Christian D. Schmidt

NMR spectroscopic investigations on VDAC

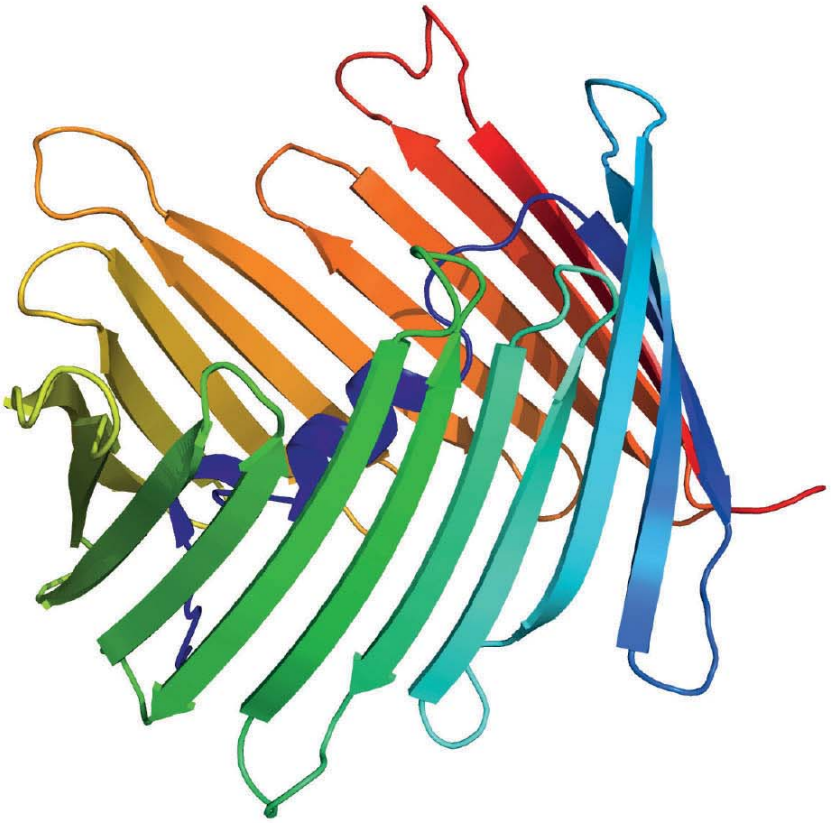

Cuvillier Verlag Göttingen
Internationaler wissenschaftlicher Fachverlag

NMR spectroscopic investigations on VDAC

Dieses Werk ist copyrightgeschützt und darf in keiner Form vervielfältigt werden noch an Dritte weitergegeben werden.
Es gilt nur für den persönlichen Gebrauch.

Dieses Werk ist copyrightgeschützt und darf in keiner Form vervielfältigt werden noch an Dritte weitergegeben werden.
Es gilt nur für den persönlichen Gebrauch.

NMR spectroscopic investigations on VDAC

Dissertation

zur Erlangung des mathematisch-naturwissenschaftlichen Doktorgrades

„Doctor rerum naturalium“

der Georg-August-Universität Göttingen

im Promotionsprogramm „Biomolecules: Structure-Function-Dynamics“

der Georg-August University School of Science (GAUSS)

vorgelegt von

Christian Daniel Schmidt

aus Leipzig

angefertigt im Max-Planck-Institut für Biophysikalische Chemie

Göttingen 2017

Dieses Werk ist copyrightgeschützt und darf in keiner Form vervielfältigt werden noch an Dritte weitergegeben werden.
Es gilt nur für den persönlichen Gebrauch.

Bibliografische Information der Deutschen Nationalbibliothek

Die Deutsche Nationalbibliothek verzeichnet diese Publikation in der Deutschen Nationalbibliographie; detaillierte bibliografische Daten sind im Internet über http://dnb.d-nb.de abrufbar.

1. Aufl. - Göttingen: Cuvillier, 2017
Zugl.: Göttingen, Univ., Diss., 2017

© CUVILLIER VERLAG, Göttingen 2017
Nonnenstieg 8, 37075 Göttingen
Telefon: 0551-54724-0
Telefax: 0551-54724-21
www.cuvillier.de

Alle Rechte vorbehalten. Ohne ausdrückliche Genehmigung des Verlages ist es nicht gestattet, das Buch oder Teile daraus auf fotomechanischem Weg (Fotokopie, Mikrokopie) zu vervielfältigen.

1. Auflage, 2017

Gedruckt auf umweltfreundlichem, säurefreiem Papier aus nachhaltiger Forstwirtschaft.

ISBN 978-3-7369-9688-5
eISBN 978-3-7369-8688-6

Dieses Werk ist copyrightgeschützt und darf in keiner Form vervielfältigt werden noch an Dritte weitergegeben werden.
Es gilt nur für den persönlichen Gebrauch.

Die vorliegende Arbeit wurde von Juni 2013 bis Juni 2017 im Max-Planck-Institut für Biophysikalische Chemie unter der Anleitung von Prof. Dr. Christian Griesinger angefertigt.

Betreuungsausschuss:

Prof. Dr. Christian Griesinger

(NMR-basierte Strukturbiologie, Max-Planck-Institut für Biophysikalische Chemie)

Prof. Dr. Claudia Steinem

(Institut für Organische und Biomolekulare Chemie, Georg-August-Universität Göttingen)

apl. Prof. Bert de Groot, Ph. D.

(Computergestützte biomolekulare Dynamik, Max-Planck-Institut für Biophysikalische Chemie)

Mitglieder der Prüfungskomission:

Referent: Prof. Dr. Christian Griesinger

(NMR-basierte Strukturbiologie, Max-Planck-Institut für Biophysikalische Chemie)

Korreferentin: Prof. Dr. Claudia Steinem

(Institut für Organische und Biomolekulare Chemie, Georg-August-Universität Göttingen)

apl. Prof. Bert de Groot, Ph. D.

(Computergestützte biomolekulare Dynamik, Max-Planck-Institut für Biophysikalische Chemie)

Prof. Dr. Markus Zweckstetter

(Proteinstrukturbestimmung mittels NMR, Max-Planck-Institut für Biophysikalische Chemie)

Prof. Dr. Claudia Höbartner

(Institut für Organische und Biomolekulare Chemie, Georg-August-Universität Göttingen)

Prof. Dr. Blanche Schwappach

(Institut für Molekulare Biologie, Universitätsmedizin Göttingen)

Tag der mündlichen Prüfung: 7. Juli 2017

Dieses Werk ist copyrightgeschützt und darf in keiner Form vervielfältigt werden noch an Dritte weitergegeben werden.
Es gilt nur für den persönlichen Gebrauch.

Dieses Werk ist copyrightgeschützt und darf in keiner Form vervielfältigt werden noch an Dritte weitergegeben werden.
Es gilt nur für den persönlichen Gebrauch.

Affidavit

I hereby declare that this thesis has been written independently and with no other sources and aids than quoted.

Christian Schmidt

Dieses Werk ist copyrightgeschützt und darf in keiner Form vervielfältigt werden noch an Dritte weitergegeben werden.
Es gilt nur für den persönlichen Gebrauch.

Dieses Werk ist copyrightgeschützt und darf in keiner Form vervielfältigt werden noch an Dritte weitergegeben werden.
Es gilt nur für den persönlichen Gebrauch.

Für meine Familie

Dieses Werk ist copyrightgeschützt und darf in keiner Form vervielfältigt werden noch an Dritte weitergegeben werden.
Es gilt nur für den persönlichen Gebrauch.

Dieses Werk ist copyrightgeschützt und darf in keiner Form vervielfältigt werden noch an Dritte weitergegeben werden.
Es gilt nur für den persönlichen Gebrauch.

Acknowledgement

Zuallererst möchte ich mich bei Prof. Dr. Christian Griesinger bedanken, der mir die Möglichkeit gegeben hat, diese Doktorarbeit in seinem Department anzufertigen und der stets ein offenes und eine offene Tür für Fragen, Sorgen, Wünsche und Probleme hatte. Ohne die exzellente Arbeitsathmosphäre und Ausstattung des Departments wäre das Anfertigen dieser Arbeit nicht möglich gewesen.

Großer Dank geht weiterhin an Prof. Dr. Bert de Groot und Prof. Dr. Claudia Steinem für die Teilnahme und Hilfestellung im Rahmen der Sitzungen meines thesis advisory committees und darüber hinaus.

Ich danke weiterhin Dr. Stefan Becker und Karin Giller für die stets unglaublich schnelle und vor allen Dingen verlässliche Bereitstellung der jeweiligen hVDAC1-Proben bzw. -Mutanten. Ein großer Dank geht zusätzlich an Stefan Becker für viele, nicht immer nur wissenschaftliche, Diskussionen.

Ich möchte mich weiterhin bei Prof. Dr. Roland Benz bedanken, der die BLM-Messungen an den VDAC-Mutanten durchführte und auch immer für Diskussionen zur Verfügung stand.

Dank für wertvollen Input und wissenschaftliche Diskussionen geht weiterhin an die übrigen (teilweise ehemaligen) Gruppenleiter im Department, Prof. Dr. Markus Zweckstetter, Dr. Rasmus Linser und Dr. Loren Andreas.

Ein Danke geht an jemanden, der gerne übersehen wird, weil er ja “nur” für funktionierende Infrastruktur sorgen muss, in Wahrheit aber mehr organisiert als mancher denkt, nämlich Dr. Dirk Bockelmann.

Für die Starthilfe im Department geht ein ganz besonderer und ausdrücklicher Dank an Dr. Saskia Villinger, die wirklich immer ein offenes Ohr hatte – auch wenn das zeitlich eigentlich gar nicht ging. Danke!

Ich danke Dr. Mariusz Jaremko und Dr. Łukasz Jaremko für die gute Zusammenarbeit und die wertvollen Hilfestellungen während der Anfertigung unserer gemeinsamen Publikation.

Für die hervorragende Zusammenarbeit im VDAC-Kosmos danke ich Dr. ShengQi Xiang und Eszter Najbauer.

Für Hilfestellungen bei diversen kleinen und großen Problemen, wissenschaftliche Diskussionen und Anregungen danke ich Dr. Pablo Trigo Moriño, Dr. ShengQi Xiang, Dr. Leo Wong, Dr. Nasrollah “Hessam” Rezaei-Ghaleh, Leif Antonschmidt, Andrei Leonov und Sergey Ryazanov.

Dieses Werk ist copyrightgeschützt und darf in keiner Form vervielfältigt werden noch an Dritte weitergegeben werden.
Es gilt nur für den persönlichen Gebrauch.

Ganz besonderer Dank für die tolle Atmosphäre im Department und die nette Aufnahme geht natürlich auch an die momentanen und ehemaligen Mitglieder des Departments, namentlich seien da Saskia, Täubi, Benni, Flo, Philip, Ann-Christin, Eibe, Manni, Leif, Michele, Sebastian, Pablo, Kris und Niels genannt. Natürlich geht auch ein Dank an alle hier nicht namentlich aufgeführten momentanen und ehemaligen Mitglieder der Abteilung.

Nicht vergessen möchte ich auch meinen ehemaligen Chef Prof. Dr. Daniel Werz und seine Mitarbeiter Dr. Tobias Schneider, Dr. Dennis Köster und Dr. Johannes Kaschel, ohne die ich wahrscheinlich auch heute nicht an dieser Stelle wäre.

Ich danke meinen Freunden aus meinem Semester: Marie, Basti, Christoph, Philip, Wuschi, Annika, Barbara, Tine für gemeinsame Urlaube, Spieleabende, das obligatorische Semesteressen und noch viel mehr. Natürlich geht dieses Dankeschön auch an die, die es in die weite Welt verschlagen hat: Anna, Rainer, Grish, Julian und Alice. Danke euch!

Ein weiterer Dank geht an alle, die ich bei meinem Fußballverein kennen lernen durfte, es sind zu viele, um sie hier aufzuzählen. Ohne euch würde mir so einiges fehlen!

Ich danke auch meiner kleinen Freundesrunde aus Gymnasiumszeiten, denn auch die alljährlichen Treffen zu Weihnachten möchte ich auf keinen Fall missen: danke Marvin, Florian, Johannes, Max und Tim!

Ich danke meinen Freunden aus meinem Wohnheim, die immer sehr verständnisvoll waren, wenn ich mal nicht so lange bleiben konnte – Jonas, Karl, Babsi, Arndt, André, Dana, Lena und alle anderen sowieso auch. ;)

Für das Korrekturlesen dieser Arbeit danke ich Marie.

Ich danke von ganzem Herzen meiner Familie! Meiner Mutter, meiner Schwester, meiner Oma, meinem verstorbenen Opa, meinem Vater. Danke, euch ist diese Arbeit gewidmet. Ein abschließendes Dankeschön geht an Marie, denn sie schafft es auch wenn ich die mieseste Laune habe, mir ein Lächeln auf’s Gesicht zu zaubern – und noch viel mehr.

Dieses Werk ist copyrightgeschützt und darf in keiner Form vervielfältigt werden noch an Dritte weitergegeben werden.
Es gilt nur für den persönlichen Gebrauch.

Abstract

This thesis is improving the understanding of the gating process of the voltage dependent anion channel (VDAC). VDAC is the most abundant protein in the outer mitochondrial membrane of eukaryotes and has a plethora of different functions there. It is the main pathway for metabolites that are going in and out the mitochondria, is interacting with many proteins in the OMM and probably also involved in the processes around cell death. Ever since its discovery in the 1970s and especially since the publication of three high resolution structures of VDAC in 2008 the mechanism of the voltage gating of the protein is a scientific question.

In this thesis, the assignment of hVDAC1 in liquid state NMR is further improved and C_β assignments are determined.

Based on a vastly improved NOE network and previously recorded R_1/R_2 relaxation data, a 3D solution state structure of E73V hVDAC1 was determined. This structure is providing evidence that the N-terminal α-helix of the protein is tightly connected to the β-barrel and has a kink feature, that has previously been described only by an X-ray 3D structure. The β-barrel shows a significant elliptic deformation that is resembling a previously determined global deformation mode of the pore and is caused by the altered lateral pressure of the surrounding micelles with respect to phospholipid membranes.

Furthermore, a hVDAC1 mutant that is stabilizing a closed state of the protein was developed and is described. This "Quintuple hVDAC1" is exhibiting properties previously determined for N-terminal deletion constructs in solid state NMR and BLM measurements, but can – contrary to the deletion constructs – still be investigated by liquid state NMR measurements. Several lines of evidence point to and suggest a partial movement of the N-terminal α-helix in this mutant. Based on the results, two possible models for a closed state of hVDAC1 are developed and discussed. The discussion is also covering differences between detergent micelles and lipid bilayer reconstituted VDAC and the respective consequences on the stability of the samples.

Dieses Werk ist copyrightgeschützt und darf in keiner Form vervielfältigt werden noch an Dritte weitergegeben werden.
Es gilt nur für den persönlichen Gebrauch.

Publication list

This thesis is based on the following publication:

- M. Jaremko, Ł. Jaremko, S. Villinger, C. D. Schmidt, C. Griesinger, S. Becker, M. Zweckstetter, High-Resolution NMR Determination of the Dynamic Structure of Membrane Proteins, Angew. Chem. Int. Ed. **2016**, *55*, 10518–10521, Angew. Chem **2016**, *128*, 10674–10678.

Dieses Werk ist copyrightgeschützt und darf in keiner Form vervielfältigt werden noch an Dritte weitergegeben werden.
Es gilt nur für den persönlichen Gebrauch.

Contents

Nomenclature **1**

1 Introduction **5**

1.1 Membrane proteins 5

1.1.1 Membrane proteins & NMR 6

1.2 Mitochondria 7

1.3 VDAC – The voltage-dependent anion channel 8

1.3.1 Voltage gating of VDAC 9

1.3.2 3D structure of VDAC 10

1.3.3 Gating models & evolution of the models 13

1.3.3.1 Physiological relevance of VDAC gating 18

1.4 Aims and Outline 20

2 Materials & Methods **21**

2.1 Materials 21

2.1.1 Chemical reagents 21

2.1.2 Bacterial strains 21

2.1.3 Growth media 22

2.1.4 SDS page gels 23

2.2 Methods 24

2.2.1 Sample preparation of hVDAC1 24

2.2.1.1 Cloning of hVDAC1 24

Dieses Werk ist copyrightgeschützt und darf in keiner Form vervielfältigt werden noch an Dritte weitergegeben werden.
Es gilt nur für den persönlichen Gebrauch.

2.2.1.2 Site directed mutagenesis 24
2.2.1.3 Expression of ^{2}H, ^{13}C and ^{15}N labelled hVDAC1 25
2.2.1.4 Refolding and purification of hVDAC1 26
2.2.2 Spin labelling 27
2.2.3 NMR spectroscopy 27
2.2.3.1 Assignment improvement and assignment of hVDAC1 mutants . . 28
2.2.3.2 Estimation of T_2 and the global correlation time τ_c 29
2.2.3.3 Determination of chemical shift differences 29
2.2.3.4 Determination of intensity changes 30
2.2.3.5 Relaxation data experiments 30
2.2.3.6 Relaxation data analysis 32
2.2.3.7 Structure calculation and refinement 34
2.2.4 BLM measurements 35
2.2.5 Calculation of PRE effect differences 35

3 Results **37**

3.1 Improving the assignment of hVDAC1 37
3.1.1 Additional C_β shifts 37
3.1.2 Improved backbone assignment 39
3.1.3 Improved backbone NOE network 42
3.2 A new NMR structure of E73V hVDAC1 45
3.2.1 A 3D structure of E73V hVDAC1 based on the improved NOE network as starting point 45
3.2.2 Improving the structure with ^{15}N spin-relaxation data 47
3.2.3 Validating the high-resolution structure of E73V hVDAC1 51
3.3 Incorporating the protein's closed state in NMR – Developing a Quintuple hVDAC1 mutant 53
3.3.1 General strategy 53

Dieses Werk ist copyrightgeschützt und darf in keiner Form vervielfältigt werden noch an Dritte weitergegeben werden.
Es gilt nur für den persönlichen Gebrauch.

3.3.2 Affixing the N-terminal helix to the β-barrel 54
3.3.2.1 A14C/C127A/S193C/C232A hVDAC1 samples are oxidized by air 55
3.3.2.2 A14C/C127A/S193C/C232A hVDAC1 in liquid state NMR 56
3.3.3 Stiffening the linker between α-helix and β-barrel 59
3.3.3.1 Changing the expression system to the pET28a expression vector . 61
3.3.3.2 Experiments on G21V/G23V hVDAC1 63
3.3.3.3 Experiments on G21V hVDAC1 68
3.3.3.4 Development of a Quintuple hVDAC1 mutant 70
3.4 Experiments on Quintuple hVDAC1 and development of a model of the closed state of hVDAC1 72
3.4.1 Quintuple hVDAC1 behaves like a ΔN construct in BLM measurements . . . 75
3.4.2 Quintuple hVDAC1 in solid state NMR measurements 78
3.4.3 Missing and new NOE contacts of Quintuple hVDAC1 80
3.4.4 Probing the new orientation of the N-terminal helix 82
3.4.5 A model for the closed state of hVDAC1 86

4 Discussion **87**
4.1 A14C/C127A/S193C/C232A hVDAC1 is not closed in NMR samples 87
4.2 The structure of hVDAC1 and the N-terminal α-helix in micelles 91
4.2.1 The shape of the β-barrel 92
4.2.2 The old NMR structure in the light of the new findings 93
4.3 Quintuple hVDAC1 as a model for the closed state 95
4.3.1 The conformation of the N-terminal helix in the closed state of Quintuple hVDAC1 99

5 Conclusion & Outlook **103**

Appendix **105**

Dieses Werk ist copyrightgeschützt und darf in keiner Form vervielfältigt werden noch an Dritte weitergegeben werden.
Es gilt nur für den persönlichen Gebrauch.

A Pulse programs **107**

A.1 Pulse program of TROSY-HNCACB 107

A.2 Pulse program for measurement of ^{15}N-R_1 relaxation rates at 900 MHz 112

A.3 Pulse program for measurement of ^{15}N-R_2 relaxation rates at 900 MHz 118

B Assignment tables of important hVDAC1 mutants **127**

B.1 Chemical shift assignment of *wt* hVDAC1 127

B.2 Chemical shift assignment of E73VC127AC232S hVDAC1 132

B.3 Chemical shift assignment of Quintuple hVDAC1 140

B.4 Chemical shift assignment of hVDAC1 in liposomes 148

C Sequence alignment of mentioned VDAC isoforms **151**

D PDB files of the models for the closed state of VDAC **153**

D.1 Model 1 153

D.2 Model 2 166

Bibliography **179**

Dieses Werk ist copyrightgeschützt und darf in keiner Form vervielfältigt werden noch an Dritte weitergegeben werden.
Es gilt nur für den persönlichen Gebrauch.

Nomenclature

ADP	adenosine 5'-diphosphate
AFM	atomic force microscopy
APS	ammonium persulfate
APSY	automated projection spectroscopy
ATP	adenosine 5'-triphosphate
BLM	black lipid membrane / bilayer lipid membrane
CEST	chemical exchange saturation transfer
CPMG	Carr–Purcell–Meiboom–Gill
CuX_2Ph	copper phenantroline
DEST	dark-state exchange saturation transfer
DMPC	dimyristoyl-phosphatidylcholine
DPhPC	diphytanoyl-phosphatidylcholine
DTT	dithiothreitol
EDTA	ethylenediaminetetraacetic acid
EM	electron microscopy
GRS	glycine rich sequence
HDL	high-density lipoprotein
HEPES	4-(2-hydroxyethyl)-1-piperazineethanesulfonic acid
HK	hexokinase
HMQC	heteronuclear multiple-quantum correlation spectroscopy
HSQC	heteronuclear single-quantum correlation spectroscopy

Dieses Werk ist copyrightgeschützt und darf in keiner Form vervielfältigt werden noch an Dritte weitergegeben werden.
Es gilt nur für den persönlichen Gebrauch.

hVDAC	human voltage dependent anion channel
HVEM	high-voltage electron microscopy
IMM	inner mitochondrial membrane
IMP	integral membrane protein
IMS	inter membrane space
IPTG	isopropyl β-D-1-thiogalactopyranoside
LDAO	lauryldimethylamine-*N*-oxide
MD	molecular dynamics
MFA	model free analysis
MTSL	*S*-(1-oxyl-2,2,5,5-tetramethyl-2,5-dihydro-1H-pyrrol-3-yl)methyl methanesulfonothioate
mVDAC	murine voltage dependent anion channel
ncVDAC	*neurospora crassa* voltage dependent anion channel
NMR	nuclear magnetic resonance
NOESY	nuclear Overhauser effect spectroscopy
OMM	outer mitochondrial membrane
OPOE	octyl polyoxyethylene
ORF	open reading frame
PB	Poisson-Boltzmann
PCA	principal component analysis
PCR	polymerase chain reaction
PDB	Protein Data Bank
PEG	polyethyleneglycol
PMSF	phenylmethanesulfonyl fluoride
PRE	paramagnetic relaxation enhancement
RDC	residual dipolar coupling
RMSD	root mean square deviation
rVDAC	rat voltage dependent anion channel

Dieses Werk ist copyrightgeschützt und darf in keiner Form vervielfältigt werden noch an Dritte weitergegeben werden.
Es gilt nur für den persönlichen Gebrauch.

S/N	signal-to-noise
scVDAC	*saccharomyces cerevisiae* voltage dependent anion channel
SD	standard deviation
SDS-PAGE	sodium dodecyl sulfate polyacrylamide gel electrophoresis
SEM	standard error of the mean
TEMED	tetramethylethylenediamine
TROSY	transverse relaxation-optimized spectroscopy
VDAC	voltage dependent anion channel
wt	wild type
zfVDAC	*zebra fish* voltage dependent anion channel

Dieses Werk ist copyrightgeschützt und darf in keiner Form vervielfältigt werden noch an Dritte weitergegeben werden.
Es gilt nur für den persönlichen Gebrauch.

Dieses Werk ist copyrightgeschützt und darf in keiner Form vervielfältigt werden noch an Dritte weitergegeben werden.
Es gilt nur für den persönlichen Gebrauch.

1 Introduction

1.1 Membrane proteins

Membrane proteins are a large subgroup of proteins along with soluble globular proteins, fibrous proteins and disordered proteins. It has been estimated by various methods that about 20 to 30% of all open reading frames (ORFs) over all organisms encode membrane proteins.[1–3] Unlike soluble proteins, that are able to fold with high variability, membrane proteins are only known to occur in two topology categories: α-helical bundles and β-barrels. Membrane proteins give the membranes their characteristical functional properties and allow them to carry out their respective activities. As such, the membrane protein content expressed as mass ratio in a membrane ranges from less than 25% (in the myelin membrane) to up to 75% (in internal membranes of mitochondria and chloroplasts).[4]

α-helical membrane proteins can be found in literally all types of biological membranes: besides occuring in the plasma membrane they are also found in the inner membranes (mitochondria, chloroplasts, endoplasmatic reticulum, peroxisomes and in bacteria). Their function comprises transport processes across membranes, metabolism, cell signaling and regulation processes and as such they are heavily adressed targets for drug discovery.[5]

In contrast to that, β-barrel membrane proteins are only found in the outer membranes of Gram-negative bacteria, scarcely in the cell walls of Gram-positive bacteria and in the outer membranes of mitochondria and chloroplasts. However, in those membranes β-barrel membrane proteins oftentimes make up the majority of the integral membran proteins. The importance of membrane proteins becomes evident with the fact, that they are targeted by more than 50% of small molecule drugs used in the treatment of human diseases: they have been and still are an intensively addressed drug target.[6]

Dieses Werk ist copyrightgeschützt und darf in keiner Form vervielfältigt werden noch an Dritte weitergegeben werden.
Es gilt nur für den persönlichen Gebrauch.

1.1.1 Membrane proteins & NMR

The fact that membrane proteins are such a prominent drug target reasons, why there is also a big interest in the scientific community in determining the 3D structures of membranes proteins. In the Membrane Protein Structures Database of the Stephen White laboratory at University of California Irvine (blanco.biomol.uci.edu/mpstruc/; status of May 2017) 692 unique membrane protein structures are deposited. Of these, only 53 structures were solved with the means of NMR spectroscopy. Until now, X-ray crystallography is still the most commonly applied technique, although structure determination by cryo-EM is becoming more and more the method of choice in recent years.[7] However, the fact that of roughly 130'000 structures in the RCSB Protein Data Bank (www.rcsb.org/pdb; status of April 2017) only about 4130 structures are membrane proteins (which is only 3 %, i.e. far less than 20 to 30 % of all structures, cf. above) shows that all three techniques are experiencing difficulties in structure determination of membrane proteins.

NMR has the unique ability to access not only rigid structures but also dynamics and different states. Furthermore, there is still ongoing advancement in liquid and solid state NMR spectroscopy, e.g. APSY[8] or non-uniform sampling[9] for liquid state NMR or the development of 0.7 mm rotors that allow spinning frequencies of up to 111 kHz and thus the direct detection of protons for solid state NMR. Further increased field strengths of at the moment up to 1 GHz proton resonance frequency raise the overall sensitivity of the spectrometers. Magnets with 1.2 GHz proton resonance frequency are being in development.

That NMR is still a viable tool to determine 3D structures of membrane proteins can be seen by the fact that in 2017 already two structures of membrane proteins or domains of proteins embedded in membranes solved with NMR have been reported: the structure of the C-terminal transmembrane domain of the HDL receptor, SR-BI,[10] and the structure of the epidermal growth factor receptor transmembrane domain dimer.[11] These are faced with 20 structures solved by X-ray diffraction or cryo-EM in 2017 (according to blanco.biomol.uci.edu/mpstruc/; status of May 2017).

Dieses Werk ist copyrightgeschützt und darf in keiner Form vervielfältigt werden noch an Dritte weitergegeben werden.
Es gilt nur für den persönlichen Gebrauch.

1.2 Mitochondria

Mitochondria are organelles found in nearly all eukaryotic organisms (monocercomonoides sp. being the only one known exception[12]) and are the main source of the cells' energy currency by generating ATP through oxidative phosphorylation.[13] They are separated from the cytoplasm of the surrounding cell by two membranes, the inner and the outer mitochondrial membrane (IMM and OMM), which in turn are separated by the inner membrane space (IMS). Following the endosymbiotic hypothesis, the two membranes are leftovers from the mitochondrias' origin as prokaryotic cells.[14] Besides their key function in the energy balance of the cell, mitochondria also play a role in the regulation of cell metabolism, cell-cycle control, development, antiviral responses and cell death.[15]

The IMM contains a series of respiratory enzyme complexes. Electrons passing through these complexes are used to build up a proton gradient across the IMM which is then enabling the ATP synthase to synthesize ATP.[13] Furthermore, the IMM containts the ADP/ATP carrier, which is catalyzing the ADP versus ATP exchange over the IMM and is thus critical for the supply of ATP from the mitochondria to the cytosol.[16,17]

The OMM is populated by four major integral membrane protein families. The translocase of the outer membrane (TOM complex), the sorting and assembly machinery (SAM complex) and the mitochondrial distribution and morphology (Mdm) complex all consist of a core subunit, which is an integral β-barrel membrane protein, and several smaller proteins that regulate the assembly and dynamics of the complexes.[18–22] These three OMM protein families are responsible for the translocation and insertion of nearly all synthesized proteins into the mitochondria.[23]

The last family is mediating the flux of all metabolites (including ADP and ATP) and ions across the OMM.[24] It is the family of voltage dependent anion channels (VDACs). They are named this way due to their anion selectivity and their voltage-dependent conductance.[25,26] In high density regions they cover up to 80 % of the membranes surface[27] and thus are the most abundant protein family in the OMM. They are known to form various oligomers[28], which was determined by EM as early as in the 1960s.[29] The following chapter will describe this family in more detail.

Dieses Werk ist copyrightgeschützt und darf in keiner Form vervielfältigt werden noch an Dritte weitergegeben werden.
Es gilt nur für den persönlichen Gebrauch.

1.3 VDAC – The voltage-dependent anion channel

VDAC, the voltage dependent anion channel, was discovered in two ways independently of each other: by electrophysiological measurements of the outer mitochondrial membrane and by electron microscopic (EM) observations of the same.[29]

Electrophysiological measurements of single-channels in membranes were made possible by the stable formation of planar membranes, which was described by Mueller *et al.* in 1962[30] and by Montal and Mueller in 1972.[31] However, in the first years after the invention of this technique, mainly channel-forming antibiotics that were reconstituted into these membranes were studied, as the patch-clamp technique was not invented before 1976.[32] Indeed, VDAC was the first intrinsic membrane channel that was reconstituted and studied at the single-channel level with planar membranes by Schein, Colombini *et al.* in the beginning of 1975, published in 1976.[25] Also the designation of the channel as "voltage dependent anion channel" is found in this paper first. Interestingly, Schein *et al.* originally wanted to study a voltage-gated calcium channel, but finally found out, that they reconstituted something completely different into the membrane. Different from what they expected, the reconstituted channels showed a conductance that depended on the applied voltage and favored anions like chloride over calcium. Since at that time the presence of channels in the mitochondrial membrane seemed to be unlikely, it was a big surprise that they were stemming from the mitochondrium. Further studies revealed that the VDAC channels were located in the OMM[25] and Marco Colombini concluded that they are the reason for its apparent "leakiness", that had functionally been described by Werkheiser and Bartley more than 20 years before.[33,34]

Studies carried out in parallel by Zalman *et al.* were not published before 1980.[35] They described a protein with an apparent molecular weight of 30 kDa obtained from rat liver mitochondria, but found this protein to be a nonspecific diffusion channel for saccharides of up to 8 kDa. This publication is the origin of the termin "mitochondrial porin". Only later it became clear that the mitochondrial porin and VDAC are the exact same protein.

Already more than ten years earlier in the middle of the 1960s, plant mitochondrial membranes had been studied with the means of negative-stain EM and revealed densely packed stain-filled subunits

Dieses Werk ist copyrightgeschützt und darf in keiner Form vervielfältigt werden noch an Dritte weitergegeben werden.
Es gilt nur für den persönlichen Gebrauch.

with 2–3 nm wide "pits", in a collaboration of Bonner, Parsons *et al.*[36] The identity of these pores was finally clarified by Carmen Mannella in the beginning of the 1980's using high-voltage electron microscopy (HVEM) and in collaboration with Parsons. Working as a PhD candidate in the lab of Bonner, she had previously found with SDS-PAGE experiments that over 50 % of the protein mass of plant outer mitochondrial membranes belong to a protein with a mass of around 30 kDa, labeled "Band I".[37] The obvious hypothesis was, that this band belonged to the subunits that Parsons *et al.* had observed with EM over ten years ago. The HVEM studies in the beginning of the 1980s finally revealed 2D crystals on the fungal outer mitochondrial membrane – which in turn were identified as being composed of VDAC, closing the circle to the observation in 1965.[38]

In the following years a wide variety of functions was described for the VDAC channels and it has been suggested that there is more than one isoform of the protein.[39] This hypothesis turned out to be true, as up to three isoforms were found, depending on the respective organism that is considered. In mammals like mice or the human, three isoforms of VDAC have been found[40,41] in tissue-specific expression-levels, while for example mitochondria from yeast contain only one or two isoforms.[42]

The isoform that was discovered in the 1970s is VDAC1, which is also by far the most abundant (factor 10 over VDAC2 and factor 100 over VDAC3 in HeLa cells) and consequently the best characterized isoform of the protein.[43] All three isoforms induce quite similar permeability when reconstituted into liposomes (molecular weight cutoff between 3.4 and 6.8 kDa based on the permeability of polyethyleneglycol). Electrophysiological studies show, that the prototypical gating properties (described in the following chapter) shown by VDAC1 are highly conserved among different species. However, VDAC2 exists in two forms, one of them with a lower conductance. VDAC3 does not insert into membranes as readily as VDAC1 and VDAC2 and generally does not show distinct gating properties.[44]

1.3.1 Voltage gating of VDAC

As described in the previous chapter, one of the most distinctive features of VDAC, and in particular of VDAC1, is its ability to show a conductance depending on the applied voltage, *i.e.* to switch from a high conducting state to a low conducting state depending on the applied potential. This property

Dieses Werk ist copyrightgeschützt und darf in keiner Form vervielfältigt werden noch an Dritte weitergegeben werden.
Es gilt nur für den persönlichen Gebrauch.

of VDAC1 is highly conserved among the different mammalian VDACs: they all show very similar conductance, selectivity and voltage-gating.[45]

All values presented here have been determined with VDAC reconstituted into planar phospholipid bilayers. The high conducting state of the pore is accessible at low voltages (below ± 20 mV) with a typical conductance of around 4 to 4.5 nS in 1 M KCl (or around 0.5 nS in 0.1 M KCl).[45–52] The conductance of the channels is linear with the KCl activity up to 4 M KCl.[53] In this state, VDAC exhibits a slight selectivity for anions ($P(Cl^-)/P(K^+) \approx 2$)[45], and is permeable to large anions such as ATP.[54] Under special conditions (a 5-fold KCl gradient across the membrane) also a cation-selective open state has once been described.[55]

At potentials above ± 20 mV, the probability of the channel to be in the high conducting ("open") state decreases until it reaches 0 % at ± 40 to 50 mV, meaning that all channels observed are in lower conducting ("closed") states.[45] The channel reaches different closed states at positive or negative potential, respectively.[53] The conductance of these closed states is usually around 50 % compared to the conductance of the open state with KCl as electrolyte in the aqueous phase – around 2 nS in 1 M KCl.[24] Deeper and more refined investigation on mVDAC1 revealed that there are two not completely identical closed substates with conductances of 2.6 nS and 1.9 nS – hence the conductance of the closed conformation of the channel is a composite of these states.[52] Upon closure, the selectivity of the channels switches to favor small cations over anions[24,56] and the pore is furthermore no longer permeable for ADP or ATP.[54,56] (See Figure 1.1.)

1.3.2 3D structure of VDAC

The 3D structure of VDAC was a long standing question that could finally be solved in 2008 – over 30 years after the protein's discovery – by three groups independently. (See below.) Before, models with 12[57–59], 13[60], 16[61–63], 18[64,65] or 19[66] β-strands and an amphipathic N-terminal α-helix had been discussed. Most of the efforts to develop these models were done by Carmen Mannella, Elizabeth Blachly-Dyson, Michael Forte and Marco Colombini over the course of over 20 years.

The number of β-strands proposed by Blachly-Dyson, Forte and Colombini increased over time from 12 to 13, while Mannella always pointed out that there is a large amount of disagreement over

Dieses Werk ist copyrightgeschützt und darf in keiner Form vervielfältigt werden noch an Dritte weitergegeben werden.
Es gilt nur für den persönlichen Gebrauch.

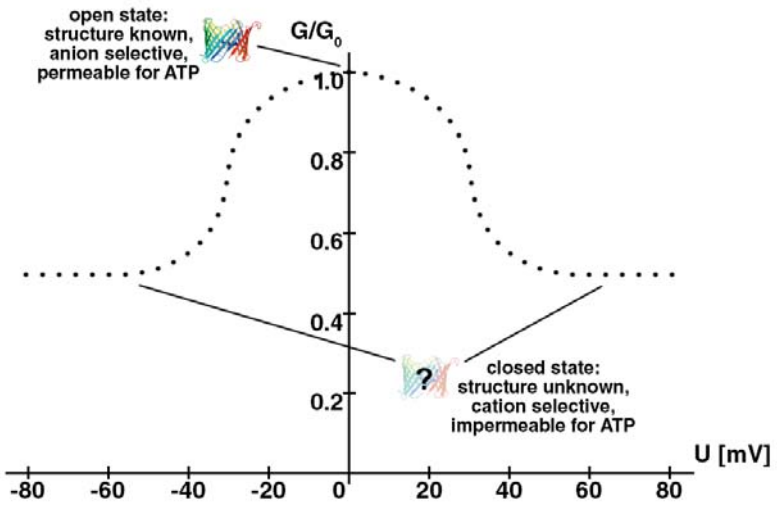

Figure 1.1: Typical voltage gating profile of VDAC. Conductance G of a VDAC channel as function of the applied potential with respect to the zero-voltage conductance G_0. The profile represents typical values yielded from studies in 1 M KCl as electrolyte. Structure shown is the 3D X-ray structure of mVDAC1 (PDB id: 3EMN).

the number of strands[67], as there are models with 16 β-strands published in the 1990s[61,62], that were never really considered by the former. The 12-β-strand model was derived in the late 1980s and early 1990s from a simple integration over the hydropathy values[68] of the amino acid side chains in groups of 10[57] and supported by site-directed mutagenesis that aimed to check for effects on channel selectivity or voltage dependence.[57,59] By biotinylation experiments the folding pattern was revised to include an N-terminal α-helix and 13 β-strands in 1998[60], which is still the model Marco Colombini prefers nowadays for the native state of the protein.[69]

By neural network-based predictors, 16 β-strands were proposed in 2002 again[63], before 18 β-strands were predicted by different authors based on computer analyses[65] and NMR data[64]. The three high resolution structures published in 2008, however, described the channel to be consisting of 19 β-strands – in line with a prediction by the Delphi algorithm from as early as 1987.[66]

In contrast to a structure from this group, that was based on a combination of X-ray crystallography and solution state NMR data[70], the other two structures were solely based on X-ray crystallography[46] or solution state NMR data[48], respectively. All three 3D structures show that the N-terminus is not part of the barrel wall and located in the interior of the pore (unstructured in the NMR structure, as an α-helix in the NMR/X-ray and X-ray structure). Furthermore, the structures showed that there is an unusual glutamate at position 73 in the sequence, which does not point

Dieses Werk ist copyrightgeschützt und darf in keiner Form vervielfältigt werden noch an Dritte weitergegeben werden.
Es gilt nur für den persönlichen Gebrauch.

to the interior of the pore, but to the surrounding hydrophobic environment. The odd number of β-strands and the fact that the N-terminal helix is not part of the barrel wall was somewhat surprising, as this implies the need of a parallel arrangement of β-strands 1 and 19 and all previously solved β-barrel structures of procaryotes had an even number of β-strands.[48] The three high resolution structures from 2008 are shown in Figure 1.2.

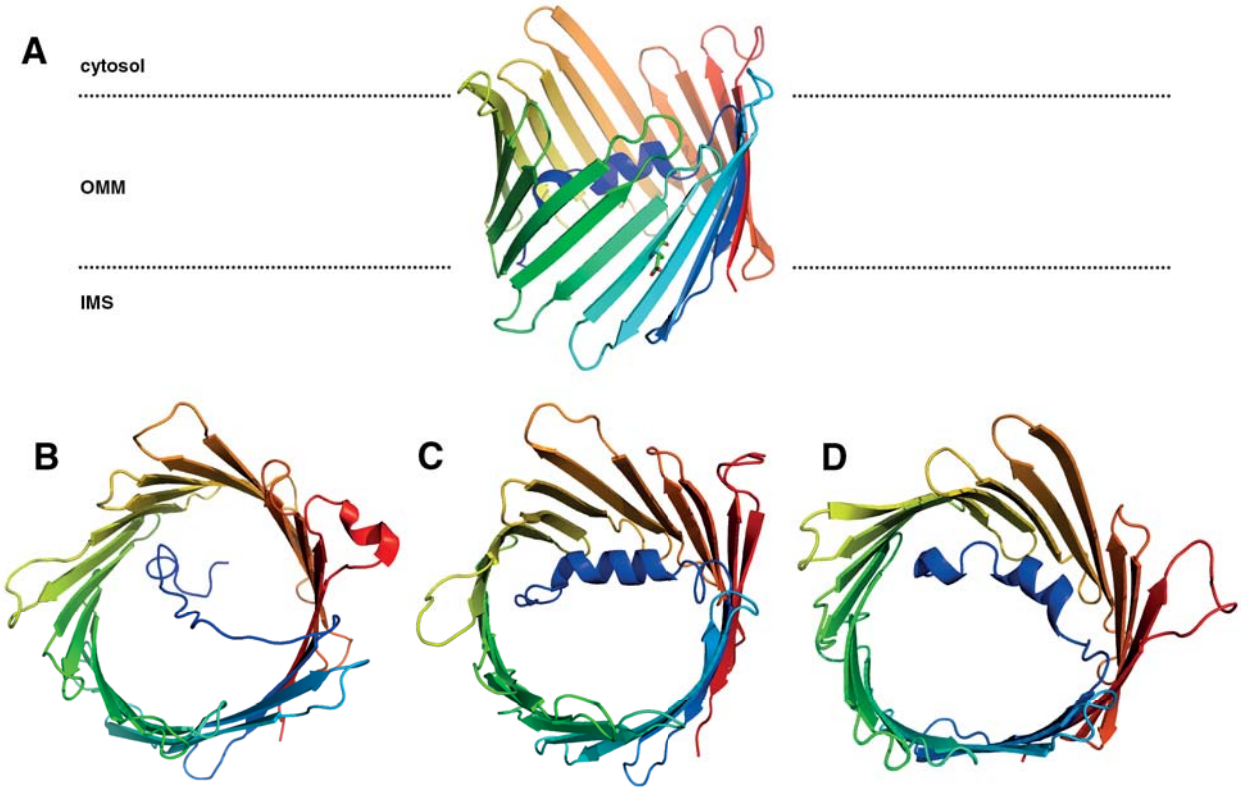

Figure 1.2: 3D structures of VDAC1 from 2008. All structures are shown in a cartoon representation and colored from N-terminus to C-terminus from blue to red. Visualization was done with PyMol.[71] A: X-ray structure of mVDAC1 (PDB id: 3EMN)[46] in a tilted view. The unusual glutamate pointing to the surrounding membrane is shown in stick representation. The dotted lines and the annotations indicate the cytosole, the Outer mitochondrial membrane (OMM) and the inter membrane space (IMS) as suggested by latest studies.[72,73] B: Lowest energy NMR structure of hVDAC1 from an ensemble of 20 structures (PDB id: 2K4T).[48] C: Combined NMR and X-ray structure of hVDAC1 (PDB id: 2JK4).[70] D: X-ray structure of mVDAC1 (PDB id: 3EMN).[46]

While the X-ray structure shows that the N-terminal helix should have a short kink from residues 10 to 12, it does not show this feature in the structure based on combined NMR and X-ray data. In the structure based on NMR data alone, the N-terminus is completely unstructured. Also, in the X-ray structure the N-terminal helix is connected tightly to the barrel, while in the structure based on combined data only the first part of the helix is connected to the barrel and in the NMR structure,

Dieses Werk ist copyrightgeschützt und darf in keiner Form vervielfältigt werden noch an Dritte weitergegeben werden.
Es gilt nur für den persönlichen Gebrauch.

the N-terminus is floating freely in the middle of the barrel. Lastly, the N-terminus is rotated by approximately 90° in the structure based on combined data with respect to the X-ray structure. It was discussed in the PhD thesis of Saskia Villinger[74], whether this is due to differences in the resolution of the structures or due to dynamics of the helix. Based on newer results, the former is most likely the case.[75]

After the publication of these structures the question was raised especially by Marco Colombini, whether these structures represent a native and functional state of the channel or are an artifact of the refolding procedure that was necessary to study the respective samples.[76] However, the diameter of the published structures is in excellent agreement with values obtained from EM and AFM experiments[27,77,78] and the tilt angle of the β-strands fits well to other resolved structures of β-barrel proteins.[79] This would not be the case for the 13-stranded model favored by Marco Colombini.[69] Except of him it is thus now universally accepted that the 3D structures published in 2008 indeed represent a native conformation of the channel.

The structures were once again confirmed by further publications in 2014, when the crystal structure of mVDAC1 in presence of ATP was solved. It reveals a low affinity binding site of ATP in the center and bottleneck of the pore: between the N-terminal helix and the C-terminal end of the sequence.[80]

Also in 2014 the first 3D high resolution structure of the VDAC2 isoform was reported. The structure of zfVDAC2 was solved by X-ray crystallography and reveals a β-barrel with 19 β-strands and an N-terminal α-helix attached to the barrel wall at the usual position and with a kink consisting of residues 10 to 12 (PDB ID: 4BUM).[75] Overall, the X-ray structure of zfVDAC2 is strikingly similar to the X-ray structure of mVDAC1 with an RMSD of 0.98 Å. The only big difference between the structures is the loop from β-strand 1 to 2 with a displacement of 10 Å. The X-ray structure of zfVDAC2 is shown in Figure 1.3.

1.3.3 Gating models & evolution of the models

The development of the gating models of VDAC happened in close connection to the amount of structural information available about the channel, as with more structural information also the mode

Dieses Werk ist copyrightgeschützt und darf in keiner Form vervielfältigt werden noch an Dritte weitergegeben werden.
Es gilt nur für den persönlichen Gebrauch.

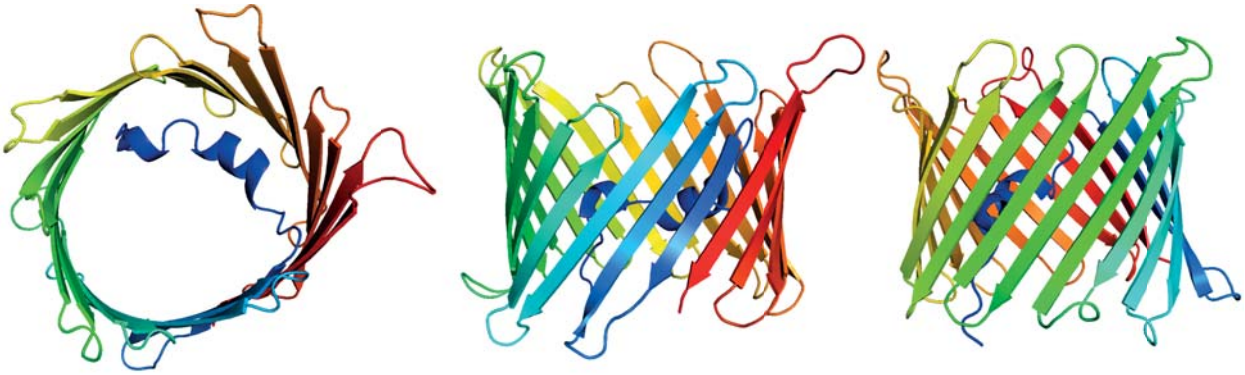

Figure 1.3: 3D structure of zfVDAC2 from 2014 (PDB ID: 4BUM). All views are shown in a cartoon representation and colored from N-terminus to C-terminus from blue to red. Visualization was done with PyMol.[71] zfVDAC2 from above shows the N-terminal helix with the characteristic kink (left) and the usual barrel fold known from the previous 3D high resolution structures (middle and right).

of gating could be proposed with more accuracy and detail. However, even with several high resolution structures available, the mode of gating is still not fully understood.

One of the earliest and most basic insights into the gating of VDAC was, that the inaccessible volume for polyethyleneglycol (PEG, a hydrophilic polymer) of the channel during closure is decreased by roughly 50 % of its initial volume in the open state. This decrease is in the order of $2 \cdot 10^4$ Å^3.[81]

Furthermore, it became evident that there is a positively charged moiety, also called "voltage sensor" region in the protein, which moves during gating and that there are actually two distinct gating processes – one at negative and one at positive potential. These gating processes can be influenced e.g. by altering the voltage sensor with the means of site-directed mutagenesis (to make the voltage dependence asymmetric, stronger or to remove it)[59,82], titration of the voltage sensor (to weaken the gating at higher pH values)[83], phosphorylation (also resulting in asymmetric gating)[84] or the composition of the membrane in which VDAC is embedded[85]. The voltage sensor was determined using a VDAC model with 12 β-strands, but based on the available 3D structures, the voltage sensor would comprise the N-terminal α-helix and parts of β-strands 2–5, 9–10 and 19.[59] (See Figure 1.4.) The residues probed in β-strands 9 and 10 (Glutamate-145 and -152 in scVDAC1, analogous to Glutamate-147 and Glutamine-154 in hVDAC1) were shown to influence only one of the two gating processes.[82] If all of the determined voltage sensor regions would move upon closure of the channel, this would entail a large scale rearrangement of the protein domains.[86]

It was proposed that the voltage sensor of the protein moves in a way, that exposes it to the membrane surface during the gating process. This was probed with site-directed mutagenesis: single

Dieses Werk ist copyrightgeschützt und darf in keiner Form vervielfältigt werden noch an Dritte weitergegeben werden.
Es gilt nur für den persönlichen Gebrauch.

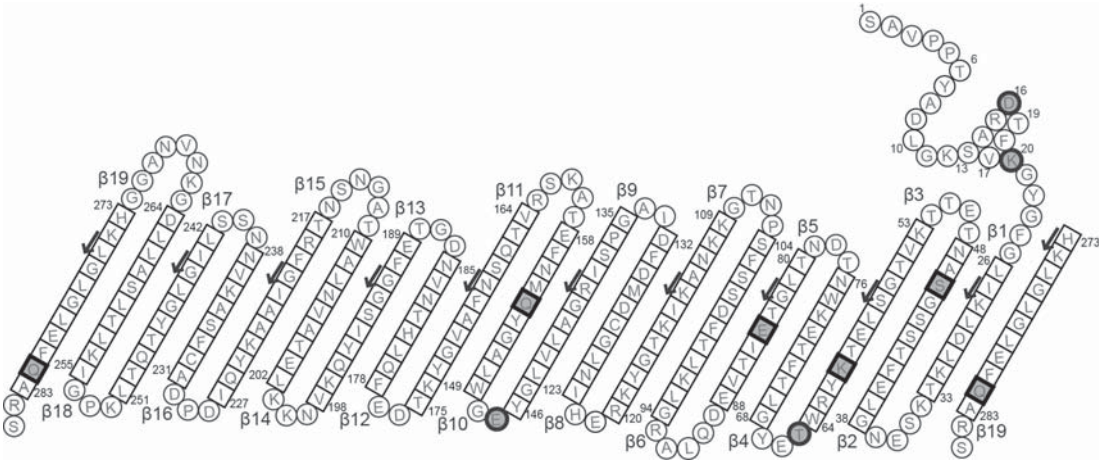

Figure 1.4: Voltage sensor in hVDAC1. Residues that were identified to move during the gating process and thus been proposed to belong to the voltage of the protein are marked. The residues were determined using a model with 12 β-strands. Glutamate-145 and -152 were shown to only influence one of the gating processes and are located in the loop from β-strand 9 to 10 and in β-strand 10.

residues were mutated to cysteine, biotinylated and tested for accessibility for streptavidin. It turned out, that it is the previously determined voltage sensor region that is accessible for streptavidin and upon binding the channels appeared to be locked in the closed state.[87] This was confirmed by N-terminal antibody studies on native OMM.[88] Based on these results the gating model shown in Figure 1.5 was developed.

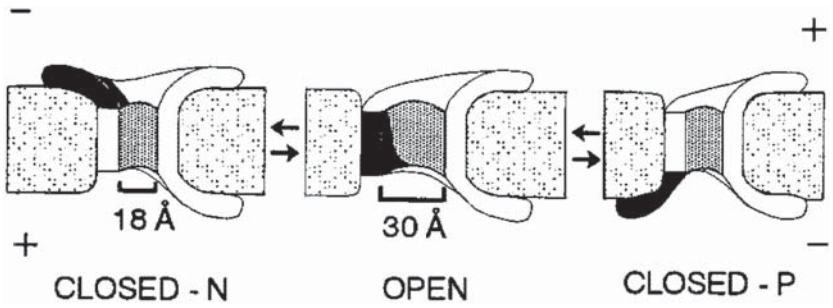

Figure 1.5: Gating processes as proposed in 1998. The voltage sensor of the protein is moving to the surface, depending on the applied potential to reach two different closed states achieved at positive and negative potential. At the same time, during gating the channel diameter decreases. Reprinted from Song *et al.* with kind permission from Elsevier.[87]

The importance of the N-terminal α-helix for the channel conductance, stability and the gating process was tested with a vast variety of deletion mutants. Interestingly, results from these experiments seem to be somewhat contradicting. As early as 1996, BLM measurements showed that Δ(2–12)-ncVDAC1 and Δ(3–20)-ncVDAC1 form instable, noisy channels with conductances mostly lower

Dieses Werk ist copyrightgeschützt und darf in keiner Form vervielfältigt werden noch an Dritte weitergegeben werden.
Es gilt nur für den persönlichen Gebrauch.

than the usual open state, but were still described to show gating properties, however significantly weakened.[50] Partly contrary to that, Δ(1–8)-scVDAC1 also shows instable, flickering channels with lower conductance than the usual open state, but has completely lost its voltage dependence.[89] In 2008, Δ(1–7)-hVDAC1 and Δ(1–19)-hVDAC1 were construed. The former shows a broad distribution of conductance values with a maximum around 2.4 nS. The latter has a predominant conductance of around 1 nS, shows only some channels with around 2.4 nS and has furthermore lost its gating properties (no information was given about that on the former construct).[90] A very similar Δ(1–20)-hVDAC1 construct however shows conductances broadly distributed between 0.5 and 3 nS (i.e. no predominant conductance of 1 nS) without voltage dependence.[91] Finally, Δ(1–26)-mVDAC1 was described to have lost its voltage dependence, but "exhibited high conductance" (no exact values were given).[47]

After it was discovered that VDAC is a 19-stranded β-barrel, these results could be rationalized, as the N-terminal α-helix obviously stabilizes the β-barrel and thus its complete or partial removal causes destabilization of the channel, resulting in (partial) collapse of the barrel structure and thus noisy and more closed state-like BLM measurements. Subsequent gating models were developed based on this combined knowledge and the available 3D structures.

The authors of the X-ray structure of mVDAC1 and two other authors had proposed detaching and movement of the N-terminal α-helix into the middle of the pore as mechanism for the gating of the channel.[46,92] This model was refined by Hiller and Wagner specifying that only the second part of the helix moves and the hydrophobic contact between Leucine-10 and the β-barrel is retained.[93] (See Figure 1.6.)

These models, however, are contradictory to the finding that the pore volume decreases upon closure.[81] Furthermore they could be ruled out also theoretically by Poisson-Boltzmann (PB) electrostatic calculations, as the helix motion proposed in these models does not show voltage dependence at all. Even a complete removal of the N-terminal α-helix out of the barrel can explain only roughly half of the voltage dependence observed in experiments and and the barrel would still be anion-selective according to these calculations. (It was, however, concluded that this motion of the helix could be part of the overall gating motion.) In the same publication it was shown with PB elec-

Dieses Werk ist copyrightgeschützt und darf in keiner Form vervielfältigt werden noch an Dritte weitergegeben werden.
Es gilt nur für den persönlichen Gebrauch.

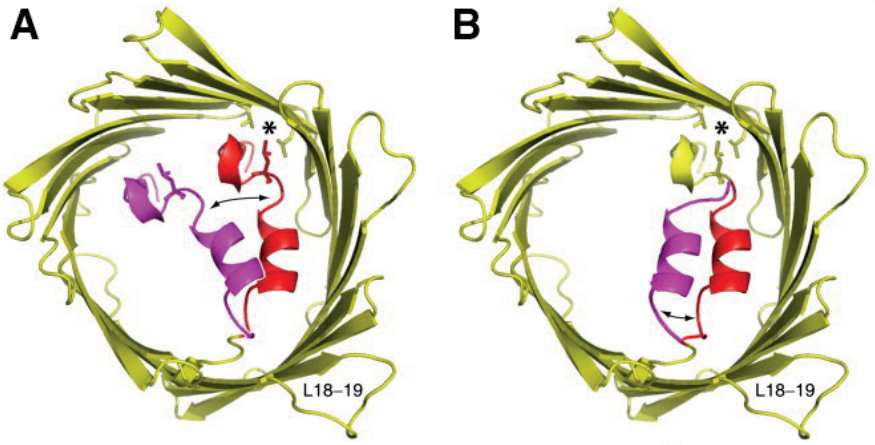

Figure 1.6: Gating as proposed in 2009. A: The N-terminal α-helix as the voltage sensor moves to the middle of the pore during gating. B: Only the second part of the helix moves, retaining the hydrophobic contact between Leucine-10, Valine-143 and Leucine-150. Reprinted from Hiller and Wagner with kind permission from Elsevier.[93]

trostatic calculations that the three high resolution 3D structures from 2008 are selective for anions and thus should be identical to the open state of the protein.[94] This was confirmed by computational electrophysiology simulations[95], from which it was likewise concluded that the published 3D structures are anion selective and have a conductance of 4.2 ± 0.2 nS (SEM) in 1 M KCl.[91] According to these simulations, a cation selective state of the pore with a conductance of approximately 2 nS can be reached by removing the N-terminal α-helix out of the barrel and collapsing the barrel to an ellipticity of around 0.5.[91] The calculated volume decrease due to this collapse would be around $1 \cdot 10^4$ Å^3, which is in the same order of magnitude compared to previous experimental values, but not completely coinciding to these. (See above, a loss of $2 \cdot 10^4$ Å^3 was determined with PEG.[81] To reach this volume decrease with an elliptic deformation, an even higher ellipticity of approximately 0.75 would be necessary.)

Further experimental evidence against the models presented in Figure 1.6 is provided by the finding, that an L10N hVDAC1 mutant (i.e. a mutant in which the hydrophobic contact between Leucine-10, Valine-143 and Leucine-150 is destroyed) is already closed at very low voltages. This indicates that increasing the mobility of the N-terminal α-helix by destroying the hydrophobic contact forces the channel into a closed state.[91]

Dieses Werk ist copyrightgeschützt und darf in keiner Form vervielfältigt werden noch an Dritte weitergegeben werden.
Es gilt nur für den persönlichen Gebrauch.

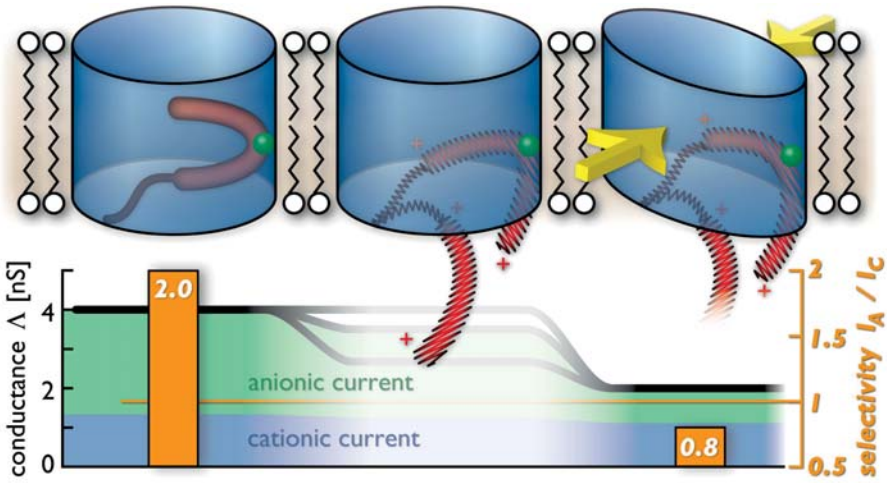

Figure 1.7: Gating as proposed in 2012. The gating process consists of the N-terminal α-helix detaching from the hydrophobic contact point and moving out of the barrel together with a partial collapse of the barrel, which is calculated to end up in a low-conducting, cation selective state. Reprinted from Zachariae *et al.* with kind permission from Elsevier.[91]

One of the most recent gating models, which seeks to comprise all available information was published in 2012 by this group and is shown in Figure 1.7.[91] The N-terminal α-helix as positively charged voltage sensor moves out of the barrel, in line with respective experimental results.[87,88] Upon this, the barrel partly collapses, explaining its lower diameter and volume in the closed state. The calculated loss of volume would be in the order of 10^4 Å^3. As mentioned above, this would, however, not completely explain the volume loss determined experimentally.[81] With these combined movements the barrel ends up in a state that is calculated to be slightly cation selective and to have a conductance of around 2 nS.

1.3.3.1 Physiological relevance of VDAC gating

The physiological relevance of the voltage gating of VDAC is still not fully understood. Because of the large permeability of the VDAC channel in both its open and closed state, it is often assumed that there cannot be a membrane potential large enough to induce closure of the channel under physiological conditions by voltage alone, which would render this special property of the channel biologically insignificant.[96] However, an electrochemical equilibrium of small ions does not necessarily mean that there is no potential across the OMM, as there are lots of charged proteins in the cytosol and the IMS, for which VDAC is not permeable. Additionally, measurements of the pH difference between

Dieses Werk ist copyrightgeschützt und darf in keiner Form vervielfältigt werden noch an Dritte weitergegeben werden.
Es gilt nur für den persönlichen Gebrauch.

the IMS and the cytosol showed that there could indeed be a transmembrane potential: two groups independently measured pH differences, that would – based on the Nernst equation – translate to potentials of ≈ 40 mV[97] or 20 to 30 mV[98], respectively. These values are exactly in the range in which VDAC switches from the open to the closed state. Thus a biological relevance of the voltage gating process of VDAC is well conceivable.

Even if the voltage gating process of VDAC is of no physiological relevance, it is still a fact that VDAC in its open state is permeable for ADP and ATP, while VDAC in its closed state is not.[99] Furthermore, it is known that VDAC interacts with many of the proteins and compounds available in the OMM and is also involved in many processes therein.[100] For example, tubulin is known to block VDAC channels by inserting its negatively charged tail into the channel in a way that is also seen during voltage gating (lower conductance, inversion of selectivity, impermeability for ATP).[101,102] Tubulin polymerizes under cellular activity, lowering the number of tubulin dimers and thus lowering the amount of VDAC blockage, which verifies the functional role of the VDAC-tubulin interaction in regulating mitochondrial respiration.[96,99] Additionally, VDAC interacts with HK-I, which induces closure of the channel[103] and many pro- and anti-apoptotic proteins, making VDAC a key protein in apoptosis.[100]

Dieses Werk ist copyrightgeschützt und darf in keiner Form vervielfältigt werden noch an Dritte weitergegeben werden.
Es gilt nur für den persönlichen Gebrauch.

1.4 Aims and Outline

Despite the efforts of over 40 years of research, a multitude of phenomenological results regarding the gating process of VDAC, and many gating models, the exact nature of the closed states (or even a single one of them) of the protein is still unknown. The aim of this thesis is to improve the existing models of the closed state of VDAC and to reach a level of information which might open the path to determining a high resolution 3D structure of the channel in its closed state.

The first part of the thesis deals with a further improvement of the assignment of the channel by the means of additionally recorded experiments such as TROSY-HNCACB and by further improving the sample preparation. This is connected with a new expression vector used for the preparation of the hVDAC1 samples. Also, the assignment of already existing and previously recorded experiments was improved dramatically, leading to an overall improvement of available information on the channel based on chemical shifts.

The second part of the thesis is based on the improved assignment of the first part. In collaboration with Mariusz Jaremko and Łukasz Jaremko, the improved assignment of a HMQC-NOESY spectrum was utilized to calculate a high resolution 3D structure of E73V hVDAC1.

The third and last part focusses on the development of a model for the closed state of VDAC. This is based on the construction of a Quintuple hVDAC1 mutant with unique gating properties. The spectral properties of this mutant are determined by NMR spectroscopy and BLM measurements are performed. A new position of the N-terminal helix was proven and probed by the means of liquid and solid state NMR spectroscopy.

Dieses Werk ist copyrightgeschützt und darf in keiner Form vervielfältigt werden noch an Dritte weitergegeben werden.
Es gilt nur für den persönlichen Gebrauch.

2 Materials & Methods

2.1 Materials

2.1.1 Chemical reagents

Lauryldimethylamine-*N*-oxide (LDAO) was purchased from Sigma-Aldrich and *S*-(1-oxyl-2,2,5,5-tetramethyl-2,5-dihydro-1H-pyrrol-3-yl)methyl methanesulfonothioate (MTSL) from Toronto Research Chemicals. ^{13}C-D-glucose (U-^{13}C6, 99 %) and $^{15}NH_4Cl$ (^{15}N, 99 %) were purchased from Cambridge Isotope Laboratories, Sigma-Aldrich or Cortecnet. Other chemicals were purchased from the usual suppliers and used without further purification. BenchMark^{TM} Protein Ladder was purchased from Invitrogen (now Thermo Fisher Scientific).

2.1.2 Bacterial strains

- *Escherichia coli* strain M15 [pRep4] (Qiagen, Hilden; phenotype: *E. coli* K12 NaI^S Str^S Rif^S Thi^- Lac^- Ara^+ Gal^+ Mtl^- F^- $RecA^+$ Uvr^+ Lon^+; carries pREP4 (*lacI* encoding repressor plasmid)) for pQE60 constructs.

- *Escherichia coli* strain BL21 [DE3] (Novagen, Merck Biosciences, Darmstadt, phenotype: *E. coli* E. coli str. B F^- ompT gal dcm lon hsdSB($r_B^-m_B^-$) λ(DE3 [lacI lacUV5-T7p07 ind1 sam7 nin5]) [$malB^+$]$_{K\text{-}12}$(λ^S)) for pET28a constructs.

Dieses Werk ist copyrightgeschützt und darf in keiner Form vervielfältigt werden noch an Dritte weitergegeben werden.
Es gilt nur für den persönlichen Gebrauch.

2.1.3 Growth media

Table 2.1: M9 minimal medium (standard/deuterated).

medium	substance	amount
M9 minimal medium	M9 salt (5x)*	200 mL
	Trace elements+	10 mL
	Thiamine HCl (5 mg/mL)	6 mL
	$CaCl_2$ (2 M)	0.05 mL
	$MgSO_4$ (1 M)	2 mL
	D-glucose or ^{13}C-D-glucose (20 % w/v)	20 mL
	$^{15}NH_4Cl$ (0.25 g/mL)	4 mL
	D_2O	758 mL
*) M9 salt (5x)	Na_2HPO_4	33.9 g
	KH_2PO_4	15 g
	NaCl	2.5 g
	D_2O	ad 1.0 L
+) Trace elements	$FeSO_4 \cdot 7H_2O$	0.6 g
	$MnCl_2 \cdot 4H_2O$	0.115 g
	$CoCl_2 \cdot 6H_2O$	0.08 g
	$ZnSO_4 \cdot 7H_2O$	0.07 g
	$CuCl_2 \cdot 2H_2O$	0.03 g
	H_3BO_3	0.002 g
	$(NH_4)_6Mo_7O_{24} \cdot 4H_2O$	0.025 g
	EDTA	0.5 g
	D_2O	ad 100 mL

Dieses Werk ist copyrightgeschützt und darf in keiner Form vervielfältigt werden noch an Dritte weitergegeben werden.
Es gilt nur für den persönlichen Gebrauch.

2.1.4 SDS page gels

Table 2.2: Resolving gel and stacking gel for SDS page.

gel	substance	amount
resolving gel 12 %	30 % Acrylamide	2.0 mL
	TrisHCl pH 8.8 (1 M)	1.88 mL
	H_2O (bidest.)	1.03 mL
	10 % SDS	50 µL
	10 % APS	50 µL
	TEMED	2.5 µL
stacking gel 3 %	30 % Acrylamide	250 µL
	TrisHCl pH 6.8 (1 M)	313 µL
	H_2O (bidest.)	1.88 mL
	10 % SDS	25 µL
	10 % APS	25 µL
	TEMED	2 µL

Dieses Werk ist copyrightgeschützt und darf in keiner Form vervielfältigt werden noch an Dritte weitergegeben werden.
Es gilt nur für den persönlichen Gebrauch.

2.2 Methods

2.2.1 Sample preparation of hVDAC1

Cloning, expression and purification of *wt* and mutant hVDAC1 with a C-terminal His_6-tag were performed as previously described in the doctoral theses of Thomas Meins[104], Monika Bayrhuber[64] and Saskia Villinger[74] by Stefan Becker and Karin Giller in the Department of NMR-based Structural Biology, Max Planck Institute for Biophysical Chemistry, Göttingen. Due to identical procedures, parts of the following chapters are identical to their theses and are marked accordingly. The preparation of hVDAC1 was done mostly as described previously.[49]

2.2.1.1 Cloning of hVDAC1[1]

The plasmid containing *wt* hVDAC1, cloned into pDS56/RBSII-6xHis vector via the *Bam*H1 and *Bgl*II restriction sites as described[49], was previously kindly provided by Thomas Meins (Max Planck Institute for Biochemistry, Martinsried). The PCR construct of *wt* hVDAC1 was amplified from this vector and ligated with the *Nco*I and *Bgl*II restriction sites in the pQE60 vector (Qiagen, Hilden). Cloning the pET28a construct of *wt* hVDAC1 was done by amplification from the pQE60 vector. For the following ligation the *Nco*I and *Xho*I restriction sites were used.

2.2.1.2 Site directed mutagenesis[1]

Point mutations into the cloned hVDAC1 coding sequence were introduced with the QuikChange Site-Directed Mutagenesis Kit (Agilent Technologies, Santa Clara), which was used essentially as recommended by Agilent. hVDAC1 mutants, vectors and primers used in this thesis are listed in Table 2.3. Successful mutagenesis was verified by DNA sequence analysis.

Table 2.3: Oligonucleotide primers for the mutagenesis of hVDAC1-His_6.

Mutation	Host	Vector	Primers (forward and reversed)
C127S	*wt*	b)	5′-CACATTAACCTGGGCTCCGACATGGATTTCGAC-3′ 3′-GTCGAAATCCATGTCGGAGCCCAGGTTAATGTG-5′
C127S/C232S	C127S	b)	5′-GACCCTGACGCCTCCTTCTCGGCTAAAGTG-3′ 3′-CACTTTAGCCGAGAAGGAGGCGTCAGGGTC-5′

[1] Due to identical procedures, parts of this section are identical to the thesis of Saskia Villinger[74]

Dieses Werk ist copyrightgeschützt und darf in keiner Form vervielfältigt werden noch an Dritte weitergegeben werden.
Es gilt nur für den persönlichen Gebrauch.

Mutation	Host	Vector	Primers (forward and reversed)
E73V	*wt*	b)	5′-CGGCCTGACGTTTACAGTGAAATGGAATACCGAC-3′ 3′-GTCGGTATTCCATTTCACTGTAAACGTCAGGCCG-5′
C127A/C232S	C127S/C232S	a)	5′-CACATTAACCTGGGCGCCGACATGGATTTCGAC-3′ 3′-GTCGAAATCCATGTCGGCGCCCAGGTTAATGTG-5′
C127A/C232A	C127A/C232S	a)	5′-GACCCTGACGCCGCCTTCTCGGCTAAAGTG-3′ 3′-CACTTTAGCCGAGAAGGCGGCGTCAGGGTC-5′
A14C/C127A/C232A	C127A/C232A	a)	5′-GCCGATCTTGGCAAATCTTGCAGGGATGTCTTCACCAAG-3′ 3′-CTTGGTGAAGACATCCCTGCAAGATTTGCCAAGATCGGC-5′
A14C/C127A/S193C/ C232A	A14C/C127A/C232A	a)	5′-GGGACAGAGTTTGGCGGCTGCATTTACCAGAAAGTGAAC-3′ 3′-GTTCACTTTCTGGTAAATGCAGCCGCCAAACTCTGTCCC-5′
E73V/C127A/C232S	C127A/C232S	c)	5′-CGGCCTGACGTTTACAGTGAAATGGAATACCGAC-3′ 3′-GTCGGTATTCCATTTCACTGTAAACGTCAGGCCG-5′
G21V	*wt*	c)	5′-GCCAGGGATGTCTTCACCAAGGTCTATGGATTTGGCTTAATAAAG-3′ 3′-CTTTATTAAGCCAAATCCATAGACCTTGGTGAAGACATCCCTGGC-5′
G21V/G23V	G21V	c)	5′-GATGTCTTCACCAAGGGCTATGTATTTGGCTTAATAAAGCTTG-3′ 3′-CAAGCTTTATTAAGCCAAATACATAGCCCTTGGTGAAGACATC-5′
G21V/E73V/C127A/ C232S	E73V/C127A/C232S	c)	5′-GCCAGGGATGTCTTCACCAAGGTCTATGGATTTGGCTTAATAAAG-3′ 3′-CTTTATTAAGCCAAATCCATAGACCTTGGTGAAGACATCCCTGGC-5′
G21V/G23V/E73V/ C127A/C232S	G21V/E73V/C127A/ C232S	c)	5′-GATGTCTTCACCAAGGGCTATGTATTTGGCTTAATAAAGCTTG-3′ 3′-CAAGCTTTATTAAGCCAAATACATAGCCCTTGGTGAAGACATC-5′
A2C/G21V/G23V/ E73V/C127A/C232S	G21V/G23V/E73V/ C127A/C232S	c)	5′-GAAGGAGATATACCATGTGTGTGCCACCCACGTATGCCG-3′ 3′-CGGCATACGTGGGTGGCACACACATGGTATATCTCCTTC-5′
A2C/E73V/C127A/ C232S	E73V/C127A/C232S	c)	5′-GAAGGAGATATACCATGTGTGTGCCACCCACGTATGCCG-3′ 3′-CGGCATACGTGGGTGGCACACACATGGTATATCTCCTTC-5′

Vectors: a) pDS56/RBSII, b) pQE60, c) pET28a

2.2.1.3 Expression of ^{2}H, ^{13}C and ^{15}N labelled hVDAC1[1]

Following transformation into *Escherichia coli* M15 [pRep4] (for pQE60 constructs) or *Escherichia coli* BL21 [DE3] (for pET28a constructs), respectively, cells were grown at 37 °C over night in M9 minimal medium containing 100 µg/mL amipicillin and 25 µg/mL kanamycin. According to the desired labelling (^{2}H(75 %)/^{13}C/^{15}N, ^{2}H(99 %)/^{13}C/^{15}N or ^{2}H(75 %)/^{15}N), glucose and NH_4Cl in the M9 minimal medium (Table 2.1) were replaced with protonated or deuterated ^{13}C-D-glucose and/or $^{15}NH_4Cl$. In order to adapt the culture to D_2O based media the cells were consecutively inoculated into M9 medium with a D_2O content of 33, 65 and 100 % and incubated at 37 °C for 24 h at each step. The fully adapted cell culture was used for inoculation of 1.5 L expression cultures with an initial OD_{600} of 0.1 AU. The culture was allowed to grow at 37 °C, until an OD_{600} of 0.8 AU was reached. Subsequently, hVDAC1-His_6 expression into inclusion bodies was induced with 1 mM IPTG. Cells were harvested 8 to 14 h (depending on the mutant) after induction by centrifugation at 5,000 g for 30 min, shock frozen in liquid N_2 and stored at -70 °C.

[1] Due to identical procedures, parts of this section are identical to the thesis of Saskia Villinger[74]

Dieses Werk ist copyrightgeschützt und darf in keiner Form vervielfältigt werden noch an Dritte weitergegeben werden.
Es gilt nur für den persönlichen Gebrauch.

2.2.1.4 Refolding and purification of hVDAC1[1]

Frozen cells were thawed, resuspended in buffer 1 (100 mM Tris/HCl pH 7.5; 1 mM EDTA; 5 mM DTT, 10 mM NaCl, 0.2 mM PMSF), and incubated with 0.1 mg/mL lysozyme for 30 min. Following lysozyme treatment, 1 mM $MgCl_2$, 0.1 mM $MnCl_2$, and 0.05 mg/mL DNAse I were added and the cells were lysed by the French press passes. Inclusion bodies were harvested by centrifugation at 5,000 g for 30 min at 4 °C at 20,000 psi. The pellet was resuspended in buffer 1 containing 3 % (w/v) OPOE, stirred for 3 h at room temperature and pelleted by centrifugation at 5,000 g for 30 min at 4 °C. Finally, the pellet was washed with buffer 1 to remove detergent contaminations. Inclusion bodies were solubilized in buffer 2 (100 mM Tris/HCl pH 7.5; 1 mM EDTAm 5 mM DTT, 6 M guanidinium chloride) and insoluble material was removed by centrifugation at 100,000 g for 45 min. The denatured hVDAC1-His_6 protein containing supernatant was adjusted with buffer 2 to 15 mg/mL and stored at -70 °C until use.

Refolding was performed at 4 °C by dropwise dilution of solubilized protein in buffer 3 (100 mM Tris/HCl pH 8.0; 1 mM EDTA; 5 mM DTT, 1 % (w/v) LDAO) until a final concentration of 0.6 M guanidinium chloride was reached. The resulting protein solution was stirred over night at 4 °C, centrifuged at 100,000 g for 45 min and finally 5-fold diluted with buffer 4 (100 mM phosphate buffer ph 7.5).

Refolded hVDAC1-His_6 was purified by immobilized metal ion affinity chromatography (IMAC). For this purpose, hVDAC1 was bound to a 5 mL Ni_2^+-Sepharose HP Column (GE Healthcare, Chalfont St Giles), washed with 100 mL buffer 5 (20 mM phosphate buffer ph 7.5; 20 mM imidazole; 0.2 % LDAO), and afterwards eluted by 50 mL buffer 6 (20 mM phosphate buffer pH 7.5, 300 mM imidazole; 0.2 % LDAO). hVDAC1 containing fractions (as judged by SDS-PAGE), were pooled. Improved sample purification was reached by an additional gel filtration step that was applied to all new mutants described in this thesis. For this purpose, the pooled hVDAC1 fractions obtained from Ni_2^+ affinity chromatography were concentrated and applied to a Superdex 200 16/60 column (GE Healthcare, Chalfont St Giles) equilibrated with buffer 7 (25 mM BisTris pH 6.8, 150 mM NaCl, 0.2 % LDAO). Eluted hVDAC1 fractions were pooled and the protein concentration was

[1] Due to identical procedures, parts of this section are identical to the thesis of Saskia Villinger[74]

Dieses Werk ist copyrightgeschützt und darf in keiner Form vervielfältigt werden noch an Dritte weitergegeben werden.
Es gilt nur für den persönlichen Gebrauch.

measured by UV absorption at 280 nm wavelength using the theoretical extinction coefficient of 38,390 M^{-1} cm^{-1}. LDAO was added to the pooled fractions in order to adjust the final concentration of a 0.6 mM hVDAC1 sample to a theoretical LDAO content of 6 % (w/v), assuming that no detergent is lost during further purification steps. After LDAO addition, the sample was dialysed against NMR buffer (25 mM BisTris/HCl pH 6.8, 0.2 % LDAO) for 4 h and concentrated with a centrifugal filter device (Amicon Ultra-30 k, Millipore) to a protein concentration of 0.4-1 mM (for pQE60 samples) or 0.15-0.4 mM (for pET28a samples), respectively. By comparison with a sample of known LDAO concentration 1D ^{1}H NMR spectroscopy revealed typical LDAO concentrations of 2-4 % (for pQE60 samples) or 1-2 % (for pET28a samples), respectively, in the final samples.

2.2.2 Spin labelling[1]

A2C/E73V/C127A/C232S hVDAC1 and A2C/G21V/G23V/E73V/C127A/C232S hVDAC1 were modified with the thiol-specific nitroxide spin label reagent MTSL. 100 µg/µL MTSL in cold acetone were added to the protein solution in a three- to five-fold molar excess prior to the refolding step and the solution was incubated for 1.5 h at room temperature. Afterwards, refolding and purification were performed as described in Chapter 2.2.1.4.

2.2.3 NMR spectroscopy

NMR spectra were recorded on ^{2}H(75 %)/^{15}N or ^{2}H(75 %)/^{13}C/^{15}N labeled samples containing 0.15–0.6 mM hVDAC1 (or the respective hVDAC1 mutant), 25 mM BisTris pH 6.8, 1–2 % (45–90 mM) LDAO and usually 10 % D_2O. Unless stated otherwise, all spectra were measured at 37 °C on Bruker 700, 800, 900 or 950 MHz Avance I, Avance III or Avance III HD spectrometers equipped with cryogenic probes. Recorded spectra were processed using NMRPipe[105] and analyzed using TopSpin[106], SPARKY[107] or CcpNmr Analysis[108].

[1] Due to identical procedures, parts of this section are identical to the thesis of Saskia Villinger[74]

Dieses Werk ist copyrightgeschützt und darf in keiner Form vervielfältigt werden noch an Dritte weitergegeben werden.
Es gilt nur für den persönlichen Gebrauch.

2.2.3.1 Assignment improvement and assignment of hVDAC1 mutants

For the improvement of the backbone resonance assignment reported earlier[64,74], a TROSY-HNCACB experiment[109,110] was recorded on E73V/C127A/C232S hVDAC1 (for the pulse program see Appendix A.1). A mixed-time parallel evolution HMQC-NOESY spectrum[111] on E73V hVDAC1 was used to further improve the inter-strand and sequential H_N-H_N NOEs. To assign the various hVDAC1 mutants described in this thesis, ^{1}H-^{15}N-TROSY spectra[112], TROSY-HNCACB spectra and HMQC-NOESY spectra were used. Furthermore, as previously, existing N_H and C_α shifts from solid state NMR experiments were taken into account.[113] All 3D spectra used in the thesis are listed in table 2.4.

Table 2.4: Experiments and parameters for hVDAC1 assignment improvement and assignment of hVDAC1 mutants.

Sample	Spectrum	Parameters	Comments
^{2}H(75 %)/^{13}C/^{15}N-E73V hVDAC1-pDS56/RBSII	TROSY-HNCA*	35×26×512 pts; ns = 72; 900 MHz	linear prediction in ^{13}C and ^{15}N dimensions
	^{15}N-NOESY-HMQC*	85×25×512 pts; ns = 26; 800 MHz mt = 240 ms	
^{2}H(75 %)/^{13}C/^{15}N-A14C/ C127A/S193C/C232A hVDAC1-pQE60	TROSY-HNCA	35×26×512 pts; ns = 92; 900 MHz	linear prediction in ^{13}C and ^{15}N dimensions
^{2}H(75 %)/^{13}C/^{15}N-E73V/ C127A/C232S hVDAC1-pET28a	TROSY-HNCACB	35×26×512 pts; ns = 52; 800 MHz	
^{2}H(75 %)/^{13}C/^{15}N-G21V/ G23V/E73V/C127A/C232S hVDAC1-pET28a	TROSY-HNCACB	35×22×512 pts; ns = 112; 950 MHz	
	^{15}N-NOESY-HMQC	85×25×512 pts; ns = 34; 800 MHz mt = 240 ms	
	TROSY-HNCO	29×26×512 pts; ns = 76 700 MHz	

Dieses Werk ist copyrightgeschützt und darf in keiner Form vervielfältigt werden noch an Dritte weitergegeben werden.
Es gilt nur für den persönlichen Gebrauch.

Sample	Spectrum	Parameters	Comments
^{2}H(75 %)/^{13}C/^{15}N-A2C/ E73V/C127A/C232S hVDAC1-pET28a + MTSL	TROSY-HNCACB	50×34×512 pts; ns = 72; 800 MHz	

* recorded by Saskia Villinger

Spectroscopic parameters are given as number of complex points in F1, F2 and F3, number of scans, field strength for ^{1}H and mixing time

2.2.3.2 Estimation of T_2 and the global correlation time τ_c

To estimate the overall transverse relaxation time of the protein, 1D ^{1}H (1–1) echo experiments were recorded.[114] Relaxation delays of 110, 1000, 2000 and 3000 µs were used for G21V/G23V hVDAC1. Transverse relaxation times T_2 were estimated from two values following the formula:

$$T_2 = \frac{2(\Delta_1 - \Delta_2)}{\ln(I_1/I_2)} \tag{2.1}$$

With Δ_1 and Δ_2 being the relaxation delays of the two points and I_1 and I_2 being the maximum signal intensities at a certain chemical shift at these two relaxation delays.

The overall rotational correlation time τ_c was then estimated as:

$$\tau_c \approx \frac{1}{5 \cdot \frac{T_2}{[ms]}} \cdot [\mu s] \tag{2.2}$$

2.2.3.3 Determination of chemical shift differences

To assess the effects of mutations on hVDAC1, ^{1}H-^{15}N-TROSY spectra were recorded in order to follow ^{1}H and ^{15}N chemical shift changes. If resonances of residues in spatial proximity to mutation sites could only be ambiguously assigned, they were excluded from the analysis. Normalized weighted average chemical shift differences (CSD), Δ_{HN}, were calculated as:

$$\Delta_{HN} = \sqrt{\frac{(\Delta\delta_N/5)^2 + (\Delta\delta_H)^2}{2}} \tag{2.3}$$

Dieses Werk ist copyrightgeschützt und darf in keiner Form vervielfältigt werden noch an Dritte weitergegeben werden.
Es gilt nur für den persönlichen Gebrauch.

where $\Delta\delta_N$ and $\Delta\delta_H$ are the chemical shift differences for the ^{15}N and ^{1}H dimensions, respectively. Errors in CSD were estimated as described in the PhD thesis of Saskia Villinger[74] and are given as average values: 0.014 ppm for ^{15}N CSD and 0.0028 ppm for the average CSD.

If CSD values were mapped to a 3D structure of VDAC1, they were mapped to the crystal structure of mVDAC1 (PDB ID: 3EMN)[46] or the new E73V hVDAC1 solution structure (PDB ID: 5JDP)[115] and visualized with PyMOL[71].

2.2.3.4 Determination of intensity changes

To follow the effects of MTSL labeling experiments, intensities were determined as absolute peak heights in the recorded ^{1}H-^{15}N-TROSY spectra. If resonances of residues in spatial proximity to mutation sites or the MTSL label, respectively, could only be ambiguously assigned, they were excluded from the analysis. Intensity ratios $I_{labeled}/I_{ref}$ were scaled according to resonances that were unaffected from the labeling and possible CSD effects.

Errors in resonance intensity ratios were calculated by error propagation using the root mean square noise of the respective spectra.

If intensity ratios were mapped to a 3D structure of VDAC1, they were mapped to the crystal structure of mVDAC1 (PDB ID: 3EMN)[46] or the new E73V hVDAC1 solution structure (PDB ID: 5JDP)[115] and visualized with PyMOL[71].

2.2.3.5 Relaxation data experiments

The recording and analysis of ^{15}N relaxation data is part of recent joint publication[115] and is therefore in big parts reproduced from the Supporting Information of that publication.

The TROSY-based pulse sequence for measurement of ^{15}N-R_2 relaxation rates was adapted from the original $R_{1\rho}$ pulse program[116] with an appropiate CPMG block introduced. (See Figure 2.1.) The sequence was tested on ^{15}N-labelled ubiquitin and yielded within the experimental accuracy the same ^{15}N-R_2 rates as determined with HSQC-based schemes (data not shown).[117,118] ^{15}N-R_1 rates were measured using the published TROSY-based pulse sequence (see Figure 2.1).[116] ^{15}N-R_1 and ^{15}N-R_2 relaxation experiments were recorded on 600 and 700 MHz Bruker Avance III and

Dieses Werk ist copyrightgeschützt und darf in keiner Form vervielfältigt werden noch an Dritte weitergegeben werden.
Es gilt nur für den persönlichen Gebrauch.

900 MHz Bruker Avance I spectrometers equipped with cryogenic probes. For all measurements the temperature was carefully adjusted to 37 °C using a standard sample or ethylene glycol. To achieve nearly complete signal recovery between experiments, the recycle delay was set to 5 s.

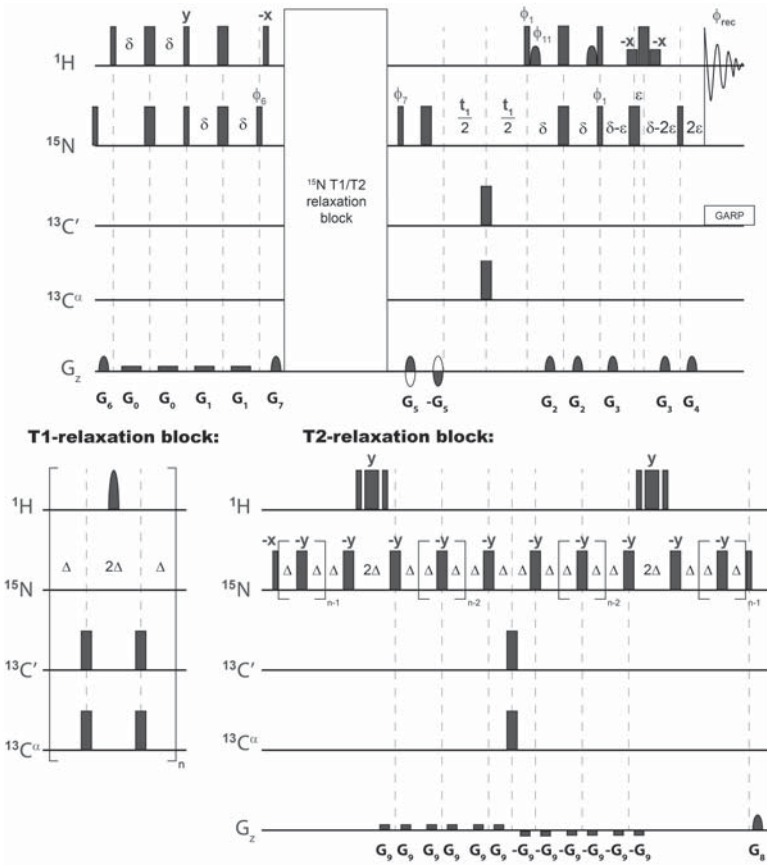

Figure 2.1: TROSY-based NMR pulse sequences for measurement of ^{15}N-R_1 and ^{15}N-R_2 relaxation rates in high-molecular weight proteins. For each experiment the appropiate temperature compensation block (T-comp) was used (not shown in the scheme for clarity). Narrow and wide rectangles correspond to 90° and 180° flip angle pulses, respectively. The lower amplitude pulses marked -x are 90° pulses with low power, shaped pulses with low amplitude are shaped pulses, all of these pulses are serving as water flip-back pulses.[119] Delay durations are δ = 2.65 ms and $\varepsilon = G_4$. Gradients are G_0 (2.65 ms, 2.1 G/cm), G_1 (2.65 ms, 1.4 G/cm), G_2 (300 μs, 7 G/cm), G_3 (1 ms, 35 G/cm) and G_9 (Δ, 0.3 G/cm) with rectangular shape and G_4 (60.8 μs, 23 G/cm), G_5 (300 μ, -23 G/cm), G_6 (1 ms, 19.6 G/cm), G_7 (200 μs, -35 G/cm) and G_8 (200 μs, 28 G/cm) with sine-bell shape. Phase cycling is done following the scheme ϕ_6 = 4(y),4(-y); ϕ_7 = y,x,-y,-x; ϕ_1 = y; ϕ_{rec} = y,-x,-y,x,-y,x,y,-x. Quadrature detection was implemented by using the Rance-Kay echo/anti-echo scheme[120] with the polarity of the gradients G_5 and -G_5 inverted, and phase ϕ_7 = y,-x,-y,x and ϕ_1 = -y for the second FID generated for each quadrature pair. (As described by Lakomek *et al.*[116]) The 180° pulse on ^{1}H in the middle of the T_1-relaxation block is a IBURP2 type pulse with a duration of 2 ms at 600 MHz. Δ in the T_2-relaxation block was set to 1.0 ms.

Dieses Werk ist copyrightgeschützt und darf in keiner Form vervielfältigt werden noch an Dritte weitergegeben werden.
Es gilt nur für den persönlichen Gebrauch.

2.2.3.6 Relaxation data analysis

The Relaxation rates were obtained by 2-parameter non-linear mono-exponential fits of the obtained signal intensities over the applied relaxation delays using the MacDonald algorithm.[121] Errors were determined from the variance covariance matrices. Only non-overlapping signals from the 2D ^{1}H-^{15}N TROSY experiments were selected for further analysis resulting in 179 R_2/R_1 pairs at each magnetic field.

In the formulation of model-free approaches (MFA), spectral density functions describe the overall tumbling as isotropic with a correlation time τ_R. Because even small degrees of motional anisotropy influence relaxation rates, reorientational anisotropy has to be taken into account to avoid determination of false parameters of internal motion. To this end, model-free approach spectral density functions are combined with a spectral density function, which describes anisotropic molecular tumbling. The latter comprises five terms and is given as:[122]

$$J(\omega) = \sum_{i=1}^{5} A_i \frac{\tau_i}{1+(\omega\tau_i)^2} \tag{2.4}$$

The correlation times τ_i are expressed by the principal components, D_k, of the rotational diffusion tensor according to $\tau_1 = (4D_1+D_2+D_3)^{-1}$, $\tau_2 = (D_1+4D_2+D_3)^{-1}$, $\tau_3 = (D_1+D_2+4D_3)^{-1}$, $\tau_4 = 6[D+(D^2-L^2)^{1/2}]^{-1}$ and $\tau_5 = 6[D+(D^2-L^2)^{1/2}]^{-1}$ where $D = (D_1+D_2+D_3)/3$ and $L^2 = (D_1D_2+D_2D_3+D_3D_1)/3$. A useful way of representing the diffusion tensor is to calculate the overall rotational correlation time τ_c, the anisotropy A and the rhombicity η according to:

$$\begin{aligned}
\tau_c &= 1/[2(D_x+D_y+D_z)] \\
A &= 2D_z/(D_x+D_y) \\
\eta &= 1.5(D_y-D_x)[D_z-0.5(D_y+D_x)]
\end{aligned}$$

with $D_x \leq D_y \leq D_z$. Directional factors A_i describe the orientation of the relaxation vector in the molecule-fixed coordinate system in terms of the directional cosines l, m and n: $A_1 = 3m^2n^2$, $A_2 = 3l^2n^2$, $A_3 = 3m^2l^2$, $A_4 = (d-e)/2$ and $A_5 = (d+e)/2$ where $d = 0.5[3(l^4+m^4+n^4)-1]$,

Dieses Werk ist copyrightgeschützt und darf in keiner Form vervielfältigt werden noch an Dritte weitergegeben werden.
Es gilt nur für den persönlichen Gebrauch.

$e = [\delta_1(3l^4+6m^2n^2-1)+\delta_2(3m^4+6l^2n^2-1)+\delta_3(3n^4+6l^2m^2-1)]/6$ and $\delta_i = (D_i-D)/(D^2-L^2)^{1/2}$.

A_i is normalized according to $A_1+A_2+A_3+A_4+A_5 = 1$. The model-free spectral density function of an anisotropically tumbling molecule according to the formalism by Lipari and Szabo[123,124] can thus be rewritten as

$$J^{MFA}(\omega) = \frac{2}{5}\sum_{i=1}^{5} A_i \left[\frac{S^2\tau_i}{1+(\omega\tau_i)^2} + \frac{(1-S^2)\tau_{\mathrm{int},i}}{1+(\omega\tau_{\mathrm{int},i})^2}\right] \tag{2.5}$$

where $1/\tau_{\mathrm{int},i} = 1/\tau_i + 1/\tau_{\mathrm{int}}$.

The spectral density function for the extended model-free approach (EMFA) of an anisotropically tumbling molecule is then (assuming the existence of an additional slow motion, with the order parameter S_s^2 and its internal time $\tau_{\mathrm{int},s}$ being outside the extreme narrowing limit and slower than S_f^2 but faster than molecular tumbling):

$$J^{EMFA}(\omega) = \frac{2}{5}\sum_{i=1}^{5} A_i \left[\frac{S_f^2 S_s^2\tau_i}{1+(\omega\tau_i)^2} + \frac{(1-S_{f,i}^2)\tau_{f,i}}{1+(\omega\tau_{f,i})^2} + \frac{S_f^2(1-S_{s,i}^2)\tau_{s,i}}{1+(\omega\tau_{s,i})^2}\right] \tag{2.6}$$

where $1/\tau_{k,i} = 1/\tau_i + 1/\tau_k$. The indices f and s correspond to fast and slow internal motions, respectively.

The experimental ^{15}N-R_1 and ^{15}N-R_2 rates of E73V hVDAC1 from three magnetic fields (proton frequency of 600, 700 and 900 MHz) were fitted according to a 2-parameter MFA with the order parameter S^2 and the time scale for internal motions τ_{int} as a model of internal motion. To this end, a grid search was performed, searching for the minimum in the global target function χ, which is given by the weighted sum of squared residuals:

$$\chi = \sum_{i=1}^{N}\Gamma_i = \sum_{i=1}^{N}\sum_{j=1}^{M}[(P_{ij,exp}-P_{ij,calc})^2/\sigma_{ij}^2] \tag{2.7}$$

where the sum is over M relaxation data for each of the N residues of E73V hVDAC1, and $P_{ij,calc}$ are the appropriate relaxation parameters calculated from the assumed model of internal motion. σ_{ij} are the standard deviations of the experimentally derived $P_{ij,exp}$. The global target function consists

Dieses Werk ist copyrightgeschützt und darf in keiner Form vervielfältigt werden noch an Dritte weitergegeben werden.
Es gilt nur für den persönlichen Gebrauch.

of the sum of partial target function Γ_i, which characterize the fit quality for the i-th residue.[125] The simple 2-parameter MFA analysis fully reproduced the experimental input. The finding that the 2-parameter model is sufficient for description of the ps–ns time scale dynamics of E73V hVDAC1 is in agreement with the magnetic field dependence of the ^{15}N-R_2 rates for each individual residue.

2.2.3.7 Structure calculation and refinement

Structure determination of E73V hVDAC1 was performed in two steps using the Xplor-NIH software platform[126]. First, an initial set of conformations was obtained by folding the extended polypeptide chain against backbone torsion angles and side-chain anglex χ_1 restraints, which were estimated by TALOS-N[127] on the basis of the experimental chemical shifts, together with distance restraints from a 3D ^{15}N-edited HMQC-NOESY experiment, as well as hydrogen bond restraints that were verified by H/D exchange experiments. Subsequently the lowest-energy structures were taken for further refinement.

In this second step, the diffusion tensor parameters τ_c, A and η were used as input in Xplor-NIH for structure refinement against the experimental ^{15}N-R_2/R_1 rates.[126,128–131] We determined initial values for τ_c, A and η through the model-free approach described above. This requires the coordinates of the protein. We used the X-ray structure of mVDAC1 (PDB ID: 3EMN)[46] for that purpose. The resulting tensor parameters were used for refinement of the 3D structure of E73V hVDAC1 yielded in the first step against 124 R_2/R_1 ratios in Xplor-NIH. During this refinement step also multidimensional torsion angle data base potentials (torsionDB[130]) and backbone H-bond data base potentials (HBDB[131]) were used. The calculated ensemble of lowest energy conformations was well converged. Next, the lowest energy conformer was selected, the directional cosines were recalculated, and the experimental relaxation rates were again fitted with the 2-parameter MFA model. This resulted in similar tensor parameters. The refined set of tensor parameters was again used for structure calculation and yielded virtually the same coordinates.

Dieses Werk ist copyrightgeschützt und darf in keiner Form vervielfältigt werden noch an Dritte weitergegeben werden.
Es gilt nur für den persönlichen Gebrauch.

2.2.4 BLM measurements

Bilayer measurements on various hVDAC1 mutants were performed by Roland Benz (Department of Life Sciences and Chemistry, Jacobs-University gGmbH, Bremen) based on a long-standing collaboration. The measurements in the planar phospholipid bilayer membranes were generally performed as described.[24] 5 µL of a solution of 1 % DiPhPC in n-decane were painted over the hole (area ≈ 0.4 mm^2) of a Teflon cuvette, creating lipid bilayers of the Mueller-Rudin type.[30] A solution of 1 M KCl, 10 mM HEPES, pH 6.0 was used as electrolyte. hVDAC1 mutants in LDAO were diluted with 1 % (w/v) Genapol to a final concentration of approximately 5 µM and mixed 1:1 with cholesterol powder suspended in 1 % (w/v) Genapol. Aliquots of VDAC (typically 1–5 µL) were added to both cuvette chambers at a standard membrane potential of 20 mV. The insertion of single channels was monitored by the increase of the current measured with the Ag/AgCl electrodes and an in-house amplifier.

Measurements with variable potentials were performed by equilibrating the system for 1–2 hours until no significant increase in current (tantamount to no further channel insertions) was observed anymore. The steady-state voltage-dependent closure of the channels was measured by increasing the potential in steps of $\pm$ 10 mV and calculating the ratio of the final (i.e. after closure) and initial (i.e. before closure) conductance at each applied voltage step.

2.2.5 Calculation of PRE effect differences

Due to the noise influenced results yielded from the PRE experiments of Quintuple hVDAC1 and A2C-Quintuple hVDAC1, respectively, the intensity changes induced due to the MTSL labeling were enhanced the following way:

For each mutant pair (A2C-Quintuple & Quintuple hVDAC1 and A2C/E73V/C127A/C232S & E73V/C127A/C232S hVDAC1), the intensity ratios I(Quint) and I(wt) were calculated for each residue. Based on residues which didn't show broadening due to the attached MTSL label, these ratios were normalized to 1. The difference in the intensity ratios was then calculated for each residue as $\Delta(I)_i = I(\text{Quint})_i - I(\text{wt})_i$.

Dieses Werk ist copyrightgeschützt und darf in keiner Form vervielfältigt werden noch an Dritte weitergegeben werden.
Es gilt nur für den persönlichen Gebrauch.

The differences of the intensity ratios were pooled in groups of five residues and normalized:

$$\Delta(\text{I,grouped})_j = \frac{\sum_{i=5j-4}^{5j} \Delta(I)_i}{5} \tag{2.8}$$

To further reduce the effects of the noise in the data, a binomial filter was applied to the floating average of three of these grouped intensity ratio differences:

$$\Delta(\text{I,filtered})_n = \frac{\Delta(\text{I,grouped})_{n-1} + 2 \cdot \Delta(\text{I,grouped})_n + \Delta(\text{I,grouped})_{n+1}}{4} \tag{2.9}$$

After all, these Δ(I,filtered) values were plotted as function of the n-th five residue group. (See Chapter 3.4.4.)

Dieses Werk ist copyrightgeschützt und darf in keiner Form vervielfältigt werden noch an Dritte weitergegeben werden.
Es gilt nur für den persönlichen Gebrauch.

3 Results

3.1 Improving the assignment of hVDAC1

VDAC backbone resonance assignment has been a challenge over the years. In 2007, 70/90 % (overall/barrel) of the backbone amide resonances of *wt* hVDAC1 were reported to be assigned in micellar solution by Monika Bayrhuber.[64,70] With the help of further experiments and due to improved sample quality, this could be increased to 85/93 % and 88/97 % (overall/barrel) for *wt* hVDAC1 and E73V hVDAC1, respectively, by Saskia Villinger. [74,132] This improvement was also made possible by chemical shift information obtained from solid-state NMR data, which delivered the necessary information to assign three residues in the N-terminal α-helix (Lysine-12, Glutamate-16 and Valine-17).[113]

In this work, the existing assignments were reviewed completely and – supported by additional recorded spectra – improved, leading to C_β shifts, improved backbone assignment (see Chapter 3.1.2), and a multitude of newly assigned H_N-H_N NOE contacts (see Chapter 3.1.3) that were used in the calculation of a 3D structure of E73V hVDAC1 (see Chapter 3.2).

3.1.1 Additional C_β shifts

In previous studies in this working group, even in fully ^{13}C labelled samples C_β resonance assignments for hVDAC1 in LDAO micelles were missing and have never been reported. Thus only the C_α resonances were available to obtain sequential information to assign the backbone resonances of the protein.[64,74] At the same time, C_β assignments were reported in the literature for samples in liquid state (hVDAC1 reconstituted in LDAO micelles)[48] as well as in solid state (hVDAC1 in

Dieses Werk ist copyrightgeschützt und darf in keiner Form vervielfältigt werden noch an Dritte weitergegeben werden.
Es gilt nur für den persönlichen Gebrauch.

DMPC liposomes).[113] Hence, it is not the protein itself which makes it generally impossible to obtain C_β shifts. It could only possibly be the complete system consisting of buffer, micelle and protein which for some reason prevents the detection of C_β resonances. If this is not the case, with the right technical approach the determination of C_β shifts should be possible.

Indeed it was found, that using a E73V/C127A/C232S hVDAC1 mutant and a slightly modified version of the standard Bruker pulse program (i.a. a shorter ^{1}H-^{15}N-INEPT delay, 1.75 ms instead of 2.3 ms (which corresponds to $1/(4J_{NH})$)), recording a 3D TROSY-HNCACB[109,110] was possible in 2 days and 14 hours with excellent results. The pulse program used can be found in Appendix A.1.

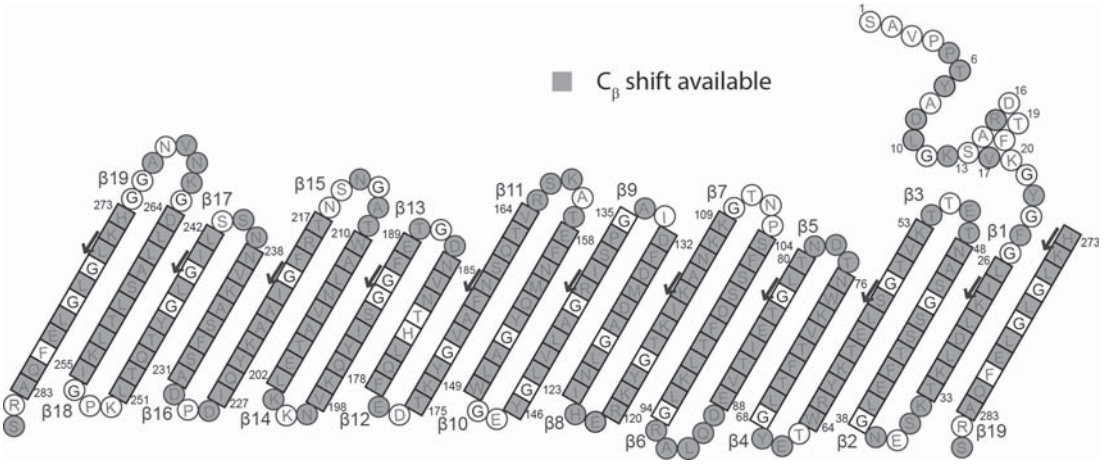

Figure 3.1: Map of the existing C_β assignments in E73V/C127A/C232S hVDAC1. Residues with available C_β shift are colored in gray, Glycine residues are lettered in black. Residues in β-strands are boxed, residues in the loops and the N-terminal α-helix are circled. The topology map was adopted and modified from previous works.[46,74]

The newly acquired HNCACB data helped to verify the existing backbone assignments. Indeed, the known assignments could be confirmed nearly completely. (See Chapter 3.1.2 for details) The current state of the assignment comprises 87.4 % of the existing C_β in the complete protein and 98.3 % in the barrel, respectively (values given for E73V/C127A/C232S hVDAC1). (See Figure 3.1) In the barrel, only Histidine-181, Threonine-182 and Phenylalanine-281 are unassigned and missing.

In the case of Histidine-181, the missing assignment is caused by the low signal strength of the corresponding HNCACB peaks that made it impossible to find the correct resonances. Threonine-182 is

Dieses Werk ist copyrightgeschützt und darf in keiner Form vervielfältigt werden noch an Dritte weitergegeben werden.
Es gilt nur für den persönlichen Gebrauch.

missing completely in all spectra and the existing assignment of Phenylalanine-281 for *wt* hVDAC1 actually has a possible equivalent in the E73V/C127A/C232S hVDAC1 spectra, but the corresponding HNCACB peaks do not fit to the previously reported values.[74]

In comparison to the assignment statistics reported by Hiller *et al.*[48], 221 instead of 194 existing C_β are assigned. In particular, the assignment in the second part of the N-terminal helix and the assignments around Glutamate-73 or Valine-73, respectively, were drastically improved. Also, in most of the loops more residues are assigned now than reported by them.

3.1.2 Improved backbone assignment

In previous works in this group, great effort had already been put into the creation and improvement of the backbone assignment of hVDAC1. β-barrel membrane proteins can be characterized relatively well by NMR and it is the helical membrane proteins that require more effort[133]. However, still there are regions of hVDAC1 that proved to be notoriously difficult to assign. Most prominent are the region around Glutamate-73 and the N-terminal helix. In the former, in the case of *wt* hVDAC1 severe peak broadening is caused by chemical exchange[132], which can be "solved" by the E73V mutation, making seven more residues in the β-strands 4 and 5 detectable (Threonine-72 to Tryptophan-75 and Glycine-82 to Glutamate-85). In the latter, the backbone assignment was improved with chemical shift information from solid-state NMR data.[74] Furthermore, also the region around Threonine-182 as well as all loops between the β-strands exhibit broadened peaks. For the loops this is obviously due to their increased conformational flexibility. In particular, loops with a Proline (loop from β-strand 6 to β-strand 7, β-strand 15 to β-strand 16 and β-strand 17 to β-strand 18) are problematic in terms of assignment, as Prolines are missing the amide proton and thus always induce breaks in the sequential connectivity.

In detail, for assignment of hVDAC1 several triple-resonance experiments were recorded (TROSY-HNCA, TROSY-HN(CO)CA, TROSY-HNCO), labeling with MTSL at various places to yield PRE data and amino acid selective labeling were done.[64] The assignment was improved with the help of triple-resonance experiments on E73V hVDAC1 (TROSY-HNCA and ^{15}N-NOESY-HMQC).[74] Since these developments took place over the course of 10 years it is not anticipated that the assign-

Dieses Werk ist copyrightgeschützt und darf in keiner Form vervielfältigt werden noch an Dritte weitergegeben werden.
Es gilt nur für den persönlichen Gebrauch.

ment will be improved drastically in the future. Nevertheless, especially with the help of the newly recorded TROSY-HNCACB spectral data further improvement of the assignment was achieved in this work.

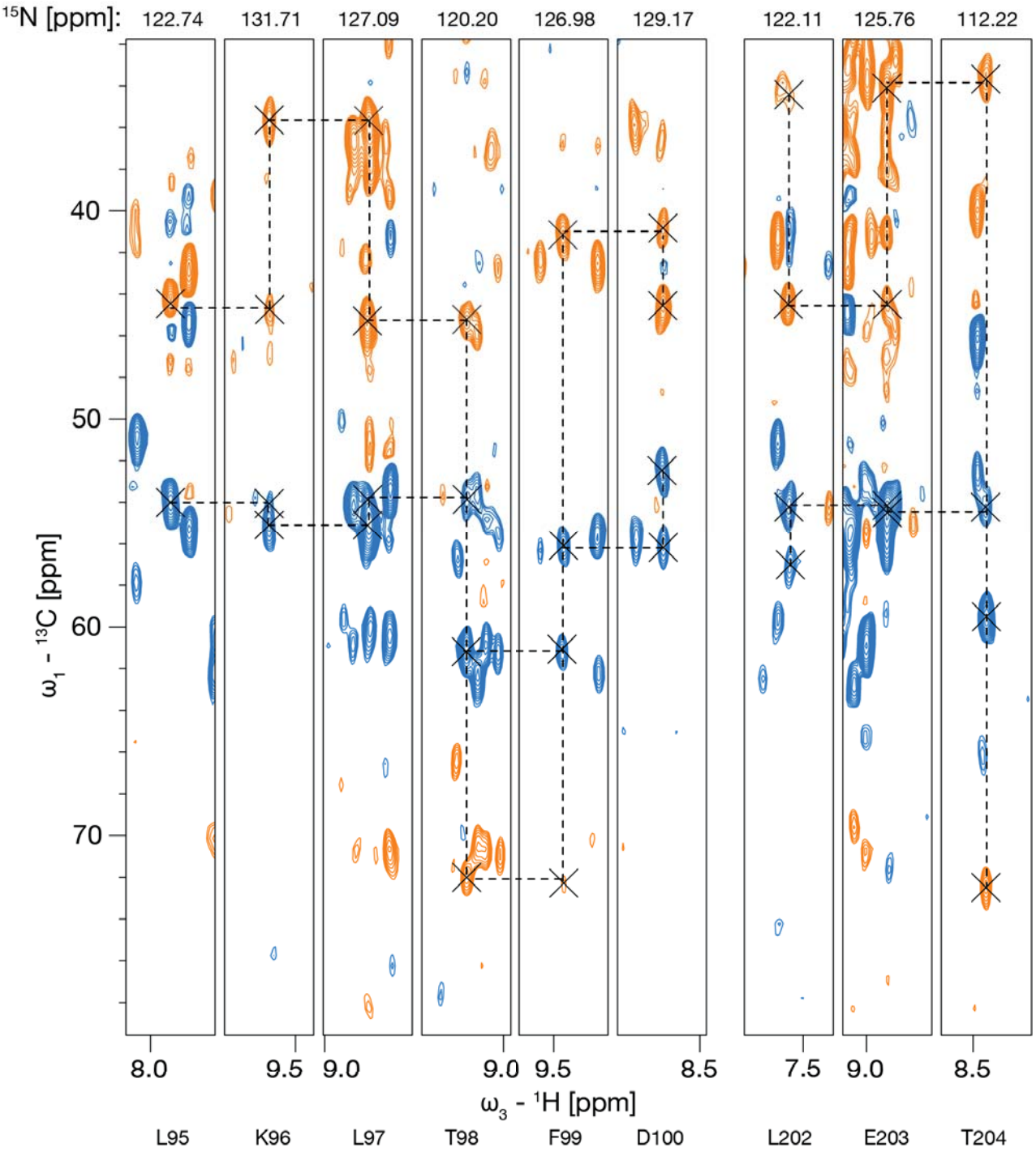

Figure 3.2: Strips of TROSY-HNCACB on E73VC127AC232S hVDAC1. Generic backbone walk shown through the example of Leucine-95 to Aspartate-100 (left). Backbone walk that lead to the assignment of Leucine-202 (right). Positive contours are shown in blue, negative contours are shown in orange.

Dieses Werk ist copyrightgeschützt und darf in keiner Form vervielfältigt werden noch an Dritte weitergegeben werden.
Es gilt nur für den persönlichen Gebrauch.

With the help of the additional C_β shift information, Leucine-202 could now be assigned. (See Figure 3.2) Interestingly, because of the very similar C_α shifts of Leucine-202 and Glutamate-203, the resonance in question had previously been assigned to Glutamate-203. This assignment had already been revised prior to the beginning of this PhD thesis, but shows that it was known that this resonance should be located in that region of the beginning of β-strand 14.

The loop from β-strand 2 to β-strand 3 had been tentatively assigned before. As it contains three Threonine residues (49, 51 and 52), the additionally recorded TROSY-HNCACB proved to be very helpful, since Threonine has a unique pattern with the C_β resonating at lower field than the C_α. This way, the previously tentative resonance assignments could now be replaced by safe assignments, at the same time confirming the NOE connectivities (see Figure 3.3).

A similar case are Leucine-91 and Alanine-92. Here, it is the unique C_β resonance position of Alanine-92, which helped to identify the resonances of these residues with more certainty. By this very same strategy the sequence of the three residues Threonine-250, Leucine-251, and Lysine-252 could additionally be assigned safely. The last additional residue found is Glutamate-177.

Regarding the N-terminal helix, the TROSY-HNCACB helped to confirm the assignments of all previously assigned residues except Alanine-8 and Alanine-14. In these two cases the characteristic C_β resonance is missing. This, however, does not prove the assignments to be wrong, as in the spectrum the Alanine-C_β resonances are always quite weak. Taken together with the overall low signal strength of the residues in the N-terminal helix it is not unlikely, that these two resonances in question are simply too weak to detect.

After all, one residue had to be deassigned because it never behaved as expected. Lysine-20 had no connections to surrounding residues in the NOESY-spectrum and furthermore does not react at all to mutations in its close proximity (G21V/G23V/E73V/C127A/C232S hVDAC1 and derivatives of this mutant). As it had been assigned only ambiguously, it was decided to remove this assignment from the list.

Overall, the backbone assignment in hVDAC1 was increased to 88.1 %/94.8 % and 92.1 %/98.4 % (overall/barrel) of the residues for *wt* hVDAC1 and E73VC127AC232S hVDAC1, respectively. (See also Figure 3.3)

Dieses Werk ist copyrightgeschützt und darf in keiner Form vervielfältigt werden noch an Dritte weitergegeben werden.
Es gilt nur für den persönlichen Gebrauch.

The largest part of the unassigend residues is now located in the last part of the N-terminal helix and the beginning of the linker from the helix to the barrel (Phenyalanine-18 to Glycine-21 and Glycine-23). Also, some loops (from β-strands 1 to 2, 3 to 4, 6 to 7, 13 to 14, 14 to 15 and 17 to 18) and residues in the C-terminal end of the protein (Phenylalanine-281, Glutamate-282, Leucine-284) are still unassigned. For all of these residues even the additional information from the TROSY-HNCACB spectrum did not help finding the assignments. (On the contrary, Lysine-20 was even deassigned.) It is thus doubtful whether they can be assigned with reasonable effort or assigned at all.

3.1.3 Improved backbone NOE network

When revising the data and spectra received from Saskia Villinger, it turned out that the 3D ^{15}N-NOESY-HMQC of the E73V hVDAC1 mutant was not completely assigned at all.

As can be seen in Figure 3.3, a significant amount of the NOE contacts in the spectrum was previously unassigned. Taken together, there were 534 NH-NH contacts assigned by Saskia Villinger (counting each resonance as a single contact, meaning that a H_N-H_N NOE that is visible in both directions is counted as two contacts).

By thorough analysis of the spectrum and by purposeful search for contacts that would be expected to be visible, 900 new H_N-H_N contacts could be found, raising the number of the overall observed contacts to 1431 (a small number of contacts was deleted) and thus increasing the number of assigned contacts nearly threefold.

As depicted in Figure 3.3, the newly assigned NOE contacts are well spread over the whole barrel. Not only are there numerous new sequential short range contacts found in all β-strands, but also a big amount of newly assigned mid and long range inter-strand contacts. Where previously often only the strong H_N-H_N contacts indicating hydrogen bonds were assigned, now basically every residue has additionally assigned inter-strand contacts. The highest density of H_N-H_N NOEs can be found in β-strands 5 to 11, where roughly 600 contacts are located alone – more than previously had been assigned in the whole protein. These β-strands are comprising the region where the N-terminal α-helix is attached to the barrel wall (hydrophophic contact patch of Valine-143 in β-strand 9 and

Dieses Werk ist copyrightgeschützt und darf in keiner Form vervielfältigt werden noch an Dritte weitergegeben werden.
Es gilt nur für den persönlichen Gebrauch.

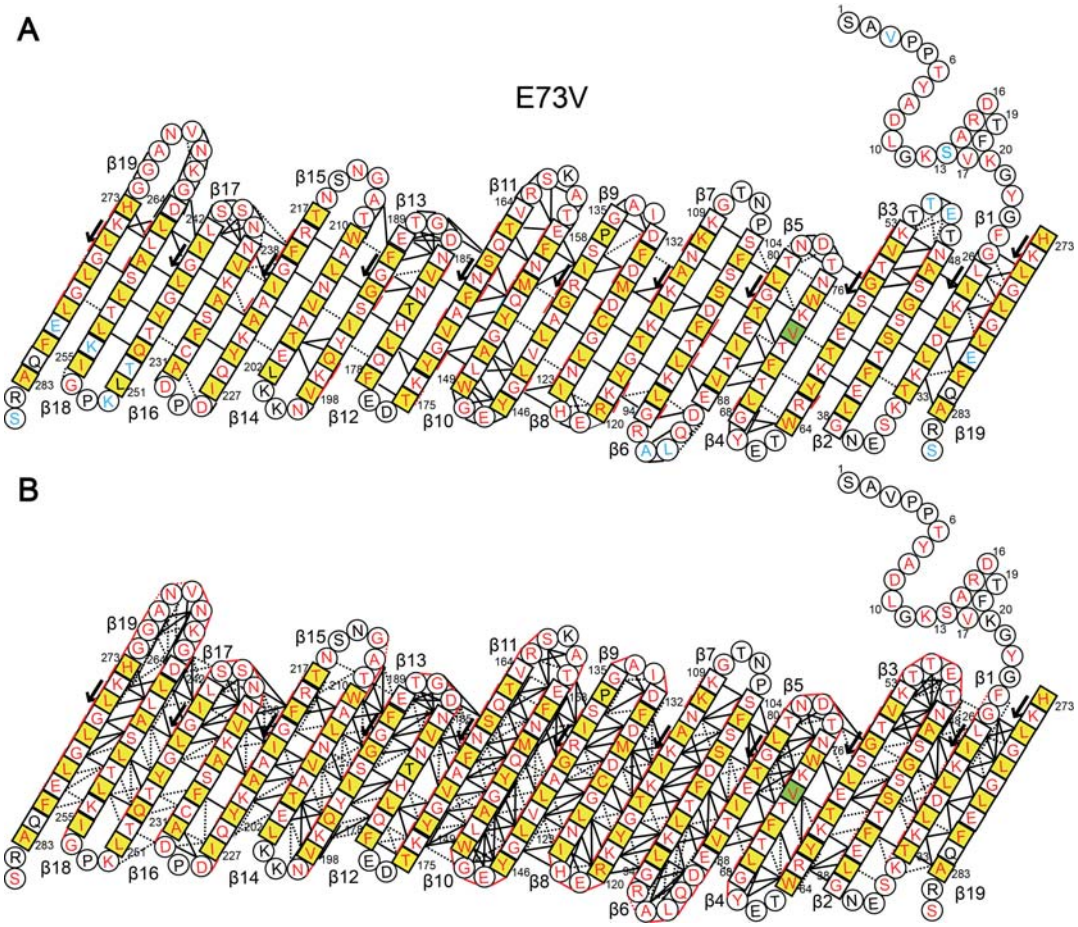

Figure 3.3: NOEs of E73V hVDAC1. Overview of the H_N-H_N NOEs obtained from a NOESY-HMQC spectrum of E73V hVDAC1 recorded by Saskia Villinger. Assigned residues are lettered in red, ambiguously assigned residues in blue and unassigned residues are lettered in black. Residues in β-strands are boxed, residues in the loops and the N-terminal α-helix are circled. Yellow shaded residues are pointing to the micelle, the mutation site E73V is highlighted in green. Solid black (solid red) lines indicate inter-strand (sequential) H_N-H_N NOEs observed in both directions, dotted black (dotted red) lines indicate inter-strand (sequential) NOEs observed only in one direction and overlapping NOEs. A: Assignment and NOE network as assigned and reported by Saskia Villinger. (This part of the figure was adapted from the PhD thesis of Saskia Villinger.[74]) B: Latest and most up to date assignment and NOE network.

Leucine-150 in β-strand 10 to Leucine-10 in the helix) and the β-strands between said region and the Valine-73 mutation site. In the β-strands 15 to 17 however, the network of NOEs is visibly least dense. This is in line with previous results, that showed that the average peak intensity for residues located in the N-terminal β-strands is significantly lower than those of the central β-strands where E73V mutation and the N-terminal α-helix are stabilizing the barrel.[132]

Interestingly, also the large number of newly assigned contacts did not result in a possible assignment for Threonine-182. Following the pattern of strong H_N-H_N contacts indicating hydrogen bonds

Dieses Werk ist copyrightgeschützt und darf in keiner Form vervielfältigt werden noch an Dritte weitergegeben werden.
Es gilt nur für den persönlichen Gebrauch.

there should be a strong NOE from Valine-171 to Threonine-182 and *vice versa*. However, no such NOE could be found, leaving the assignment of Threonine-182 an open question.

There are also some new contacts between residues in the N-terminal α-helix found. The number of internal contacts in the helix was increased from 21 to 32 inter residue contacts plus 9 intra residue contacts. For example, there are four new contacts from and to Lysine-12 alone, which had no contacts before at all. (Data not shown here.)

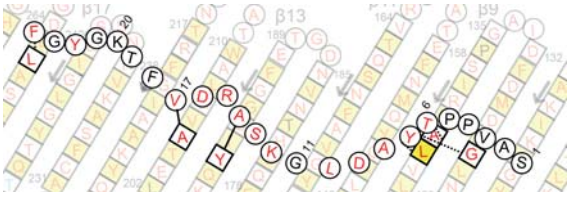

Figure 3.4: NOEs of E73V hVDAC1 between N-terminal α-helix and β-barrel. Assigned residues are lettered in red and unassigned residues are lettered in black. Residues in β-strands are boxed, residues in the loops and the N-terminal α-helix are circled. Yellow shaded residues are pointing to the micelle. Solid black lines indicate H_N-H_N NOEs observed in both directions, dotted black lines indicate NOEs observed only in one direction. Residues in the barrel without contact to helix residues are greyed out for clarity.

Finally, the contacts between N-terminal α-helix and β-barrel were completely revised and improved. Although there are still only 7 contacts between α-helix and β-barrel, these contacts can be translated into constraints that are not violated when calculating a 3D structure based on the NOE data (see Chapter 3.2). From the previously existing three contacts between α-helix and β-barrel, two had to be removed (Threonine-6 to Methionine-155 and *vice versa*) because they were violating the structure and the contact between Alanine-14 and Isoleucine-194 was altered to be a better fitting contact between Alanine-14 and Tyrosine-195 that is now assigned in both directions. An overview of the contacts between α-helix and β-barrel is shown in Figure 3.4.

Dieses Werk ist copyrightgeschützt und darf in keiner Form vervielfältigt werden noch an Dritte weitergegeben werden.
Es gilt nur für den persönlichen Gebrauch.

3.2 A new NMR structure of E73V hVDAC1

As mentioned above in Chapters 3.1.2 and 3.1.3, not only the assignment of hVDAC1 could be improved to a previously unprecedented level, but also the NOE network in E73V hVDAC1 could be improved drastically. In connection with ^{15}N spin-relaxation data from E73V hVDAC1 and by once again revising the E73V hVDAC1 H/D exchange data, this was used to determine a 3D structure of E73V hVDAC1 based solely on NMR data that by far exceeds the accuracy and quality of the previously published NMR structure of hVDAC1[48].

The following chapter describes how this was done and achieved. This chapter of this PhD thesis is part of a recent collaborative publication[115] and thus parts of this chapter are reproduced from this publication and contain some identical text passages. The calculations described in the following were performed by Mariusz Jaremko, Łukasz Jaremko and Markus Zweckstetter.

3.2.1 A 3D structure of E73V hVDAC1 based on the improved NOE network as starting point[1]

In previous works, to compensate for the sparsity of long-range structural information based on NOE-based interproton restraints (due to the fact that hVDAC1 in micelles is a system so large it requires deuteration[134–136]), it was tried to record residual dipolar couplings (RDCs), as they often prove useful in that purpose.[137,138] However, it turned out to be impossible to align hVDAC1 in LDAO micelles in liquid crystalline alignment media. In charged polyacrylamide gels the partial alignment of hVDAC1 in LDAO micelles was possible, but overall the resulting spectra and data were of poor quality.[74]

These limitations were addressed by exploiting the long-range order that is encoded in the nuclear magnetic spin relaxation of macromolecules like hVDAC1 in LDAO micelles due to their anisotropic rotational diffusion.[129,139] (This approach was previously never applied to membrane proteins.) A combination of these information from heteronuclear relaxation rates together with NOE data and the

[1] This section is based on a recent joint publication[115] and contains akin text passages.

Dieses Werk ist copyrightgeschützt und darf in keiner Form vervielfältigt werden noch an Dritte weitergegeben werden.
Es gilt nur für den persönlichen Gebrauch.

application of empiric potentials to hydrogen bonds determined from the aforementioned E73V hVDAC1 H/D exchange data[131] lead to a structure of E73V hVDAC1 in unprecedented resolution.

Based on the improved assignment of 92.1 % of the backbone H^N and N resonances and the corresponding C_α and C' shifts, the backbone torsion angles ψ, ϕ and the side-chain angle χ^1 were estimated using TALOS-N.[127] (See Figure 3.5.)

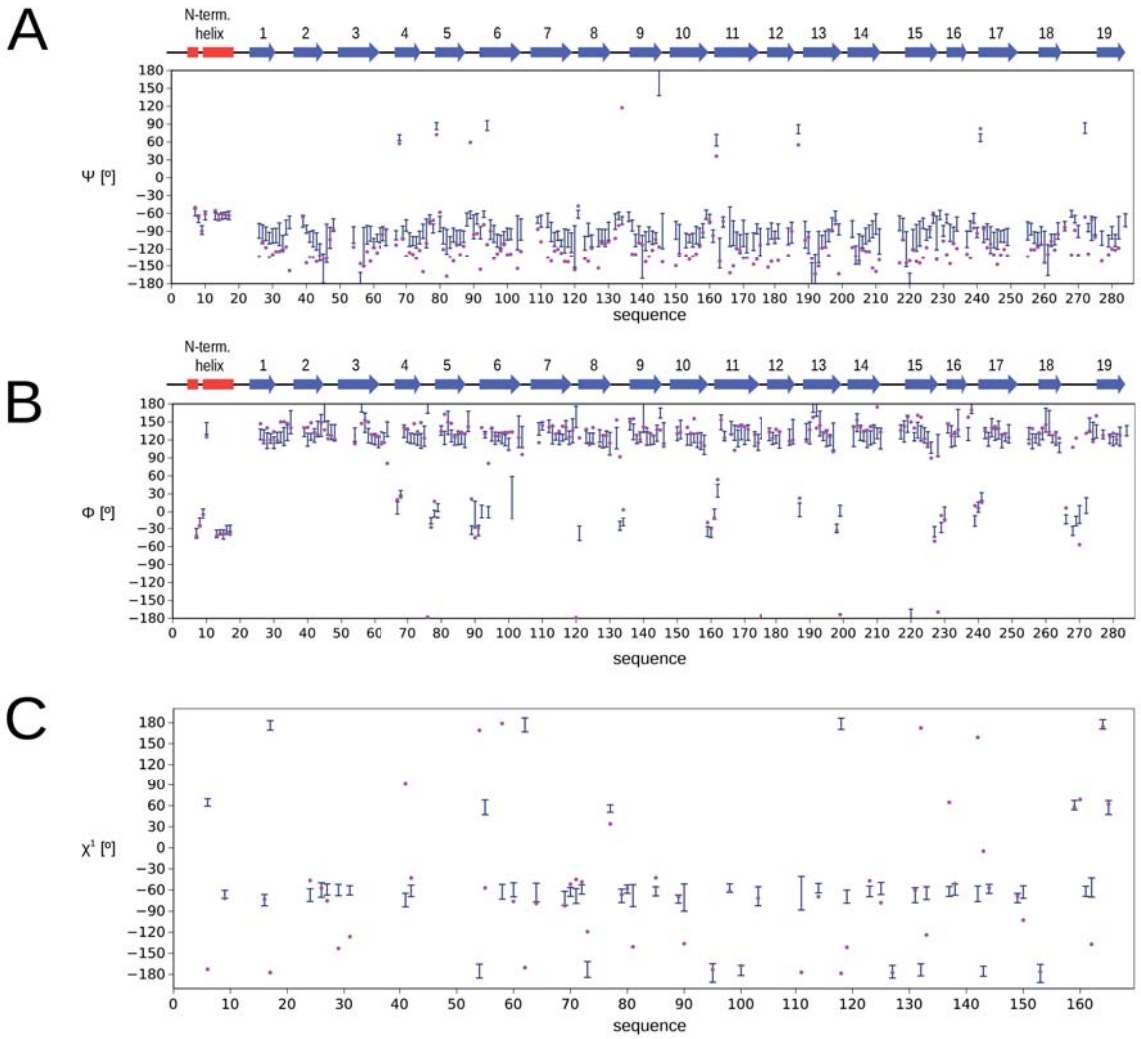

Figure 3.5: Torsion angle information from experimental chemical shifts. Angles on the basis of the experimental backbone H^N, N, C_α, C' chemical shifts in E73V hVDAC1. Pink dots show the values observed in the crystal structure of mVDAC1. (PDB ID: 3EMN)[46] A: Backbone dihedral angle ψ. B: Backbone dihedral angle ϕ. C: Backbone torsion angle χ^1. Figure was adapted from our joint publication[115] under the terms of the Creative Commons License CC BY-NC-ND.

After refinement, the aforementioned NOE data (see Figures 3.3 and 3.4) provided 656 sequential, medium- and long-range proton-proton distance restraints. 128 hydrogen bond restraints from the E73V hVDAC1 H/D exchange data were also present. (Originally from our group and published in

Dieses Werk ist copyrightgeschützt und darf in keiner Form vervielfältigt werden noch an Dritte weitergegeben werden.
Es gilt nur für den persönlichen Gebrauch.

Bayrhuber *et al.*[70], refined data not shown.) The combined data (NOE restraints, hydrogen bond restraints and backbone angle restraints) were used to fold the protein from the extended polypeptide with a simulated annealing protocol using the platform Xplor-NIH.[126]

The resulting ensemble of the 20 lowest energy structures had a backbone RMSD of 2.5 Å and like in other previously published NOE-based structures[48,70] the definition of the barrel shape and the conformation and position of the N-terminal helix could only be determined with modest accuracy. Nevertheless, in the majority of these 20 structures the N-terminal helix shows the kink between Leucine-10 and Lysine-12, a structural feature that previously had not been described based on NMR data. (See Figure 3.6.)

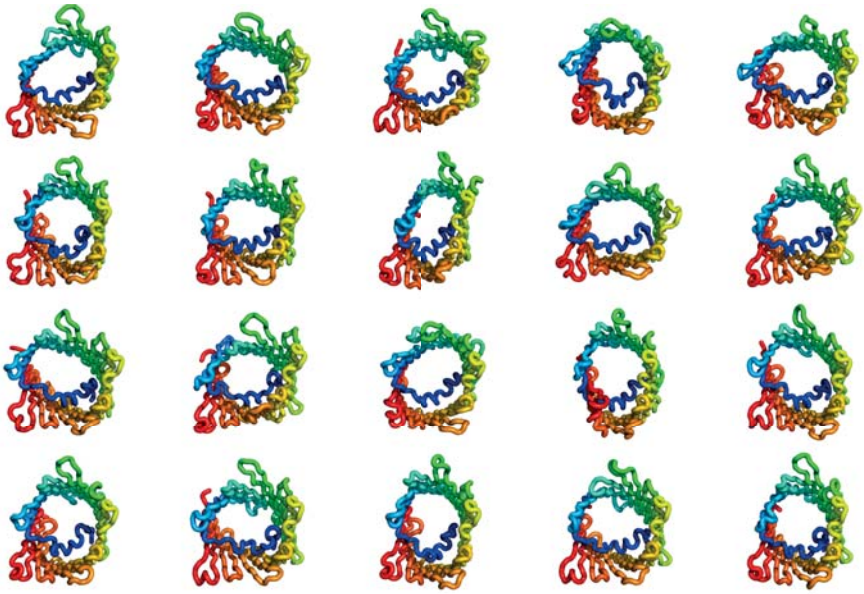

Figure 3.6: 20 lowest energy structures. E73V hVDAC1 calculated exclusively from the NOE- and hydrogen bond-based distance and chemical shift-derived angular restraints. The structres are colored from the N- to the C-terminus from blue to red. Figure was adapted from our joint publication[115] under the terms of the Creative Commons License CC BY-NC-ND.

3.2.2 Improving the structure with ^{15}N spin-relaxation data[1]

The accuracy and precision of the E73V hVDAC1 could now be further improved by ^{15}N spin-relaxation data derived from measurements at magnetic fields corresponding to 60 to 90 MHz nitrogen frequency. (The measurements were performed by Saskia Villinger, the analysis of the data was

[1] This section is based on a recent joint publication[115] and contains akin text passages.

Dieses Werk ist copyrightgeschützt und darf in keiner Form vervielfältigt werden noch an Dritte weitergegeben werden.
Es gilt nur für den persönlichen Gebrauch.

performed by Mariusz Jaremko, Łukasz Jaremko and the author of this thesis. The pulse programs used can be found in Appendix A.2 and A.3.) The measurements were performed using the TROSY approach.[116] This way, 537 pairs of R_1 and R_2 relaxation rates of E73V hVDAC1 were obtained with average errors of 2.7 % at 60 MHz, 3.1 % at 70 MHz and 4.4 % at 90 MHz.

By measuring at several magnetic fields possible contributions of R_{ex} (chemical exchange motions slower than the overall tumbling but fast enough to average the chemical shifts, *i.e.* motions in the range from µs to ms) to the transverse relaxation rate R_2 can be assessed. The contributions from R_{ex} would enhance the R_2 rates and the enhancement would scale quadratically with the magnetic field.[140] Thus, plotting the ratio of R_2 rates at two magnetic fields, $R_{2(B_1)}/R_{2(B_2)}$, as a function of the residue number can provide evidence for R_{ex}. As can be seen in Figure 3.7 there is no evidence of significant contributions from R_{ex} in E73V hVDAC1.

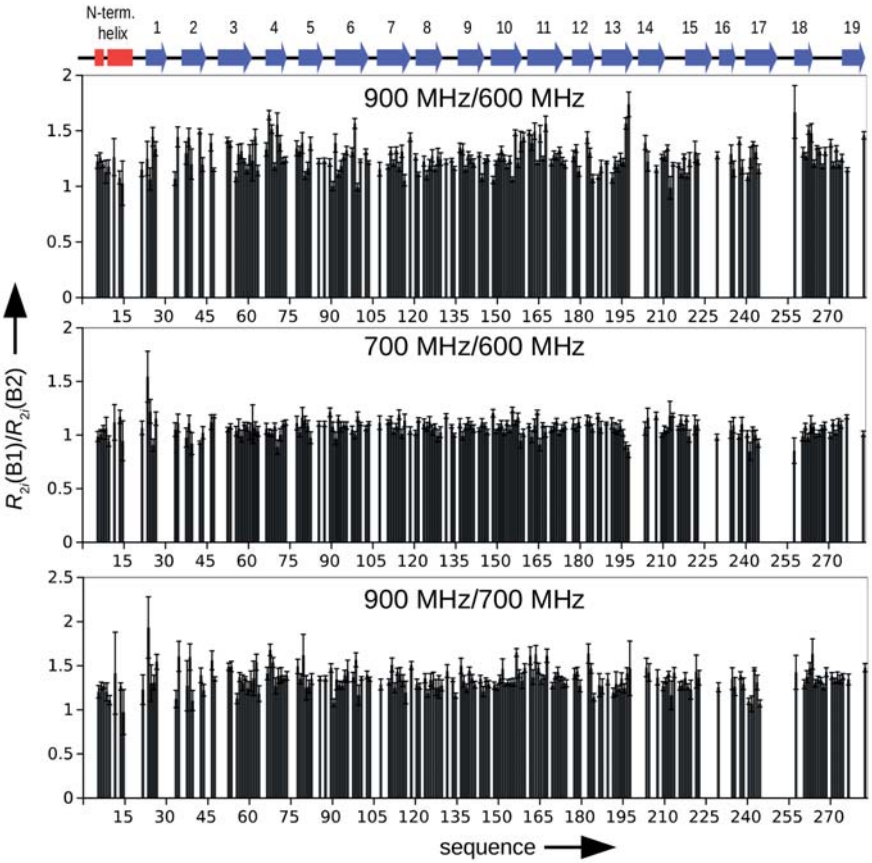

Figure 3.7: Dynamic information encoded in ^{15}N spin-relaxation rates. Residue-specific ratios of ^{15}N-R_2 relaxation rates $[R_{2i(B_1)}/R_{2i(B_2)}]$ from three magnetic fields. Error bars show one SD. Figure was adapted from our joint publication[115] under the terms of the Creative Commons License CC BY-NC-ND.

Dieses Werk ist copyrightgeschützt und darf in keiner Form vervielfältigt werden noch an Dritte weitergegeben werden.
Es gilt nur für den persönlichen Gebrauch.

Additionally, with measuring at three magnetic fields the overall quality of the data can better be evualuated and ps–ns motions can be determined with more accuracy.[141] By applying MFA analysis[142] on the relaxation rates it was demonstrated that the majority of the residues in the 19 β-strands of E73V hVDAC1 are rigid on the ps–ns time scale and only a few residues in the N-terminal β-strands had elevated values for fast internal motion. The loops nevertheless showed higher flexibility, in particular the long loop between β-strands 18 and 19. (With rigid residues being defined by a Lipari–Szabo order parameter $S^2 > 0.85$ and a correlation time for internal motions $\tau_i < 500$ ps. See Figure 3.8.)

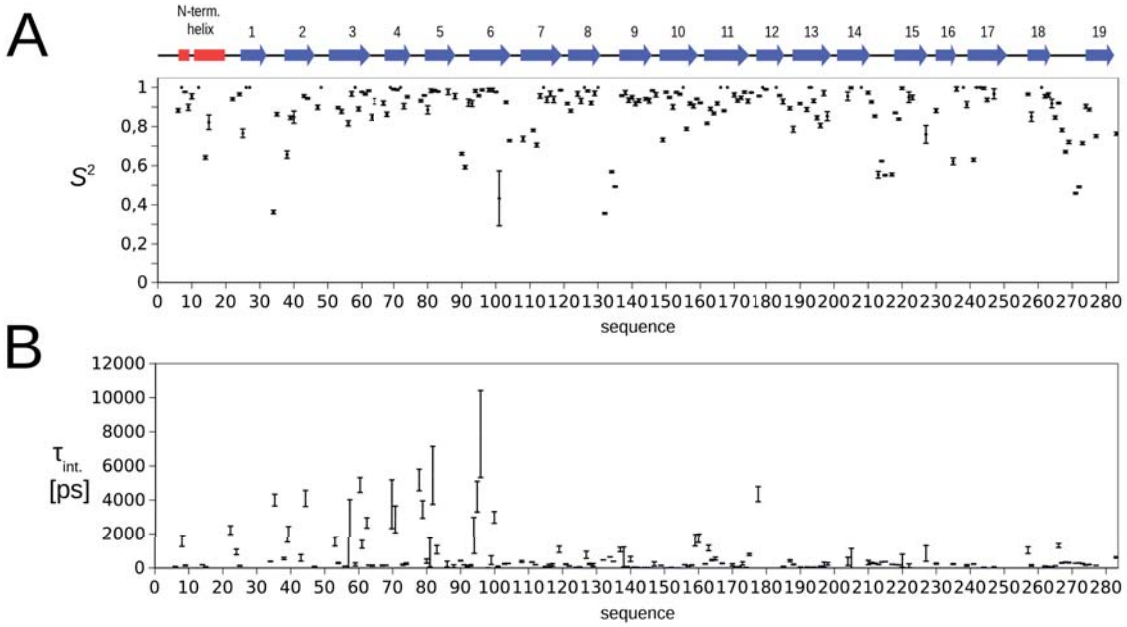

Figure 3.8: Model-free analysis of the ^{15}N relaxation data of E73V hVDAC1 (2-parameter MFA model with S^2_f and $\tau_{int,f}$ and fully anisotropic reorientation. A: Residue-specific S^2_f order parameters. B: Internal total correlation time ($\tau_{int,f}$) describing ps–ns time scale motions of individual residues. Errors were estimated by 200 Monte Carlo simulations and represent one SD. Figure was adapted from our joint publication[115] under the terms of the Creative Commons License CC BY-NC-ND.

It was now made use of the fact, that the dependence of the transverse and longitudinal relaxation rates on the rotational diffusion anisotropy of the protein provides information not only on internal motion but also on long-range structure.[129] It had already been show by MFA analysis that E73V hVDAC1 is very rigid in comparison to *wt* hVDAC1.[132] Thus, it was expected that information on the long-range order with could be extracted with higher accuracy in E73V hVDAC1. As shown in the last paragraphs, exactly this assumption holds true. The residues with order parameters

Dieses Werk ist copyrightgeschützt und darf in keiner Form vervielfältigt werden noch an Dritte weitergegeben werden.
Es gilt nur für den persönlichen Gebrauch.

$S^2 > 0.85$, *i.e.* the most rigid ones, were now selected to be analyzed for that purpose. 124 residues mainly found in the β-strands were selected. This corresponds to 124 R_1 and R_2 values at 3 fields, respectively, so all in all 372 R_1 and 372 R_2 rates or 744 experimental values in total. The respective residues are shown in Figure 3.9.

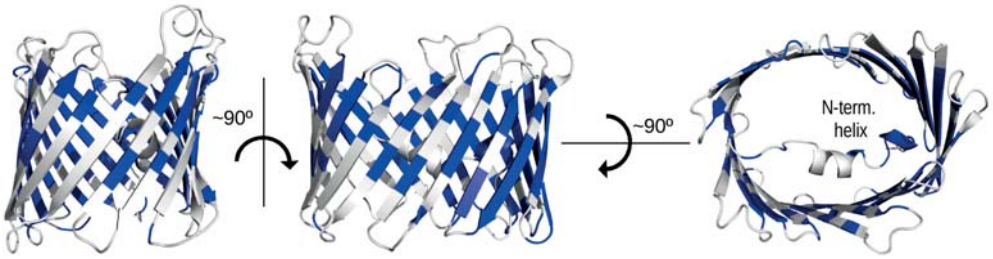

Figure 3.9: ^{15}N-R_2/R_1 rates used for structure refinement. Residues for which R_2/R_1 rates were used during structure refinement are shown in blue. Data is mapped on the lowest-energy conformation of E73V hVDAC1 after refinement. Figure was adapted from our joint publication[115] under the terms of the Creative Commons License CC BY-NC-ND.

To extract the structural information encoded in the relaxation rates, the rotation correlation time τ_c, the anisotropy A and the rhombicity η of the diffusion tensor have to be known *a priori*. These parameters were estimated by applying MFA analysis[142] to the lowest-energy NOE-based structure of E73V hVDAC1 obtained previously (cf. Figure 3.6). This structure of E73V hVDAC1 was then refined against the experimental ^{15}N-R_2/R_1 rates of the 124 previously selected residues. This was done with a specially designed Xplor-NIH protocol that makes use of the knowledge-based potentials torsionDB and HBDB[130,131] to optimize the geometry of the torsion angles and hydrogen bonds. The potentials were used to narrow the conformational space in which the protein can move during refinement to the physically most justified conformations as they are found among the highest-quality X-ray structures. Additionally, they prevent overfitting of the orientational restraints, in particular in the case of outliers.[129]

To check the robustness and stability of this approach the same calculations were performed with diffusion tensor parameters obtained by MFA analysis of the previously published VDAC1 structures with the PDB IDs 3EMN[46] and 2JK4[70]. Also, the tensor parameters A and η, which were derived from the R_2/R_1 refined E73V hVDAC1 structure were taken, altered by ± 0.2 units and −50 % and +100 %, respectively, and the calculation was repeated using these values. As with previous

Dieses Werk ist copyrightgeschützt und darf in keiner Form vervielfältigt werden noch an Dritte weitergegeben werden.
Es gilt nur für den persönlichen Gebrauch.

results with this approach from globular proteins and their complexes[139,143], all these calculations converged to highly similar 3D structures, proving the high robustness and stability of the protocol. The 20 lowest-energy structures of E73V hVDAC1 obtained by refinement as described above are shown in Figure 3.10, the lowest energy structure can be seen in Figure 3.9.

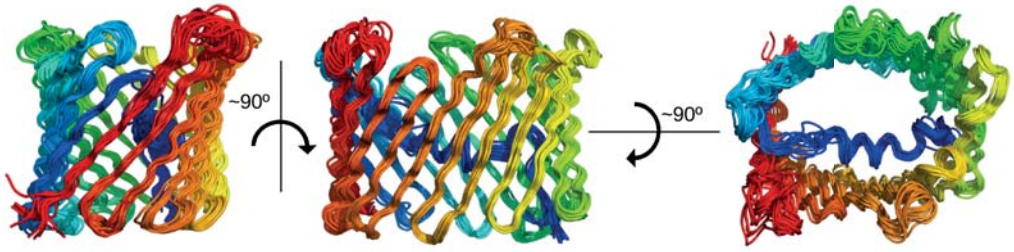

Figure 3.10: 20 lowest-energy structures of E73V hVDAC1 after refinement against R_2/R_1 rates. Structures are colored from the N- to the C-terminus from blue to red. Figure was adapted from our joint publication[115] under the terms of the Creative Commons License CC BY-NC-ND.

The ensemble of the 20 lowest-energy structures tightly clusters around a single conformation and exhibits a backbone RMSD of 1.1 Å for all 283 residues. Each of the 19 β-strands is well defined and the N-terminal α-helix is rigidly attached to the barrel wall with no sign of flexibility. The most flexible part of the structure is the linker, which connects the N-terminal helix to β-strand 1.

3.2.3 Validating the high-resolution structure of E73V hVDAC1[1]

When comparing the high-resolution structure of E73V hVDAC1 described here to the previously reported crystal structure of mVDAC1[46], it becomes obvious that the former is more anisotropic. It can be shown that this is a direct consequence of the experimental R_2/R_1 rates, as the R_2/R_1 rates fit better to the solution structure of E73V hVDAC1 than to the crystal structure of mVDAC1. (See Figure 3.11.)

The largest deviations between the experimental rates and the values back-calculated from the crystal structure of mVDAC1 are found in β-strands 9 and 10. Interestingly, as can also be seen in Figure 3.11, the ellipsoidal shape of the solution structure of E73V hVDAC1 as it is encoded in the R_2/R_1 rates is more similar to an anisotropic barrel shape found during a 100 ns MD trajectory of membrane-embedded mVDAC1[132] than to the starting X-ray structure of mVDAC1[46]. (C_α

[1] This section is based on a recent joint publication[115] and contains akin text passages.

Dieses Werk ist copyrightgeschützt und darf in keiner Form vervielfältigt werden noch an Dritte weitergegeben werden.
Es gilt nur für den persönlichen Gebrauch.

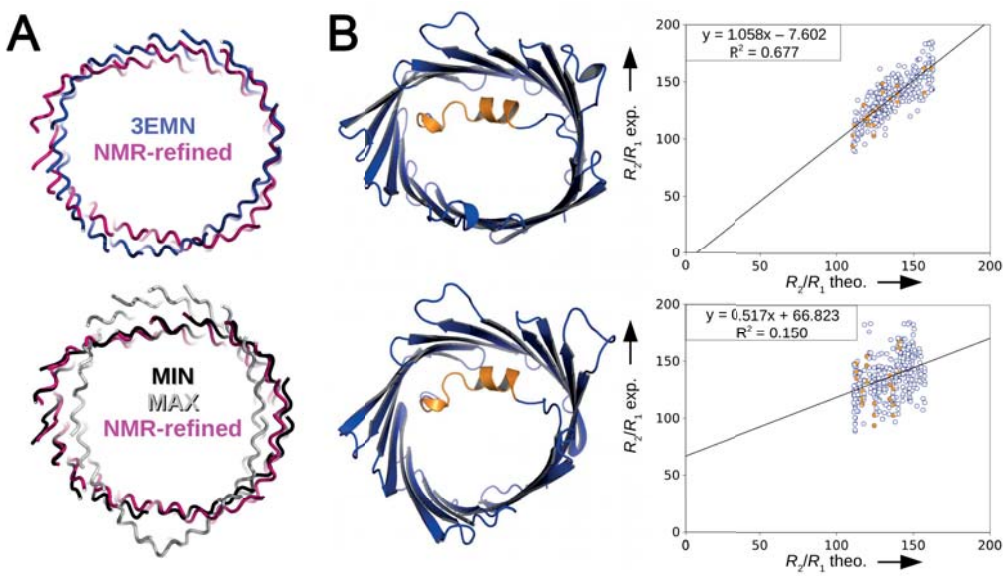

Figure 3.11: Validation of the high-resolution structure of E73V hVDAC1. A: Comparisons of the lowest-energy structure of E73V hVDAC1 to previous structures. The new structure (pink) is more anisotropic than the previously published crystal structure of mVDAC1.[46] (top) The barrel shape of E73V hVDAC1 (pink) is similar to one of the two maximum excursions (black and grey) observed in a 100 ns MD trajectory of mVDAC1 embedded in a phospholipid bilayer.[132] (bottom) B: Left side: Solution structure of E73V hVDAC1 (PDB ID: 5JDP, top) and crystal structure of mVDAC1(PDB ID: 3EMN, bottom). Right Side: Correlation of experimental R_2/R_1 rates from three magnetic fields (scaled according to the theoretical field dependence) with values back-calculated from the respective structure to the left. The residues of the N-terminal helix together with their determined R_2/R_1 rates on the correlation plots are shown in orange. Figure was adapted from our joint publication[115] under the terms of the Creative Commons License CC BY-NC-ND.

RMSD of residues 26–283 of 2.1 Å to the MD structure versus 3.3 Å to the crystal structure.) This suggests that the E73V mutation and/or the micellar environment stabilize a conformation that the VDAC1 pore can adopt in a phospholipid bilayer according to molecular dynamics simulations. Nevertheless, implications of this finding for possible gating pathways or movements of the channel remain unclear.

The NMR ensemble of E73V hVDAC1 refined against the R_2/R_1 rates was deposited together with the experimental data in the Protein Data Bank (PDB ID 5JDP and 30065).

Dieses Werk ist copyrightgeschützt und darf in keiner Form vervielfältigt werden noch an Dritte weitergegeben werden.
Es gilt nur für den persönlichen Gebrauch.

3.3 Incorporating the protein's closed state in NMR – Developing a Quintuple hVDAC1 mutant

3.3.1 General strategy

As shown and discussed above in Chapter 1.3.3, the mode of gating and the nature and structure of the closed state (or its variety of several quite alike closed states) of VDAC1 are a long-standing question in the scientific community. One of the main goals of this thesis was to tackle this question by the means of NMR spectroscopy.

For quite obvious reasons it is not possible to apply a voltage to a liquid state NMR sample like it can be applied to a BLM, because the complexes of the protein and the detergent molecules are tumbling freely in the samples and there are no defined compartments as there are in e.g. BLM measurements. These compartments make it possible to study proteins embedded in a membrane under various parameters such as different ionic strength, pH or medium composition on both sides of the membrane.[144] Solid state NMR samples exhibit the same drawback, because also they lack defined compartments.

It is thus necessary to find other approaches to study the closed state of VDAC1 with NMR. Since it is known that the N-terminal α-helix plays a key role in the gating of the pore[100], many studies focused also on mutations of the helix or other parts of the protein, to gain more insight about the behavior of the helix in the gating process (cf. Chapter 1.3.3). In the course of these studies some groups found VDAC1 mutants that showed unusual or altered gating properties, respectively.

The approach of this thesis is thus, to use hVDAC1 mutants which stabilize the closed state or alter the gating process in a fashion that it can be expected to see the closed state enriched in NMR samples, *i.e.* also at zero voltage. The first of these mutants affixes the N-terminal helix to the β-barrel[52] (see Chapter 3.3.2), the second of these mutants features a stiffened linker between α-helix and β-barrel which significantly changes the gating properties of the mutant[145] (see Chapter 3.3.3).

Dieses Werk ist copyrightgeschützt und darf in keiner Form vervielfältigt werden noch an Dritte weitergegeben werden.
Es gilt nur für den persönlichen Gebrauch.

3.3.2 Affixing the N-terminal helix to the β-barrel

Studies on A14C/C127A/S193C/C232A hVDAC1 were performed based on a publication by Mertins *et al.* from 2012[52], where this mutant, albeit based on mVDAC1, had been described. The two native Cysteine residues in this mutant had been replaced by Alanine. Based on the crystal structure of mVDAC1 (PDB ID: 3EMN)[46] two new artificial Cysteines had been added by mutating Alanine-14 and Serine-193. This should allow the formation of a disulfide bond between the N-terminal α-helix and β-strand 13 of the β-barrel. Indeed Mertins *et al.* could observe the formation of the desired disulfide bond, attesting the 3D structures published in 2008. In the oxidized state, *i.e.* with the disulfide bond formed, this mutant had been described to have special gating properties that seemed to be useful for NMR studies. In general, the mutant has a "usual" open state with conductance of 3.74 ± 0.09 nS (oxidized mutant) and 3.75 ± 0.12 nS (reduced mutant), respectively, and closed states with conductances of 1.85 ± 0.07 nS (oxidized mutant) and 2.55 ± 0.12 nS as well as 1.67 ± 0.09 nS (reduced mutant, all values measured in 1 M KCl, 5 mM $CaCl_2$), respectively.

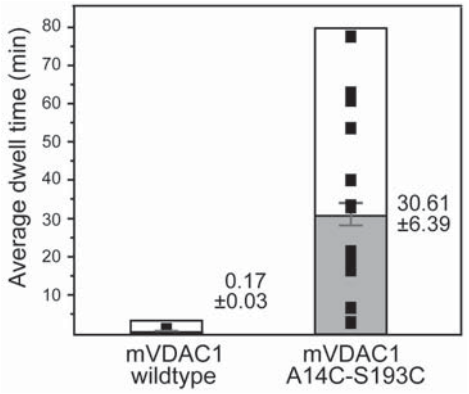

Figure 3.12: Dwelling times of *wt* mVDAC1 and A14C/C127A/S193C/C232A mVDAC1. Reprinted from Mertins et al.[52] under the terms of Creative Commons Attribution License.

Oxidation and reduction of the mutant had been performed by treatment with CuX_2Ph and DTT, respectively. The special gating properties of the oxidized mutant are as follows: when a potential of 40 mV is applied, instead of switching into a closed state after seconds like *wt* VDAC1 is doing, the mutant dwells in the open state for over 30 minutes on average. (See Figure 3.12) Switching into the closed state additionally occurred only in 8 % of the traces, that were recorded. The authors of the study hypothesized, that the closure of the cross-linked channel is mediated by mechanical

Dieses Werk ist copyrightgeschützt und darf in keiner Form vervielfältigt werden noch an Dritte weitergegeben werden.
Es gilt nur für den persönlichen Gebrauch.

strain effects due to the covalent bond between α-helix and β-barrel and that closure is caused by the barrel collapsing, the N-terminal helix irreversibly unfolding or a combination of these two.

The fact that this particular mutant in the oxidized state is failing to reopen once it closed, raised our interest. In principle, also at zero voltage and also when the closed state itself is attained with strongly reduced probability, as the authors conclude[52], there should – based on the argument of Boltzmann distribution – still be a very small but certain amounts of channels, that are in the closed state. That the mutant is not able to reopen, should cause the closed state of the protein to be enriched in the sample over time. This might make it observable at zero voltage in NMR samples.

3.3.2.1 A14C/C127A/S193C/C232A hVDAC1 samples are oxidized by air

A14C/C127A/S193C/C232A hVDAC1 was expressed, refolded in LDAO and purified following the procedures described in Materials & Methods. To make sure the mutant is in the oxidized state (*i.e.* to make sure the disulfide bond is formed), SDS-PAGE experiments were performed, following a similar procedure as in the publication. As shown in Figure 3.13, hVDAC1 exhibits the expected behavior like described by Mertins *et al.* In all cases that are described in the following, the hVDAC1 samples were taken directly out of the NMR buffer.

First, conditions were chosen such that it should be possible to reach reference states of the mutant (completely oxidized and completely reduced). Line A shows the mutant under the influence of oxidant CuX_2Ph, line B shows the mutant treated with the reductants DTT and β-mercaptoethanol. The increased electrophoretic mobility in line A indicates the formation of the disulfide cross-link, whereas the disulfide bridge is reduced in line B, being completely in line with the results of Mertins *et al.* and showing that the creation of the desired reference states was successful.

Next, the behavior of the mutant under varying conditions was investigated. Line C shows the mutant without oxidizing or reducing treatment and stored at 37 °C for 6 hours before loading, while line F shows the mutant without treatment and stored at room temperature before loading. In these two cases the mutant behaves like the one that was oxidized by CuX_2Ph, indicating that air oxygen is sufficient to oxidize the protein and form the disulfide bond independently from the temperature. This points to that the protein in the NMR buffer and consequently also in the NMR

Dieses Werk ist copyrightgeschützt und darf in keiner Form vervielfältigt werden noch an Dritte weitergegeben werden.
Es gilt nur für den persönlichen Gebrauch.

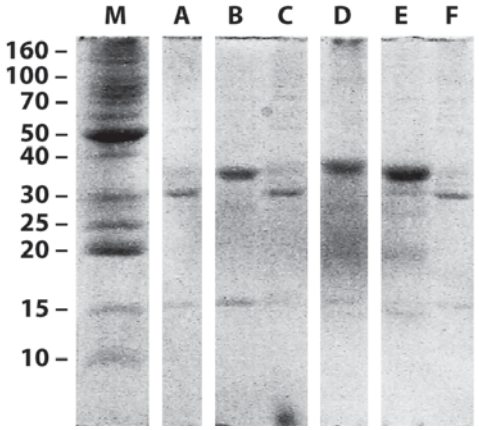

Figure 3.13: SDS-PAGE, stained with Coomassie blue. M: Molecular weight marker with molecular weights marked on the left, A: A14C/C127A/S193C/C232A hVDAC1 treated with CuX_2Ph, B: A14C/C127A/S193C/C232A hVDAC1 treated with DTT and β-mercaptoethanol, C: A14C/C127A/S193C/C232A hVDAC1 stored at 37 °C, D: V75C hVDAC1, E: C127S/C232S hVDAC1, F: A14C/C127A/S193C/C232A hVDAC1 stored at room temperature.

samples is in the state that showed the special gating properties and of which it was hypothesized that it should allow the enriching of the closed state of the protein over time.

To cross-check this hypothesis, line D was loaded with V75C hVDAC1 and line E was loaded with Cysteine-free hVDAC1 (C127S/C232S hVDAC1). In these two cases the protein behaves like in line B – giving further indication that in this case there are indeed no disulfide bridges formed (which is in the case of Cysteine-free hVDAC1 obviously not possible at all). Furthermore, in none of the lines there is a sign of significant oligomerization or intermolecular disulfide bridges formed, as there is no spot with higher molecular weight than approximately 30 kDa.

3.3.2.2 A14C/C127A/S193C/C232A hVDAC1 in liquid state NMR

A14C/C127A/S193C/C232A hVDAC1 delivers well dispersed spectra (see Figure 3.14), that allowed the assignment of 85.6 % of the assignable backbone amide groups. This is only slightly worse than in the *wt* hVDAC1, where at the current state 88.1 % of the backbone amide resonances are assigned (for further information about the current assignment statistics and the improved assignment of hVDAC1 see Chapter 3.1).

The assignment was performed with the help of the already existing assignments of the *wt* hVDAC1 and – which is especially true for the shifted residues – was supported and completely

Dieses Werk ist copyrightgeschützt und darf in keiner Form vervielfältigt werden noch an Dritte weitergegeben werden.
Es gilt nur für den persönlichen Gebrauch.

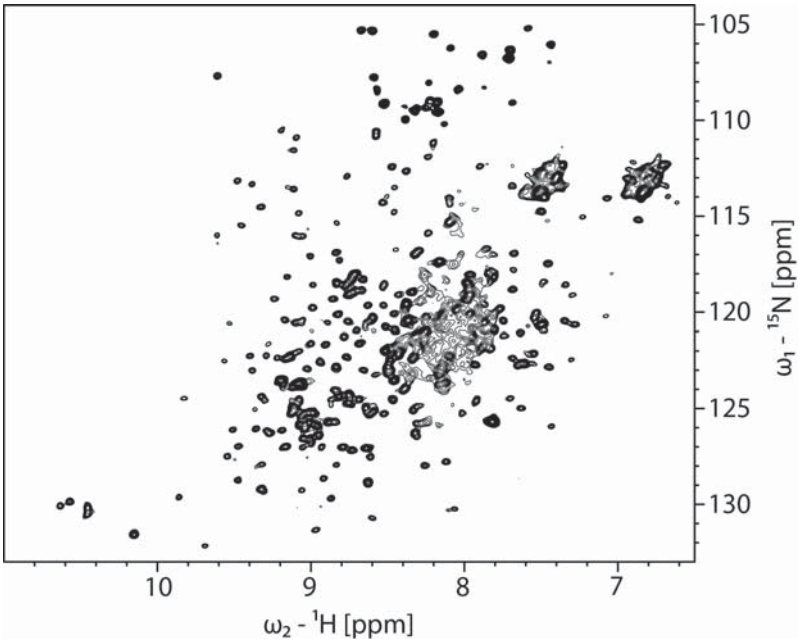

Figure 3.14: ^{1}H,^{15}N TROSY spectrum of A14C/C127A/S193C/C232A hVDAC1.

reviewed via three-dimensional spectra for sequential assignment (TROSY-HNCA and TROSY-HNCO). This way, 81.8 % of the C_α resonances and 72.2 % of the C' resonances could be assigned. All assignments are well spread over the whole protein, including residues in the N-terminal helix as well as residues in the β strands and loops.

To probe for structural and conformational differences between *wt* hVDAC1 and A14C/C127A/S193C/C232A hVDAC1, the chemical shift differences (CSD) of combined ^{1}H and ^{15}N chemical shift between the two proteins were determined. The threshold for unshifted residues was set to 0.05 ppm.

As can be seen in Figure 3.15, the largest CSDs are present in spatial proximity around the four mutation sites. For Alanine-14, shifts are visible in the N-terminal helix and the first half of the linker between α-helix and β-barrel. For the mutations in the β-barrel, the residues with CSD over 0.05 ppm are mostly located in the neighbouring β-strands 7 to 9 (Alanine-127) and β strands 15 to 17 (Alanine-232), respectively. The newly introduced Cysteine-193 causes CSDs of over 0.05 ppm in a slightly bigger range, spanning from β-strand 12 to 14 and including scattered residues in strands 11 and 15, which can explained by the fact that this residue is attached by the likewise newly introduced disulfide bond to the N-terminal helix and Cysteine-14, respectively. Thus, this mutation

Dieses Werk ist copyrightgeschützt und darf in keiner Form vervielfältigt werden noch an Dritte weitergegeben werden.
Es gilt nur für den persönlichen Gebrauch.

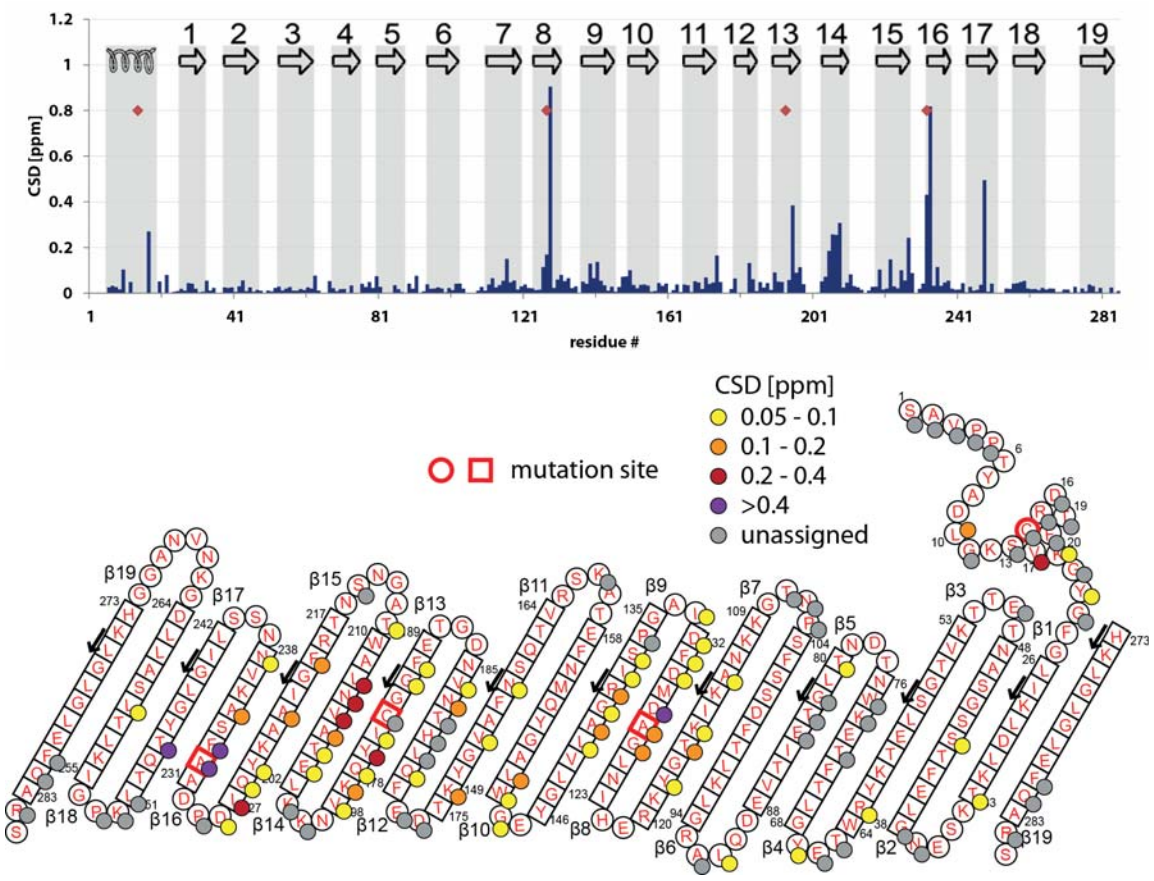

Figure 3.15: CSD of A14C/C127A/S193C/C232A hVDAC1 in comparison to *wt* hVDAC1. Chemical shift differences induced by the A14C/C127A/S193C/C232A quadruple mutations in dependence of the residue number (top) and mapped to the topology map of hVDAC1 (bottom). In the upper plot, the mutation sites are marked with red diamonds and the secondary structure of the protein is indicated.

is causing larger conformational disturbances in the direct neighbourhood because the distance between these two residues is roughly, but not perfectly the same as the length of the S-S bond. Based on the X-ray structure of mVDAC1, mutagenesis with PyMol shows that the newly introduced Sulfides are 1.7 Åapart from each other, while a disulfide bridge is approximately 2.05 Ålong.

Additionally, two residues in β strand 12 (Leucine-180 and Histidine-181) that were previously assigned in the wild type spectra as well as the mutated Cysteine-193 itself could not be assigned. In general, the residues which show significant CSD in the β strands are shifted by considerable amounts of up to nearly 1 ppm. However, in the barrel and helix regions that are distant to the mutation sites, the CSDs are significantly lower and are nearly completely falling under the threshold of 0.05 ppm.

Dieses Werk ist copyrightgeschützt und darf in keiner Form vervielfältigt werden noch an Dritte weitergegeben werden.
Es gilt nur für den persönlichen Gebrauch.

These findings can be compared with the spectral behaviour of C127S/C232S hVDAC1 in comparison to *wt* hVDAC1. As can be seen in the according plot, the CSD profile looks very similar to the one obtained by comparing A14C/C127A/S193C/C232A hVDAC1 with *wt* hVDAC1. (See Figure 3.16) Only difference are the high CSD values around the two mutation sites Alanine-14 and Serine-193 missing or being there additionally, respectively. It is known that C127S/C232S hVDAC1 is behaving like *wt* hVDAC1 in BLM measurements and is in the open state in liquid state NMR samples.[146] Taken together with the fact that the CSD profiles caused by the mutations A14C and S193C do not differ significantly from the ones observed for C127S and C232S in extent and strength, it is concluded that the CSDs visible in A14C/C127A/S193C/C232A hVDAC1 are solely caused by the mutations being present and are no sign for conformational changes in the mutant or the mutant being in the closed state of the protein.

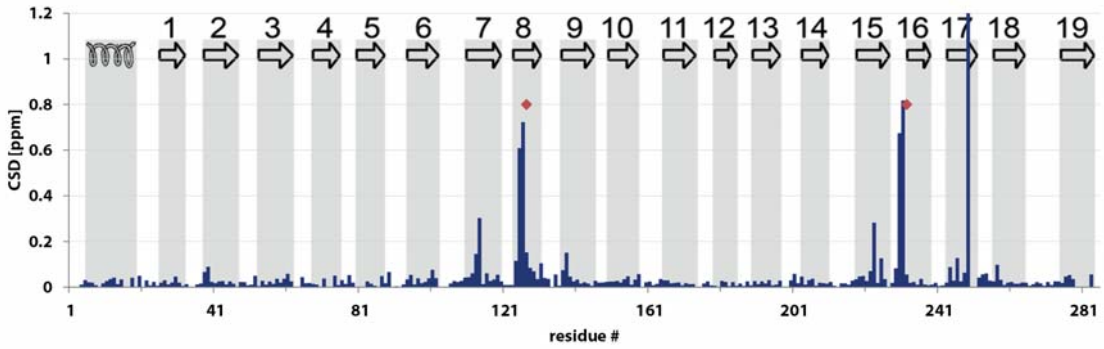

Figure 3.16: CSD of C127SC232S hVDAC1 in comparison to *wt* hVDAC1. Chemical shift differences induced by the C127S/C232S mutations in dependence of the residue number. The mutation sites are marked with red diamonds and the secondary structure of the protein is indicated.

3.3.3 Stiffening the linker between α-helix and β-barrel

The approach presented here is based on a publication by Geula *et al.* from 2012.[145] In that paper the authors describe a G21V/G23V rVDAC1 mutant with interesting properties.

The linker between α-helix and β-barrel in rVDAC1 consists of a triple-Glycine motif $G^{21}YGFG^{25}$ that is highly conserved among mammals.[147] (For example, the respective five residue sequence is identically present also in mVDAC1 and hVDAC1.) As there is a plethora of evidence that the N-terminal helix plays an important role and is moving during the gating process of the channel[100], mutations in the linker might have a crucial influence on the gating. Glycine is the

Dieses Werk ist copyrightgeschützt und darf in keiner Form vervielfältigt werden noch an Dritte weitergegeben werden.
Es gilt nur für den persönlichen Gebrauch.

only non-chiral proteinogenic amino acid and as such has a larger conformational freedom than all other proteinogenic amino acids, being at the same time able to behave as a quasi L and quasi D conformer.[148] Because of this, Glycine rich sequences (GRS) are often found in hinge regions of proteins, allowing flexibility in these regions.

In the described mutant two of the three Glycines in the linker region are replaced by Valine. This obviously makes the linker more stiff and at the same time restricts the conformational freedom of linker and N-terminal helix. As such, an impact of this mutation on the gating properties of the channel can be expected – and this was in deed described by Geula *et al.* (see Figure 3.17).

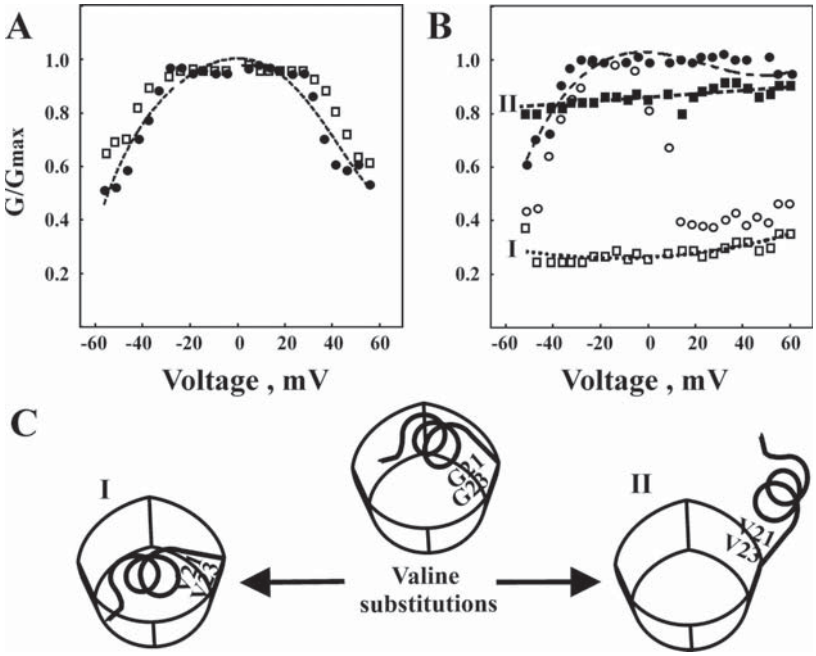

Figure 3.17: G21V/G23V rVDAC1 showing various gating profiles. A: Gating profile of the mutant in which the mutant (empty squares) is behaving like the *wt* rVDAC1 (black circles). B: Representative gating profiles of the same channel of the mutant in which the channel is closed in all voltages (empty squares, type I), open in all voltages (black squares, type II) or gating in totally unusal manner (empty circles, black circles). C: Interpretation of the gating types as provided by Geula *et al.* Type I (fixed in closed state) has the helix fixed inside the pore, type II (fixed in open state) has the helix pointing out of the channel. The figure is reproduced from Geula *et al.*[145]

While the bilayer-reconstituted mutant is able to show a gating behavior that is similar to the one of the *wt* rVDAC1 (and such also as hVDAC1 and mVDAC1) in approximately 50 % of the recorded traces, it also often fails to do so. In the other 50 % of the recorded traces the authors saw unusual behavior, reaching from cases where the mutant is locked in the closed state independently from the applied voltage, over cases where the mutant is locked in the open state independently

Dieses Werk ist copyrightgeschützt und darf in keiner Form vervielfältigt werden noch an Dritte weitergegeben werden.
Es gilt nur für den persönlichen Gebrauch.

from the applied voltage, to cases where the mutant is switching between open and closed state at unusual voltages or only in negative or positive potentials. The authors conclude, that these results demonstrate the function of the GRS in conferring flexibility to the N-terminal helix.

There are two interesting points in their findings and theory, respectively. First, they give a number of 50 % for the share of channels that are gating normally (and thus another 50 % share of channels that are gating annormally). Usually the number of channels where a gating event during a single voltage scan can be observed is significantly lower and not unusually just around 10 %. (E.g. the previously studied mutant described by Mertins *et al.*[52] shows gating in 8 % of the recorded traces, according to them.) The mutant thus shows gating behavior of any kind with much higher probability than usual. Second, the gating model they are proposing (see Figure 3.17) is directly contradictory to the nowadays widest accepted models and calculations, where the helix is moving out of the channel during closure and is staying inside of the pore in the open state.[91]

Nevertheless, the findings of Geula *et al.* are also very interesting in the light of NMR spectroscopy. The described type-I-gating features pores that are in the closed state when there is no potential applied – exactly the same situation as one has it in the the NMR tube. It is thus expectable to see the closed state of the protein at least to some extent when expressing and refolding it to micelles and studying it with the means of NMR spectroscopy.

The following chapters are describing the results with the G21V/G23V hVDAC1 mutant expressed for NMR spectrospic investigations, the development of a Quintuple hVDAC1 mutant and the results yielded with this construct as well as the development of a model for the closed state based on modifications of Quintuple hVDAC1.

3.3.3.1 Changing the expression system to the pET28a expression vector

Because all previous studies in our group were performed on hVDAC1 and the crucial part of the mutant described by Geula *et al.*, namely the GRS in the linker between α-helix and β-barrel is conserved between rVDAC1 and hVDAC1, it was decided to express a hVDAC1 mutant instead of a rVDAC1 mutant with the same mutations as described – G21V/G23V hVDAC1.

Dieses Werk ist copyrightgeschützt und darf in keiner Form vervielfältigt werden noch an Dritte weitergegeben werden.
Es gilt nur für den persönlichen Gebrauch.

It became then evident that the G21V/G23V hVDAC1 mutant does not express in the previously used pQE60 vector which allows the expression of hVDAC1 with the correct N-terminus lacking RGS after the starting Methionine. After scanning possible expression vectors it was possible to express the G21V/G23V hVDAC1 mutant with the pET28a expression vector. To validate that hVDAC1 samples expressed in this new system are folded correctly, a *wt* hVDAC1 sample as reference sample was produced by using the pET28a expression vector.

This *wt* hVDAC1 sample shows nicely dispersed ^{15}N-TROSY spectra that allowed the assignment of basically all for the wild type known residues without the need to record any further experiments just by comparing the ^{15}N-TROSY spectra of the *wt* hVDAC1 samples expressed in the different expression vectors. (See Figure 3.18)

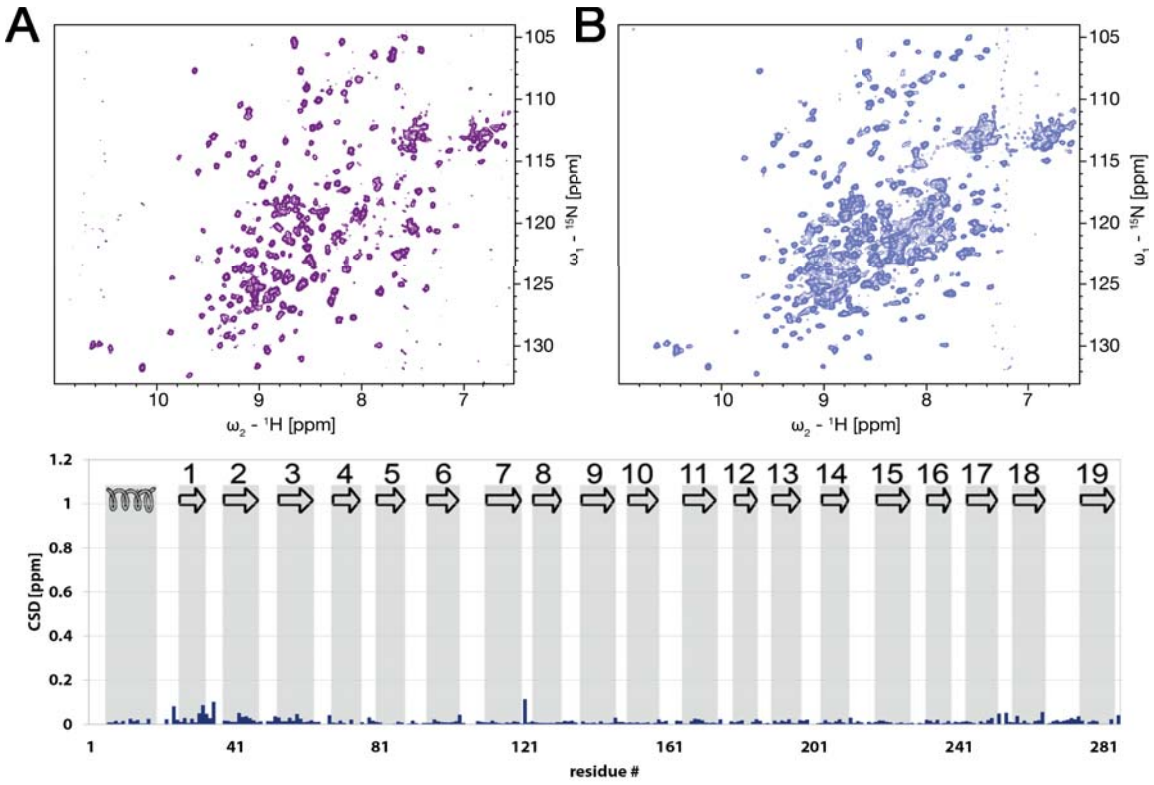

Figure 3.18: Comparison of *wt* hVDAC1 samples expressed in different expression vectors. The ^{15}N-TROSY spectra of *wt* hVDAC1 expressed in the pQE60 vector (A) and the pET28a vector (B) are nearly identical. This is represented in the CSD graph (C).

Although the *wt* hVDAC1 spectrum expressed with the new pET28a vector shows higher amounts of miss-folded protein (regions at proton shift of 8 ppm and 9 ppm with broadened signals), nearly all defined resonances are at identical positions as in the spectrum of *wt* hVDAC1 expressed with the old

Dieses Werk ist copyrightgeschützt und darf in keiner Form vervielfältigt werden noch an Dritte weitergegeben werden.
Es gilt nur für den persönlichen Gebrauch.

pQE60 vector. The only exceptions are a very few residues in loops (e.g. Glutamate-121 being the most prominent one) and residues in the spatial proximity of the C-terminal end, where for technical reasons the sequence does not end with RS but with LE, which could be interpreted as double-mutation that is causing slight resonance shifts. It was thus concluded that the pET28a expression vector is suitable to express hVDAC1 samples and does not have any influence on the folding or properties of the final protein after the expression, opening the possibility to study G21V/G23V hVDAC1 with NMR spectroscopic methods.

3.3.3.2 Experiments on G21V/G23V hVDAC1

After G21V/G23V hVDAC1 could finally be expressed, a ^{1}H-^{15}N-TROSY spectrum was recorded to evaluate the sample quality and to start the assignment procedure. Unlike in the most previous cases, the spectral behavior of this mutant turned out the be quite bad. Although the protein was obviously folded correctly, as the signals were dispersed in the usual range (from circa 7.0 to 10.0 ppm in the proton dimension) at 37 °C, the linewidths of the signals were increased significantly. (See Figure 3.19.)

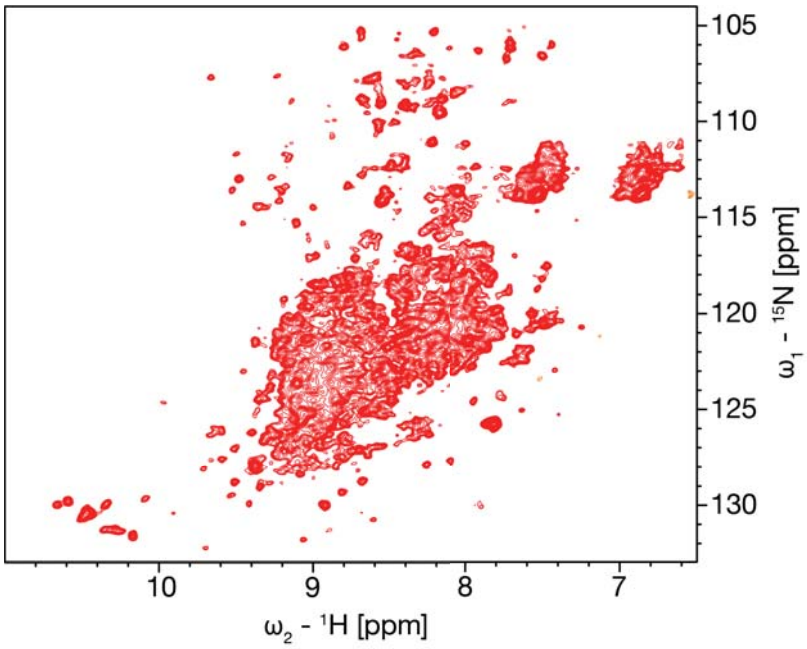

Figure 3.19: ^{1}H-^{15}N-TROSY spectrum of G21V/G23V hVDAC1 at 37 °C. The signals are dispersed in the usual range, but are severely broadened, preventing an assignment *via* 3D spectra.

Dieses Werk ist copyrightgeschützt und darf in keiner Form vervielfältigt werden noch an Dritte weitergegeben werden.
Es gilt nur für den persönlichen Gebrauch.

Despite the severe broadening of the observed resonances it was tried to perform a tentative assignment of the resonances that could at least be identified as single resonance, even if broadened. This tentative assignment was based on simple comparison of the existing 2D ^{1}H-^{15}N-TROSY spectra, as 3D spectra for sequential assignment were not available for G21V/G23V hVDAC1 and recording them was, given the severe broadening of the lines, scrapped as it would not have any prospect of success.

Based on this approach there were some resonances that could be assigned with relatively high certainty. Either because they are isolated in both the TROSY-spectra of G21V/G23V hVDAC1 and *wt* hVDAC1 (which is true for Threonine-6, Glycine-38 or Glycine-145, for example) or they are isolated in the spectrum of *wt* hVDAC1 and there is a clear maximum in the immediate proximity in the mutant spectrum. Even if it might be located in the region where the broadened resonances are completely merged (which is true for Cysteine-127, Alanine-151 or Tryptophane-210, for example). Also, there are some resonances from the *wt* hVDAC1 spectrum where this kind of assignment is only possible with high uncertainty.

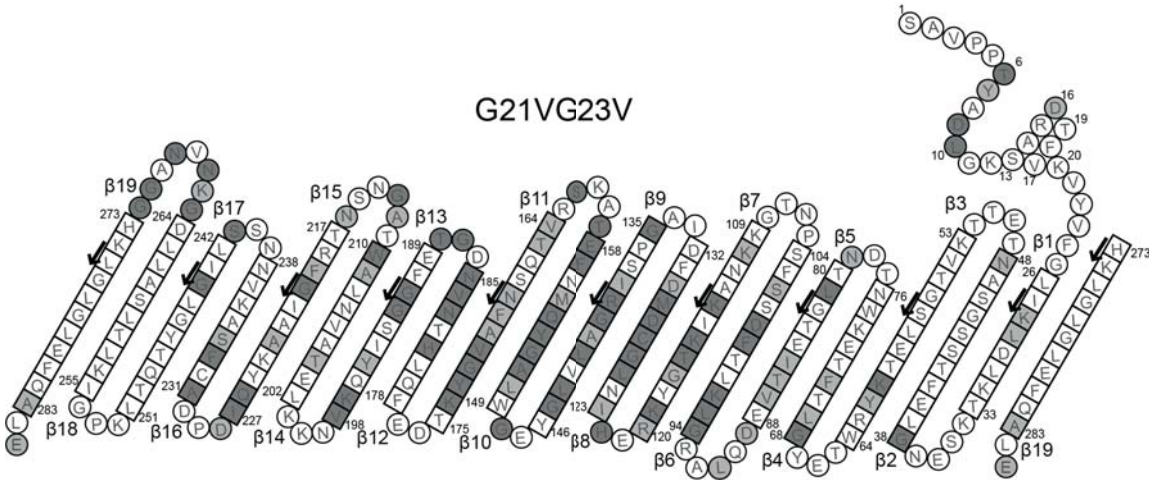

Figure 3.20: Topology map of G21V/G23V hVDAC1 with possible assignments based on similar resonance positions in comparison to *wt* hVDAC1. Residues that have a possible assignment that is relatively clear are colored in dark gray. Resonances where the assignment is very ambiguous are colored in light gray.

All in all, even based on this very non-conservative approach there are just 106 resonances that could be identified as single resonance and are placed at a similar frequency like resonances in the existing *wt* hVDAC1 spectra. The overview of these resonances is shown in Figure 3.20. They comprise 38.1 % of the assignable residues in the whole sequence or 41.7 % of the residues in the

Dieses Werk ist copyrightgeschützt und darf in keiner Form vervielfältigt werden noch an Dritte weitergegeben werden.
Es gilt nur für den persönlichen Gebrauch.

β-barrel, respectively. Interestingly, there is a clear prevalence of these possible assignments in the region where in the high-resolution 3D structures of hVDAC1 the N-terminal α-helix is connected to the β-barrel. This points to that the α-helix is still stabilizing the barrel in that region to some extent.

To get more insight into why the resonances in the ^{1}H-^{15}N-TROSY spectrum are broadened, several more experiments were performed. The recording of the ^{1}H-^{15}N-TROSY spectra was repeated at a lower temperature than the usually used 37 °C as this could slow down possible motion in the protein to make the broadened lines split up into several lines. As it turns out, reducing the temperature does not help to better resolve the broadened resonances. Instead it quenches the signal yielded from the protein as barely any resonances are retained at 5 °C. (See Figure 3.21)

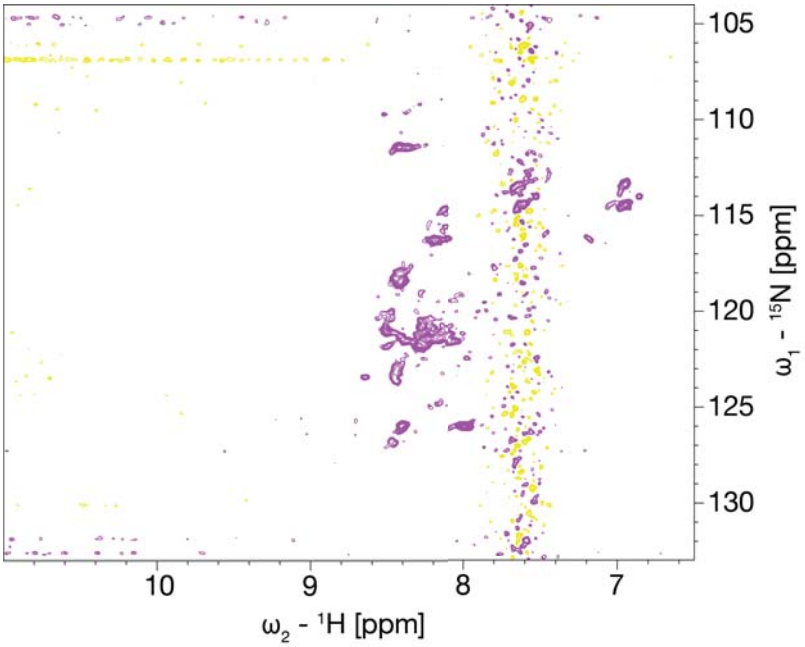

Figure 3.21: ^{1}H-^{15}N-TROSY spectrum of G21V/G23V hVDAC1 at 5 °C.

To also exclude the possibility that the lines in the ^{1}H-^{15}N-TROSY spectrum are broadened because for some reason the G21V/G23V hVDAC1 mutant is prone to oligomerization or dimerization and the emerging oligomers are to large to be detected by transverse relaxation-optimized spectroscopy (as it was observed for T19C/C127S/C232S hVDAC1 by Saskia Villinger)[74], ^{1}H 1D (1–1) echo experiments were performed to estimate the overall rotational correlation time of the protein.[114] Bigger entities than the usual combination of one hVDAC1 channel and the surrounding

Dieses Werk ist copyrightgeschützt und darf in keiner Form vervielfältigt werden noch an Dritte weitergegeben werden.
Es gilt nur für den persönlichen Gebrauch.

LDAO micelle, weighing usually roughly 140 kDa, should have a significantly elevated rotational correlation time. However, this could be ruled out. Based on the measurements, for G21V/G21V hVDAC1 rotational correlation times of 26 ns in the folded and 37 ns in the unfolded region (^{1}H shift of 9.25 ppm and 7.5 ppm as representative positions, respectively) were estimated, which fits well to previously reported values for the *wt* hVDAC1 of 23 ns in the folded and 35 ns in the unfolded region, respectively. (For the dimer-forming T19C/C127S/C232S hVDAC1 values of 50–60 ns were reported.)

Finally, the behavior of the resonances that could be found in the ^{1}H-^{15}N-TROSY spectrum was examined in regard of the linewidth these resonances are showing in dependence of the magnetic field used for measurement. Solely based on the TROSY effect one would expect that the lines should become sharper due to the improved compensation of the transversal relaxation time T_2 when switching from 600 Mhz to 800 MHz measurement frequency [149,150]. However, as can be seen in figure 3.22, the opposite is the case.

For this analysis, not only completely isolated resonances were taken into account, but also some resonances in the region where the single resonances are due to shifts and line broadening to a large extent not identifiable anymore. The linewidths were determined by CcpNmr Analysis. All resonances had thus to be strong enough in both analyzed spectra that their linewidth could be calculated by the program without distortions due to neighboring resonances. The analyzed resonances were refined and cases where shoulders or neighboring resonances distorted the result, are excluded. As Figure 3.22 B shows, there are some few resonances that don't broaden with increasing field strength, but the overall tendency is clearly visible: higher field strength is broadening the resonances.

All in all it was concluded that the resonances in G21V/G23V hVDAC1 are broadened due to chemical exchange that is intermediate on the NMR timescale, which does not allow a deeper analysis of the spectra yielded. This could indeed be seen in line with the results of Geula *et al.*, as they showed that the mutant is switching between open and closed state to a large part totally independent of the applied potential. If this is happening in a speed which is intermediate on the NMR timescale, this would totally explain the results that we got. Also the fact that certain resonances don't broaden

Dieses Werk ist copyrightgeschützt und darf in keiner Form vervielfältigt werden noch an Dritte weitergegeben werden.
Es gilt nur für den persönlichen Gebrauch.

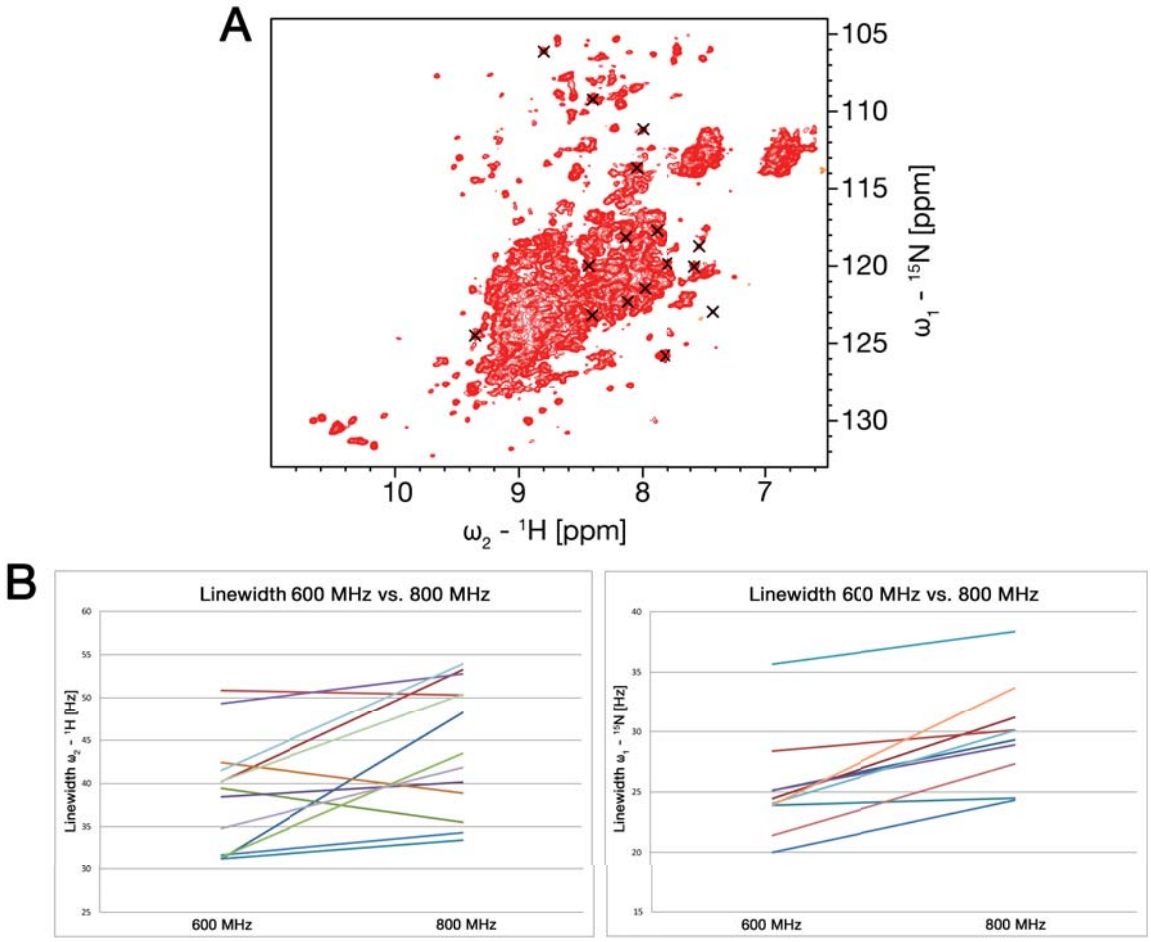

Figure 3.22: Linewidths of several residues in G21V/G23V hVDAC1. A: Resonances that were chosen for analysis are marked with "x". B: Linewidths of the respective resonances at 600 and 800 MHz in proton (left) and nitrogen dimension (right). Although there are some outliers the overall trend is that the linewidth of every resonance is increasing with increasing field strength.

with increasing field could just mean that they are less affected by the motion that underlies the broadening effect.

Nevertheless, to check the results described by Geula *et al.*, in collaboration with Roland Benz (Department of Life Sciences and Chemistry, Jacobs University Bremen gGmbH) we performed own BLM measurements on G21V/G23V hVDAC1. Due to lack of material, the voltage dependency of the protein could not be investigated. Still it could be shown that there are some pores with the usual conductance of 3.9 nS in 1 M KCl and a lot of pores with lower conductance – being in line with the results published. (Data not shown.)

Dieses Werk ist copyrightgeschützt und darf in keiner Form vervielfältigt werden noch an Dritte weitergegeben werden.
Es gilt nur für den persönlichen Gebrauch.

3.3.3.3 Experiments on G21V hVDAC1

After the result that spectra of G21V/G23V hVDAC1 are broadened due to intermediate exchange in NMR and are thus not usable for deeper analysis as described in the last chapter, the next step was to have a look into which of the two mutated Glycines or introduced Valines, respectively, might be more important for the properties Geula *et al.* described for the mutant. When checking the conformation of the two Glycines in the crystal structure of mVDAC1, it turns out that Glycine-23 adopts a conformation that also L amino acids can adopt, while Glycine-21 has a conformation that, when replaced by Valine, only D-Valine could adopt. (ϕ(G21) = 82.6°, ϕ(G23) = −151.2°, See Figure 3.23) Therefore we hypothesized that the mutation G21V could have bigger responsibility for the mutant properties and at the same time by only replacing one instead of two Glycines in the linker, the stiffening effect could be weakened such that a timescale of movement is reached that makes it possible to study the mutant by NMR spectroscopy again.

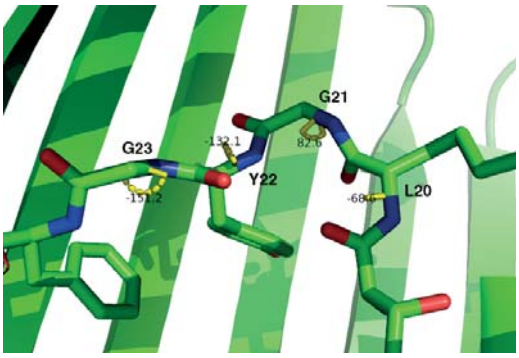

Figure 3.23: Glycine-21 and Glycine-23 in the 3D structure of mVDAC1. While Glycine-23 adopts a L like configuration (ϕ(G23) = −151.2°), Glycine-21 could only be replaced by D-Valine without changing the backbone angles (ϕ(G21) = 82.6°).

G21V hVDAC1 could be expressed in the pET28a expression vector and was studied with ^{1}H-^{15}N-TROSY experiments. As it turns out, similar like it was the case with G21V/G23V hVDAC1, also this mutant delivers spectra that show severe resonance broadening, although this broadening effect is far less strong than with G21V/G23V hVDAC1 and the ^{1}H-^{15}N-TROSY spectrum is overall of significantly better quality. (See Figure 3.24)

As described for G21V/G23V hVDAC1 a tentative assignment by comparing the available 2D ^{1}H-^{15}N-TROSY spectra was also performed for G21V hVDAC1. The number of residues for which

Dieses Werk ist copyrightgeschützt und darf in keiner Form vervielfältigt werden noch an Dritte weitergegeben werden.
Es gilt nur für den persönlichen Gebrauch.

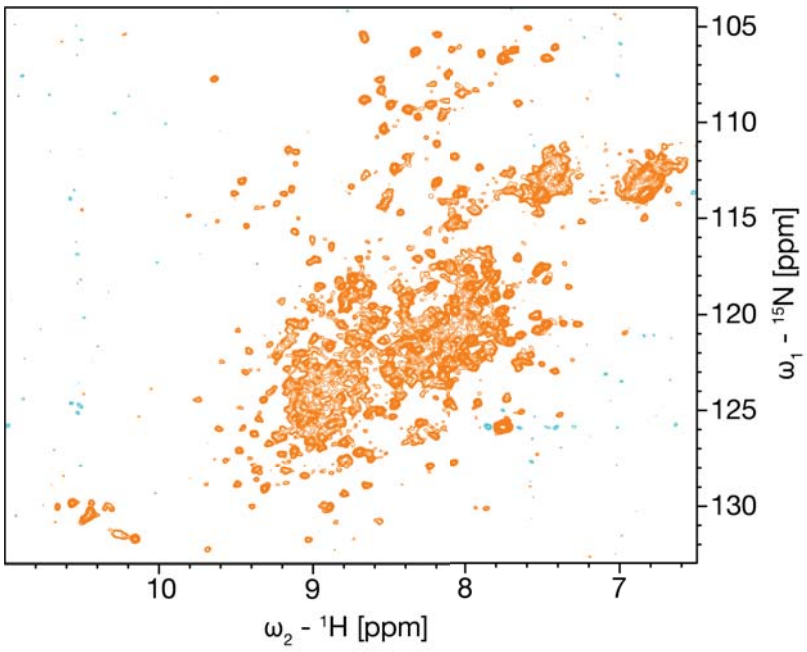

Figure 3.24: ^{1}H-^{15}N-TROSY spectrum of G21V hVDAC1 at 37 °C. The resonances are dispersed in the right range for folded proteins, but are broadened due to intermediate exchange.

for which assignments can be made by matching the amide signals with those from *wt* hVDAC1 is increased in G21V hVDAC1 to 144 residues, which corresponds to 51.8 % of the whole protein sequence or 56.3 % of the β-strands. Again, in the region where in the high resolution 3D structures of mVDAC1 and hVDAC1 the α-helix is anchored to the barrel, *i.e.* in the β-strands 7 to 13, the number of these possible assignments is significantly increased. Still, the number of possible assignments based on this approach is far from what can be assigned in *wt* hVDAC1 or E73V hVDAC1. (See Figure 3.25)

The ^{1}H-^{15}N-TROSY spectra of G21V hVDAC1 are of better quality than these of G21V/G23V hVDAC1, but still show signs of broadening due to intermediate exchange (which was understood as movement causing the special gating properties described by Geula *et al.*). Based on this fact it was hypothesized that it might – contrary to G21V/G23V hVDAC1 – be possible to reach a better assignment. To do this and to confirm the assignments that are until now only based on similar resonance positions a 3D TROSY-HNCA spectrum was recorded. After recording this spectrum it turned out that this assumption was wrong, as the recorded TROSY-HNCA does not show any signals above the noise level. Additionally, after recording the TROSY-HNCA, the sample presented itself com-

Dieses Werk ist copyrightgeschützt und darf in keiner Form vervielfältigt werden noch an Dritte weitergegeben werden.
Es gilt nur für den persönlichen Gebrauch.

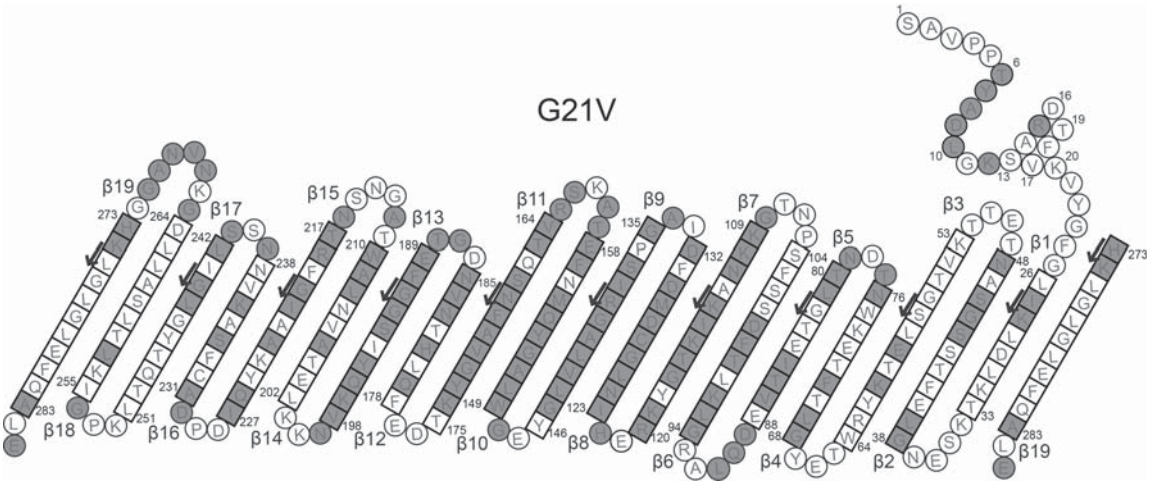

Figure 3.25: Topology map of G21V hVDAC1 with possible assignments based on similar resonance positions in comparison to *wt* hVDAC1. Residues that have a possible assignment are colored in dark gray.

pletely unfolded in the subsequently recorded ^{1}H-^{15}N-TROSY, pointing to that the G21V mutation is decreasing the sample's stability at the measurement temperature of 37 °C dramatically.

Also the G21V hVDAC1 mutant has been studied with BLM measurements in collaboration with Roland Benz, Jacobs-University Bremen. In these measurements, only the normal gating channels were taken into account. G21V hVDAC1 has an open channel conductance of 3.8 $\pm$ 0.16 nS in 1 M KCl, which is slightly lower than for *wt* hVDAC1. Furthermore, it shows significantly more distinct gating, meaning that it is gating at way lower potentials than usual: the voltage dependency starts already at around 20 mV and is completely shaped at potentials of around 50 mV. Interestingly, for this mutant one could not observe channels that are already closed at zero potential.

3.3.3.4 Development of a Quintuple hVDAC1 mutant

After the results with G21V/G23V hVDAC1 and G21V hVDAC1, the available information was reinterpreted. From the ^{1}H-^{15}N-TROSY spectra of these two mutants is was obvious that the barrel is too much destabilized such that intermediate exchange is causing severe resonance broadening in these spectra. On the other hand, it is known since several years, that the E73V mutation is stabilizing the barrel and improving the spectra quality dramatically. This had theoretically been proven by Villinger *et al.* [132] and can practically be seen in that this spectra quality lead to the

Dieses Werk ist copyrightgeschützt und darf in keiner Form vervielfältigt werden noch an Dritte weitergegeben werden.
Es gilt nur für den persönlichen Gebrauch.

dramatically improved NOE network, the possibility to record a TROSY-HNCACB spectrum and the new high resolution 3D structure of E73V hVDAC1 described in this thesis.

Furthermore, the BLM measurements performed by Roland Benz showed, that it is necessary to have both the G21V and the G23V mutation present in the sample to be able to observe channels that are in the closed state at low or zero potentials applied to the membrane, as this could only be observed for G21V/G23V hVDAC1 but not for G21V hVDAC1.

Additionally, the fact that G21V hVDAC1 presented itself completely unfolded after the measurement of the TROSY-HNCA, calls for stabilization of the mutant not only dynamically but also thermodynamically such that the stability over time at 37 °C has to be improved. For this, additionally to the E73V mutation the two native Cysteines were removed, which is taking the system the possibility to denaturize or dimerize, respectively, by forming disulfide bonds. As mentioned earlier the removal of the Cysteines has already been shown to have no influence on the gating properties of the channel.[146] Given the fact that Cysteine-127 is pointing to the micelle, Cysteine-232 is pointing to the water inside the pore and with the aim to replace the Cysteines with the most similar other amino acids possible it was decided to replace Cysteine-127 by Alanine (which is apolar and thus disturbing the micelle less) and Cysteine-232 by Serine (which is polar and thus better fitting to the water filled interior of the channel).

All in all this leads to a Quintuple hVDAC1 construct, namely G21V/G23V/E73V/C127A/C232S hVDAC1, which was designed to combine the desired special gating properties with the necessary stability for NMR measurements.

Dieses Werk ist copyrightgeschützt und darf in keiner Form vervielfältigt werden noch an Dritte weitergegeben werden.
Es gilt nur für den persönlichen Gebrauch.

3.4 Experiments on Quintuple hVDAC1 and development of a model of the closed state of hVDAC1

Quintuple hVDAC1 was expressed in the pET28a expression vector as it was done with G21V/G23V hVDAC1 and G21V hVDAC1. Unlike these two mutants, Quintuple hVDAC1 indeed delivers ^{1}H-^{15}N-TROSY spectra in which the resonances are not broadened due to intermediate exchange. (See Figure 3.26)

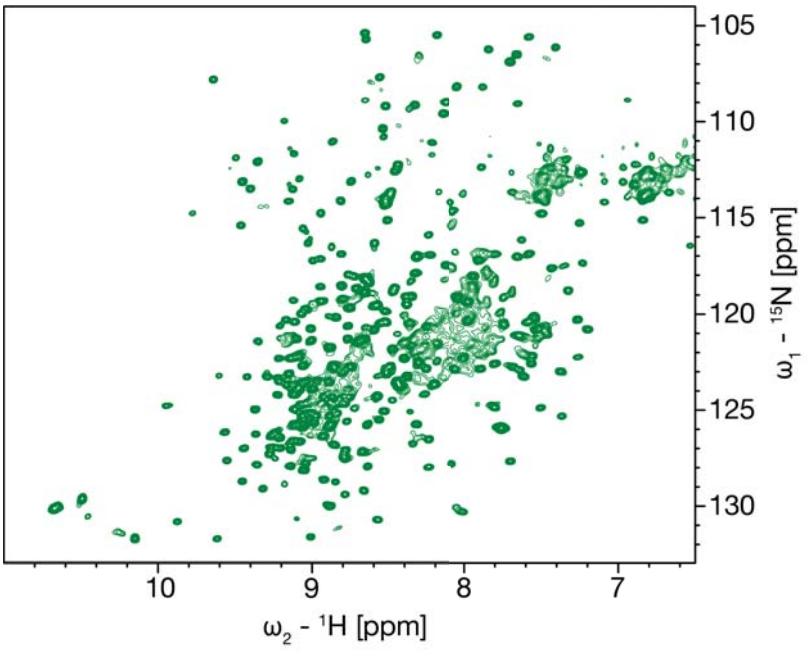

Figure 3.26: ^{1}H-^{15}N-TROSY spectrum of Quintuple hVDAC1 at 37 °C. The dispersion of the resonances is indicating a correct fold of the protein. Different from G21V and G21V/G23V hVDAC1, the resonances are not broadened in a way which renders interpretation of the spectra impossible.

Based on the good spectral behavior of Quintuple hVDAC1, assignment of the protein was possible and because of the importance of this mutant a lot of effort has been put into it. To assign Quintuple hVDAC1, ^{1}H-^{15}N-TROSY spectra and already existing assignments for *wt* hVDAC1 were used first. To support the assignment an E73V/C127A/C23S hVDAC1 mutant was also expressed in the pET28a vector as a wild-type-like reference sample (as in comparison Quintuple hVDAC1 and E73V/C127A/C232S hVDAC1 just differ by the G21V/G23V mutation). This is the mutant where as described in Chapter 3.1.1 recording a TROSY-HNCACB spectrum was successful for the first time. This way, a good reference spectrum and reference assignment was available that could then

Dieses Werk ist copyrightgeschützt und darf in keiner Form vervielfältigt werden noch an Dritte weitergegeben werden.
Es gilt nur für den persönlichen Gebrauch.

be used to assign Quintuple hVDAC1. Additionally, the assignment was performed with the help of further recorded spectra: a mixed-time parallel evolution HMQC-NOESY as described and previously recorded for other hVDAC1 mutants by Saskia Villinger[74,111] to yield spatial connections between the residues, a TROSY-HNCA to yield the sequential connections and – after it turned out with E73V/C127A/C232S hVDAC1, that recording a TROSY-HNCACB spectrum is possible – also a TROSY-HNCACB spectrum.

With the help of these spectra, it was possible to nearly reach a level of assigned backbone resonances similar to E73V/C127A/C232S hVDAC1. Presently, the assignment statistics are as follows: There are 254 assigned amide backbone groups in the overall protein, corresponding to 91.4 % of the assignable amide groups (for comparison 88.1 % are assigned in *wt* hVDAC1 and 92.1 % are assigned in E73VC127AC232S hVDAC1). In the β-strands, 189 amide backbone groups are assigned, which is corresponding to 98.4 % of the assignable amide groups (*wt* hVDAC1: 94.8 %, E73V/C127A/C232S hVDAC1: 98.4 %). Thus, the backbone amide assignment in Quintuple hVDAC1 is of even better quality than it can be reached with *wt* hVDAC1 and only slightly worse than in the reference E73V/C127A/C232S hVDAC1. With the TROSY-HNCA and the TROSY-HNCACB also the C_α and C_β resonances could be assigned. However, in the triple-resonance spectra the differences in overall sample quality, sample stability and signal strength are, due to the generally decreased sensitivity in these kind of spectra and the required measurement time, more pronounced, such that here the level of assignment is significantly lower for Quintuple hVDAC1. Presently, 90.2 % of the C_α and 54.1 % of the C_β atoms are assigned, which is less than for E73V hVDAC1 or E73V/C127A/C232S hVDAC1 (C_α: 95.4 %, C_β: 87.4 %), respectively. Importantly, there is generally only one set of resonances that could be observed in the Quintuple hVDAC1 spectra.

To now assess differences between Quintuple hVDAC1 and E73V/C127A/C232S hVDAC (which will from now on be used as a wild-type-like reference mutant as the only difference between these two mutants is the G21V/G23V mutation that is inducing the protein to be partly closed), the chemical shift differences (CSD) and intensity changes between the two mutants were investigated. As can be seen in Figure 3.27, only small CSDs can be observed in the β-strands 4 to 13 of the barrel. The largest CSDs are located in the β-strands 14 to 19 and β-strand 1 as well as in the proximity

Dieses Werk ist copyrightgeschützt und darf in keiner Form vervielfältigt werden noch an Dritte weitergegeben werden.
Es gilt nur für den persönlichen Gebrauch.

of the loop from β-strand 2 to 3, indicating conformational changes in these regions. The α-helix nevertheless seems to be only affected in the C-terminal end, which anyway has to be taken with care, as due to the missing sequential links in the helix assignment of a possible second conformation is difficult to impossible. However, this is strongly suggesting that the N-terminal helix is not unfolding upon the changes that can be observed in this mutant.

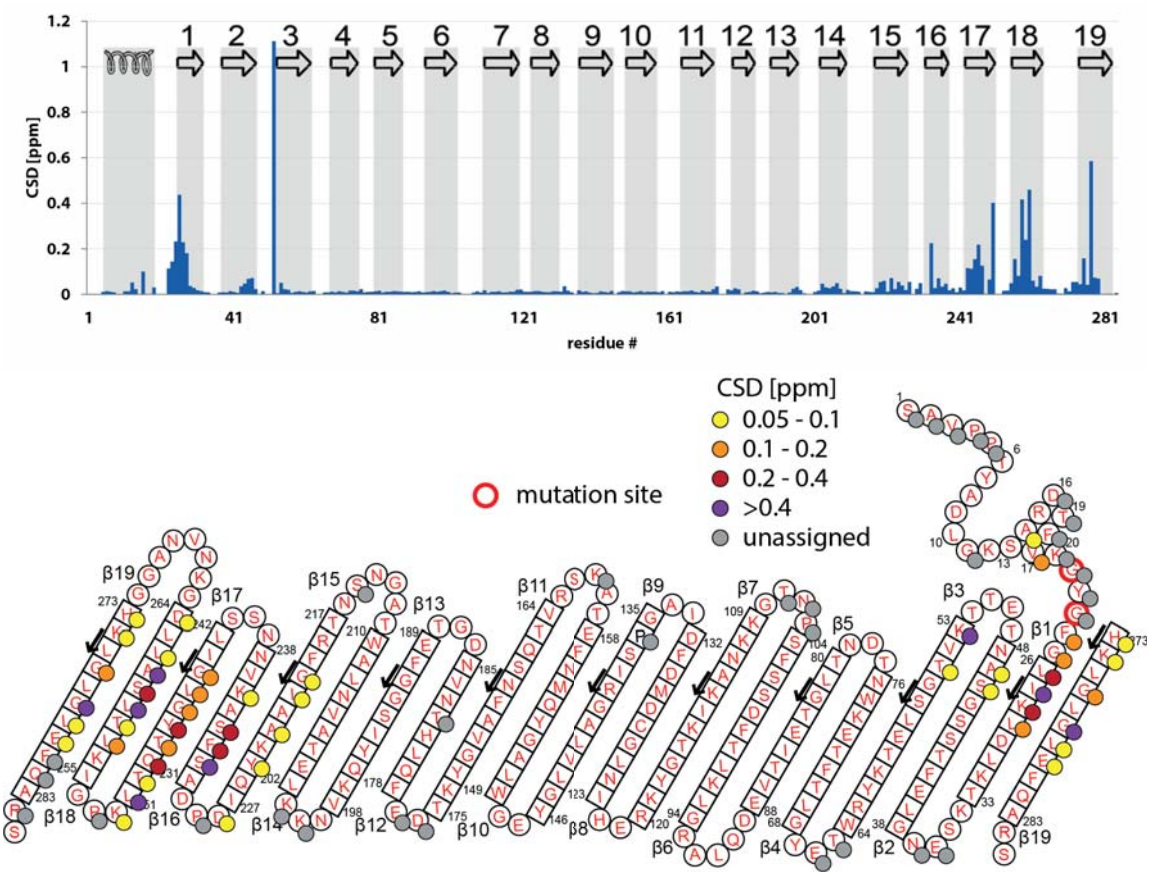

Figure 3.27: CSD of Quintuple hVDAC1 in comparison to E73V/C127A/C232S hVDAC1. Chemical shift differences induced by the G21V/G23V mutations in dependence of the residue number (top) and mapped to the topology map of hVDAC1 (bottom).

Still, the CSDs observable in the last β-strands point to conformational changes there. Additionally, the change of intensity values to asses possible changes in dynamics were investigated. The respective graph can be seen in Figure 3.28. Obviously, some residues in the β-strands 15 to 19 are severely broadened in the Quintuple hVDAC1 mutant, pointing to increased dynamics in these strands. The same is true for residues in the linker and in β-strand 1.

Taken together, by analyzing the ^{1}H-^{15}N-TROSY spectra, first experimental evidence is pointing to some conformational and dynamical changes in the C-terminal β-strands of the β-barrel as well

Dieses Werk ist copyrightgeschützt und darf in keiner Form vervielfältigt werden noch an Dritte weitergegeben werden.
Es gilt nur für den persönlichen Gebrauch.

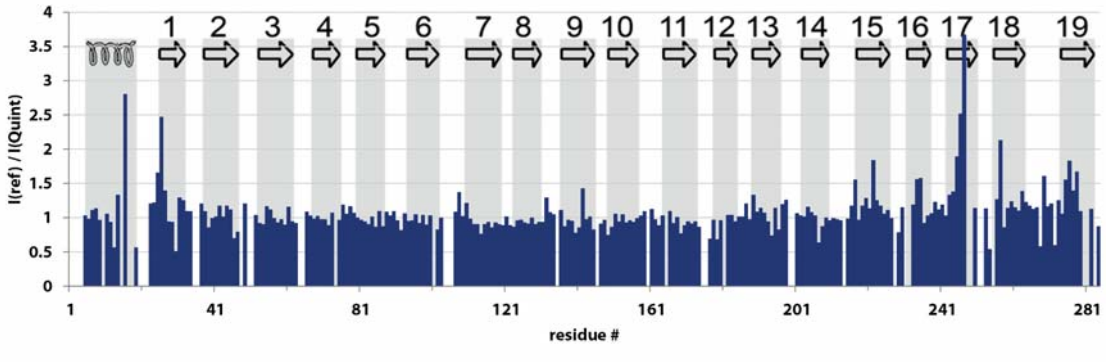

Figure 3.28: Intensity of the resonances of Quintuple hVDAC1 in comparison to E73V/C127A/C232S hVDAC1. The intensity ratio of the resonances of the two mutants E73V/C127A/C232S hVDAC1 and Quintuple hVDAC1 is plotted against the residue number. Ratios greater than 1 indicate weaker resonances in the Quintuple hVDAC1.

as the linker between barrel and helix and the proximity of the point where to linker is connected to the barrel.

3.4.1 Quintuple hVDAC1 behaves like a ΔN construct in BLM measurements

As the experiments on Quintuple hVDAC1 are following the assumption that this mutant is exhibiting the same or very alike gating properties like the G21V/G23V hVDAC1 mutant described by Geula *et al.*, BLM measurements had to be performed with the mutant to confirm this. The BLM measurements were performed by Roland Benz (Department of Life Sciences and Chemistry, Jacobs University Bremen gGmbH), with a part of the NMR sample containing Quintuple hVDAC1 reconstituted in LDAO micelles.

As depicted in Figure 3.29, besides pores with the usual conductance of around 4 nS, Quintuple hVDAC1 shows a lot of pores with lower conductance of slightly above 2 nS at small potentials that are usually not sufficient to induce closing of the channel (10 to 20 mV). While the former channels can close at higher potentials of ± 50 mV, the latter type of channels does never show closure. The channels with conductances of around 4 nS are obviously Quintuple hVDAC1 channels in the open state and thus can close when a higher potential is applied. On the other hand the channels with conductances of slightly above 2 nS resemble channels that are already closed at lower potentials and thus they are not showing gating when the applied potentials are increased. Notably, the channels with closed state-like conductance are showing relatively noisy traces. Overall, the BLM

Dieses Werk ist copyrightgeschützt und darf in keiner Form vervielfältigt werden noch an Dritte weitergegeben werden.
Es gilt nur für den persönlichen Gebrauch.

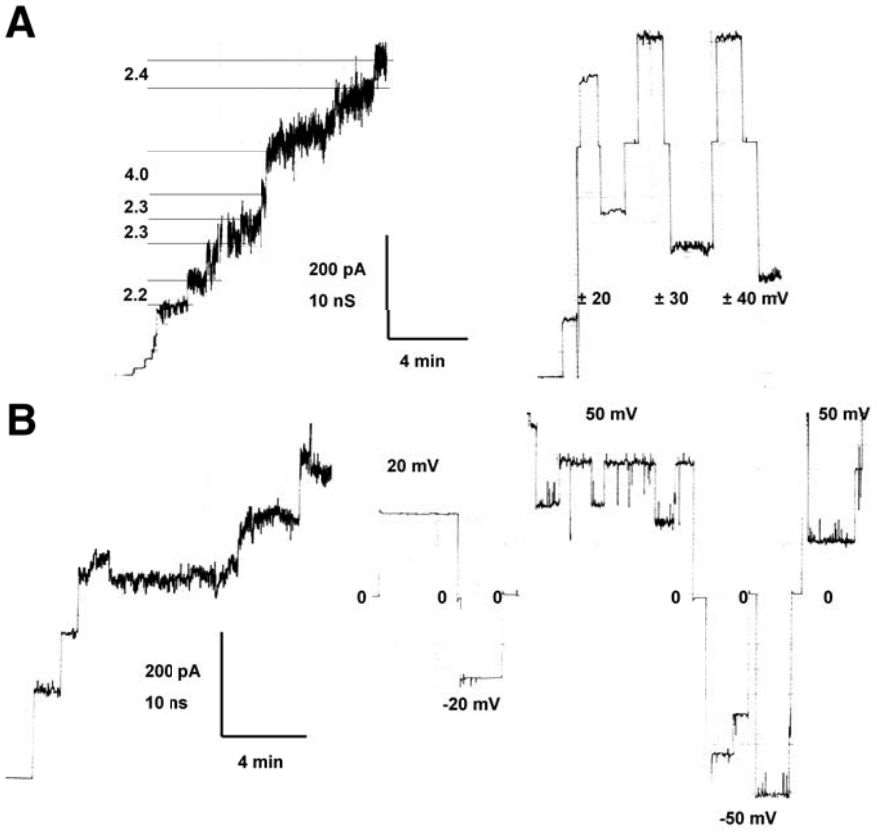

Figure 3.29: BLM measurements on Quintuple hVDAC1. A: There are a lot of channels with closed state-like conductances that do not show gating at higher potentials. B: There are also channels with usual open state-like conductances that show gating at higher potentials.

traces are showing that Quintuple hVDAC1 has – compared to *wt* hVDAC1 – significantly altered gating properties with the protein being in the closed state at unusual voltages. This is confirming that Quintuple hVDAC1 shows the desired properties that are similar to G21V/G23V rVDAC1 like it was described by Geula *et al.*

Similar traces as Quintuple hVDAC1 (Figure 3.29 A) have already been described for a completely different VDAC mutant. In this group, a Δ(1–31)-hVDAC2 construct has been studied.[151] hVDAC2 is eleven residues longer than hVDAC1, having the extension at the N-terminal end (see sequence alignment in Appendix C). The sequence identity of this construct with the corresponding part of hVDAC1 is 74.9 % and the percentage of strongly similar amino acids is 91.6 % according to Clustal Omega[152], such that the Δ(1–31)-hVDAC2 construct is basically the same as a Δ(1–20)-hVDAC1 construct – being a hVDAC variant where the N-terminal helix is deleted. Such a construct has

Dieses Werk ist copyrightgeschützt und darf in keiner Form vervielfältigt werden noch an Dritte weitergegeben werden.
Es gilt nur für den persönlichen Gebrauch.

been shown by computational electrophysiology simulations to have a Cation-selective state with a conductance of around 2 nS at an ellipticity of approximately 0.5.[91]

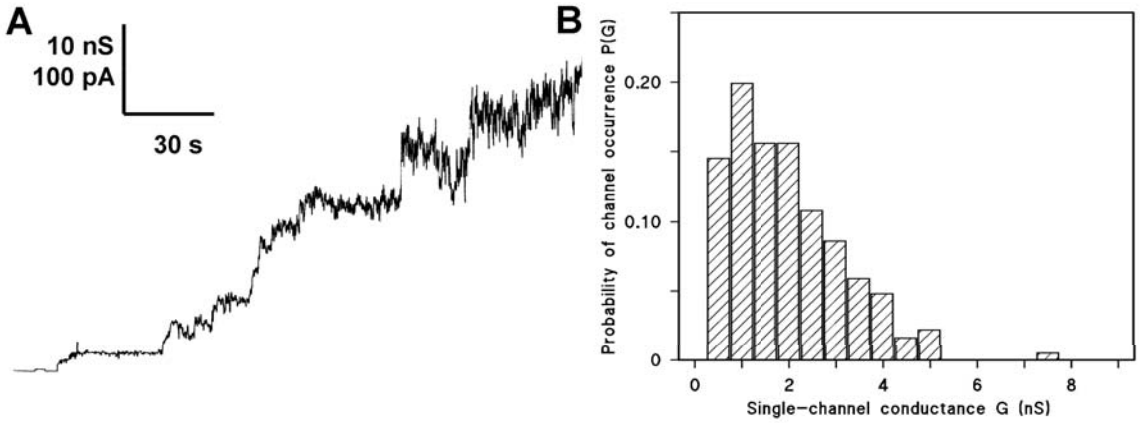

Figure 3.30: BLM measurements on Δ(1–31)-hVDAC2. Illustration is reprinted from Gattin *et al.*[151] with permission from SpringerLink.

For the Δ(1–31)-hVDAC2 construct, roughly 2 nS are the most often observed conductance value in BLM measurements. However, Δ(1–20)-hVDAC1 and Δ(1–31)-hVDAC2 could not be studied by liquid state NMR spectroscopy due to too big instability in the barrel caused by the missing N-terminal helix. Taking this together, Quintuple hVDAC1 partly behaves like a ΔN construct in BLM measurements, although it still possesses the N-terminal helix and is still being able to studied by liquid state NMR. The ΔN construct as well as Quintuple hVDAC1 show conductances of around 2 nS and by computational methods is was shown that this state most likely is Cation-selective – exactly like the closed state of the protein.

All this is pointing towards that the N-terminal helix in Quintuple hVDAC1 moves away from its original position, causing ΔN construct-like BLM traces, and this movement resembles the closed state of the protein. Notably, this seems to be contradictory to the fact that no elevated CSD values are visible in the open-state contact region between α-helix and β-barrel in liquid state NMR spectra. This, however, could also be caused by the different environments of the protein in the two measurement methods (micelles in liquid state NMR and phospholipid membranes in BLM measurements).

Dieses Werk ist copyrightgeschützt und darf in keiner Form vervielfältigt werden noch an Dritte weitergegeben werden.
Es gilt nur für den persönlichen Gebrauch.

3.4.2 Quintuple hVDAC1 in solid state NMR measurements

With the knowledge that Quintuple hVDAC1 behaves like a Δ(1–31)-hVDAC2 construct in BLM measurements and given the fact, that the similar Δ(1–20)-hVDAC1 construct could be studied with solid state NMR but not with liquid state NMR, the decision was taken to also produce a Quintuple hVDAC1 sample that was reconstituted into DPhPC liposomes for solid state NMR measurements.

As described by Schneider *et al.* [113], Δ(1–20)-hVDAC1 and *wt* hVDAC1 show several differences in the solid state spectra due to the N-terminal helix missing in the former construct. In particular, in a ^{13}C-^{13}C PDSD spectrum with a mixing time of 300 ms, the Leu-142-Val-143-Leu-144 motif could be assigned together with some sequential, long-range and internal contacts of these three residues for *wt* hVDAC1. Valine-143 forms a hydrophobic patch together with Leucine-150 that points to the interior of the barrel and is anchor point for Leucine-10 of the N-terminal helix. In the Δ(1–20)-hVDAC1 construct however, nearly all the sequential, internal and long-range contacts for these three residues are missing.

A similar 300 ms ^{13}C-^{13}C PDSD spectrum was recorded for Quintuple hVDAC1 by ShengQi Xiang. The overall quality of the resulting spectrum was good, such that the resonances in question were examined. The results are shown in Table 3.1.

Table 3.1: Assignability of PDSD contacts

		Assignable in	
resonance	*wt* hVDAC1	Δ(1–20)-hVDAC1	Quint-hVDAC1
L142CA-CB	yes	no	unclear
V143CA-L10CG	yes	no	no
V143CA-L144CG	yes	no	yes
V143CB-L10CG	yes	no	no
V143CB-CG1	yes	no	yes
V143CB-CG2	yes	yes	yes
V143CB-L144CG	yes	no	yes
L144CA-CB	yes	no	no

Dieses Werk ist copyrightgeschützt und darf in keiner Form vervielfältigt werden noch an Dritte weitergegeben werden.
Es gilt nur für den persönlichen Gebrauch.

Obviously, Quintuple hVDAC1 does not behave completely identical to Δ(1–20)-hVDAC1, but quite similar. While the internal and sequential contacts involving C_γ atoms are retained, all other contacts are not visible anymore. (The C_α-C_β contact of Leucine-142 is unclear, see below.) That means that in particular the contacts from the N-terminal helix to the β-barrel are missing, indicating once again, that the N-terminal α-helix has moved from its original position at least partly. As with the BLM measurements, this seems to contradict the fact that no elevated CSD values are visible in the open-state contact region between α-helix and β-barrel in liquid state NMR spectra. However, also in this case the two environments in question into which hVDAC1 is reconstituted are very different. (Micelles in liquid state NMR and liposomes in solid state NMR.) This points to that the environment of the protein plays a large role in to which extent the special properties of Quintuple hVDAC1 are visible. More membrane-like environments seem to result in more strongly altered protein properties.

Yet, the impact of the movement of the helix is not as strong as its complete removal, as not all contacts in the region of the hydrophobic patch are broadened beyond detection as it happens in Δ(1–20)-hVDAC1, but just some.

As it was possible to measure an HNCACB on Quintuple hVDAC1 in liquid state, both measurement methods can be compared regarding the C_α and C_β resonances. Indeed, for both Leucine-142 and Leucine-144, C_α and C_β are assigned in the HNCACB. While for Leucine-142 no broadening of the C_β resonance is observed, the opposite is the case for Leucine-144, where the height of the C_β resonance is just 60 % of the expected height (based on the HNCACB of E73V/C127A/C232S hVDAC1 and the height of the C_α resonance; data not shown). So at least for Leucine-144, the broadening of the C_α-C_β contact beyond detection can be justified with the liquid state spectra. On the other hand, as Leucine-142 is showing once again, liquid state and solid state NMR spectra do not necessarily deliver completely identical results.

To rule out the possibility that the missing PDSD contacts are caused by the resonances shifting into bulk regions near them, the respective ^{13}C chemical shifts in the liquid state HNCACB experiment were used. For Leucine-142 the C_β resonance in the Quintuple HNCACB actually shifts by approximately -0.2 ppm in comparison to E73V/C127A/C232S hVDAC1, and as the respective

Dieses Werk ist copyrightgeschützt und darf in keiner Form vervielfältigt werden noch an Dritte weitergegeben werden.
Es gilt nur für den persönlichen Gebrauch.

resonance is a shoulder of the Leucine bulk, the possibility that it is shifting into the latter is existing. Thus, in the above table the visibility of this resonance in the Quintuple PDSD is assessed as unclear. For Leucine-144 however, C_β is barely shifting at all (not more than 0.02 ppm) and C_α shifts by 0.25 ppm upfield, which would put the resonance even further away from the bulk. Accordingly, the possibility that the respective PDSD contact is relocated into the bulk is very unlikely. (The respective chemical shift values can be found in Appendices B.2 and B.3.)

3.4.3 Missing and new NOE contacts of Quintuple hVDAC1

To further test the hypothesis that the N-terminal helix is displaced in Quintuple hVDAC1 and to probe for spatial information in Quintuple hVDAC1, a 3D ^{15}N HMQC-NOESY was recorded with the usual mixing time of 240 ms. The NOE contacts between N-terminal helix and β-barrel were taken into special consideration, as they are a main source of information about the position of the N-terminal helix.

As it turns out, all 7 previously in E73V hVDAC1 assigned NOE contacts between N-terminal helix and β-barrel are broadened below the noise level, see Figure 3.31.

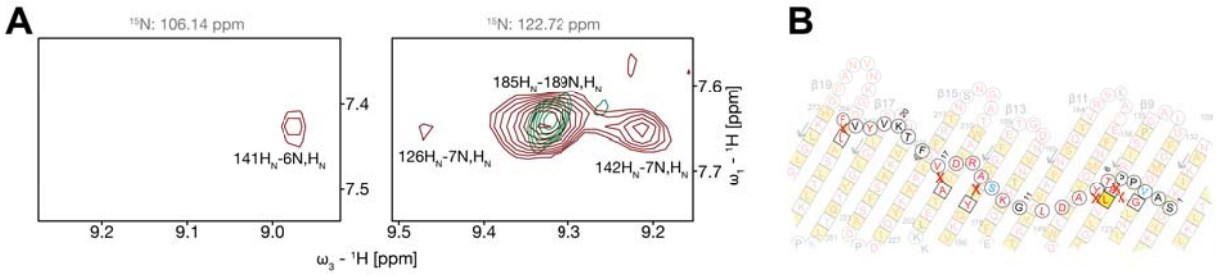

Figure 3.31: Missing NOEs in Quintuple hVDAC1. A: HMQC-NOESY spectra of Quintuple hVDAC1 (green) and E73V hVDAC1 (brown), showing the missing contacts of Threonine-6 (left) and Tyrosine-7 (right) while other correlations are visible. (Missing: A141-T6, G126-Y7, L142-Y7, Visible: N185-E189) B: Map of the missing NOE contacts plotted to the corresponding fragment of the topology map of hVDAC1.

As shown, other contacts in the spectrum are well retained. It should be noted that the signal strength in the two spectra is quite different, the spectrum of Quintuple hVDAC1 has a significantly worse S/N ratio. Based on the respective diagonal peaks and the reference resonances in the NOESY spectrum of E73V hVDAC1, there are the following contacts that are, however, expected to be visible: A141-T6 (expected Peak height $2.01 \cdot 10^6$ a.u.), L142-Y7 (expected $1.54 \cdot 10^6$ a.u.), A14-

Dieses Werk ist copyrightgeschützt und darf in keiner Form vervielfältigt werden noch an Dritte weitergegeben werden.
Es gilt nur für den persönlichen Gebrauch.

Y195 (expected $1.74 \cdot 10^6$ a.u.) and V17-A205 (expected $2.28 \cdot 10^6$ a.u.). The graphically determined maximum noise level in the spectrum is $1.42 \cdot 10^6$ a.u. However, except of the contact L142-Y7 where the data height at the position of the expected resonance is $1.29 \cdot 10^6$ a.u. – slightly below the noise cutoff, which could mean that this peak is retained, but just influenced by noise – all other resonances are clearly no longer visible. Given this, the broadening of the resonance is pointing to that the N-terminal helix is partially displaced and partially still in place, which would be in line with the BLM and solid state measurements presented in the last chapters. (Also the results from these measurement methods did rather show a partial than a complete displacement of the helix.) Taken together, the previously reported NOEs between N-terminal helix and β-barrel are missing or at least broadened significantly. On the other hand, for the residues in the N-terminal helix there are new resonances visible above the noise level. Examples for these are shown in figure 3.32 A – the additional resonances are marked with "x" in the green Quintuple hVDAC1 spectra.

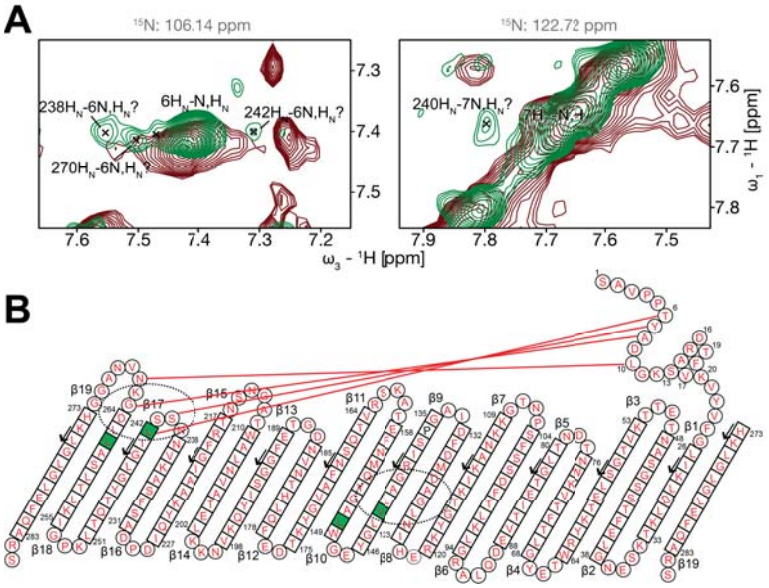

Figure 3.32: Examples for additional NOEs in Quintuple hVDAC1. A: HMQC-NOESY spectra of Quintuple hVDAC1 (green) and E73V hVDAC1 (brown), showing possible new contacts of Threonine-6 (left, possible contacts to Asparagine-238, Leucine-242, Alanine-270) and Tyrosine-7 (right, possible contact to Serine-240). B: Map of some possible new NOE contacts plotted to the the topology map of hVDAC1. Residues in green are residues with hydrophobic sidechain that are pointing to the interior of the pore. The old contact region between N-terminal helix and β-barrel and a possible new region based on the experimental results are circled.

It was not possible to assign the here described resonances safely until now. A set of possible assignments is shown in Figure 3.32 B: T6-L242, Y7-S240, A8-G265, L10-N267. These possible

Dieses Werk ist copyrightgeschützt und darf in keiner Form vervielfältigt werden noch an Dritte weitergegeben werden.
Es gilt nur für den persönlichen Gebrauch.

assignments, i.e. the possible new contacts for the residues in the α-helix, are clustered in the loop from β-strand 16 to 17 and in the loop from β-strand 18 to 19.

This leads to the assumption that the α-helix, which is – based on results from BLM and solid state NMR measurements – expected to move away from its original position at least partially, is replaced to the C-terminal β-strands. This would be in line with the results described at the beginning of this Chapter (significantly elevated CSDs and intensity changes in the last β-strands in comparison to E73V/C127A/C232S hVDAC1). Based on this, a new contact region between α-helix and β-barrel was identified and was marked in Figure 3.32 C. However, it should again be noted that in the open-state contact region (also marked in Figure 3.32 C) no elevated CSDs could be found in the liquid state NMR spectra of Quintuple hVDAC1. In the proposed new contact region the barrel possesses a pattern of two amino acids with hydrophobic sidechains that are pointing to the interior of the barrel, namely Leucine-242 and Leucine-262. A similar pattern of Valine-143 and Leucine-150 is forming a hydrophobic patch, where Leucine-10 of the α-helix is anchored in the open state of the pore. Thus, this pattern of Leucine-242 and Leucine-262 could be the anchor point for the helix in a second state of the protein. (The two residues are colored in green in Figure 3.32 C.) It is hypothesized that this second state is a closed state of hVDAC1 – as this is the state in which the protein is situated in BLM measurements to a large amount. The pattern of Leucine-242 and Leucine-262 is furthermore conserved in a high number of VDAC isoforms (see Appendix C).

3.4.4 Probing the new orientation of the N-terminal helix

To accumulate more experimental evidence about the N-terminal helix moving from the old contact site at β-strands 8 to 10 to the proposed new contact site at β-strands 16 to 18, the movement and new orientation of the helix was probed with MTSL labeling.

Based on Quintuple hVDAC1, an additional mutation was introduced at residue 2. Alanine-2 was mutated to Cysteine and the MTSL label was attached at that position. The resulting hexuple mutant (A2C-Quintuple hVDAC1) should show less resonance broadening due to the attached MTSL label at the old position of the N-terminal helix or of the N-terminus, respectively, than *wt* hVDAC1 labeled at this position. On the contrary, the region where the N-terminal helix is displaced to, should

Dieses Werk ist copyrightgeschützt und darf in keiner Form vervielfältigt werden noch an Dritte weitergegeben werden.
Es gilt nur für den persönlichen Gebrauch.

be broadened more. As mentioned earlier, the wild-type-like reference sample used for experimente on Quintuple hVDAC1 is E73V/C127A/C232S hVDAC1, thus the reference mutant for the MTSL labeling is A2C/E73V/C127A/C232S hVDAC1.

E73V/C127A/C232S hVDAC1 and Quintuple hVDAC1 have been described earlier in this thesis. The two MTSL-labeled mutants were expressed in the pET28a expression vector as usual and were labeled with MTSL prior to the refolding to avoid dimerization (see Materials and Methods for further details). Both MTSL mutants yielded nice $^{1}H,^{15}N$-TROSY spectra without signs of resonance broadening due to intermediate chemical exchange or dimerization. Assignment of these mutants was done based on the existing assignments for E73V/C127A/C232S hVDAC1 and Quintuple hVDAC1, respectively.

To confirm that the A2C mutation and the attached MTSL label are not changing the gating properties of the channel, the MTSL labeled A2C-Quintuple hVDAC1 mutant was tested in BLM measurements. The BLM measurements were performed by Roland Benz (Department of Life Sciences and Chemistry, Jacobs University Bremen gGmbH), as usual with a part of the liquid state NMR sample reconstituted in LDAO micelles.

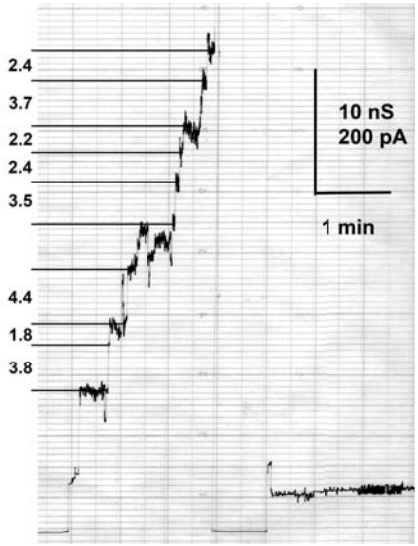

Figure 3.33: BLM measurements on MTSL labelled A2C-Quintuple hVDAC1. Similar to Quintuple hVDAC1 there are channels with conductances around 4 nS, resembling the open state of the protein, as well as channels with conductances around 2 nS, resembling a closed state of the protein.

Similar to Quintuple hVDAC1, also A2C-Quintuple hVDAC1 labeled with MTSL shows a great amount of channels with conductances of around 2 nS or slightly above 2 nS at low potentials that

Dieses Werk ist copyrightgeschützt und darf in keiner Form vervielfältigt werden noch an Dritte weitergegeben werden.
Es gilt nur für den persönlichen Gebrauch.

are usually not large enough to induce a closure of the channel, but also pores with 4 nS can be observed. (See Figure 3.33) This is exactly the behavior of the mutant that was expected and it is the same as for Quintuple hVDAC1. It is thus concluded that the A2C mutation and the MTSL label at this position are not interfering with the gating properties of the channel and that A2C-Quintuple hVDAC1 is still stabilizing a closed state of the pore like Quintuple hVDAC1 is doing it.

The effect of the MTSL labels was now determined for both sets of mutants and the resulting intensity ratios are given in Figure 3.34.

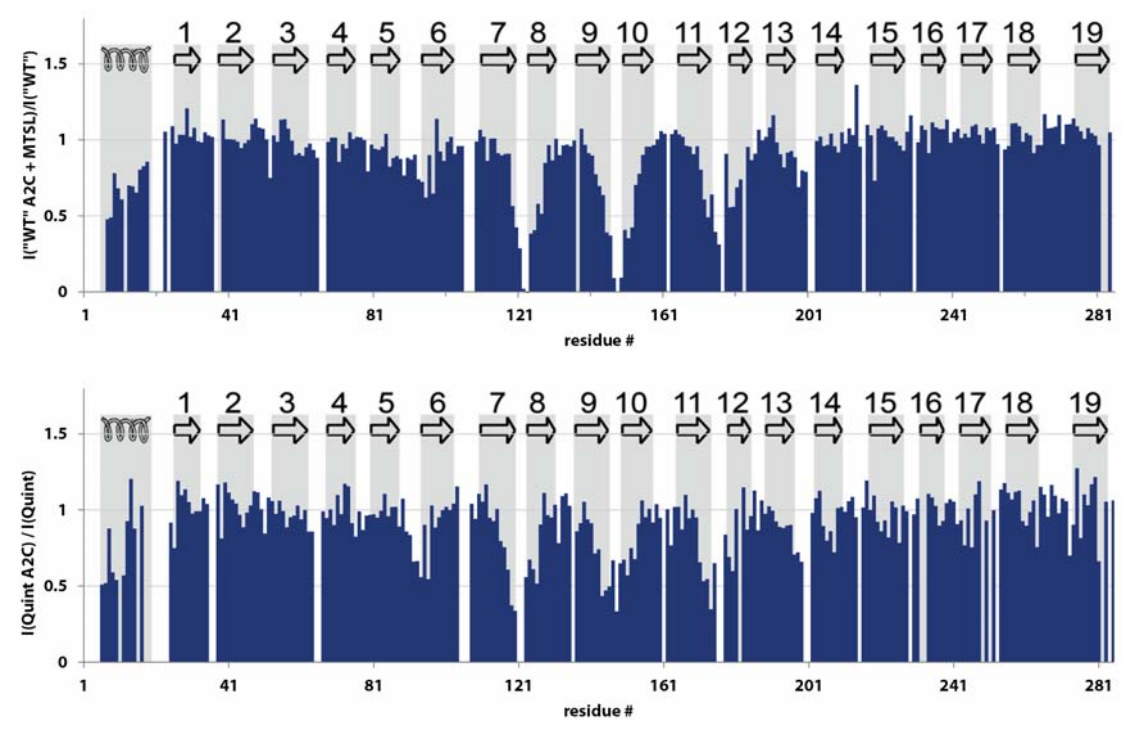

Figure 3.34: Comparison of PRE effects between Quintuple hVDAC1 and E73V/C127A/C232S hVDAC1. The PRE effects induced by an MTSL label introduced at residue 2 are shown by plotting the intensity ratios of the resonances of labeled and unlabeled E73V/C127A/C232S hVDAC1 (top) and Quintuple hVDAC1 (bottom) against the residue number.

Obviously in both sets of mutants the MTSL label induces PREs in a region, where the label should be located if the helix is still at its old position, *i.e.* the position that it has in the open state of the pore. However, there are some residues in the C-terminal β-strands that also show broadening due to PRE in the Quintuple/A2C-Quintuple hVDAC1 mutant pair. As the results for this particular mutant pair are visibly more influenced by noise than the results for the other mutant pair, the difference

Dieses Werk ist copyrightgeschützt und darf in keiner Form vervielfältigt werden noch an Dritte weitergegeben werden.
Es gilt nur für den persönlichen Gebrauch.

between the two mutant pairs was enhanced in the following way: The difference between the PRE effects of the two mutant pairs was calculated as a binomial filtered floating average of the intensity change of 3 five-residue groups, respectively. (See Chapter 2.2.5.) The result of this can be seen in Figure 3.35.

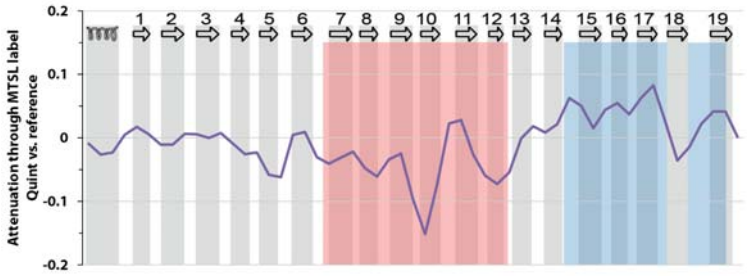

Figure 3.35: Difference of PRE effects between Quintuple hVDAC1 and E73V/C127A/C232S hVDAC1. The difference between the PRE effects shown in Figure 3.34 is calculated as a binomial filtered floating average of the intensity of 3 five-residue groups. Negative values indicate less pronounced PRE effects in Quintuple hVDAC1, while positive values indicate stronger PRE effects in Quintuple hVDAC1.

Obviously, the PRE effect is weaker at the old contact region for the mutant pair based on Quintuple hVDAC1 (resulting in a negative difference in Figure 3.35 around β-strand 10) and stronger in the proposed new contact region (resulting in a positive difference in Figure 3.35 around β-strand 17). This further supports the assumption that the N-terminal helix is replaced from its original position in Quintuple hVDAC1.

Yet, the difference between the two PRE profiles is far less pronounced than expected from BLM measurements and the results from solid state NMR that were presented in the last chapters. Based on the BLM experiments, at least 50 % of the Quintuple hVDAC1 channels should be situated in a closed state. Based on the PRE profile, however, probably not more than 10 % of the channels are closed, as the maximal attenuation of the residue intensities caused by the MTSL label is around 10 % of the normalized intensities in both regions. Obviously the micelle environment is intrinsically pushing the system to the open state, as based on methods where hVDAC1 is reconstituted into more membrane like environments far bigger amounts of closed hVDAC1 are observed.

Still, based on the collected results presented in the last chapters, a model of hVDAC1 in the closed state was derived that will be described in the following chapter.

Dieses Werk ist copyrightgeschützt und darf in keiner Form vervielfältigt werden noch an Dritte weitergegeben werden.
Es gilt nur für den persönlichen Gebrauch.

3.4.5 A model for the closed state of hVDAC1

Taking all experimental data together, there is clear evidence that in Quintuple hVDAC1 the N-terminal α-helix is replaced from its old position at the middle of the β-barrel to a new position. All the data available (CSD values, Intensity ratio Quintuple vs. E73V/C127A/C232S hVDAC1, NOE contacts, sequence analysis, PRE effects from MTSL labeling) are suggesting, that this new position of the N-terminal helix is in the C-terminal end of the β-barrel, in the β-strands 16 to 18.

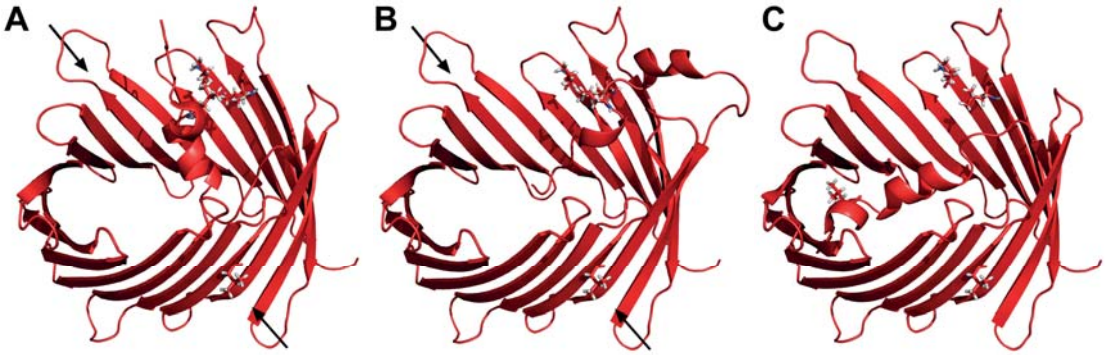

Figure 3.36: Models of the closed state of hVDAC1 incorporated in Quintuple hVDAC1. A: Model where the N-terminal α-helix is "bending back" to the C-terminal β-strands. B: Model in which the linker pulls the helix out of the barrel. In both models Leucine-10 is connected to the hydrophobic patch formed of Leucine-242 and Leucine-262. Arrows indicate further elliptic deformation following the displacement of the helix. Models are based on the NMR structure of E73V hVDAC1. C: NMR structure of E73V hVDAC1 with the α-helix attached at the open-state contact site. Residues Leucine-10, Valine-73, Leucine-242 and Leucine-262 are shown by stick representations.

This thesis thus proposes a model, where a) the linker between helix and barrel is – coming from the β-barrel – conformationally largely unchanged until the G21VG23V mutation, which induces the α-helix to bend back to the loops between the β-strands 16 to 17 and 18 to 19. Or b), the linker between helix and barrel is, due to the G21V/G23V mutation, displaced to out of the barrel, pulling the N-terminal helix into the new position attached to β-strands 16 to 18. Both models are depicted in Figure 3.36.

In either model, Leucine-10 is positioned such that it is now attached to the hydrophobic patch that is consisting of Leucine-242 and Leucine-262. A detailed discussion of the two models will be provided in Chapter 4.3.1.

Modeling was done with PyMol[71], starting from the NMR structure of E73V (PDB ID: 5JPD). The resulting PDB files can be found in Appendix D.

Dieses Werk ist copyrightgeschützt und darf in keiner Form vervielfältigt werden noch an Dritte weitergegeben werden.
Es gilt nur für den persönlichen Gebrauch.

4 Discussion

4.1 A14C/C127A/S193C/C232A hVDAC1 is not closed in NMR samples

Opening and closing of VDAC is a process that usually happens on the timescale of seconds (closing) and microseconds to milliseconds (opening) in BLM measurements.[45] Is has been phenomenologically shown that the opening of the channels can, however, be slowed down by holding the channel in the closed state for longer times (which is done by applying elevated potentials for longer times).[45] Exact values for the state switching behavior of VDAC were determined by Mertins *et al.*, they yielded an average dwelling time of 0.17 ± 0.03 minutes in either of the states for mVDAC1. Contrary to that, the mutant A14C/C127A/S193C/C232A mVDAC1 usually takes a far longer time to switch into the closed state. It takes about 30.61 ± 6.39 minutes (SEM), meaning that the process of closing is slowed down by two orders of magnitude, or factor 180, respectively, in this mutant. Afterwards it fails to reopen again.[52]

A kinetic description of the opening and closing process of VDAC has been provided by Marco Colombini[153]. The switching between the open and the closed state of the channel can be described with the transition state theory: $k = \frac{k_B T}{h} \cdot \exp(\frac{-\Delta G}{RT})$ with ΔG being the height of the energy barrier, k_B the Boltzmann constant, h the Planck constant, R the Gas constant and T the temperature. A deceleration of the closing process like observed by Mertins *et al.* by the factor of 180 would then be equivalent to a raise of this energy barrier ΔG for the reaction between open and closed state of 12.9 kJ/mol at 298 K. Based on his own findings[154], according to Colombini the influence of the

Dieses Werk ist copyrightgeschützt und darf in keiner Form vervielfältigt werden noch an Dritte weitergegeben werden.
Es gilt nur für den persönlichen Gebrauch.

applied voltage on the velocity of the closing process can be corrected with $E = nFV$, F being the Faraday constant, V the applied potential and n the number of charges moving. In the case of VDAC the observed values can be fitted to $n = 3$. ΔG is then corrected by E and the resulting corrected rate constants for the closing of the channel at different applied potentials fit very well to the observed values. The values Mertins *et al.* reported were measured at 40 mV.

Following the model of Colombini, the difference between 40 mV (applied potential by Mertins *et al.*) and 0 mV (potential in the NMR samples) would be equivalent to a further raise of the energy barrier between open and closed state by 11.6 kJ/mol relative to the open state. Going back to the transition state theory, this would be equivalent to a further reduction of the rate constant of closing of the channel by a factor of 107, meaning that A14C/C127A/S193C/C232A hVDAC1 has a dwelling time in the open state of at least 54.6 hours in NMR samples.

The energy difference between the open and the closed state of *wt* VDAC amounts to around 10 kJ/mol.[93] According to Boltzmann distribution in *wt* hVDAC1 the closed state is populated to about 2 % also at zero potential[93]. Given the extremely high dwelling time of A14C/C127A/S193C/C232A mVDAC1 at zero voltages it is thus very questionable, whether this population is enriched to values that would render the closed state observable by conventional TROSY experiments, as also overall denaturation of the protein over time has to be taken into account. There are ways to detect "invisible" states with NMR: CPMG relaxation dispersion experiments usually only work as long as the rates of exchange between the "visible" ground state and the "invisible" excited state lie between $\approx$ 200 and 2000 s^{-1} and the population of the excited state is at least 0.5 %.[155] CEST experiments are able to access slower processes, with exchange rates of $\approx$ 20 to 200 s^{-1}. DEST experiments can probe exchange processes with even lower rates of $\approx$ 1 to 100 s^{-1}.[156] However, the rate of exchange in A14C/C127A/S193C/C232A hVDAC1 is obviously slower than all of these measurement methods require.

Spectroscopically, the mutant does not show elevated CSD values in regions that are distant from the mutation sites. This does not point to large conformational changes, like they are expected for the protein when it switches into the closed state. Quite the contrary to this, the mutant shows a CSD profile that is very similar to C127S/C232S hVDAC1, a mutant that does not show an unusual

Dieses Werk ist copyrightgeschützt und darf in keiner Form vervielfältigt werden noch an Dritte weitergegeben werden.
Es gilt nur für den persönlichen Gebrauch.

gating behavior in BLM measurements at all.[146] Thus also based on this line of evidence there is no hint that A14C/C127A/S193C/C232A hVDAC1 is in a different state than it is usually manifested in NMR sample – which is the open state of the protein.

There is even the open question, whether the closed state Mertins *et al.* are seeing in their publication is really the usual closed state like it is described for *wt* hVDAC1. The fact that the mutant is trapped in the closed state contradicts the usual behavior that opening of the channel is occuring even faster than closing.[45] Furthermore, there is plethora of experimental and theoretical evidence that movement of the N-terminal helix is essential for the channel to reach a cation selective closed state. This starts with the findings that the N-terminus is part of a voltage-sensor that is moving during closure of the channel and that it is leaving the pore at least partially.[53,87,88] It continues with theoretical calculations that show that a large movement of the helix is necessary to explain the voltage dependence that is seen and that the channel can only reach a cation selective state under large deformation and without the N-terminal helix in the interior of the pore.[91,94] Furthermore, BLM measurements on a large number of mutants do also point in that direction. [90,91]

Basically there is only one publication from 2012 which suggests that VDAC can reach a closed state without movement of the N-terminal helix: Teijido *et al.* reported a L10C/C127A/A170C/C232A mVDAC1 mutant, that according to them is showing undisturbed gating.[157] Similar to the mutant studied in this thesis, the N-terminal α-helix is affixed to the β-barrel, particularly to β-strand 11. The authors conclude their findings with two possible explanations, namely that either the N-terminal helix is staying inside the pore during gating or that it moves in an concerted fashion together with the rest of the voltage sensor to reach the outside of the lumen. However, β-strand 11 does not belong to the regions that could form the voltage sensor (but as probed by mutations that affect the voltage gating, the neighboring β-strands 9 and 10 do).[59] Furthermore, movement of just one or two β-strands during gating would imply that a large number of hydrogen bonds to these strands has to be broken during gating. As mentioned above, the gating can however be described with an energy difference of 10 kJ/mol.[93] To break one hydrogen bond in a β-sheet alone already 6.6 kJ/mol are needed.[158] This renders the possibility that the N-terminal α-helix is moving together with one or two β-strands very unlikely. Additionally, the au-

Dieses Werk ist copyrightgeschützt und darf in keiner Form vervielfältigt werden noch an Dritte weitergegeben werden.
Es gilt nur für den persönlichen Gebrauch.

thors do not report measurements about the selectivity of their construct in the closed state that they are seeing.[157] Lastly, their claim that the mutant behaves "indistinguishably from the endogenous protein"[157] is in disagreement with their own data. Their data clearly shows that the mutant even closes at lower positive potentials than *wt* mVDAC1 – a behavior that remains unexplained. All in all, the publication by Teijido *et al.* does not seem to be reliable basis on which to reason that there is the possibility for the VDAC channel to close in the usual way when the N-terminal α-helix is covalently bound to the β-barrel.

Taking all this together the most likely explanation for the behavior of A14C/C127A/S193C/C232A hVDAC1 in BLM measurements is indeed, that the β-barrel is collapsing, *i.e.* losing its overall structural integrity completely, due to the applied potential and that the channel closure one can see is not a real gating but just the macroscopic effect of the channel collapse. Consequently, the spectra A14C/C127A/S193C/C232A hVDAC1 delivers are spectra of the protein in the open state.

Dieses Werk ist copyrightgeschützt und darf in keiner Form vervielfältigt werden noch an Dritte weitergegeben werden.
Es gilt nur für den persönlichen Gebrauch.

4.2 The structure of hVDAC1 and the N-terminal α-helix in micelles

Based on the three 3D structures of VDAC1 published in 2008[46,48,70] it was previously argued whether the visible difference of the appearance of the N-terminal α-helix is due to different resolutions of the structures or due to dynamics of the helix. Especially the tilt of the α-helix of ≈90° between the X-ray structure of mVDAC1 and the combined NMR/X-Ray structure of hVDAC1 and the different length of the helix in these two structures raised suspicion.[74] However, as mentioned in the introduction, with the new data available, this question can most likely be answered.

Based on revised chemical shift data of E73V hVDAC1 already the by TALOS-N predicted backbone torsion angles ψ and ϕ indicate a kink in the N-terminal helix at position 10. (See Figure 3.5) This is confirmed by the refined NOE network, in which the first part of the helix from residues 6 to 10 is showing the characteristic (i,i+1) and (i,i+2) NOE connections. The same is true for the second part of the helix from residues 13 to 17. Between these two parts, however, the (i,i+1) NOE connections are missing.[115] Furthermore, the distance of the two residues directly before and after the kink in the X-ray structure is 5.0 Å and in the new NMR structure is 4.8 Å, which is very similar to the usual pitch of an α-helix of 5.4 Å. The resolution of the combined NMR/X-ray structure by our group was only 4.1 Å, which explains why the kink can very easily be modeled as a further turn of the α-helix without any problems. The presence of the kink in the N-terminal α-helix, that could not be resolved in the combined NMR/X-ray by our group in 2008, is thus encoded in the NMR data and not just stemming from different dynamics of the helix in micelles and crystals.

The same arguments are true for the tilt of the N-terminal α-helix that was previously observed when comparing the different structures. Refining the NOE network lead to different connections between α-helix and β-barrel compared to what was assumed and assigned previously. This was described in detail in Chapter 3.1.3. It is very likely that this revision of the contacts between the two characteristic parts of the protein lead to the helix being positioned in the E73V hVDAC1 NMR structure the same way as in the mVDAC1 X-ray structure. The reasoning for this is that information about the linker between α-helix and β-barrel is still very sparsely, thus the α-helix is not pushed into

Dieses Werk ist copyrightgeschützt und darf in keiner Form vervielfältigt werden noch an Dritte weitergegeben werden.
Es gilt nur für den persönlichen Gebrauch.

one certain orientation by this very part of the protein. Rather the connection information between α-helix and β-barrel have a large impact on how the helix is modeled. The new assignments and connections are not only more numerous than before (7 versus 3) but also the chemical shifts of the assigned resonances fit better to the shifts of the respective connected residues. Thus, the outcome with the α-helix having the same position, length and rotation in both the old X-ray and the new NMR liquid state structure is really encoded in the NOE data.

Concluding this, this answers the question raised in the thesis of Saskia Villinger, where the differences between the appearance of the α-helix in the X-ray and the combined NMR/X-ray structure are stemming from. They are clearly caused by the different resolution of these two structures. A better resolved NMR structure is able to depict the α-helix in the same accuracy as it was depicted in the X-ray structure previously.

4.2.1 The shape of the β-barrel

The overall shape of the β-barrel is very much determined by the relaxation rates R_1 and R_2 or the anisotropy of the diffusion tensor of the protein that was determined by the relaxation rates, respectively. The resulting lowest energy structure shows a clear elliptic deformation with the minor axis of the ellipse going through Valine-73. This deformation of the barrel is resembling one of the two extremes yielded from a combination of four PCA eigenmodes generated from MD simulations using the X-ray structure of mVDAC1 and three modified versions (modifications at E73: deprotonated charged, E73V and E73Q) thereof.[132] (See Figure 3.11) The MD simulations revealed that E73V mVDAC1 embedded in a lipid bilayer is only slightly less circular than *wt* mVDAC1 (i.e. the X-ray structure of mVDAC1), having a relative excursion of no more than 0.2 nm along the eigenvector of this first eigenmode with respect to the latter. In absolute values the most probable excursion along this vector is ≈ 0.7 nm for E73V mVDAC1 in a phospholipid bilayer.

The newly published and in this thesis described E73V hVDAC1 NMR structure, however, matches to an excursion of 6 nm along this eigenvector. An ellipticity that large was only observed for the deprotonated charged modification ($E73^-$) of mVDAC1 in the MD simulations – and even for this modification this is the largest observed excursion along the eigenvector, reached only with low

Dieses Werk ist copyrightgeschützt und darf in keiner Form vervielfältigt werden noch an Dritte weitergegeben werden.
Es gilt nur für den persönlichen Gebrauch.

probability.[132] It is exactly this deprotonated charged modification that in the MD simulations also perturbated the DMPC membrane in which it was embedded. The membrane was thinning out at the position of E73 by roughly 0.5 nm with respect to the E73V mVDAC1. Thinning of the membrane may reduce the lateral pressure the membrane is exerting on the protein on that particular side – it could also increase the lateral pressure on the protein from the opposite side –, which then in turn can undergo conformational changes and in particular this global deformation more easily. Detergent micelles do usually also exert a different lateral pressure on IMPs than membranes.[159] The large deformation of E73V hVDAC1 in LDAO micelles, *i.e.* the large excursion along the calculated eigenvector, is thus pointing to an altered lateral pressure exerted on the protein.

Interestingly, the effect of the different lateral pressure is much more pronounced in E73V hVDAC1 in detergent micelles than in $E73^-$ in DMPC membranes. The 3D NMR structure, which is of course a structure that is resembling a mean structure out of an ensemble of present structures, is way more elliptic than $E73^-$ mVDAC1 in the MD simulations. The most probable excursion along the eigenvector of the global deformation mode is no more than 2.8 nm for $E73^-$ mVDAC1 – 3.2 nm less than E73V hVDAC1 in detergent micelles. It was this same global elliptic deformation mode that was shown to being able to lead to a closed state of the protein.[91] This obviously raises the question, whether exactly this might be the state of E73V hVDAC1 in LDAO micelles. According to Zachariae *et al.* an ellipticity of 0.5 is needed to reach a cation selective state with halved conductance in comparison to the circular channel. However, fitting the lowest energy structure of E73V hVDAC1 to an ellipse delivers a fit with an ellipticity of just 0.2 – and the long and short axis of the ellipse are swapped with respect to what was reported by Zachariae *et al.* Furthermore, the NMR data suggest that the N-terminal α-helix is tightly anchored to the β-barrel wall, although it should leave the pore lumen according to the simulations.[91]

4.2.2 The old NMR structure in the light of the new findings

These findings also shed light on the NMR structure of hVDAC1 that was published in 2008.[48] The definition of the barrel in the deposited structures (PDB ID: 2K4T) is only very modest. While the lowest energy structure that is always depicted in comparisons of the 3D structures from 2008 is

Dieses Werk ist copyrightgeschützt und darf in keiner Form vervielfältigt werden noch an Dritte weitergegeben werden.
Es gilt nur für den persönlichen Gebrauch.

nearly circular, a large number of the 20 deposited structures are very deformed, partly reaching even higher ellipticities than E73V hVDAC1. Some of the 20 deposited structures are not deformed as suggested by the global mode that was calculated, but the biggest part of the structures is. Together with the knowledge that the E73V mutation is increasing the overall stability of the β-barrel of the protein this leads to the conclusion that the high conformational space the 20 structures of 2K4T are occupying is an expression of the (with respect to E73V hVDAC1) unstabilized β-barrel together with the different lateral pressure the LDAO micelles are exerting on the protein with respect to membranes.

It is thus not that E73V hVDAC1 in micelles is more elliptic than *wt* hVDAC1 in micelles, but rather is the E73V mutation stabilizing the β-barrel to a single of the anyway existing deformed protein conformations.

Dieses Werk ist copyrightgeschützt und darf in keiner Form vervielfältigt werden noch an Dritte weitergegeben werden.
Es gilt nur für den persönlichen Gebrauch.

4.3 Quintuple hVDAC1 as a model for the closed state

The assumption that Quintuple hVDAC1 delivers spectra of the pure closed state of the protein has one big flaw. Similar to A14C/C127A/S193C/C232A hVDAC1, large parts of the protein do not show significantly elevated CSD values with respect to the reference (in this case E73V/C127A/C232S hVDAC1, see Figure 3.27). There are especially no elevated CSDs in the β-strands 4 to 13, which is an indication against the possibility that large conformational changes are happening in the β-barrel. To completely rule this out, however, further measurements about the relaxation behavior of the residues in these strands – similar to the ones that were determined for E73V hVDAC1 – are needed. Nevertheless, the observable shifts point to some conformational changes in the beginning of β-strand 1, in the loop from β-strand 2 to 3 and in the last five β-strands of the barrel. For "just" two mutation sites that are additionally very close to each other, the range of these conformational changes seems to be quite large.

Additionally, there are several lines of evidence that are not based on the simple 2D TROSY spectrum, that Quintuple hVDAC1 behaves differently from previously studied *wt*-like hVDAC1 mutants. There are the following points: a) There are significant intensity changes of the resonances in Quintuple hVDAC1 with respect to E73V/C127A/C232S hVDAC1. Resonances in the C-terminal end of the α-helix and β-strands 1, 9 and 15 to 19 as well as some in the loops from β-strands 6 to 7 and 8 to 9 are significantly broadened, pointing to changes in dynamics in these regions of the protein. b) In BLM measurements Quintuple hVDAC1 is often behaving like a Δ(1-31)-hVDAC2 construct and not always like *wt* hVDAC1. It is thus to a significant percentage behaving like a mutant which is lacking the N-terminal α-helix which implements the closed state. c) In solid state PDSD spectra Quintuple hVDAC1 is lacking several intra- und inter-residue correlations that are visible in *wt* hVDAC1 and are missing in Δ(1-20)-hVDAC1, too. Taking these two points together, according to solid state NMR measurements Quintuple hVDAC1 shows features previously described for a construct lacking the N-terminal α-helix and is in the closed state electrophysiologically. d) In liquid state HMQC-NOESY spectra the contacts between N-terminal α-helix and β-barrel are missing or broadened beyond the noise level, respectively. Instead, possible new resonances are emerging for

Dieses Werk ist copyrightgeschützt und darf in keiner Form vervielfältigt werden noch an Dritte weitergegeben werden.
Es gilt nur für den persönlichen Gebrauch.

the residues in the α-helix that can tentatively be assigned to residues in the loops between β-strands 16 to 17 and 18 to 19, where a pattern of two hydrophobic residues is pointing to the interior of the pore. This in turn could have the same function as the respective pattern in β-strands 9 and 10. e) MTSL labeling at position 2 shows that resonances of residues in the β-strands 7 to 12 are less broadened in Quintuple hVDAC1 with respect to E73V/C127A/C232S hVDAC1, while resonances of residues in the β-strands 15 to 17 and 19 are showing stronger PRE effects.

As calculated and discussed in Chapter 4.1, based on the small energy difference between open and closed state, in *wt* hVDAC1 roughly 2 % of the channels should be in the closed state of the protein. The findings listed in the last paragraph point to that Quintuple hVDAC1 is situated in the closed state to a higher percentage, roughly 10 %, in liquid state samples, i.e. if reconstituted into detergent micelles. This quantitative conclusion will be derived in the following.

The finding that G21V/G23V hVDAC1 delivers non-interpretable liquid state NMR spectra can be explained with what has been discussed in Chapter 4.2: The detergent micelles exert a different lateral pressure on the protein in comparison to phospholipid bilayers. This weakens the structural integrity of the protein in the micelles. This would explain that even E73V hVDAC1 (with the E73V mutation that is stabilizing the β-barrel) adopts a structure that is considerably more elliptic compared to what is expected for E73V hVDAC1 embedded in lipid bilayers by MD simulations. The structure rather resembles an extreme case of a global deformation mode that is expected for charged $E73^{-}$ hVDAC1.[115,132] This points to that especially in detergent micelles the N-terminal α-helix has a crucial function of stabilizing the protein in its overall structure. Interestingly as mentioned in Chapter 4.2.1, the long and short axis of the ellipse in the NMR structure of E73V hVDAC1 are swapped with respect to an elliptic collapsed structure that was found under low uniaxial membrane membrane stress (approximately -10 mN/m) in MD simulations.[91]

This in turn can explain why it is not possible to study a Δ(1-20)-hVDAC1 construct reconstituted into detergent micelles: The barrel without the helix is destabilized that strongly, that the different lateral pressure of the detergent micelles with respect to phospholipid membranes leads to a barrel collapse. The observations made with G21V/G23V hVDAC1 are very analogous to that: based on BLM measurements it is expected that a significant relative share of the protein is in its closed

Dieses Werk ist copyrightgeschützt und darf in keiner Form vervielfältigt werden noch an Dritte weitergegeben werden.
Es gilt nur für den persönlichen Gebrauch.

state.[145] If this is comprising movement of the helix, the same destabilization effect like what was observed for Δ(1-20)-hVDAC1 is kicking in, resulting in non-interpretable spectra. The different lateral pressure that lipid bilayers are exerting on the protein can however stabilize the conformation of the β-barrel, resulting in the possibility to record interpretable solid state spectra and BLM measurements. Detergent micelles are thus inherently demanding the protein to be mostly open, because it is otherwise destabilized and collapsing.

This problem is tackled by combining the G21V/G23V mutation with the E73V mutation. While the former is inducing the movement of the N-terminal helix, respectively pushing the protein towards the closed state, the latter is stabilizing the barrel and ensures that the protein can still be studied by liquid state NMR. The result is a protein which is still mostly in the open state, but where due to the G21V/G23V mutation the energy difference between the open and the closed state is further reduced, thus a larger relative share of the channels is in the closed state of the protein than usual.

This assumption allows an explanation for the observations made with liquid state NMR. If the protein is still mostly open the fact that for large parts of the protein no elevated CSD values can be observed can be understood. The larger share of protein in the closed state, however, is manifesting itself in the CSDs in the last β-strands 15 to 19 and the resonance intensity changes observed (and pointing to changes in dynamics) in the very same β-strands.

How large the relative share of Quintuple hVDAC1 in the closed state is can be estimated with the MTSL labeling experiments. The comparison of the PRE effects of a label at residue 2 in Quintuple hVDAC1 and E73V/C127A/C232S hVDAC1 (See Figure 3.35) shows a maximal difference of the intensity ratios of roughly 0.1. The values presented there are normalized to the peak intensity of the single amino acid. Assuming that the maximal difference of the intensity ratios is stemming from residues that are affected in the strongest possible way by the MTSL label, *i.e.* that are broadened beyond detection if the MTSL label is near them in one state and are completely unaffected if the label is far away from them in the other state, this corresponds to approximately 10 % population difference of the open and closed state between Quintuple hVDAC1 and E73V/C127A/C232S hV-

Dieses Werk ist copyrightgeschützt und darf in keiner Form vervielfältigt werden noch an Dritte weitergegeben werden.
Es gilt nur für den persönlichen Gebrauch.

DAC1. Thus it can be estimated that the share of Quintuple hVDAC1 situated in the closed state of the protein in detergent micelles is roughly 10 %, as already stated above.

The results from solid state NMR and BLM experiments do also fit into this explanation. Both of these systems are better able to stabilize the channel also in the moments when the helix is not in the interior of the pore. Thus, in these two systems Quintuple hVDAC1 is appearing to be closed to an even higher extent: far more than 10 % of the BLM traces are showing Quintuple hVDAC1 to be closed at low applied potentials as described by Geula *et al.*[145] and shown by our own measurements (see Chapter 3.4.1). The solid state PDSD spectra are also suggesting a higher share of protein without N-terminal helix in the interior as the mentioned missing contacts are quite prominent in *wt* hVDAC1 (see Chapter 3.4.2). However, that open channels can be observed in the BLM measurements and that not all PDSD contacts in question are invisible in solid state NMR experiments also suggests, that in both methods also open channels are still present.

At the same time all these results are pointing to that the N-terminal α-helix is indeed moving between the open and the closed state of the channel, as the results are delivering a coherent picture with exactly this assumption. However, the question arises where exactly the N-terminal helix is moving in the closed state of the protein.

All experimental evidence presented in this thesis suggests that the C-terminal β-strands 15 to 19 are the place where the helix is moving. These strands are where the largest CSD values and the biggest resonance intensity changes are observed. The tentative new NOE contacts of the helix residues are pointing there. Also the PRE effects observed suggest a stronger effect of the MTSL label in these strands in Quintuple hVDAC1. Lastly, there is a unique and often conserved pattern of two residues with hydrophobic sidechains that are pointing to the interior of the channel in β-strands 17 and 18 (Leucine-242 and Leucine-262), which could form a hydrophobic patch Leucine-10 is anchored to in the closed state of the protein – similar to the hydrophobic patch formed by Valine-143 and Leucine-150.

This lead to the two possible models shown in Figure 3.36; the helix is either “bending back” to the C-terminal β-strands or pulled out by the linker between helix and barrel.

Dieses Werk ist copyrightgeschützt und darf in keiner Form vervielfältigt werden noch an Dritte weitergegeben werden.
Es gilt nur für den persönlichen Gebrauch.

4.3.1 The conformation of the N-terminal helix in the closed state of Quintuple hVDAC1

Both the models presented in this thesis seem to reasonably fulfill the experimental restraints that were found, although some of them fit better to one or the other of the two models. The two models are shown here together with the an open state of the protein as it is observed with E73V hVDAC1.

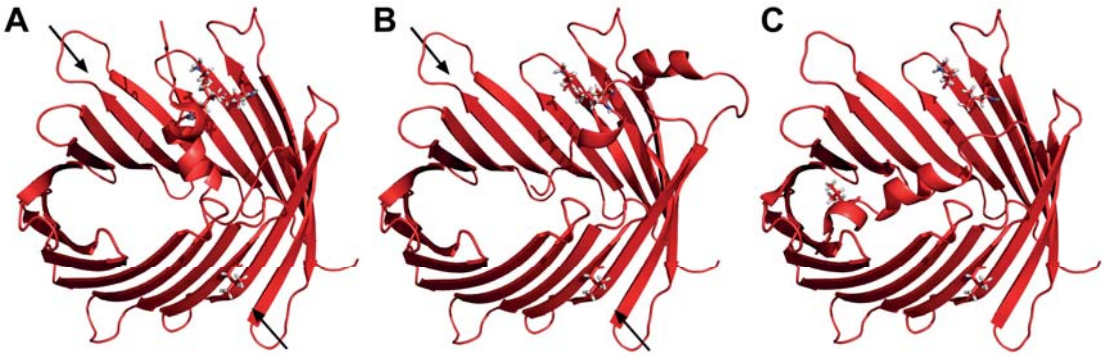

Figure 4.1: Models of the closed state of hVDAC1 incorporated in Quintuple hVDAC1. A: Model where the N-terminal α-helix is "bending back" to the C-terminal β-strands. B: Model in which the linker pulls the helix out of the barrel. In both models Leucine-10 is connected to the hydrophobic patch formed of Leucine-242 and Leucine-262. Arrows indicate further elliptic deformation following the displacement of the helix. Models are based on the NMR structure of E73V hVDAC1. C: NMR structure of E73V hVDAC1 with the α-helix attached at the open-state contact site. Residues Leucine-10, Valine-73, Leucine-242 and Leucine-262 are shown by stick representations.

Model A in Figure 4.1 comprises a movement of the α-helix that leads to it bending back to the loops of the C-terminal β-strands ("bending model"). The second part of the α-helix would then be in closer spatial proximity to the C-terminal β-strands. This could cause conformational changes in these β-strands, which would explain the elevated CSD values there. If this also causes changes in dynamics, it would also explain the altered residue intensities. As is visible in the structural model, this special conformation would also induce a pull on the linker between α-helix and β-barrel, resulting in conformational changes in the first β-strand – again explaining the observed elevated CSD values. Depending on the exact conformation of the first part of the helix, with this model furthermore the tentative NOE assignments could be confirmed, as the first part of the helix can be located there where it can explain the possible new NOE contacts. The model would, however, be problematic when trying to explain the cation selectivity of the closed state, as the N-terminal helix is, although significantly tilted, still completely located in the interior of the pore. Also, the

Dieses Werk ist copyrightgeschützt und darf in keiner Form vervielfältigt werden noch an Dritte weitergegeben werden.
Es gilt nur für den persönlichen Gebrauch.

position of the MTSL would be quite far outside of the pore: The distance from Alanine-2 would be around 28 Å from the middle of β-strand 17 (Glycine-246) in this model (C_α-C_α distance). As the PRE effect of the MTSL is detectable up to approximately 25 Å, this renders it unclear whether the observed PRE profile can be explained with the MTSL in this position.

Model B, where the linker between helix and barrel is more or less pulling the helix away from its old position ("pulling model"), would better explain the observed PRE profile. In this model, the above mentioned distance between Alanine-2 and Glycine-246 would be around 13 Å (C_α-C_α distance). Adding the length of the MTSL label, it seems to be very likely, that large parts of the C-terminal β-strands undergo broadening due to PRE in this state. The model would also be more reasonable to form a state that has cation selectivity, as the helix in this case is visibly moved to the very rim of the pore. This is obviously better resembling the "empty barrel" that was used for the MD simulations which came out with a collapsed, cation-selective state. Furthermore, this model would probably also fit better to the observations that the N-terminal helix as voltage sensor is moving to the surface of the pore during gating. As is visible in in the figure, also this model requires conformational changes in the N-terminal β-strands, explaining the elevated CSD values there. The elevated CSD values and intensity changes in the C-terminal β-strands can be explained with the proximity of the N-terminal part of the α-helix to these β-strands. The pulling model, however, would not confirm the tentative NOE connections, as the N-terminal part of the α-helix would not be located in the proximity of the loops from β-strand 16 to 17 and 18 to 19, where the tentative NOE contacts are located. As mentioned, it would rather be in the middle of these β-strands.

Both models can explain that by the suggested movement of the N-terminal α-helix the β-barrel becomes less stabilized and thus collapses to a very elliptic state which is needed to explain the lower conductance and inversed ion selectivity of the closed state. Solely based on the new positions of the α-helix, however, it can not be predicted whether this elliptic, collapsed state resembles the ellipse observed in the NMR structure of E73V[115] (long axis running through β-strands 1 and 9) or the one found with MD simulations on the empty barrel under uniaxial membrane stress (long axis running through β-strands 4 and 14).[91]

Dieses Werk ist copyrightgeschützt und darf in keiner Form vervielfältigt werden noch an Dritte weitergegeben werden.
Es gilt nur für den persönlichen Gebrauch.

In the light of the results of Choudhary *et al.*[94], the pulling model might be a bit more feasible. They showed that a large displacement of the α-helix is needed to explain the observed voltage dependence of the gating process. In the pulling model the helix is rather moving in its entirety for a significant distance, while the bending model involves a smaller movement of the helix.

Both models are equally able to explain the results from Marco Colombini.[87] He determined a number of residues in scVDAC1 that are influencing the steepness of the voltage gating process in scVDAC1 and thus proposed that they belong to the voltage sensor, that is moving during the gating process. They will be discussed in detail in the following. Aspartate-15 and Lysine-19 are conserved among the VDACs from different species, are part of the N-terminal α-helix and are thus obviously moving in the models presented here. Lysine-46 in scVDAC1 is equivalent to Serine-46 in hVDAC1. This residue is located in the C-terminal end of β-strand 2, which is also involved into the movements that are induced by the respective rearrangements of the linker between α-helix and β-barrel in both proposed models. Lysine-61, Lysine-65 and Lysine-84 are equivalent to Lysine-61, Threonine-65 and Glutamate-84 in hVDAC1. These residues are located in the proximity of one of the axes of the proposed elliptic deformation that is connected with the closure of the channel. Thus, upon this elliptic deformation they are located in the region which is exhibiting the largest displacements – explaining why they have been identified as moving during the gating. The same argument is true for Glutamate-145 and Glutamate-152 (equivalent to Glutamate-147 and Glutamine-154 in hVDAC1), with the only difference that they are located near the second of the two axes of the proposed ellipse. Thus, for all these residues the findings of Colombini can be explained with the models proposed in this thesis. The only residue where the explanation of its movement has to remain unclear is Aspartate-282 (equivalent to Glutamine-282), as this residue does not move in both models proposed here.

Which of the two suggested models is more realistic has to be probed with further experiments – see Chapter 5. The possibility that each of the suggested models implements one of the two gating processes of VDAC (the one at positive and the one at negative potential) might be imaginable too.

Dieses Werk ist copyrightgeschützt und darf in keiner Form vervielfältigt werden noch an Dritte weitergegeben werden.
Es gilt nur für den persönlichen Gebrauch.

Dieses Werk ist copyrightgeschützt und darf in keiner Form vervielfältigt werden noch an Dritte weitergegeben werden.
Es gilt nur für den persönlichen Gebrauch.

5 Conclusion & Outlook

The results of this thesis shed further light into the gating process of VDAC and increase the overall understanding of how VDAC is behaving in lipid bilayers and reconstituted into detergent micelles and which influence these environments have on the channel gating. Also, new information about structural changes during the gating process have been obtained.

The liquid state NMR assignment, which is the basis for further analysis of the channel with the means of NMR spectroscopy, was once again revised and improved in this thesis. The current assignment statistics are as follows: for *wt* hVDAC1, 88.1 %/94.8 % (whole protein/barrel) of the NH backbone resonances are assigned now. For E73VC127AC232S hVDAC1, a mutant in which the overall barrel is stabilized, the respective values are 92.1 % and 98.4 % (whole protein/barrel). For Quintuple hVDAC1, a mutant in which the closed state of the protein is stabilized, 91.4 % of the whole protein's NH backbone groups and 98.4 % of the NH backbone groups in the barrel are assigned.

Furthermore, by recording TROSY-HNCACB experiments, the assignment of the C_β resonances in the protein was finally possible. This lead to 87.4 % of the C_β resonances being assigned in E73VC127AC232S hVDAC1 and 54.1 % of the same being assigned in Quintuple hVDAC1.

Lastly, the existing NOE network in E73V hVDAC1 was dramatically improved. 900 new H_N-H_N NOE contacts raised the overall number of contacts to 1431, which is a nearly threefold improvement with respect the previous values.

Based on the improved NOE network, the improved overall assignment and previously recorded relaxation data, a new 3D structure of E73V hVDAC1 reconstituted into LDAO micelles was determined and published. The structure features an elliptic β-barrel that implements the maximal ex-

Dieses Werk ist copyrightgeschützt und darf in keiner Form vervielfältigt werden noch an Dritte weitergegeben werden.
Es gilt nur für den persönlichen Gebrauch.

cursion of a previously calculated global elliptic deformation mode of the channel. The N-terminal α-helix is, as in the X-ray structure from 2008, tightly bound to the β-barrel and has a short kink from residues 10 to 12. As shown in the Discussion, the ellipticity of the β-barrel is the manifestation of both the different lateral pressure, the detergent micelles are exerting on the barrel, and the E73V mutation.

A publication from 2012 lead to the development of a G21V/G23V/E73V/C127A/C232S hVDAC1 mutant, called Quintuple hVDAC1. It has been shown that this mutant is significantly stabilizing the closed state of the protein. Based on the NMR structure of E73V hVDAC1 and previously published results about the gating mechanism of the channel, seemingly contradictory results about how large the relative share of closed channels in this mutant is, have been understood: reconstitution in detergent micelles is causing an inherent necessity of the channel to be open. Based on MTSL labeling experiments and as shown in the Discussion, an estimated 10 % of the Quintuple hVDAC1 channels in liquid state NMR are situated in a closed state of the channel.

Several lines of evidence point to a) a movement of the N-terminal α-helix upon gating and b) that the new location of the helix is at the cytosolic side of the channel at the C-terminal β-strands. Based on these results, two possible models for the movement of the helix upon gating have been developed and are proposed in this thesis. One of the models comprises a movement of the α-helix such that it is bending back to the respective C-terminal β-strands. The second model proposes that the α-helix is pulled out of the channel by the linker between α-helix and β-barrel.

Further experiments or calculations are recommended to gain more insight into which of the models is a better representation of a closed state of the channel. For example, the PRE profile which is expected based on MTSL labeling at residue 2 from both of these models could be calculated and compared with the already known experimental PRE profile.

To circumvent the problems the different lateral pressure of the detergent micelles is causing, it could be tried to study Quintuple hVDAC1 reconstituted into covalently circularized nanodiscs. This system has already been shown by Nasr *et al.*[160] to deliver very nice spectra with VDAC. If these nanodiscs are better stabilizing the channel when the α-helix has moved from its original position, this system could further improve the results on Quintuple hVDAC1. Also solid state NMR

Dieses Werk ist copyrightgeschützt und darf in keiner Form vervielfältigt werden noch an Dritte weitergegeben werden.
Es gilt nur für den persönlichen Gebrauch.

experiments on 2D crystals of Quintuple hVDAC1 could deliver further insights, first experiments on this system seem to be very promising.

Additionally, the observed resonance intensity changes in the C-terminal β-strands in Quintuple hVDAC1 should be further investigated. It should be checked with Het-NOE or CPMG measurements, in how far the dynamics of these β-strands change in Quintuple hVDAC1 with respect to *wt* hVDAC1 and E73V hVDAC1, respectively, and also, which implication that has for the channel and for the closed state of the channel.

Dieses Werk ist copyrightgeschützt und darf in keiner Form vervielfältigt werden noch an Dritte weitergegeben werden.
Es gilt nur für den persönlichen Gebrauch.

Dieses Werk ist copyrightgeschützt und darf in keiner Form vervielfältigt werden noch an Dritte weitergegeben werden.
Es gilt nur für den persönlichen Gebrauch.

Appendix A Pulse programs

In the following the pulse program used for the acquisition of the TROSY-HNCACB and the pulse programs used for measuring the ^{15}N relaxation data are given.

A.1 Pulse program of TROSY-HNCACB

```
;trhncacbetgp3d
;avance-version (07/08/13)
;TROSY-HNCACB
;3D sequence with
;   inverse correlation for triple resonance
;      via TROSY and inept transfer steps
;
;      F1(H) -> F3(N) -> F2(Caliph.,t1) -> F3(N,t2) -> F1(H,t3)
;
;on/off resonance Ca and C=O pulses using shaped pulse
;phase sensitive (t1)
;phase sensitive using Echo/Antiecho gradient selection (t2)
;using constant time in t2
;with H-1 180degree pulses in t1
;uncompensated version d25=d26
;(use parameterset TRHNCACBETGP3D)
;
;T. Schulte-Herbrueggen & O.W. Sorensen, J. Magn. Reson. 144,
;   123 - 128 (2000)
;A. Eletsky, A. Kienhoefer & K. Pervushin,
;   J. Biomol. NMR 20, 188-180 (2001)
;(M. Salzmann, G. Wider, K. Pervushin, H. Senn & K. Wuethrich,
;   J. Am. Chem. Soc. 121, 844-848 (1999))
;
;$CLASS=HighRes
;$DIM=3D
;$TYPE=
;$SUBTYPE=
;$COMMENT=


prosol relations=<triple>


#include <Avance.incl>
#include <Grad.incl>
#include <Delay.incl>


define list<gradient> EA5 = { 0.8750 1.0000}
```


Dieses Werk ist copyrightgeschützt und darf in keiner Form vervielfältigt werden noch an Dritte weitergegeben werden.
Es gilt nur für den persönlichen Gebrauch.

```
define list<gradient> EA7 = { 1.0000 0.6667}
define list<gradient> EA9 = { 0.6595 1.0000}


"p2=p1*2"
"p22=p21*2"
"d11=30m"
"d12=20u"

"d19=1.75m"        ;shorter 1h-15n-inept delay
"d23=11m"
"d25=2.3m"
"d26=2.3m"
"d28=3.6m"


"d0=3u"
"d10=3u"
"d30=d23/2-d25/2-p14/2-p16/2-d16/2-2u"

"in0=inf1/4"
"in10=inf2/4"

"in30=in10"


"DELTA=d0*4+p2*2+larger(p14,p22)-p14-4u"
;"DELTA1=d26-p16-d16"
"DELTA1=d19-p16-d16"        ;shorter 1h-15n-inept delay
;"DELTA2=d23-p16-d16"
"DELTA2=d23-d16"            ;deleted gradient at this place
"DELTA3=d28-p16-d16"
"DELTA4=d23/2-d25/2-p14/2-d10+p21*2/3.1416"
"DELTA5=d23/2-d25/2-p14/2-d10-p16-d16-p11+p21*2/3.1416-8u"
"DELTA6=d25-p16-d16"
"DELTA7=d26-p11-p16-d16-8u"


"spoff2=0"
"spoff3=0"
"spoff5=bf2*(cnst21/1000000)-o2"
"spoff8=0"


aqseq 321


1 d11 ze
2 d11
3 d1 pl1:f1
  50u UNBLKGRAD

  4u pl0:f1
  (p11:sp1 ph2:r):f1
  4u
  4u pl1:f1

  4u pl3:f3    ;new line, loading power level on 15n

  (p1 ph3):f1
  p16:gp1
  d16
  DELTA1
  (center (p2 ph2) (p22 ph1):f3 )
  DELTA1
  p16:gp1
  d16
  (p1 ph2):f1

  (p21 ph1):f3
```


Dieses Werk ist copyrightgeschützt und darf in keiner Form vervielfältigt werden noch an Dritte weitergegeben werden.
Es gilt nur für den persönlichen Gebrauch.

```
d16                ;deleted gradient here
DELTA2
(center (p14:sp3 ph1):f2 (p22 ph1):f3 )
DELTA2
d16
(p21 ph2):f3

(p13:sp2 ph6):f2
p16:gp3
d16
DELTA3
(p14:sp3 ph1):f2
DELTA3
p16:gp3
d16
(p13:sp8 ph2):f2

d0
(p2 ph1):f1
d0
(center (p14:sp5 ph1):f2 (p22 ph1):f3 )
d0
(p2 ph1):f1
d0
(p14:sp3 ph1):f2
DELTA
(p14:sp5 ph1):f2
4u

(p13:sp2 ph9):f2
p16:gp4
d16
DELTA3
(p14:sp3 ph1):f2
DELTA3
p16:gp4
d16
(p13:sp8 ph10):f2

(p21 ph5):f3
d30
(p14:sp5 ph1):f2
d30
(center (p14:sp3 ph1):f2 (p22 ph1):f3 )
DELTA4
d10
(p14:sp5 ph1):f2
d10
DELTA5
p16:gp5*EA5
d16 pl0:f1
(p11:sp1 ph3:r):f1
4u
4u pl1:f1

(p1 ph7)
p16:gp6
d16
DELTA6
(center (p2 ph2) (p22 ph2):f3 )  ;deleted 13c pulse here
DELTA6
p16:gp6
d16
(p1 ph1)

p16:gp7*EA7
d16
4u

(p21 ph1):f3
```


Dieses Werk ist copyrightgeschützt und darf in keiner Form vervielfältigt werden noch an Dritte weitergegeben werden.
Es gilt nur für den persönlichen Gebrauch.

```
  p16:gp8
  d16
  DELTA7 pl0:f1
  (p11:sp1 ph4:r):f1
  4u
  4u pl1:f1
  (center (p2 ph2) (p22 ph2):f3 )
  4u pl0:f1
  (p11:sp1 ph4:r):f1
  4u
  DELTA7
  p16:gp8
  d16 pl1:f1
  (p21 ph8:r):f3

  p16:gp9*EA9
  d16
  4u BLKGRAD

  go=2 ph31
  d11 mc #0 to 2
     F1PH(rd10 & rd30 & rp5 & rp31 & dp9 & dp10, id0)
     F2EA(igrad EA5 & igrad EA7 & igrad EA9 & ip7*2 & ip8*2, id10 & dd30 & ip5*2 & ip31*2)

exit


ph1=0
ph2=1
ph3=2
ph4=3
ph5=0 2
ph6=0 0 2 2
ph7=3
ph8=3
ph9=0
ph10=1
ph31=0 2 2 0


;pl0 : 120dB
;pl1 : f1 channel - power level for pulse (default)
;pl3 : f3 channel - power level for pulse (default)
;sp1: f1 channel - shaped pulse  90 degree  (H2O on resonance)
;sp2: f2 channel - shaped pulse  90 degree  (Cali on resonance)
;sp3: f2 channel - shaped pulse 180 degree  (Cali on resonance)
;sp5: f2 channel - shaped pulse 180 degree  (C=O off resonance)
;sp8: f2 channel - shaped pulse  90 degree  (Cali on resonance)
;                  for time reversed pulse
;p1 : f1 channel -  90 degree high power pulse
;p2 : f1 channel - 180 degree high power pulse
;p11: f1 channel -  90 degree shaped pulse             [1 msec]
;p13: f2 channel -  90 degree shaped pulse
;p14: f2 channel - 180 degree shaped pulse
;p16: homospoil/gradient pulse                         [1 msec]
;p21: f3 channel -  90 degree high power pulse
;p22: f3 channel - 180 degree high power pulse
;d0 : incremented delay (F1 in 3D)                     [3 usec]
;d1 : relaxation delay; 1-5 * T1
;d10: incremented delay (F2 in 3D)                     [3 usec]
;d11: delay for disk I/O                               [30 msec]
;d16: delay for homospoil/gradient recovery
;d23: 1/(4J(NCa)                                       [11 msec]
;d25: 1/(4J'(NH)                                       [2.3 msec]
;d26: 1/(4J(NH)                                        [2.3 msec]
;d28: 1/(8J(CaCb)                                      [3.6 msec]
;d30: decremented delay (F2 in 3D) = d23/2-d25/2-p14/2-p16/2-d16/2-2u
;cnst21: CO chemical shift (offset, in ppm)
;cnst23: Caliphatic chemical shift (offset, in ppm)
;o2p: Caliphatic chemical shift (cnst23)
```


Dieses Werk ist copyrightgeschützt und darf in keiner Form vervielfältigt werden noch an Dritte weitergegeben werden.
Es gilt nur für den persönlichen Gebrauch.

```
;inf1: 1/SW(Cali) = 2 * DW(Cali)
;inf2: 1/SW(N) = 2 * DW(N)
;in0: 1/(4 * SW(Cali)) =  (1/2) DW(Cali)
;nd0: 4
;in10: 1/(4 * SW(N)) = (1/2) DW(N)
;nd10: 4
;in30: = in10
;NS: 8 * n
;DS: >= 16
;td1: number of experiments in F1
;td2: number of experiments in F2       td2 max = 2 * d30 / in30
;FnMODE: States-TPPI (or TPPI) in F1
;FnMODE: echo-antiecho in F2


;use gradient ratio:  gp 1:gp 2:gp 3:gp 4:gp 5:gp 6:gp 7:gp 8: gp 9
;                        2:   2:   2:   2: -80:   2:  30:  45:30.13

;for z-only gradients:
;gpz1: 2%
;gpz2: 2%
;gpz3: 2%
;gpz4: 2%
;gpz5: -80%
;gpz6: 2%
;gpz7: 30%
;gpz8: 45%
;gpz9: 30.13%

;use gradient files:
;gpnam1: SINE.100
;gpnam2: SINE.100
;gpnam3: SINE.100
;gpnam4: SINE.100
;gpnam5: SINE.100
;gpnam6: SINE.100
;gpnam7: SINE.100
;gpnam8: SINE.100
;gpnam9: SINE.100



;Processing

;PHC0(F1): 90
;PHC0(F2): 22.5



;$Id: trhncacbetgp3d,v 1.4.2.1 2007/09/14 16:17:35 ber Exp $
```


Dieses Werk ist copyrightgeschützt und darf in keiner Form vervielfältigt werden noch an Dritte weitergegeben werden.
Es gilt nur für den persönlichen Gebrauch.

A.2 Pulse program for measurement of ^{15}N-R_1 relaxation rates at 900 MHz

```
; 15N-T1 relaxation experiment with TROSY read-out
; for 15N, 15N13C, 2H15N and 2H15N13C labelled proteins
; modified from NL by savi 15/08/2012
; see footnotes
; as pseudo-3D

#include <Avance.incl>
#include <Grad.incl>
#include <Delay.incl>

define list<loopcounter> t1list=<$VCLIST>

define loopcounter COUNTER1
define loopcounter COUNTER2



;#define LABEL_CN  ; switch on for 13C labelled samples
#define TEMP_COMPENSATION


"in0=inf2/2"


# ifdef LABEL_CN
"d0=97u-p4*2+p7*0.66-p1*0.5"
"d25=20m-p15*0.5-p4*4-8u"
#else
"d0=100u+p7*0.66-p1*0.5"
"d25=20m-p15*0.5"
#endif /*LABEL_CN*/

"d11=30m"
"d21=500u-p30*0.5"
"DELTA=2.65m"
"DELTA1=2.65m"
"DELTA2=2.65m-p22-p11-300u"
"DELTA3=2.65m-p23-p10-300u"
"DELTA4=260u-p24-p1*0.66"


"d27=p24+35u"
"d30=d21*4+p2*2"



"l1=1"
"l2=1"



"cnst21=176"
"cnst22=56"
"cnst18=-1"
"cnst23=9"

"spoff4=bf2*((cnst22-cnst21)/1000000)"


aqseq 312
```


Dieses Werk ist copyrightgeschützt und darf in keiner Form vervielfältigt werden noch an Dritte weitergegeben werden.
Es gilt nur für den persönlichen Gebrauch.

```
1       ze
        d11


; ----- start ----------------------------------------------------------------

        3m
        3m
2       d11 do:f2
        1m LOCKH_OFF
        2m BLKGRAD
        10u pl1:f1
        10u pl4:f2
        10u pl7:f3

        "COUNTER1=t1list"
        "COUNTER2=cnst23*4"

        (p7 ph0):f3     ; purge pulse for 15N magnetization before d1
        5u

;-------- Temperature compensation and d1 recovery delay----------------
# ifdef TEMP_COMPENSATION

        "d17=d1-40u-((d21*2+p30)*cnst23*4)"   ; cnst23 is the highest repeat used
in T2 experiment +1

        10u fq=cnst18(bf ppm):f3
        10u pl30:f3

10      d21
        (p30 ph16):f3             ; 15N pulses are applied almost on-resonance
        d21
        lo to 10 times COUNTER2

        10u
        10u fq=0:f3
        d17

# else
        d1
# endif
        1m UNBLKGRAD
        10u pl7:f3

;------- kill steady state 15N ------------
        (p7 ph0):f3
        5u
        p20:gp6
        200u

;------- first INEPT Hz-> 2HxNz -----------
        (p1 ph0):f1
        5u
        DELTA gron0 ; soft gradient to prevent radiation damping
        5u  groff
        (center(p1*2 ph0):f1 (p7*2 ph0):f3)
        5u
        DELTA gron0
        5u groff

;------- rephase  2HxNz to Nz------ --------
        (p1 ph5):f1  (p7 ph0):f3
        5u
        DELTA1 gron1 ; soft gradient to prevent radiation damping
        5u groff
        (center (p1*2 ph0):f1 (p7*2 ph0):f3)
        5u
        DELTA1 gron1
```


Dieses Werk ist copyrightgeschützt und darf in keiner Form vervielfältigt werden noch an Dritte weitergegeben werden.
Es gilt nur für den persönlichen Gebrauch.

```
        5u groff
        (p7 ph6):f3 ; phase-cycle Nz, -Nz for Freeman-Hill decay
        5u
;-----------------------------------------
        (p1 ph2):f1 ; purge pulse to kill any residual HzNz
        5u
        p21:gp7  ; cleaning gradient
        100u
        100u pl0:f1
;------15N T1 relaxation period--------------

if "COUNTER1==0" goto 77  ; jump to 77 for zero relaxation data point, (0 in t1list)

70       d25*0.5
#  ifdef LABEL_CN
         3u pl4:f2
         (p4*2 ph0 3u 3u pl2 p4*2:sp4 ph0):f2
#  endif
         d25*0.5
         (p15:sp5 ph0):f1
         d25*0.5
#  ifdef LABEL_CN
         3u pl4:f2
         (p4*2 ph0 3u 3u pl2 p4*2:sp4 ph0):f2
# endif
        d25*0.5
        lo to 70 times COUNTER1   ; delay=t1list*2*d25 (40ms)

;------Echo/ Anti-echo encoding for TROSY read-out------------
 77     3u
        3u pl4:f2
        3u pl1:f1
        if "l1==1"
        {
        (p7 ph7):f3
        10u
        p25:gp5
        200u
        (p7*2 ph7):f3
        10u
        p25:gp5*-1
        }
        else
        {
        (p7 ph17):f3
        10u
        p25:gp5*-1
        200u
        (p7*2 ph17):f3
        10u
        p25:gp5
        }
;------ t1 (15N) evolution period ------------------------------
        d0
# ifdef LABEL_CN
        (p4*2 ph0 3u 3u pl2 p4*2:sp4 ph0):f2
# endif
        d0
;------ start TROSY read-out-----------------------------------
        if "l1==1"
        {
        (p1 ph1):f1    ; Echo
        3u
        3u pl0:f1
        (p11:sp11 ph11:r):f1
        6u
        }
        else
        {
        (p1 ph3):f1   ; Anti-Echo
```


Dieses Werk ist copyrightgeschützt und darf in keiner Form vervielfältigt werden noch an Dritte weitergegeben werden.
Es gilt nur für den persönlichen Gebrauch.

```
        3u
        3u pl0:f1
        (p11:sp11 ph13:r):f1
        6u
        }
        5u pl1:f1
;goto 999 ; optimization of  water supression
        DELTA2
        p22:gp2
        300u
        (center (p1*2 ph0):f1 (p7*2 ph0):f3)
        7u
        p22:gp2
        DELTA2
        300u pl0:f1
;-------------------------------------------------
        (p11:sp12 ph12:r):f1
        5u
        3u pl1:f1
        if "l1==1"
        {
        (p1 ph0):f1 (p7 ph1):f3  ; Echo
        }
        else
        {
        (p1 ph0):f1 (p7 ph3):f3     ; Anti-Echo
        }
        ;goto 999 ; for optimization of  water supression
        DELTA3
        p23:gp3
        200u
        100u pl10:f1
        (center(p10 ph10:r 5u pl1 p1*2 ph0 5u pl10 p10 ph10:r):f1 (p7*2 ph0 d27):f3)
        5u
;goto 999 ; for optimization of  water supression
        p23:gp3
        DELTA3
        DELTA4
        (p7 ph0):f3
        5u
        p24:gp4 ; Echo/Anti-echo decoding gradient
999     5u
        5u pl31:f2
        20u BLKGRAMP

; ----- Acquisition and looping for T1 and E/AE --------------------------------

        go=2 ph31 cpds2:f2
        1m do:f2
        1m LOCKH_OFF
        d11 do:f2 mc #0 to 2
           F1QF(t1list.inc & iu2)
           F2EA(t1list.res & iu1 & ru2, id0 & ru1)
d30
1m BLKGRAD
exit

ph0=0
ph1=1
ph2=2
ph3=3
ph5=1
ph6=1 1 1 1  3 3 3 3
ph10=2
ph11=3
ph12=0
ph13=1
ph16=1
ph7=1 0 3 2
ph17=1 2 3 0
```


Dieses Werk ist copyrightgeschützt und darf in keiner Form vervielfältigt werden noch an Dritte weitergegeben werden.
Es gilt nur für den persönlichen Gebrauch.

```
ph31=1 2 3 0  3 0 1 2


;-------------NOTES----------------------

;o1p = 4.7 ppm
;o2p=176 ppm (CO)
;o3p=119 ppm

;NS=8*n
;in0=inf/2
;SW=1/(2*in0)
;echo-antiecho in N15 (process as Complex in NmrDraw before splitting the spectra)


; 1H pulses

;p1:  90 deg hard 1H pulse @pl1
;pl1: 1H 90 deg
;pl0: 120 dB
;p10: 1200u (@ 600 MHz) 90 deg soft rectangular water flip-back pulse
;p11: 1900u (@ 600 MHz) 90 deg Sinc1.1000 water flip-back pulse (sp11,sp12)
;p15: 2000u (@ 600 MHz) 180 deg IBurp2 pulse on 1H (sp15)
;sp5: 180 deg IBurp2 pulse on 1H (sp15)
;sp11: 90 deg Sinc1.1000 water flip-back pulse
;sp12: 90 deg Sinc1.1000 water flip-back pulse
;spnam5: IBurp2
;spnam11: Sinc1.1000
;spnam12: Sinc1.1000
;spoffs5: 2340Hz @ 600 MHz (8.6 ppm) , should be centered in amide region but not touch the water

; 13C pulses

;p4: 13CO selective 180 deg (23.7*2us @ 600 MHz) @pl4
;pl2: 120 dB
;pl4: 13C 90 deg

;sp4: 13CA selective 180 deg (23.7*2us @ 600 MHz)
;CPDPRG2: garp (aq C' decoupling)
;pcpd5: C' decoupling (140u or 280u @pl31)
;pl31: C' decoupling power

;15N pulses
;p7 : 90 deg hard 15N pulse @pl7
;p18 : maximum duration of spin-lock; temperature compensation
;pl7 :15N 90 deg

; gradients
;p20: 1000u
;p21: 200u
;p22: 300u
;p23: 1000u
;p24: 60.8u Echo/Anti-echo decoding gradient
;p25: 300u Echo/Anti-echo half-encoding gradient

;for z-only gradients
;gpz0: 3%
;gpz1: 2%
;gpz2: 10%
;gpz3: 50%
;gpz4: 33%
;gpz5: -33%
;gpz6: 30%
;gpz7: -50%

;gpnam2 SINE.10
;gpnam3 SINE.50
;gpnam4 SINE.10
;gpnam5 SINE.10
```


Dieses Werk ist copyrightgeschützt und darf in keiner Form vervielfältigt werden noch an Dritte weitergegeben werden.
Es gilt nur für den persönlichen Gebrauch.

```
;gpnam6 SINE.10
;gpnam7 SINE.10
```


Dieses Werk ist copyrightgeschützt und darf in keiner Form vervielfältigt werden noch an Dritte weitergegeben werden.
Es gilt nur für den persönlichen Gebrauch.

A.3 Pulse program for measurement of ^{15}N-R_2 relaxation rates at 900 MHz

```
; 15N-T2 relaxation experiment with TROSY read-out
; for 15N, 15N13C, 2H15N and 2H15N13C labelled proteins
; written according to NL by savi 15/08/2012
; see footnotes

#include <Avance.incl>
#include <Grad.incl>
#include <Delay.incl>

define list<loopcounter> cpmglist=<$VCLIST>

define loopcounter vc_max

define loopcounter COUNTER1
define loopcounter COUNTER2
define loopcounter COUNTER3

;#define LABEL_CN  ; switch on for 13C labelled samples
#define TEMP_COMPENSATION


"in0=inf2*0.5"

# ifdef LABEL_CN
"d0=97u-p4*2+p7*0.66-p1*0.5"
#else
"d0=100u+p7*0.66-p1*0.5"
#endif /*LABEL_CN*/

"d11=30m"
"d21=500u-p30*0.5"
"DELTA=2.65m"
"DELTA1=2.65m"
"DELTA2=2.65m-p22-p11-300u"
"DELTA3=2.65m-p23-p10-300u"
"DELTA4=260u-p24-p1*0.66"
"DELTA5=d21-p1*2.15-3u"
"DELTA6=d21-p1*2.15-13u"
"DELTA7=d21-10u"
"DELTA8=d21-13u-p4*2"

"d27=p24+35u"

"l1=1"
"l2=1"
"l3=td1"


"cnst21=176"
"cnst22=56"
"cnst18=-1"



"spoff4=bf2*((cnst22-cnst21)/1000000)"

aqseq 312



1       ze
        1m
```


Dieses Werk ist copyrightgeschützt und darf in keiner Form vervielfältigt werden noch an Dritte weitergegeben werden.
Es gilt nur für den persönlichen Gebrauch.

```
        "vc_max=0"

; ----- Count maximum number of cpmg points from cpmglist ----------------------

9       20u
        if "cpmglist > vc_max"
           {
           20u
           "vc_max=cpmglist"
           }

        3m cpmglist.inc
        lo to 9 times l3

        3m cpmglist.res

; ----- start ------------------------------------------------------------------


2       d11 do:f2
        1m LOCKH_OFF
        3m
3       1m
        1m
4       3m
5       2m BLKGRAD
        10u pl1:f1
        10u pl4:f2
        10u pl7:f3

; ------ set counters for cpmg loop and temperature correction -----------------

        20u
        "COUNTER1=cpmglist-1"
        20u
        "COUNTER2=(vc_max-cpmglist+2)*4"
        20u
        "COUNTER3=cpmglist-2"
        20u

        (p7 ph0):f3     ; purge pulse for 15N magnetization before d1
        5u


;---------temperature compensation and d1 recovery delay---------
# ifdef TEMP_COMPENSATION

 "d17=d1-40u-((d21*2+p30)*COUNTER2)"

        10u fq=cnst18(bf ppm):f3
        10u pl30:f3

        if "COUNTER2>=1"
        {
10      d21
        (p30 ph16):f3
        d21
        lo to 10 times COUNTER2
        }
                   ; 15N pulses are applied far off-resonance
        10u
        10u fq=0:f3
        d17
# else
        d1
# endif
        1m UNBLKGRAD
        10u pl7:f3

;------- kill steady state 15N ------------
```


Dieses Werk ist copyrightgeschützt und darf in keiner Form vervielfältigt werden noch an Dritte weitergegeben werden.
Es gilt nur für den persönlichen Gebrauch.

```
        (p7 ph0):f3
        5u
        p20:gp6
        200u

;------- first INEPT Hz-> 2HxNz -----------
        (p1 ph0):f1
        5u
        DELTA gron0 ; soft gradient to prevent radiation damping
        5u  groff
        (center(p1*2 ph0):f1 (p7*2 ph0):f3)
        5u
        DELTA gron0
        5u groff

;------- rephase  2HxNz to Nz------ --------
        (p1 ph5):f1  (p7 ph0):f3
        5u
        DELTA1 gron1 ; soft gradient to prevent radiation damping
        5u groff
        (center (p1*2 ph0):f1 (p7*2 ph0):f3)
        5u
        DELTA1 gron1
        5u groff
        (p7 ph6):f3 ; phase-cycle Nz, -Nz for Freeman-Hill decay
        5u
;-----------------------------------------
        (p1 ph2):f1 ; purge pulse to kill any residual HzNz
        5u
        p21:gp7  ; cleaning gradient
        100u
        100u

;------15N T1 relaxation period--------------
;------ excitation pulse ------------------------------------------------------

        (p7 ph18):f3 ; rotate -Nz to Ny

;---- N-1 loop ---------------
        if "COUNTER1==0" goto 20
        if "COUNTER1>=1"
        {
14      5u
        DELTA7 pl30:f3
        5u
        (p30 ph16):f3
        d21
        lo to 14 times COUNTER1
        }

;---- 1 times with 1H decoupling composite pulse -----------------------------
        d21
        (p30 ph16):f3
        DELTA5
        (p1 ph0 3u p1*2.3 ph1 3u p1 ph0):f1
        5u
        DELTA6 gron9
        5u groff
        (p30 ph16):f3
        5u
        DELTA7 gron9
        5u groff

;---- N-2 loop ---------------------------------------------------------------
        if "COUNTER3>=1"
        {
15      5u
        DELTA7 gron9
        5u groff
        (p30 ph16):f3
```


Dieses Werk ist copyrightgeschützt und darf in keiner Form vervielfältigt werden noch an Dritte weitergegeben werden.
Es gilt nur für den persönlichen Gebrauch.

```
        5u
        DELTA7 gron9
        5u groff
        lo to 15 times COUNTER3
        }

;----1x with 13C decoupling in the middle ----------------------------------------
        5u
        DELTA7 gron9
        5u groff
        (p30 ph16):f3
        5u
        DELTA8 gron9
        5u groff
        (p4*2 ph0 3u 3u pl2 p4*2:sp4 ph0):f2
        5u
        DELTA8 gron9*-1
        5u groff
        (p30 ph16):f3
        5u
        DELTA7 gron9*-1
        5u groff

;----N-2 loop ---------------------------------------------------------------
       if "COUNTER3>=1"
        {
16      5u
        DELTA7 gron9*-1
        5u groff
        (p30 ph16):f3
        5u
        DELTA7 gron9*-1
        5u groff
        lo to 16 times COUNTER3
        }

;---- 1x with 1H decoupling composite pulse -------------------------------------
        5u
        DELTA7 gron9*-1
        5u groff
        (p30 ph16):f3
        5u
        DELTA6 gron9*-1
        5u groff
        (p1 ph0 3u p1*2.3 ph1 3u p1 ph0):f1
        DELTA5
        (p30 ph16):f3
        d21

;---- N-1 loop ------------------------------------------------------------------
        if "COUNTER1>=1"
        {
17      5u
        DELTA7 pl30:f3
        5u
        (p30 ph16):f3
        5u
        DELTA7 pl7:f3
        5u
        lo to 17 times COUNTER1
        }
        goto 21

;--- if counter1 is 0 ----------------------------------------------------------
20      5u
        DELTA7 pl30:f3
        5u
        (p30 ph16):f3
        DELTA5
        (p1 ph0 3u p1*2.3 ph1 3u p1 ph0):f1
```


Dieses Werk ist copyrightgeschützt und darf in keiner Form vervielfältigt werden noch an Dritte weitergegeben werden.
Es gilt nur für den persönlichen Gebrauch.

```
;----1x with 13C decoupling in the middle ----------------------------------------
        5u
        DELTA6 gron9
        5u groff
        (p30 ph16):f3
        5u
        DELTA8 gron9
        5u groff
        (p4*2 ph0 3u 3u pl2 p4*2:sp4 ph0):f2
        5u
        DELTA8 gron9*-1
        5u groff
        (p30 ph16):f3
        5u
        DELTA6 gron9*-1
        5u groff
        (p1 ph0 3u p1*2.3 ph1 3u p1 ph0):f1
        DELTA5
        (p30 ph16):f3
        5u
        DELTA7 pl7:f3
        5u
;-------------------------------------------------------------------------------


;----- flip back to Nz/-Nz-------------------------------------------------------
21
        (p7 ph8):f3  ; rotate back to -Nz

        5u
        p21:gp8  ; cleaning gradient
        100u
        100u

;------Echo/ Anti-echo encoding for TROSY read-out------------
77      3u
        3u pl4:f2
        3u pl1:f1
        if "l1==1"
        {
        (p7 ph7):f3
        10u
        p25:gp5
        200u
        (p7*2 ph7):f3
        10u
        p25:gp5*-1
        }
        else
        {
        (p7 ph17):f3
        10u
        p25:gp5*-1
        200u
        (p7*2 ph17):f3
        10u
        p25:gp5
        }
;------ t1 (15N) evolution period ------------------------------
        d0
# ifdef LABEL_CN
        (p4*2 ph0 3u 3u pl2 p4*2:sp4 ph0):f2
# endif
        d0
;------ start TROSY read-out-----------------------------------
        if "l1==1"
        {
        (p1 ph1):f1    ; Echo
        3u
```


Dieses Werk ist copyrightgeschützt und darf in keiner Form vervielfältigt werden noch an Dritte weitergegeben werden.
Es gilt nur für den persönlichen Gebrauch.

```
        3u pl0:f1
        (p11:sp11 ph11:r):f1
        6u
        }
        else
        {
        (p1 ph3):f1   ; Anti-Echo
        3u
        3u pl0:f1
        (p11:sp11 ph13:r):f1
        6u
        }
        5u pl1:f1
;goto 999 ; optimization of  water supression
        DELTA2
        p22:gp2
        300u
        (center (p1*2 ph0):f1 (p7*2 ph0):f3)
        7u
        p22:gp2
        DELTA2
        300u pl0:f1
;-----------------------------------------------
        (p11:sp12 ph12:r):f1
        5u
        3u pl1:f1
        if "l1==1"
        {
        (p1 ph0):f1 (p7 ph1):f3  ; Echo
        }
        else
        {
        (p1 ph0):f1 (p7 ph3):f3     ; Anti-Echo
        }
        ;goto 999 ; for optimization of  water supression
        DELTA3
        p23:gp3
        200u
        100u pl10:f1
        (center(p10 ph10:r 5u pl1 p1*2 ph0 5u pl10 p10 ph10:r):f1 (p7*2 ph0 d27):f3)
        5u
;goto 999 ; for optimization of  water supression
        p23:gp3
        DELTA3
        DELTA4
        (p7 ph0):f3
        5u
        p24:gp4 ; Echo/Anti-echo decoding gradient
999     5u
        5u pl31:f2
        20u BLKGRAMP
        go=2 ph31 cpds2:f2
        1m do:f2
        1m LOCKH_OFF

        d11 do:f2 mc #0 to 2
        F1QF(cpmglist.inc & iu2)
        F2EA(cpmglist.res & iu1 & ru2, id0 & ru1)

1m
1m BLKGRAD
exit

ph0=0
ph1=1
ph2=2
ph3=3
ph5=1
ph6=1 1 1 1  3 3 3 3
ph8=0
```


Dieses Werk ist copyrightgeschützt und darf in keiner Form vervielfältigt werden noch an Dritte weitergegeben werden.
Es gilt nur für den persönlichen Gebrauch.

```
ph10=2
ph11=3
ph12=0
ph13=1
ph16=3
ph7=1 0 3 2
ph17=1 2 3 0
ph18=2
ph31=1 2 3 0  3 0 1 2


;-------------NOTES----------------------

;o1p = 4.7 ppm
;o2p=176 ppm (CO)
;o3p=119 ppm

;NS=8*n
;in0=inf/2
;SW=1/(2*in0)
;echo-antiecho in N15 (process as Complex in NmrDraw before splitting the spectra)


; 1H pulses

;p1:  90 deg hard 1H pulse @pl1
;pl1: 1H 90 deg
;pl0: 120 dB
;p10: 1200u (@ 600 MHz) 180 deg soft rectangular water flip-back pulse
;p11: 1900u (@ 600 MHz) 90 deg Sinc1.1000 water flip-back pulse (sp11,sp12)
;p15: 2000u (@ 600 MHz) 180 deg IBurp2 pulse on 1H (sp15)
;sp5: 180 deg IBurp2 pulse on 1H (sp15)
;sp11: 90 deg Sinc1.1000 water flip-back pulse
;sp12: 90 deg Sinc1.1000 water flip-back pulse
;spnam5: IBurp2
;spnam11: Sinc1.1000
;spnam12: Sinc1.1000
;spoffs5: 2340Hz @ 600 MHz (8.6 ppm) , should be centered in amide region but not touch the water

; 13C pulses

;p4: 13CO selective 180 deg (23.7*2us @ 600 MHz) @pl4
;pl2: 120 dB
;pl4: 13C 90 deg

;sp4: 13CA selective 180 deg (23.7*2us @ 600 MHz)
;CPDPRG2: garp (aq C' decoupling)
;pcpd5: C' decoupling (140u or 280u @pl31)
;pl31: C' decoupling power

;15N pulses
;p7 : 90 deg hard 15N pulse @pl7
;p18 : maximum duration of spin-lock; temperature compensation
;pl7 :15N 90 deg
;pl8: 15N spin-lock power

; gradients
;p20: 1000u
;p21: 200u
;p22: 300u
;p23: 1000u
;p24: 60.8u Echo/Anti-echo decoding gradient
;p25: 300u Echo/Anti-echo half-encoding gradient

;for z-only gradients
;gpz0: 3%
;gpz1: 2%
;gpz2: 10%
;gpz3: 50%
;gpz4: 33%
```


Dieses Werk ist copyrightgeschützt und darf in keiner Form vervielfältigt werden noch an Dritte weitergegeben werden.
Es gilt nur für den persönlichen Gebrauch.

```
;gpz5: -33%
;gpz6: 30%
;gpz7: -50%
;gpz8: 40%

;gpnam2 SINE.10
;gpnam3 SINE.50
;gpnam4 SINE.10
;gpnam5 SINE.10
;gpnam6 SINE.50
;gpnam7 SINE.10
;gpnam8 SINE.10
```


Dieses Werk ist copyrightgeschützt und darf in keiner Form vervielfältigt werden noch an Dritte weitergegeben werden.
Es gilt nur für den persönlichen Gebrauch.

Dieses Werk ist copyrightgeschützt und darf in keiner Form vervielfältigt werden noch an Dritte weitergegeben werden.
Es gilt nur für den persönlichen Gebrauch.

Appendix B Assignment tables of important hVDAC1 mutants

B.1 Chemical shift assignment of *wt* hVDAC1

Table B.1: Backbone chemical shifts of *wt* hVDAC1

	H_i	N	$C_{\alpha i}$	$C_{\alpha i-1}$	C'_{i-1}*		H_i	N	$C_{\alpha i}$	$C_{\alpha i-1}$	C'_{i-1}*
M1	-	-	-	-	-	Y22	6.608	113.7	55.82	44.27	-
A2	-	-	-	-	-	G23	-	-	-	-	-
V3	-	-	-	-	-	F24	7.081	120.2	56.17	-	-
P4	-	-	-	-	-	G25	8.141	110.2	45.40	56.19*	-
P5	-	-	-	-	-	L26	7.487	118.3	53.09	45.24*	172.9
T6	7.411	106.1	60.20	61.18	174.4	I27	8.696	120.9	59.72	52.97	176.6
Y7	7.659	122.5	62.08	60.25	176.2	K28	8.760	126.8	54.87	59.87	175.0
A8	8.404	119.1	53.59	62.13*	178.7	L29	8.725	124.1	53.35	54.91	173.9
D9	7.237	115.2	53.61	53.61	177.6	D30	8.475	123.1	53.49	53.49	174.4
L10	7.366	125.4	56.04	53.43*	177.5	L31	9.112	123.9	53.67	53.67	173.9
G11	-	-	-	-	-	K32	8.611	125.3	55.05*	-	-
K12	7.278	122.2	59.54	44.58*	175.5	T33	9.017	115.9	60.13	55.06	172.2
S13	-	-	-	-	-	K34	8.131	123.7	55.18	60.01	172.9
A14	8.320	121.9	54.86	-	-	S35	8.820	120.3	57.00	55.04	175.8
R15	7.307	117.2	59.70	54.91*	-	E36	-	-	-	-	-
D16	8.559	118.6	-	-	-	N37	-	-	-	-	-
V17	7.495	120.4	66.26	-	-	G38	7.862	106.5	45.22	52.78	175.4
F18	-	-	-	-	-	L39	7.617	122.5	54.99	45.29	-
T19	-	-	-	-	-	E40	8.841	124.5	54.95	54.95	-
K20	-	-	-	-	-	F41	8.743	124.5	56.43	54.97	-
G21	-	-	-	-	-	T42	8.886	120.3	61.10*	-	-

Dieses Werk ist copyrightgeschützt und darf in keiner Form vervielfältigt werden noch an Dritte weitergegeben werden.
Es gilt nur für den persönlichen Gebrauch.

	H_i	N	$C_{\alpha i}$	$C_{\alpha i-1}$	C'_{i-1}*		H_i	N	$C_{\alpha i}$	$C_{\alpha i-1}$	C'_{i-1}*
S43	9.262	121.9	56.62	-	-	L81	8.601	127.3	53.30	62.84	173.7
S44	8.631	120.4	56.48	56.48	173.0	G82	-	-	-	-	-
G45	9.095	111.4	44.98	-	173.3	T83	-	-	-	-	-
S46	9.087	116.0	56.64	44.92	172.0	E84	-	-	-	-	-
A47	9.163	123.8	49.39	56.62	172.3	I85	9.196	127.3	60.03	-	-
N48	8.320	122.3	52.52	49.44	175.3	T86	9.076	123.7	60.77	59.97	174.5
T49	-	-	-	-	-	V87	9.321	124.4	59.88	60.72	173.1
E50	8.517	119.6	57.47	64.31	-	E88	-	-	-	-	-
T51	8.095	114.1	-	-	-	D89	8.721	118.1	57.14	55.17	-
T52	7.848	108.3	-	-	-	Q90	7.847	116.6	55.36	-	175.2
K53	7.525	120.1	56.34	64.14*	172.2	L91	8.141	117.3	58.26	-	-
V54	8.595	125.1	59.77	56.41	176.8	A92	-	-	-	-	-
T55	8.760	118.5	59.78	59.78	175.2	R93	8.839	124.0	57.58	-	-
G56	8.302	109.4	45.33	59.76*	172.4	G94	9.415	115.4	45.08	57.62	177.3
S57	9.156	113.4	57.12	-	-	L95	7.909	122.7	53.72	45.09	173.7
L58	9.128	122.3	54.03	57.14	172.4	K96	9.678	132.3	55.18	53.77	175.3
E59	9.059	124.6	54.60	-	-	L97	8.716	127.0	53.52	55.09	-
T60	9.046	120.4	60.70	54.55	-	T98	9.152	120.4	61.15	53.55	174.6
K61	8.909	126.9	54.52	60.69	172.7	F99	9.470	127.0	55.96	61.11	172.9
Y62	9.343	125.1	56.92	54.52	-	D100	8.648	128.8	52.30	56.01	-
R63	8.073	124.9	-	-	-	S101	8.759	119.1	56.57	52.24	174.5
W64	8.940	126.4	54.15	-	-	S102	8.695	118.8	57.07	56.55	-
T65	-	-	-	-	-	F103	8.913	122.3	55.73	57.17	-
E66	-	-	-	-	-	S104	7.810	120.7	52.95	55.79	-
Y67	6.572	114.5	-	-	-	P105	-	-	-	-	-
G68	7.572	105.1	46.71	-	-	N106	-	-	-	-	-
L69	7.336	120.5	53.83	46.67	175.7	T107	-	-	-	-	-
T70	9.086	120.6	62.08	53.74	176.7	G108	8.230	111.9	45.27	-	-
F71	9.335	128.0	55.93	62.04	-	K109	7.468	120.5	56.43	45.28	173.7
T72	-	-	-	-	-	K110	8.463	124.4	54.80	56.43	175.8
E73	8.940	126.2	54.09	-	-	N111	8.571	120.1	52.65	54.75	175.2
K74	-	-	-	-	-	A112	8.577	124.9	51.31	52.65	176.7
W75	-	-	-	-	-	K113	9.008	119.7	54.55	51.34	-
N76	7.567	122.4	51.75	-	174.1	I114	8.795	120.4	59.25	54.67	175.7
T77	8.013	108.4	63.58	-	-	K115	9.281	126.7	54.62	59.34	174.9
D78	7.701	121.0	53.88	-	-	T116	8.688	117.1	60.13	54.77	175.9
N79	8.441	114.7	54.25	53.94*	176.0	G117	9.161	113.6	44.48	60.13	174.5
T80	7.393	113.0	62.66	-	174.1	Y118	9.153	123.5	56.55	44.51	171.1

Dieses Werk ist copyrightgeschützt und darf in keiner Form vervielfältigt werden noch an Dritte weitergegeben werden.
Es gilt nur für den persönlichen Gebrauch.

	H_i	N	$C_{\alpha i}$	$C_{\alpha i-1}$	C'_{i-1}*		H_i	N	$C_{\alpha i}$	$C_{\alpha i-1}$	C'_{i-1}*
K119	7.615	125.0	52.90	56.51	172.3	F157	9.554	127.5	56.15	52.24	173.4
R120	8.721	118.1	53.63	52.96	173.0	E158	8.076	127.7	54.87	56.23	173.5
E121	8.476	120.7	59.41	53.83	174.5	T159	7.645	117.0	64.89	54.83	177.1
H122	7.883	112.3	59.44	59.44	177.1	A160	9.152	125.0	54.44	64.96	177.1
I123	7.940	118.0	59.92	59.49	173.5	K161	-	-	-	-	-
N124	8.976	125.3	52.78	59.91	171.9	S162	7.486	114.7	58.36	54.63	175.3
L125	9.471	128.8	53.25	52.76	174.5	R163	6.834	115.0	53.71	58.34	173.1
G126	9.494	113.6	44.76	53.25	175.8	V164	8.815	124.3	62.01	53.76	174.5
C127	8.533	121.3	58.11	44.73	171.9	T165	8.634	118.8	61.27	61.93	177.0
D128	9.383	129.9	52.41	58.08	172.7	Q166	7.442	121.0	55.31	61.32*	174.6
M129	9.406	123.0	54.42	52.41	175.0	S167	8.336	119.0	57.05	55.31	174.6
D130	8.559	124.9	52.78	54.35	173.0	N168	9.120	127.2	51.53	56.93	172.7
F131	8.521	123.0	57.88	52.73	176.0	F169	8.615	118.2	56.10	51.46	171.9
D132	7.394	122.8	54.05	57.81	-	A170	8.830	122.7	51.02	56.08	173.4
I133	8.448	124.2	62.95	54.06	-	V171	8.226	116.8	60.14	51.03	176.2
A134	8.469	123.4	52.45	63.03	176.8	G172	9.445	113.0	45.70	60.16	175.5
G135	7.679	106.2	44.51	52.44	177.9	Y173	8.595	119.4	56.59	45.63	170.1
P136	-	-	-	-	-	K174	8.778	129.4	55.50	56.66	173.8
S137	8.836	118.2	57.37	62.90	177.1	T175	8.647	118.1	59.56	55.38	174.0
I138	9.103	122.5	59.58	57.36	172.7	D176	-	-	-	-	-
R139	9.043	128.4	53.86	59.58	173.4	E177	-	-	-	-	-
G140	8.741	113.3	43.76	53.83	176.1	F178	7.526	119.9	56.32	64.17*	173.9
A141	8.948	123.9	50.90	43.77	170.8	Q179	8.692	122.6	53.71	56.25	174.1
L142	9.236	123.8	53.64	50.85	174.8	L180	9.350	127.7	53.44	53.63	173.8
V143	9.006	125.2	60.91	53.60	174.1	H181	9.165	128.9	-	-	-
L144	9.358	126.1	51.99	60.94	174.7	T182	-	-	-	-	-
G145	8.178	105.4	44.64	52.00	176.2	N183	8.862	116.4	52.99	59.87*	171.8
Y146	8.501	122.9	58.87	44.73	173.0	V184	8.931	118.4	59.97	52.97	172.7
E147	9.043	125.8	57.14	58.90	173.6	N185	9.320	129.2	51.23	60.00	175.0
G148	8.117	108.8	45.22	56.94*	175.3	D186	9.032	125.1	55.85	51.32	174.9
W149	8.180	121.4	57.20	45.12	173.3	G187	8.648	105.3	46.01	55.75	175.9
L150	8.961	123.5	53.52	57.13	177.3	T188	7.644	109.0	62.47	46.11	173.3
A151	8.871	121.6	50.70	53.52	175.4	E189	7.636	122.8	54.83	62.41	-
G152	9.629	107.7	45.22	50.68	175.5	F190	8.878	125.6	55.77	54.76	174.3
Y153	9.209	122.1	56.03	45.27	171.2	G191	8.543	110.3	44.44	55.74	175.7
Q154	8.219	127.9	53.09	56.00	171.9	G192	8.635	105.6	45.42	44.49	171.7
M155	8.750	121.3	52.93	52.93	172.2	S193	9.783	114.7	56.14	45.45	171.4
N156	7.983	119.4	52.23	52.88	174.3	I194	8.784	119.0	59.60	56.26	173.3

Dieses Werk ist copyrightgeschützt und darf in keiner Form vervielfältigt werden noch an Dritte weitergegeben werden.
Es gilt nur für den persönlichen Gebrauch.

	H_i	N	$C_{\alpha i}$	$C_{\alpha i-1}$	C'_{i-1}*		H_i	N	$C_{\alpha i}$	$C_{\alpha i-1}$	C'_{i-1}*
Y195	8.780	127.4	55.61	59.65	173.4	F233	9.249	127.8	55.61	56.29	-
Q196	8.264	125.5	53.65	55.58	172.9	S234	9.321	124.4	57.54	55.60	-
K197	8.916	130.4	55.71	53.61	174.5	A235	8.036	122.7	50.72	57.45	-
V198	8.585	131.0	64.83	55.73	176.1	K236	9.050	114.8	54.61	50.74	175.7
N199	8.159	113.5	-	-	-	V237	8.967	116.9	59.47	54.69	174.1
K200	-	-	-	-	-	N238	7.585	122.3	50.80	59.48	174.0
K201	-	-	-	-	-	N239	8.475	113.5	54.89	50.69	176.5
L202	7.548	122.1	54.07	-	-	S240	7.820	116.9	58.27	55.11*	175.2
E203	8.842	125.5	54.11	54.11	-	S241	8.158	109.5	59.62	58.37*	172.8
T204	8.399	112.2	59.39	54.13	174.8	L242	7.299	118.5	53.75	59.76	172.3
A205	9.038	122.4	50.75	59.37	171.6	I243	9.045	126.6	59.45	53.72	176.7
V206	8.967	116.9	59.47	50.75	174.6	G244	9.300	114.5	43.99	59.49	174.8
N207	8.885	122.5	51.96	59.34	174.4	L245	9.391	122.2	53.31	44.02	171.4
L208	8.705	121.4	54.08	51.94	172.5	G246	9.185	110.4	44.61	53.45	-
A209	9.189	126.3	51.86	54.11	175.2	Y247	9.101	125.4	56.26	44.68	170.9
W210	8.991	121.3	57.64	51.88	175.4	T248	8.367	124.3	60.74	56.22	174.0
T211	8.519	120.5	60.35	57.78	173.3	Q249	9.045	126.0	52.52	60.76*	-
A212	8.670	127.0	53.22	60.33	173.7	T250	9.250	126.0	62.56	52.49	-
G213	8.406	110.1	45.02	53.29	-	L251	8.931	130.1	-	-	-
N214	7.973	119.2	52.39	45.00	-	K252	8.776	126.6	-	-	-
S215	-	-	-	-	-	P253	-	-	-	-	-
N216	8.371	120.4	53.04	59.05	174.3	G254	8.586	110.9	47.03	62.53	-
T217	8.384	119.4	62.66	53.03	174.8	I255	8.246	121.6	59.89	46.97	-
R218	9.040	125.7	54.96	62.68	174.2	K256	8.694	127.0	54.82	59.97	175.0
F219	8.043	119.1	55.84	54.92	175.1	L257	8.809	127.7	52.98	54.71	-
G220	8.576	107.7	45.04	55.81	173.5	T258	9.597	122.8	61.12	53.15	174.3
I221	8.815	118.6	59.59	45.01	171.0	L259	9.251	129.4	52.95	61.22	-
A222	8.872	126.2	50.13	59.59	172.1	S260	8.815	115.3	56.71	52.93	-
A223	9.210	119.3	50.22	50.22	175.3	A261	9.547	120.6	51.14	56.83	172.8
K224	8.769	122.5	56.06	50.13	-	L262	8.735	124.7	52.44	51.07	173.3
Y225	9.863	128.9	55.27	56.19	-	L263	9.495	126.1	52.33	52.33	175.2
Q226	9.012	131.6	54.39	55.29	173.7	D264	9.850	124.5	52.31	52.31	175.3
I227	7.825	129.9	64.61	54.31	173.8	G265	8.465	112.3	46.01	52.32	176.8
D228	8.439	118.4	52.68	64.39	175.6	K266	8.141	117.3	56.85	46.03	173.8
P229	-	-	-	-	-	N267	7.434	117.4	51.79	56.83	177.1
D230	8.517	114.4	53.71	65.64	176.1	V268	8.511	122.0	65.05	51.80	175.0
A231	7.679	124.2	51.74	51.61	174.9	N269	8.322	117.0	54.34	65.08	177.4
C232	8.468	119.0	56.10	51.68*	175.1	A270	7.497	120.6	51.68	54.39	175.7

Dieses Werk ist copyrightgeschützt und darf in keiner Form vervielfältigt werden noch an Dritte weitergegeben werden.
Es gilt nur für den persönlichen Gebrauch.

	H_i	N	$C_{\alpha i}$	$C_{\alpha i-1}$	C'_{i-1}*		H_i	N	$C_{\alpha i}$	$C_{\alpha i-1}$	C'_{i-1}*
G271	7.692	106.7	44.71	51.64	177.7	L279	8.684	124.5	53.33	44.17	171.7
G272	8.525	109.1	45.56	44.75	174.0	E280	8.813	125.7	-	53.50*	-
H273	7.251	120.7	54.53	45.49	173.9	F281	-	-	-	-	-
K274	8.854	119.3	54.71	54.71	176.0	Q282	-	-	-	-	-
L275	8.667	121.5	53.51	54.82	175.2	A283	8.301	126.4	51.22	53.95	174.5
G276	9.098	110.9	45.06	53.56	178.0	R284	-	-	-	-	-
L277	8.222	120.9	53.83	45.15	171.0	S285	7.816	125.6	57.05	55.73	174.1
G278	9.597	115.8	44.28	53.74	-						

*: Shift obtained from RGS-*wt* hVDAC1

Dieses Werk ist copyrightgeschützt und darf in keiner Form vervielfältigt werden noch an Dritte weitergegeben werden.
Es gilt nur für den persönlichen Gebrauch.

B.2 Chemical shift assignment of E73VC127AC232S hVDAC1

Table B.2: Backbone chemical shifts of E73VC127AC232S hVDAC1

	Hi	Ni	$C_{\alpha i}$	$C_{\alpha i-1}$	$C_{\beta i}$	$C_{\beta i-1}$	C'_{i-1}*
M1	-	-	-	-	-	-	-
A2	-	-	-	-	-	-	-
V3	-	-	-	-	-	-	-
P4	-	-	-	-	-	-	-
P5	-	-	-	-	-	-	-
T6	7.419	106.1	60.39	61.62	69.85	31.49	174.4
Y7	7.690	122.6	62.12	60.16	39.22	70.15	176.1
A8	8.403	119.0	53.84	62.11	-	38.97	178.9
D9	7.262	115.2	53.82	53.82	39.98	-	177.7
L10	7.369	125.3	56.13	53.60	39.01	40.05	177.4
G11	-	-	-	-	-	-	-
K12	7.278	122.2	59.48	44.91	32.64	-	-
S13	8.101	115.4	-	-	-	-	-
A14	8.328	122.0	55.22	62.70*	-	-	-
R15	7.322	117.4	59.67	55.33	29.58	-	-
D16	8.550	118.5	-	-	-	-	-
V17	7.534	120.5	66.55	56.90*	31.23	-	-
F18	-	-	-	-	-	-	-
T19	-	-	-	-	-	-	-
K20	-	-	-	-	-	-	-
G21	-	-	-	-	-	-	-
Y22	6.601	113.3	55.69	44.56	39.91	-	-
G23	-	-	-	-	-	-	-
F24	7.031	120.2	56.15*	-	-	-	174.5
G25	8.153	110.1	45.54	56.29	-	38.03	177.0
L26	7.485	118.4	53.28	45.29*	46.15	-	172.8
I27	8.699	120.9	60.02	52.93	38.24	45.97	176.5
K28	8.777	126.9	54.95	59.83	36.25	38.12	175.1
L29	8.753	124.2	53.30	55.07	45.70	36.33	173.9
D30	8.484	123.3	53.77	53.30	45.40	45.40	174.4
L31	9.113	123.6	53.58	53.58	44.90	45.40	173.9
K32	8.542	125.0	55.23	53.92	35.71	44.35	-
T33	9.044	116.3	60.28	55.35	70.04	35.88	172.1
K34	8.217	123.6	55.39	60.41	35.02	69.97	172.7

Dieses Werk ist copyrightgeschützt und darf in keiner Form vervielfältigt werden noch an Dritte weitergegeben werden.
Es gilt nur für den persönlichen Gebrauch.

	Hi	Ni	$C_{\alpha i}$	$C_{\alpha i-1}$	$C_{\beta i}$	$C_{\beta i-1}$	C'_{i-1}*
S35	8.767	119.7	56.91	55.36	64.83	35.24	175.6
E36	-	-	-	-	-	-	-
N37	-	-	-	-	-	-	-
G38	7.852	106.2	45.26	53.02	-	37.65	-
L39	7.815	122.5	55.30	45.37	42.84	-	-
E40	8.936	124.3	54.96	55.30	32.40	42.73	175.9
F41	8.810	124.6	56.48	54.87*	42.08	32.14	174.7
T42	8.856	120.1	60.80	56.35	71.24	42.08	174.6
S43	9.218	120.6	56.67	61.05	66.44	71.57	173.3
S44	8.604	120.4	56.62	56.62	66.01	66.46	172.9
G45	9.108	111.3	45.08	56.53	-	65.93	173.1
S46	9.094	116.0	56.78	45.08	66.45	-	172.1
A47	9.213	124.0	49.68	56.61	21.26	66.30	172.3
N48	8.305	122.4	52.74	49.66	39.41	21.06	175.5
T49	8.495	118.6	-	52.54*	-	-	-
E50	8.523	119.8	57.65	64.17*	30.19	67.47	174.2
T51	8.107	114.2	56.46*	-	-	-	176.5
T52	7.841	108.2	-	-	-	-	-
K53	7.548	120.2	56.58	64.02	36.14	68.56	172.3
V54	8.650	125.8	60.04	56.57	33.06	36.02	176.6
T55	8.785	118.7	59.83	59.83	71.47	33.06	175.2
G56	8.345	109.3	45.59	59.84	-	71.25	172.6
S57	9.100	113.1	57.33	45.50	66.27	-	171.4
L58	9.089	122.2	55.79	57.31	45.76	66.45	172.3
E59	9.046	123.5	54.77	55.71	33.45	46.23	174.8
T60	9.085	119.9	60.81	54.77	70.67	33.41	175.2
K61	8.864	126.8	54.20	60.85	36.67	70.83	171.8
Y62	9.237	124.2	57.09	54.24	42.83	36.15	174.2
R63	7.706	127.6	54.37	57.16	31.23	42.85	173.6
W64	9.152	127.9	53.46	54.38	30.91	31.23	-
T65	-	-	-	-	-	-	-
E66	-	-	-	-	-	-	-
Y67	6.486	114.0	56.20	59.14	39.20	28.20	176.2
G68	7.588	105.5	47.05	56.37	-	39.42	173.7
L69	7.276	120.2	53.66	46.67*	45.67	-	175.6
T70	9.126	120.4	62.33	53.71	70.52	45.74	176.6
F71	9.291	127.3	55.64	62.28	42.52	-	172.6
T72	9.022	120.7	61.25	55.53	70.79	42.73	174.0

Dieses Werk ist copyrightgeschützt und darf in keiner Form vervielfältigt werden noch an Dritte weitergegeben werden.
Es gilt nur für den persönlichen Gebrauch.

	Hi	Ni	$C_{\alpha i}$	$C_{\alpha i-1}$	$C_{\beta i}$	$C_{\beta i-1}$	C'_{i-1}*
V73	9.000	125.6	60.61	61.45	33.67	71.06	173.6
K74	9.123	125.7	54.47	60.80	36.23	33.58	173.6
W75	9.127	124.1	55.79	54.35	32.48	36.13	174.1
N76	7.603	123.2	51.39	55.63	41.28	32.72	174.7
T77	8.041	108.0	63.71	51.50	68.22	41.31	-
D78	7.652	121.1	54.31	63.64*	39.09	-	175.2
N79	8.523	115.2	54.02	54.20	37.23	39.04	176.0
T80	7.226	112.6	62.59	54.37	69.46	36.93	174.0
L81	8.658	128.0	53.24	62.60	44.80	69.48	173.4
G82	9.373	112.2	44.45	53.09	-	-	175.8
T83	8.826	114.1	59.59	44.50	71.66	-	172.6
E84	8.900	124.6	54.53	59.60	33.27	71.55	172.7
I85	9.146	126.6	60.27	54.53	41.25	33.07	175.2
T86	9.009	123.8	60.61	60.23	71.83	41.16	174.5
V87	9.378	124.9	59.90	60.62	33.76	71.66	173.0
E88	9.064	128.1	55.34	59.78	33.23	33.83	174.5
D89	8.781	117.9	57.32	55.45	38.58	33.05	175.4
Q90	7.913	117.1	55.31	57.18	28.77	-	175.3
L91	8.340	117.8	58.53	55.22	40.48	28.78	177.3
A92	7.588	116.8	51.25	58.42	20.66	41.18	176.8
R93	8.779	123.9	57.52*	51.05*	-	-	176.3
G94	9.467	115.4	45.37	57.79	-	28.41	177.3
L95	7.901	122.8	54.00	45.01*	44.46	-	173.8
K96	9.624	131.7	55.09	54.06	35.64	44.74	175.3
L97	8.794	127.0	53.86	55.10	45.29	35.66	174.0
T98	9.179	120.2	61.18	53.86	72.00	45.22	174.7
F99	9.457	127.0	56.09	61.07	41.15	72.28	172.9
D100	8.678	129.2	52.47	56.18	44.55	40.82	173.0
S101	8.672	118.8	56.90	52.32	66.38	-	174.8
S102	8.659	118.2	56.82	56.93	66.29	66.29	174.8
F103	9.112	121.3	56.06	56.89	42.59	66.30	173.1
S104	7.981	120.3	53.45	56.05	63.72	42.59	173.5
P105	-	-	-	-	-	-	-
N106	-	-	-	-	-	-	-
T107	-	-	-	-	-	-	-
G108	8.229	111.7	45.22*	-	-	-	-
K109	7.524	120.7	56.78	45.46	32.51	-	173.8
K110	8.444	123.7	54.94	56.69	34.74	32.49	175.9

Dieses Werk ist copyrightgeschützt und darf in keiner Form vervielfältigt werden noch an Dritte weitergegeben werden.
Es gilt nur für den persönlichen Gebrauch.

	Hi	Ni	$C_{\alpha i}$	$C_{\alpha i-1}$	$C_{\beta i}$	$C_{\beta i-1}$	C'_{i-1}*
N111	8.596	119.5	52.82	55.05	41.88	34.82	175.0
A112	8.585	124.3	51.44	52.74	21.88	41.62	173.5
K113	9.053	119.7	54.79	51.59	36.68	21.85	174.9
I114	8.781	120.6	59.43	54.83	40.46	36.46	175.4
K115	9.276	126.3	54.71	59.28	33.95	40.62	175.0
T116	8.818	116.8	59.99	54.66	71.37	33.39	175.8
G117	9.136	113.5	44.76	59.99	-	71.55	174.6
Y118	9.161	123.1	56.90	44.78	42.26	-	171.0
K119	7.507	124.8	52.96	56.87	34.62	-	172.2
R120	8.734	117.9	53.79	52.99	30.80	34.54	173.1
E121	8.623	120.8	59.61	53.68*	27.96	30.69	174.6
H122	7.905	112.4	59.48	59.80	32.95	28.09	177.0
I123	7.946	118.0	59.95	59.32	42.05	32.56	173.5
N124	8.988	125.3	52.86	59.95	42.02	41.12	171.9
L125	9.465	128.7	53.39	52.86	45.79	40.94	174.5
G126	9.408	113.4	45.35	53.60	-	-	175.8
A127	8.413	122.3	51.39	45.40	20.47	-	171.9
D128	9.179	123.7	52.10	51.40	42.87	20.65	172.6
M129	9.433	123.2	54.53	52.25	35.66	42.92	175.0
D130	8.580	125.5	53.02	54.53	42.86	35.69	173.1
F131	8.532	122.8	58.00	53.02	37.94	42.87	176.0
D132	7.386	122.9	54.05	58.01	42.94	38.22	174.6
I133	8.451	123.6	63.02*	53.86*	-	-	-
A134	8.457	123.5	52.72	63.13	18.23	-	176.8
G135	7.671	106.5	44.45	52.63	-	18.04	177.8
P136	-	-	-	-	-	-	-
S137	8.826	118.4	57.49	63.07	65.41	31.97	177.2
I138	9.147	122.2	59.48	57.36	40.92	65.21	172.8
R139	8.935	128.6	53.99	59.50	31.75	41.31	173.4
G140	8.756	113.1	43.97	54.09	-	31.58	176.1
A141	9.095	123.9	51.11	43.59	22.74	-	170.8
L142	9.220	123.5	53.84	50.95	46.13	22.57	174.9
V143	9.018	125.1	60.95	53.79	34.70	46.07	-
L144	9.374	126.2	52.30	61.11	45.16	34.93	174.8
G145	8.199	105.5	44.79	52.45	-	-	176.3
Y146	8.506	122.7	58.86	44.83	41.41	-	173.0
E147	9.070	125.8	57.09	58.96	33.11	41.17	173.7
G148	8.143	109.0	45.27	56.83*	-	-	175.2

Dieses Werk ist copyrightgeschützt und darf in keiner Form vervielfältigt werden noch an Dritte weitergegeben werden.
Es gilt nur für den persönlichen Gebrauch.

	Hi	Ni	$C_{\alpha i}$	$C_{\alpha i-1}$	$C_{\beta i}$	$C_{\beta i-1}$	C'_{i-1}*
W149	8.207	121.4	57.29	45.21	30.31	-	173.4
L150	8.977	123.4	53.80	57.29	46.89	30.59	177.3
A151	8.893	121.7	50.90	53.77	21.73	46.93	175.4
G152	9.649	107.8	45.51	50.99	-	21.91	175.3
Y153	9.227	122.3	56.04	45.57	43.63	-	171.2
Q154	8.254	127.9	53.28	56.05	31.46	43.66	172.0
M155	8.780	121.3	53.05	53.29	35.16	31.37	172.2
N156	7.988	119.3	52.66	53.07	42.69	34.99	174.3
F157	9.561	127.6	56.32	52.56	42.14	42.68	173.4
E158	8.095	127.7	55.00	56.30	30.02	42.00	173.5
T159	7.667	117.0	65.21	55.02	68.01	29.92	177.0
A160	9.103	124.9	54.36	64.91*	-	-	177.1
K161	-	-	-	-	-	-	-
S162	7.505	114.7	58.44	54.79	61.75	32.86	175.2
R163	6.847	115.1	53.94	57.81	33.26	61.73	173.0
V164	8.831	124.4	62.18	53.99	30.92	33.23	174.4
T165	8.672	118.8	61.43	62.21	68.63	31.13	177.0
Q166	7.471	121.0	55.62	61.41	32.52	-	174.6
S167	8.371	119.0	57.23	55.52	63.70	32.48	174.7
N168	9.146	127.0	51.65	57.12	41.28	63.87	172.7
F169	8.647	118.3	56.20	51.65	35.83	41.39	172.0
A170	8.865	122.8	51.15	56.51	23.46	36.12	173.4
V171	8.250	116.8	60.35	51.15	35.39	-	176.2
G172	9.456	113.1	45.79	60.33	-	-	175.4
Y173	8.609	119.5	56.70	45.81	43.25	-	170.1
K174	8.813	129.4	55.76	56.60	35.90	-	173.8
T175	8.647	117.9	59.69	55.30*	71.30	-	174.0
D176	-	-	-	-	-	-	-
E177	8.439	124.7	58.00	60.69	31.20	-	-
F178	7.553	120.0	56.40	57.97	42.04	-	173.9
Q179	8.734	122.7	53.88	56.52	31.87	41.94	174.1
L180	9.358	127.7	53.59	53.91	45.18	-	173.9
H181	9.178	128.8	55.01*	-	-	-	-
T182	-	-	-	-	-	-	-
N183	8.884	116.6	53.14	59.86*	-	-	171.8
V184	8.958	118.5	60.07	53.05	32.96	42.95	172.7
N185	9.323	129.1	51.50	59.97	38.07	32.84	175.0
D186	9.072	125.2	55.74	51.25	40.90	-	174.9

Dieses Werk ist copyrightgeschützt und darf in keiner Form vervielfältigt werden noch an Dritte weitergegeben werden.
Es gilt nur für den persönlichen Gebrauch.

	Hi	Ni	$C_{\alpha i}$	$C_{\alpha i-1}$	$C_{\beta i}$	$C_{\beta i-1}$	C'_{i-1}*
G187	8.664	105.3	46.02	55.80*	-	40.44	-
T188	7.659	109.0	62.69	46.02	71.27	-	173.2
E189	7.649	122.8	54.86	62.46*	30.80	71.41	172.5
F190	8.903	125.9	55.82	54.48*	41.12	30.97	174.3
G191	8.554	110.3	44.63	55.89	-	40.97	175.6
G192	8.660	105.7	45.57	44.58	-	-	171.7
S193	9.777	114.8	56.11	45.53	66.95	-	171.5
I194	8.799	119.2	59.88	56.07*	41.64	-	173.3
Y195	8.803	127.5	55.57	59.51	42.21	-	173.4
Q196	8.305	125.6	53.92	55.58	31.81	42.56	172.9
K197	8.907	130.3	55.91	53.87	31.44	31.82	174.4
V198	8.599	130.8	64.91	55.90	31.89	31.38	-
N199	8.178	113.6	52.56	-	37.52	-	-
K200	-	-	-	-	-	-	-
K201	-	-	-	-	-	-	-
L202	7.569	122.1	54.23	57.01	44.48	34.42	175.2
E203	8.903	125.8	54.49	54.15	34.11	44.49	-
T204	8.438	112.3	59.51	54.23	72.49	33.68	174.9
A205	9.094	122.6	50.99	59.64	23.67	72.47	171.6
V206	8.990	117.0	59.46	50.87	35.62	24.13	174.6
N207	8.916	122.7	52.32	59.55	42.32	35.55	174.4
L208	8.746	121.8	54.21	52.32	46.07	42.32	172.6
A209	9.191	126.3	52.18	54.16	22.34	45.85	175.3
W210	9.012	121.4	57.92	51.99	32.10	22.79	175.3
T211	8.536	120.3	60.47	57.84	70.74	32.15	173.3
A212	8.683	127.1	53.37	60.43	18.51	70.66	173.7
G213	8.455	110.2	44.97*	53.07*	-	-	-
N214	7.988	119.3	52.27	45.00*	39.90	-	-
S215	-	-	-	-	-	-	-
N216	8.377	120.4	52.99*	58.93*	-	-	174.3
T217	8.399	119.5	62.63	53.00*	-	-	174.8
R218	9.069	125.7	54.87	62.80	31.16	69.52	174.2
F219	8.070	119.2	55.78	54.87	42.23	31.13	175.1
G220	8.614	108.0	45.25	55.77	-	42.16	173.5
I221	8.832	119.0	59.64	45.18	41.50	-	171.0
A222	8.917	126.4	50.28	59.70	22.02	41.46	172.2
A223	9.221	119.4	50.35	50.35	23.16	22.14	175.2
K224	8.817	122.9	56.22	50.35	35.68	23.34	-

Dieses Werk ist copyrightgeschützt und darf in keiner Form vervielfältigt werden noch an Dritte weitergegeben werden.
Es gilt nur für den persönlichen Gebrauch.

	Hi	Ni	$C_{\alpha i}$	$C_{\alpha i-1}$	$C_{\beta i}$	$C_{\beta i-1}$	C'_{i-1}*
Y225	9.949	130.8	55.74	56.38	42.33	35.68	-
Q226	9.007	131.4	54.76	55.69	27.18	42.24	-
I227	7.982	130.3	64.87	54.31	38.46	27.41	-
D228	8.489	118.3	52.79	64.49*	40.14	-	175.5
P229	-	-	-	-	-	-	-
D230	8.539	114.4	54.20	65.54	43.06	-	176.0
A231	7.760	124.6	51.77	54.39	22.17	-	-
S232	8.714	114.4	56.41	51.74	66.28	22.25	-
F233	9.084	122.1	55.24	56.41	44.25	66.26	-
S234	9.345	124.8	57.73	55.30	65.33	44.20	-
A235	8.067	122.6	50.87	57.87	22.93	65.39	-
K236	9.039	114.6	54.72	50.78	35.91	23.15	175.7
V237	8.974	116.9	59.62	54.67	34.07	35.62	174.1
N238	7.620	122.4	51.18	59.58	41.26	34.17	174.1
N239	8.483	113.6	55.07	41.53	36.72	-	176.4
S240	7.829	116.8	58.14*	54.80*	63.05	-	-
S241	8.162	109.5	59.62*	58.08*	-	-	172.8
L242	7.321	118.6	54.04	59.56*	40.73	-	172.3
I243	9.062	126.6	59.55	54.02	40.58	40.58	176.7
G244	9.305	114.5	44.29	59.65	-	40.45	174.8
L245	9.375	122.2	53.70	44.30	46.39	-	171.4
G246	9.188	111.1	44.81	53.66	-	46.64	-
Y247	9.091	125.6	55.55	44.89	42.92	-	170.9
T248	8.533	124.8	60.95	55.60	71.37	43.09	-
Q249	9.029	126.2	52.76	52.44*	32.82	71.52	-
T250	9.203	125.8	63.05	52.27*	68.88	68.43	-
L251	8.958	130.1	56.37	-	42.50	-	-
K252	8.794	126.7	54.69*	-	-	-	-
P253	-	-	-	-	-	-	-
G254	8.558	110.8	47.14	62.43*	-	-	-
I255	8.285	121.6	59.95	47.24	39.93	-	-
K256	8.710	127.0	55.33	59.86*	36.51	-	174.9
L257	8.828	127.7	53.24	55.07	45.78	36.00	-
T258	9.583	122.7	61.14	53.14	71.25	45.64	-
L259	9.345	129.9	53.03	61.25	45.10	71.04	-
S260	8.809	115.0	56.74	53.14	66.74	45.05	-
A261	9.549	120.6	51.26	56.95	22.59	-	172.7
L262	8.764	124.8	52.95	51.26	42.55	22.87	173.4

Dieses Werk ist copyrightgeschützt und darf in keiner Form vervielfältigt werden noch an Dritte weitergegeben werden.
Es gilt nur für den persönlichen Gebrauch.

	Hi	Ni	$C_{\alpha i}$	$C_{\alpha i-1}$	$C_{\beta i}$	$C_{\beta i-1}$	C'_{i-1}*
L263	9.516	126.2	52.56	52.86	43.14	42.59	175.2
D264	9.847	124.5	52.63	52.63	39.92	43.32	175.3
G265	8.478	112.3	46.19	52.60	-	39.93	176.8
K266	8.161	117.4	56.92	46.09	31.50	-	173.8
N267	7.460	117.6	52.07	56.91	38.15	31.43	177.0
V268	8.505	121.9	65.10	52.06	31.12	38.18	175.0
N269	8.325	117.0	54.31*	65.07*	-	-	177.4
A270	7.531	120.7	51.93	54.34*	18.30	-	175.8
G271	7.725	106.7	45.00	51.66	-	-	177.5
G272	8.516	109.1	45.44	44.97	-	-	174.0
H273	7.269	120.6	54.67	45.63	31.22	-	174.0
K274	8.863	119.4	54.88	54.88	36.27	31.10	176.2
L275	8.685	121.7	54.13	54.93	45.63	36.46	175.1
G276	9.083	110.8	45.30	54.40	-	-	-
L277	8.241	121.0	54.07	45.13	46.80	-	171.1
G278	9.597	116.0	44.49	54.21	-	46.29	175.4
L279	8.741	124.8	53.34	44.17	45.86	-	171.7
E280	8.865	125.8	54.16	53.33	32.81	45.39	174.9
F281	-	-	-	-	-	-	-
Q282	-	-	-	-	-	-	-
A283	8.246	126.6	51.37	54.19	18.88	30.90	174.5
L284	-	-	-	-	-	-	-
E285	7.764	125.9	56.97	55.58*	30.57	-	174.0

*: Shift obtained from RGS-E73V hVDAC1

Dieses Werk ist copyrightgeschützt und darf in keiner Form vervielfältigt werden noch an Dritte weitergegeben werden.
Es gilt nur für den persönlichen Gebrauch.

B.3 Chemical shift assignment of Quintuple hVDAC1

Table B.3: Backbone chemical shifts of Quintuple hVDAC1

	Hi	Ni	$C_{\alpha i}$	$C_{\alpha i-1}$	$C_{\beta i}$	$C_{\beta i-1}$	C'_{i-1}*
M1	-	-	-	-	-	-	-
A2	-	-	-	-	-	-	-
V3	-	-	-	-	-	-	-
P4	-	-	-	-	-	-	-
P5	-	-	-	-	-	-	-
T6	7.406	106.1	60.25	61.12	70.08	31.55	174.3
Y7	7.683	122.7	62.09	60.22	-	70.15	176.1
A8	8.396	119.1	53.73	62.09	-	-	-
D9	7.251	115.3	53.66	53.66	40.43	-	177.7
L10	7.367	125.3	55.94	53.85	-	-	177.7
G11	-	-	-	-	-	-	-
K12	7.261	122.2	59.54	44.70	-	-	-
S13	8.089	115.4	-	-	-	-	-
A14	8.354	121.6	54.85	-	-	-	-
R15	7.346	117.5	59.49	54.80	-	-	-
D16	-	-	-	-	-	-	-
V17	7.521	121.2	66.27	-	-	-	-
F18	-	-	-	-	-	-	-
T19	-	-	-	-	-	-	-
K20	-	-	-	-	-	-	-
V21	-	-	-	-	-	-	-
Y22	-	-	-	-	-	-	-
V23	-	-	-	-	-	-	-
F24	6.960	120.9	-	-	-	-	-
G25	8.224	111.1	45.46	54.09	-	-	-
L26	7.232	117.4	53.15	45.50	-	-	173.0
I27	8.360	118.3	59.81	-	-	-	-
K28	9.043	127.8	54.74	59.92	36.24	-	175.0
L29	8.885	125.3	53.29	54.64	45.49	-	174.0
D30	8.518	123.1	53.64	53.35	45.31	45.31	174.5
L31	9.078	123.8	53.80	53.61	-	-	174.0
K32	8.532	125.1	55.12	53.88	35.83	-	-
T33	9.025	116.3	60.19	55.15	-	-	-
K34	8.207	123.7	55.31	60.19	-	-	175.2

Dieses Werk ist copyrightgeschützt und darf in keiner Form vervielfältigt werden noch an Dritte weitergegeben werden.
Es gilt nur für den persönlichen Gebrauch.

	Hi	Ni	$C_{\alpha i}$	$C_{\alpha i-1}$	$C_{\beta i}$	$C_{\beta i-1}$	C'_{i-1}*
S35	8.754	119.7	56.99	55.35	64.49	34.64	172.5
E36	-	-	-	-	-	-	-
N37	-	-	-	-	-	-	-
G38	7.841	106.2	45.09	52.78	-	-	-
L39	7.803	122.6	55.06	45.03	42.94	-	-
E40	8.925	124.3	54.96	54.96	-	42.47	-
F41	8.792	124.7	56.48	54.80	-	-	174.8
T42	8.843	120.2	60.81	56.49	71.69	41.94	174.5
S43	9.208	120.6	56.58	60.82	66.43	-	173.6
S44	8.557	120.5	56.50	56.50	66.19	66.19	-
G45	9.117	111.7	45.03	56.38	-	-	173.3
S46	9.059	115.6	56.75	45.01	66.16	-	171.9
A47	9.111	124.0	49.37	56.70	-	-	-
N48	8.311	122.5	52.85	49.38	-	-	175.4
T49	8.473	118.8	52.74	52.74	-	-	-
E50	8.526	119.9	57.55	-	30.25	-	-
T51	8.099	114.2	-	-	-	-	-
T52	7.879	108.2	61.17	-	-	-	-
K53	8.523	114.0	56.37	-	-	-	-
V54	8.643	125.8	59.99	56.38	33.36	-	176.8
T55	8.715	118.7	59.73	60.01	71.69	33.32	175.3
G56	8.332	109.1	45.57	59.69	-	-	-
S57	9.082	113.0	57.26	45.63	-	-	171.4
L58	9.089	122.2	54.05	57.27	45.83	-	172.5
E59	9.044	123.6	54.75	54.07	33.18	-	174.7
T60	9.071	120.0	60.68	54.74	70.38	-	175.3
K61	8.856	126.8	54.16	60.67	36.79	-	171.8
Y62	9.227	124.2	57.11	54.12	-	-	174.6
R63	7.700	127.7	54.30	57.14	31.21	42.70	173.5
W64	9.146	128.0	53.47	54.30	30.05	-	173.6
T65	-	-	-	-	-	-	-
E66	-	-	-	-	-	-	-
Y67	6.476	114.0	55.94	59.17	39.10	-	-
G68	7.578	105.6	46.75	56.03	-	-	-
L69	7.262	120.3	53.61	46.73	45.58	-	175.5
T70	9.114	120.4	62.12	53.61	70.64	-	-
F71	9.274	127.3	55.54	62.16	42.46	-	172.5
T72	9.008	120.8	61.24	55.59	70.49	-	174.0

Dieses Werk ist copyrightgeschützt und darf in keiner Form vervielfältigt werden noch an Dritte weitergegeben werden.
Es gilt nur für den persönlichen Gebrauch.

	Hi	Ni	$C_{\alpha i}$	$C_{\alpha i-1}$	$C_{\beta i}$	$C_{\beta i-1}$	C'_{i-1}*
V73	8.990	125.7	60.64	61.21	33.83	-	173.7
K74	9.114	125.8	54.45	60.55	36.03	33.44	173.6
W75	9.096	124.0	55.58	54.47	-	-	-
N76	7.616	123.2	51.35	55.62	40.83	-	174.7
T77	8.047	108.2	63.76	51.37	-	-	-
D78	7.642	121.1	53.95	63.85	39.33	-	-
N79	8.509	115.2	54.01	54.01	37.16	-	-
T80	7.241	112.6	62.62	54.06	-	-	174.0
L81	8.640	128.0	53.00	62.62	44.55	-	173.4
G82	9.353	112.1	44.42	52.98	-	-	175.9
T83	8.816	114.1	59.59	44.41	71.92	-	172.5
E84	8.884	124.6	54.44	59.52	33.65	72.10	172.7
I85	9.130	126.6	60.20	54.44	41.46	-	175.3
T86	8.994	123.9	60.68	60.14	71.95	-	-
V87	9.369	125.0	59.65	60.77	33.83	71.56	173.0
E88	9.056	128.2	55.13	59.72	32.94	-	174.5
D89	8.766	118.0	57.14	55.14	38.77	33.08	175.5
Q90	7.904	117.2	55.13	57.09	-	-	175.4
L91	8.331	117.9	58.46	55.15	40.50	-	177.4
A92	7.577	116.9	51.21	58.44	-	-	176.9
R93	8.769	124.0	57.68	51.05	-	-	-
G94	9.462	115.4	45.12	57.68	-	-	177.3
L95	7.892	122.8	53.86	45.08	44.14	-	173.9
K96	9.616	131.8	55.09	53.88	35.01	-	175.5
L97	8.785	127.1	53.65	55.21	45.22	-	174.2
T98	9.169	120.3	61.21	53.65	72.11	-	174.7
F99	9.442	127.0	56.03	61.20	41.10	-	172.9
D100	8.664	129.3	52.32	56.00	44.97	41.39	173.0
S101	8.660	118.9	57.01	52.33	66.51	-	174.8
S102	8.651	118.2	56.98	56.98	66.45	66.45	-
F103	9.102	121.3	55.85	57.10	42.60	-	173.1
S104	7.975	120.3	53.26	55.88	63.59	42.66	173.6
P105	-	-	-	-	-	-	-
N106	-	-	-	-	-	-	-
T107	-	-	-	-	-	-	-
G108	8.223	111.7	-	-	-	-	-
K109	7.514	120.8	56.59	45.31	32.86	-	173.8
K110	8.435	123.7	54.73	56.59	34.82	-	176.0

Dieses Werk ist copyrightgeschützt und darf in keiner Form vervielfältigt werden noch an Dritte weitergegeben werden.
Es gilt nur für den persönlichen Gebrauch.

	Hi	Ni	$C_{\alpha i}$	$C_{\alpha i-1}$	$C_{\beta i}$	$C_{\beta i-1}$	C'_{i-1}*
N111	8.572	119.5	52.70	54.74	42.30	-	175.1
A112	8.578	124.3	51.57	52.71	22.35	-	173.5
K113	9.040	119.8	54.66	51.54	36.63	-	175.0
I114	8.768	120.6	59.29	54.67	40.34	-	175.3
K115	9.257	126.4	54.56	59.18	33.66	-	174.9
T116	8.811	116.9	59.90	54.56	-	32.92	175.8
G117	9.125	113.5	44.63	59.90	-	-	174.4
Y118	9.151	123.1	56.70	44.62	-	-	171.0
K119	7.504	124.9	52.97	56.63	34.83	-	172.2
R120	8.730	118.1	53.86	52.99	30.91	-	-
E121	8.597	120.8	59.60	53.82	-	-	174.6
H122	7.889	112.4	59.60	59.78	28.32	-	-
I123	7.943	118.0	59.95	59.59	41.95	-	-
N124	8.975	125.3	52.82	59.96	41.10	-	-
L125	9.452	128.8	53.30	52.84	45.78	-	174.4
G126	9.399	113.5	45.19	53.22	-	-	175.9
A127	8.404	122.3	51.32	45.19	20.64	-	171.2
D128	9.167	123.7	52.34	51.31	42.73	-	175.3
M129	9.423	123.3	54.43	52.30	35.41	-	174.9
D130	8.565	125.5	52.83	54.40	42.92	35.90	173.2
F131	8.515	122.9	57.80	52.98	37.90	42.74	175.9
D132	7.374	123.0	53.94	57.81	42.84	37.91	174.7
I133	8.425	123.8	63.03	54.05	37.60	-	-
A134	8.442	123.6	52.48	63.04	18.48	-	176.8
G135	7.660	106.5	44.33	52.47	-	18.33	177.8
P136	-	-	-	-	-	-	-
S137	8.809	118.5	57.35	62.87	65.53	-	177.2
I138	9.138	122.3	59.46	57.35	41.09	-	172.8
R139	8.921	128.7	53.83	59.42	31.74	-	173.4
G140	8.746	113.1	43.72	53.93	-	-	176.1
A141	9.089	123.9	51.00	43.75	23.00	-	170.8
L142	9.212	123.5	53.72	50.91	45.92	22.89	174.9
V143	9.008	125.2	60.97	53.73	34.82	-	-
L144	9.367	126.3	52.06	61.00	45.18	34.89	174.7
G145	8.189	105.5	44.73	52.05	-	-	176.2
Y146	8.491	122.7	59.00	44.74	-	-	172.9
E147	9.060	125.8	57.25	58.94	-	-	173.7
G148	8.129	109.0	45.28	57.31	-	-	-

Dieses Werk ist copyrightgeschützt und darf in keiner Form vervielfältigt werden noch an Dritte weitergegeben werden.
Es gilt nur für den persönlichen Gebrauch.

	Hi	Ni	$C_{\alpha i}$	$C_{\alpha i-1}$	$C_{\beta i}$	$C_{\beta i-1}$	C'_{i-1}*
W149	8.193	121.5	57.26	45.10	-	-	173.2
L150	8.968	123.5	53.56	57.27	-	-	177.3
A151	8.886	121.8	50.74	53.55	21.91	-	175.4
G152	9.640	107.8	45.29	50.76	-	-	-
Y153	9.217	122.3	55.97	45.28	43.57	-	171.2
Q154	8.243	128.0	53.12	56.02	31.55	-	172.0
M155	8.770	121.3	52.93	53.17	34.82	-	172.2
N156	7.976	119.4	52.34	52.83	42.72	-	-
F157	9.552	127.7	56.21	52.36	42.27	-	173.4
E158	8.087	127.8	54.87	56.14	29.93	41.84	173.6
T159	7.656	117.0	64.96	54.93	-	-	176.9
A160	9.112	125.0	54.48	65.01	-	-	-
K161	-	-	-	-	-	-	-
S162	7.493	114.8	58.41	54.59	61.51	-	175.2
R163	6.840	115.1	53.79	58.35	33.32	-	173.1
V164	8.822	124.5	62.02	53.78	30.87	-	174.5
T165	8.660	118.9	61.31	61.92	68.50	-	-
Q166	7.455	121.1	55.39	-	-	-	-
S167	8.355	119.1	57.16	55.40	63.83	-	174.8
N168	9.138	127.1	51.53	57.14	41.45	-	172.7
F169	8.634	118.3	56.15	51.50	43.93	-	172.0
A170	8.856	122.8	51.07	56.16	23.68	-	-
V171	8.233	116.9	60.20	51.08	-	-	176.1
G172	9.452	113.1	45.72	60.13	-	-	-
Y173	8.603	119.6	56.63	45.67	43.21	-	-
K174	8.787	129.5	55.48	56.66	-	-	-
T175	8.651	118.2	59.45	-	-	-	173.7
D176	-	-	-	-	-	-	-
E177	-	-	-	-	-	-	-
F178	7.545	120.2	56.38	-	-	-	-
Q179	8.753	122.8	53.76	56.34	-	-	174.1
L180	9.356	127.9	53.38	53.69	-	-	-
H181	9.179	128.9	-	-	-	-	-
T182	-	-	-	-	-	-	-
N183	8.874	116.5	53.05	-	-	-	-
V184	8.945	118.6	60.04	52.98	32.87	-	172.7
N185	9.319	129.2	51.34	60.03	38.43	-	175.0
D186	9.062	125.3	55.78	51.32	40.87	-	174.9

Dieses Werk ist copyrightgeschützt und darf in keiner Form vervielfältigt werden noch an Dritte weitergegeben werden.
Es gilt nur für den persönlichen Gebrauch.

	Hi	Ni	$C_{\alpha i}$	$C_{\alpha i-1}$	$C_{\beta i}$	$C_{\beta i-1}$	C'_{i-1}*
G187	8.659	105.4	46.03	55.85	-	-	-
T188	7.651	109.1	62.52	46.09	-	-	-
E189	7.640	122.9	54.70	62.44	-	-	-
F190	8.894	125.9	55.82	-	-	-	174.4
G191	8.541	110.4	44.54	55.86	-	41.64	175.6
G192	8.650	105.7	45.54	44.49	-	-	171.6
S193	9.777	114.8	56.26	-	67.46	-	-
I194	8.798	119.2	59.59	56.36	-	-	-
Y195	8.791	127.5	55.45	59.55	35.86	-	-
Q196	8.324	125.8	53.73	55.65	31.83	-	172.9
K197	8.884	130.1	55.71	53.68	31.46	31.46	174.5
V198	8.573	130.8	64.91	55.70	-	-	-
N199	8.177	113.7	52.12	-	-	-	-
K200	-	-	-	-	-	-	-
K201	-	-	-	-	-	-	-
L202	7.559	122.2	54.09	56.72	44.48	-	175.2
E203	8.879	125.8	54.16	-	33.71	-	174.1
T204	8.463	112.6	59.46	54.19	72.69	-	-
A205	9.061	122.7	50.71	59.47	23.57	-	171.7
V206	8.995	117.2	59.46	50.65	-	-	-
N207	8.869	122.6	51.95	59.45	41.87	-	-
L208	8.700	121.5	54.20	51.98	45.93	-	-
A209	9.208	126.5	51.94	54.25	-	-	175.3
W210	9.006	121.4	57.68	51.91	-	-	175.3
T211	8.522	120.4	60.35	57.58	-	-	173.3
A212	8.674	127.2	53.23	60.36	17.52	-	173.8
G213	8.437	110.2	-	-	-	-	-
N214	7.976	119.4	-	-	-	-	-
S215	-	-	-	-	-	-	-
N216	8.366	120.5	53.12	-	-	-	-
T217	8.385	119.5	62.63	53.06	-	-	-
R218	9.060	125.8	55.01	62.73	31.32	-	174.3
F219	8.038	119.1	55.84	54.95	42.34	-	-
G220	8.560	107.7	45.10	55.85	-	-	-
I221	8.809	118.5	59.59	45.16	41.77	-	171.0
A222	8.927	126.4	50.21	59.60	22.40	-	172.4
A223	9.123	119.3	50.33	50.20	23.06	-	-
K224	8.805	123.1	56.25	50.35	35.43	-	-

Dieses Werk ist copyrightgeschützt und darf in keiner Form vervielfältigt werden noch an Dritte weitergegeben werden.
Es gilt nur für den persönlichen Gebrauch.

	Hi	Ni	$C_{\alpha i}$	$C_{\alpha i-1}$	$C_{\beta i}$	$C_{\beta i-1}$	C'_{i-1}*
Y225	9.875	130.9	55.48	56.24	-	-	-
Q226	9.009	131.7	54.58	55.39	27.36	-	173.7
I227	8.009	130.3	64.59	54.52	-	-	-
D228	8.463	118.7	52.66	64.57	40.09	-	-
P229	-	-	-	-	-	-	-
D230	8.521	114.3	54.03	65.74	43.02	-	176.3
A231	7.803	124.9	51.68	53.94	-	-	-
S232	9.068	124.7	-	-	-	-	-
F233	9.289	123.3	56.07	-	-	-	-
S234	9.027	124.6	57.45	55.97	-	-	-
A235	8.060	122.8	50.73	57.43	-	-	-
K236	8.944	114.8	54.63	50.65	-	-	-
V237	8.946	117.1	59.59	54.62	-	-	173.7
N238	7.563	122.6	50.83	59.54	41.15	-	174.0
N239	8.488	113.7	54.85	50.68	-	-	176.3
S240	7.796	116.9	58.24	-	-	-	-
S241	8.149	109.6	59.69	58.18	-	-	172.8
L242	7.325	118.8	53.88	59.76	40.56	-	172.2
I243	9.078	126.7	59.39	53.82	40.29	-	176.8
G244	9.154	114.2	43.75	59.44	-	-	175.1
L245	9.349	121.4	53.39	43.66	-	-	171.7
G246	9.180	110.0	44.69	53.29	-	-	-
Y247	9.208	127.0	55.91	44.63	-	-	-
T248	8.365	125.1	54.05	56.11	-	-	-
Q249	8.894	123.5	53.10	-	-	-	171.8
T250	9.237	126.3	62.89	53.09	68.73	-	174.8
L251	9.470	128.8	61.04	-	-	-	-
K252	8.794	127.3	54.89	60.85	-	-	-
P253	-	-	-	-	-	-	-
G254	8.536	110.8	47.09	62.49	-	-	-
I255	8.268	121.7	59.90	47.07	-	-	-
K256	8.685	127.3	54.67	60.02	-	-	-
L257	8.848	128.8	53.09	54.87	45.26	-	-
T258	9.603	123.2	61.44	53.12	-	-	-
L259	9.266	127.0	53.12	61.59	-	-	-
S260	8.595	116.3	56.30	53.10	67.56	-	-
A261	9.222	123.4	50.92	56.24	-	-	-
L262	8.848	124.7	52.74	50.88	42.71	-	173.7

Dieses Werk ist copyrightgeschützt und darf in keiner Form vervielfältigt werden noch an Dritte weitergegeben werden.
Es gilt nur für den persönlichen Gebrauch.

	Hi	Ni	$C_{\alpha i}$	$C_{\alpha i-1}$	$C_{\beta i}$	$C_{\beta i-1}$	C'_{i-1}*
L263	9.563	126.2	52.40	52.80	43.14	-	175.2
D264	9.946	124.8	52.36	52.36	39.57	-	-
G265	8.445	112.3	46.03	52.38	-	40.10	176.7
K266	8.131	117.5	56.83	46.03	31.35	-	173.7
N267	7.431	117.6	51.82	56.72	38.20	-	177.0
V268	8.480	121.8	65.06	51.83	30.84	-	175.1
N269	8.320	117.0	54.30	-	-	-	-
A270	7.532	120.8	51.69	54.53	-	-	175.6
G271	7.700	106.9	44.83	51.89	-	-	-
G272	8.524	109.2	45.65	44.94	-	-	174.1
H273	7.197	120.8	54.54	45.58	31.34	-	174.0
K274	8.940	119.3	54.61	54.61	37.12	-	-
L275	8.673	121.4	53.40	54.54	45.75	-	175.1
G276	8.866	111.0	45.68	53.55	-	-	-
L277	8.254	120.7	53.70	45.65	-	-	-
G278	9.494	111.9	43.85	53.71	-	-	-
L279	8.761	124.3	53.45	43.83	-	-	-
E280	8.775	125.6	54.07	53.38	-	-	174.7
F281	9.068	125.8	-	54.11	-	-	-
Q282	-	-	-	-	-	-	-
A283	8.243	126.6	51.32	-	30.36	-	174.4
L284	-	-	-	-	-	-	-
E285	7.759	125.9	57.17	55.80	30.40	-	174.1

Dieses Werk ist copyrightgeschützt und darf in keiner Form vervielfältigt werden noch an Dritte weitergegeben werden.
Es gilt nur für den persönlichen Gebrauch.

B.4 Chemical shift assignment of hVDAC1 in liposomes

Table B.4: Chemical shifts of hVDAC1 in liposomes

	N	C'	C_α	C_β	C_γ
A2			52.164*	18.995*	
V3			59.906*	31.682*	
P4			61.536*	30.622*	
P5		174.244#	61.352*	31.988*	27.093*
T6	106.236+	176.106#	60.473*	69.720*	
Y7	122.926#		62.248*	40.038*	
A8	119.378+		53.998*	18.596*	
D9		177.388*	53.883*	40.268*	
L10	125.543+		56.447*	39.136*	
G11		175.187*	45.100*		
K12	122.932+		59.807*	33.442*	
S13			59.976*	63.294*	
A14	122.001+		55.286*	18.233*	
R15	116.568+		60.302*	30.483*	28.04*
D16	118.244+		57.303*	40.349*	
V17			66.58*	31.286*	
T19			66.289*	68.507*	
K32	126.050+		55.162+	36.847+	
T42	120.948+		61.712+	71.390+	
S46	116.408+		56.798*	66.116*	
T55	118.003+		59.973*	71.825*	
T72	120.761+		61.724+	71.327+	
N76	122.297+		51.999+	39.418+	
L81	127.813+		53.823+	45.911+	
T86	123.304+		61.008*	71.754*	
P105			65.367*	31.072*	
G108		174.616*	45.528*		
K109	119.963#				
A112	125.073+	174.833#	51.987*	23.008*	
K113	121.372#				
K115	126.495+	175.830#	54.875+	33.907+	
T116	116.602#				
I123	117.851+		59.694*	42.49*	
S137	117.726+		57.607+	67.534+	
I138		173.629#	59.861#		
R139	128.035#	175.623#	54.103#		
G140	112.480#	171.271#	44.849#		
A141	124.369+		51.100+	23.711+	
L142			53.842*	47.717*	

Dieses Werk ist copyrightgeschützt und darf in keiner Form vervielfältigt werden noch an Dritte weitergegeben werden.
Es gilt nur für den persönlichen Gebrauch.

	N	C'	C_α	C_β	C_γ
V143		174.819#	61.186*	35.703*	23.553* & 22.251*
L144	126.074#	176.217#	52.113*	46.328*	
G145	105.414#				
A151		175.212#	51.202*	24.078*	
G152	107.812#				
S167	118.904+		57.131+	66.071+	
F169	118.472+	174.427#	56.518*	42.418*	
A170	121.901+	176.555#	50.916*	22.615*	
V171	117.409+	175.594#	60.456+	36.150+	
G172	113.565#				
Q179	122.615+		53.955+	32.274+	
Q196	125.772+		54.046+	32.402+	
S193			56.353*	67.534*	
E203		174.809#	54.529#		
T204	112.136+	172.117#	59.688*	72.539*	
A205	122.775+	174.588#	50.916*	23.971*	
V206	117.073+		59.804+	35.868+	
W210	121.628+		58.041+	30.264+	
A212	127.751+		51.805+	23.079+	
A222	125.687+	175.149#	50.711+	22.937+	
A223	119.402+	175.743#	50.595*	23.936*	
K224	120.766#				
Q226	130.995+		54.306*	27.968*	
A231	124.160+		51.855+	22.870+	
A235	122.972+	175.761#	51.100+	23.985+	
K236	114.518#				
V237	117.834+	173.995#	59.801+	35.869+	
N238	122.859#				
S240	117.716+		58.867*	62.976*	
L245	121.688+		53.894+	46.875+	
P253			65.919*	32.086*	
L257	127.823+		53.451+	45.928+	
T258	123.395+		61.686*	71.112*	

* = from PDSD
+ = from NCACB
# = from NCOCA

Dieses Werk ist copyrightgeschützt und darf in keiner Form vervielfältigt werden noch an Dritte weitergegeben werden.
Es gilt nur für den persönlichen Gebrauch.

Dieses Werk ist copyrightgeschützt und darf in keiner Form vervielfältigt werden noch an Dritte weitergegeben werden.
Es gilt nur für den persönlichen Gebrauch.

Appendix C Sequence alignment of mentioned VDAC isoforms

The sequences of VDAC isoforms that were mentioned in this thesis (and for completeness also including zfVDAC1) were aligned with Clustal Omega[152] and visualized with Jalview 2.10.1[161]. The figure is – due to space restrictions – following on the next page.

Dieses Werk ist copyrightgeschützt und darf in keiner Form vervielfältigt werden noch an Dritte weitergegeben werden.
Es gilt nur für den persönlichen Gebrauch.

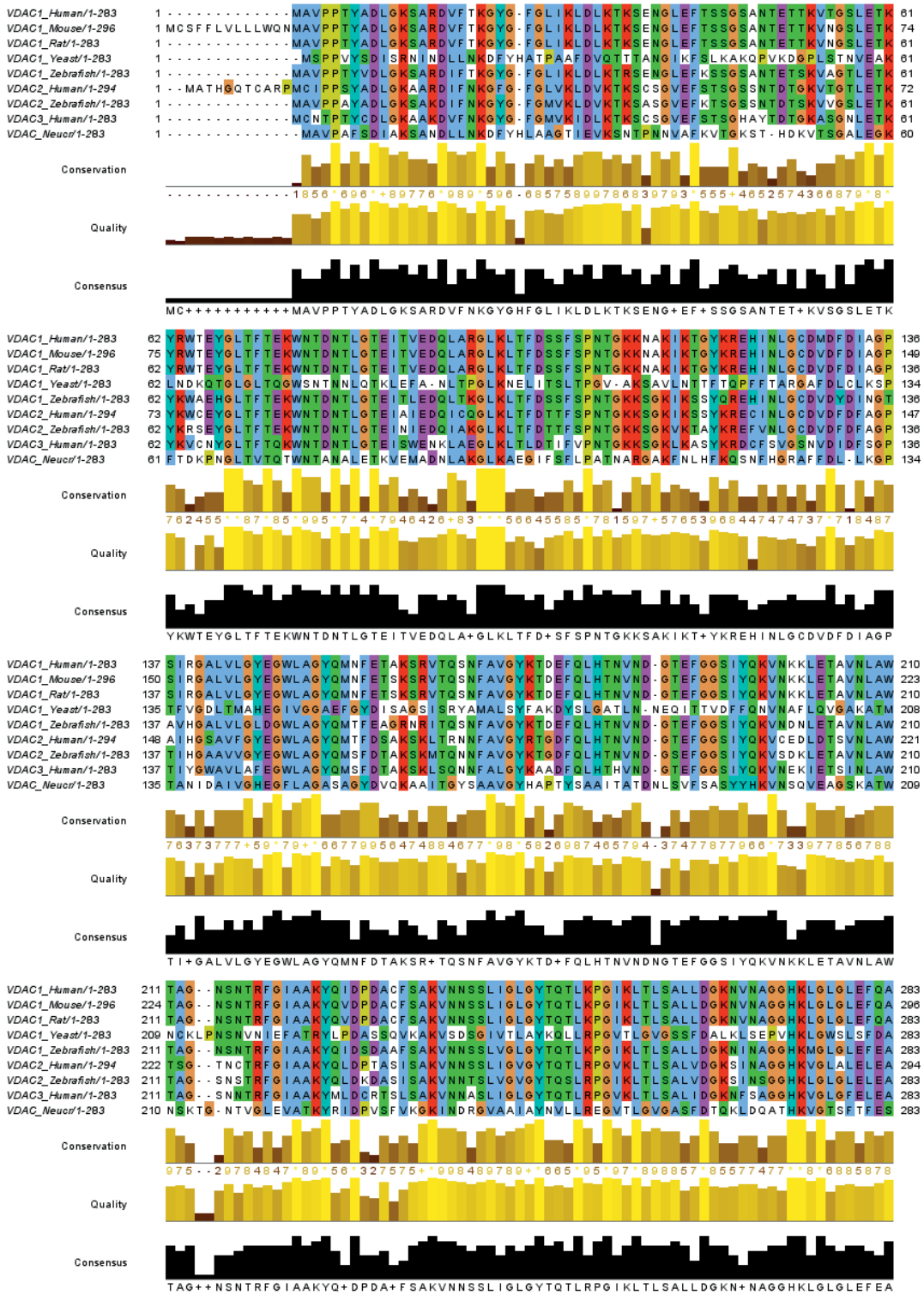

Figure C.1: Alignment of VDAC sequences. VDAC1 from *homo sapiens* (VDAC1_Human), VDAC1 from *mus musculus* (VDAC1_Mouse), VDAC1 from *rattus norvegicus* (VDAC1_Rat), VDAC1 from *saccharomyces cerevisiae* (VDAC1_Yeast), VDAC1 from *danio rerio* (VDAC1_Zebrafish), VDAC2 from *homo sapiens* (VDAC2_Human), VDAC2 from *danio rerio* (VDAC2_Zebrafish), VDAC3 from *homo sapiens* (VDAC3_Human) and VDAC from *neurospora crassa* (VDAC_Neucr) were aligned with Clustal Omega [152] and visualized with Jalview 2.10.1 [161].

Dieses Werk ist copyrightgeschützt und darf in keiner Form vervielfältigt werden noch an Dritte weitergegeben werden.
Es gilt nur für den persönlichen Gebrauch.

Appendix D PDB files of the models for the closed state of VDAC

In the following, the PDB files for the two models of the closed state of VDAC are given. Due to space restrictions, only the coordinates of the N, C_α, C' and O atoms are printed.

D.1 Model 1

```
HEADER 5jdp_close1c
ATOM      1  N   SER A   1     -14.364  12.935  18.289  1.00  0.00           N
ATOM      2  CA  SER A   1     -13.382  12.614  19.359  1.00  0.00           C
ATOM      3  C   SER A   1     -12.511  11.470  18.871  1.00  0.00           C
ATOM      4  O   SER A   1     -11.378  11.296  19.322  1.00  0.00           O
ATOM     14  N   ALA A   2     -13.035  10.720  17.906  1.00  0.00           N
ATOM     15  CA  ALA A   2     -12.280   9.632  17.327  1.00  0.00           C
ATOM     16  C   ALA A   2     -11.054  10.245  16.708  1.00  0.00           C
ATOM     17  O   ALA A   2      -9.969   9.672  16.746  1.00  0.00           O
ATOM     24  N   VAL A   3     -11.246  11.482  16.142  1.00  0.00           N
ATOM     25  CA  VAL A   3     -10.246  12.451  15.751  1.00  0.00           C
ATOM     26  C   VAL A   3      -9.285  11.629  14.953  1.00  0.00           C
ATOM     27  O   VAL A   3      -8.195  11.578  15.345  1.00  0.00           O
ATOM     40  N   PRO A   4      -9.733  10.754  14.006  1.00  0.00           N
ATOM     41  CA  PRO A   4      -8.708   9.843  13.446  1.00  0.00           C
ATOM     42  C   PRO A   4      -8.119  10.817  12.434  1.00  0.00           C
ATOM     43  O   PRO A   4      -8.676  11.217  11.434  1.00  0.00           O
ATOM     68  N   THR A   6      -6.338  10.524   9.580  1.00  0.00           N
ATOM     69  CA  THR A   6      -6.698   9.087   9.832  1.00  0.00           C
ATOM     70  C   THR A   6      -5.339   8.387   9.774  1.00  0.00           C
ATOM     71  O   THR A   6      -4.786   8.801   8.794  1.00  0.00           O
ATOM     82  N   TYR A   7      -4.919   7.511  10.625  1.00  0.00           N
ATOM     83  CA  TYR A   7      -3.508   7.048  10.816  1.00  0.00           C
ATOM     84  C   TYR A   7      -2.748   6.624   9.522  1.00  0.00           C
ATOM     85  O   TYR A   7      -1.538   6.836   9.500  1.00  0.00           O
ATOM    103  N   ALA A   8      -3.421   6.151   8.483  1.00  0.00           N
ATOM    104  CA  ALA A   8      -2.824   6.080   7.126  1.00  0.00           C
ATOM    105  C   ALA A   8      -2.643   7.473   6.461  1.00  0.00           C
ATOM    106  O   ALA A   8      -1.539   7.729   5.967  1.00  0.00           O
ATOM    113  N   ASP A   9      -3.662   8.293   6.473  1.00  0.00           N
ATOM    114  CA  ASP A   9      -3.627   9.719   5.994  1.00  0.00           C
ATOM    115  C   ASP A   9      -3.067  10.745   7.042  1.00  0.00           C
ATOM    116  O   ASP A   9      -3.452  11.957   6.905  1.00  0.00           O
ATOM    125  N   LEU A  10      -2.172  10.278   7.872  1.00  0.00           N
ATOM    126  CA  LEU A  10      -0.914  11.326   9.072  1.00  0.00           C
ATOM    127  C   LEU A  10      -0.192  12.645   8.838  1.00  0.00           C
ATOM    128  O   LEU A  10       0.962  12.879   9.158  1.00  0.00           O
ATOM    144  N   GLY A  11      -0.981  13.515   8.164  1.00  0.00           N
ATOM    145  CA  GLY A  11      -0.479  14.706   7.492  1.00  0.00           C
ATOM    146  C   GLY A  11       0.171  14.327   6.158  1.00  0.00           C
ATOM    147  O   GLY A  11       1.338  13.881   6.267  1.00  0.00           O
ATOM    151  N   LYS A  12      -0.551  14.453   5.006  1.00  0.00           N
ATOM    152  CA  LYS A  12      -0.341  13.553   3.898  1.00  0.00           C
ATOM    153  C   LYS A  12       0.328  14.278   2.704  1.00  0.00           C
ATOM    154  O   LYS A  12       1.107  13.480   2.207  1.00  0.00           O
ATOM    173  N   SER A  13      -0.006  15.493   2.046  1.00  0.00           N
```


Dieses Werk ist copyrightgeschützt und darf in keiner Form vervielfältigt werden noch an Dritte weitergegeben werden.
Es gilt nur für den persönlichen Gebrauch.

```
ATOM    174  CA  SER A  13       0.805  16.230   1.059  1.00  0.00           C
ATOM    175  C   SER A  13       2.295  16.178   1.388  1.00  0.00           C
ATOM    176  O   SER A  13       3.112  15.906   0.507  1.00  0.00           O
ATOM    184  N   ALA A  14       2.720  15.961   2.668  1.00  0.00           N
ATOM    185  CA  ALA A  14       4.006  15.350   3.089  1.00  0.00           C
ATOM    186  C   ALA A  14       4.201  13.881   3.046  1.00  0.00           C
ATOM    187  O   ALA A  14       5.462  13.624   2.774  1.00  0.00           O
ATOM    194  N   ARG A  15       3.401  12.885   3.356  1.00  0.00           N
ATOM    195  CA  ARG A  15       3.675  11.441   3.141  1.00  0.00           C
ATOM    196  C   ARG A  15       3.561  11.102   1.670  1.00  0.00           C
ATOM    197  O   ARG A  15       4.594  10.514   1.223  1.00  0.00           O
ATOM    218  N   ASP A  16       2.564  11.327   0.852  1.00  0.00           N
ATOM    219  CA  ASP A  16       2.511  10.713  -0.505  1.00  0.00           C
ATOM    220  C   ASP A  16       3.436  11.440  -1.522  1.00  0.00           C
ATOM    221  O   ASP A  16       3.246  11.059  -2.713  1.00  0.00           O
ATOM    230  N   VAL A  17       4.412  12.288  -1.175  1.00  0.00           N
ATOM    231  CA  VAL A  17       5.665  12.460  -1.962  1.00  0.00           C
ATOM    232  C   VAL A  17       6.855  11.931  -1.111  1.00  0.00           C
ATOM    233  O   VAL A  17       7.776  11.424  -1.843  1.00  0.00           O
ATOM    246  N   PHE A  18       7.001  11.933   0.194  1.00  0.00           N
ATOM    247  CA  PHE A  18       8.004  11.132   0.980  1.00  0.00           C
ATOM    248  C   PHE A  18       8.011   9.610   0.654  1.00  0.00           C
ATOM    249  O   PHE A  18       9.103   9.033   0.755  1.00  0.00           O
ATOM    266  N   THR A  19       6.892   9.052   0.195  1.00  0.00           N
ATOM    267  CA  THR A  19       6.846   7.851  -0.662  1.00  0.00           C
ATOM    268  C   THR A  19       6.692   8.245  -2.147  1.00  0.00           C
ATOM    269  O   THR A  19       5.653   7.848  -2.733  1.00  0.00           O
ATOM    280  N   LYS A  20       7.664   8.948  -2.736  1.00  0.00           N
ATOM    281  CA  LYS A  20       7.858   8.920  -4.173  1.00  0.00           C
ATOM    282  C   LYS A  20       9.370   8.734  -4.532  1.00  0.00           C
ATOM    283  O   LYS A  20      10.101   9.713  -5.161  1.00  0.00           O
ATOM    302  N   GLY A  21       9.692   7.196  -4.225  1.00  0.00           N
ATOM    303  CA  GLY A  21      10.538   6.404  -5.261  1.00  0.00           C
ATOM    304  C   GLY A  21      10.900   6.726  -3.925  1.00  0.00           C
ATOM    305  O   GLY A  21      10.796   7.849  -2.757  1.00  0.00           O
ATOM    309  N   TYR A  22      11.792   5.344  -3.756  1.00  0.00           N
ATOM    310  CA  TYR A  22      11.018   4.066  -3.460  1.00  0.00           C
ATOM    311  C   TYR A  22      10.610   3.896  -2.028  1.00  0.00           C
ATOM    312  O   TYR A  22       9.375   3.504  -1.956  1.00  0.00           O
ATOM    330  N   GLY A  23      11.277   4.096  -0.925  1.00  0.00           N
ATOM    331  CA  GLY A  23      10.618   3.943   0.391  1.00  0.00           C
ATOM    332  C   GLY A  23      11.512   4.381   1.560  1.00  0.00           C
ATOM    333  O   GLY A  23      12.660   3.898   1.541  1.00  0.00           O
ATOM    337  N   PHE A  24      11.024   5.208   2.469  1.00  0.00           N
ATOM    338  CA  PHE A  24      11.687   5.640   3.729  1.00  0.00           C
ATOM    339  C   PHE A  24      10.838   5.329   4.963  1.00  0.00           C
ATOM    340  O   PHE A  24       9.661   4.961   4.792  1.00  0.00           O
ATOM    357  N   GLY A  25      11.360   5.464   6.194  1.00  0.00           N
ATOM    358  CA  GLY A  25      10.497   5.273   7.358  1.00  0.00           C
ATOM    359  C   GLY A  25      11.142   5.449   8.734  1.00  0.00           C
ATOM    360  O   GLY A  25      11.423   6.586   9.133  1.00  0.00           O
ATOM    364  N   LEU A  26      11.337   4.376   9.499  1.00  0.00           N
ATOM    365  CA  LEU A  26      11.549   4.437  10.965  1.00  0.00           C
ATOM    366  C   LEU A  26      13.031   4.421  11.326  1.00  0.00           C
ATOM    367  O   LEU A  26      13.767   4.834  10.333  1.00  0.00           O
ATOM    383  N   ILE A  27      13.700   4.059  12.425  1.00  0.00           N
ATOM    384  CA  ILE A  27      15.140   3.722  12.459  1.00  0.00           C
ATOM    385  C   ILE A  27      15.102   2.375  11.698  1.00  0.00           C
ATOM    386  O   ILE A  27      14.864   1.430  12.374  1.00  0.00           O
ATOM    402  N   LYS A  28      15.300   2.436  10.392  1.00  0.00           N
ATOM    403  CA  LYS A  28      15.102   1.346   9.426  1.00  0.00           C
ATOM    404  C   LYS A  28      16.442   0.930   8.812  1.00  0.00           C
ATOM    405  O   LYS A  28      16.976   1.919   8.229  1.00  0.00           O
ATOM    424  N   LEU A  29      16.887  -0.330   8.942  1.00  0.00           N
ATOM    425  CA  LEU A  29      18.105  -0.820   8.307  1.00  0.00           C
ATOM    426  C   LEU A  29      17.664  -1.567   7.045  1.00  0.00           C
ATOM    427  O   LEU A  29      16.868  -2.499   7.308  1.00  0.00           O
ATOM    443  N   ASP A  30      18.081  -1.162   5.831  1.00  0.00           N
ATOM    444  CA  ASP A  30      17.722  -1.827   4.577  1.00  0.00           C
ATOM    445  C   ASP A  30      18.957  -2.329   3.841  1.00  0.00           C
ATOM    446  O   ASP A  30      19.923  -1.590   3.639  1.00  0.00           O
ATOM    455  N   LEU A  31      18.905  -3.598   3.442  1.00  0.00           N
ATOM    456  CA  LEU A  31      20.002  -4.237   2.720  1.00  0.00           C
ATOM    457  C   LEU A  31      19.539  -4.554   1.294  1.00  0.00           C
ATOM    458  O   LEU A  31      18.509  -5.217   1.117  1.00  0.00           O
ATOM    474  N   LYS A  32      20.244  -4.052   0.271  1.00  0.00           N
ATOM    475  CA  LYS A  32      20.037  -4.365  -1.166  1.00  0.00           C
ATOM    476  C   LYS A  32      21.195  -5.208  -1.686  1.00  0.00           C
ATOM    477  O   LYS A  32      22.322  -5.085  -1.222  1.00  0.00           O
ATOM    496  N   THR A  33      20.137  -6.301  -2.446  1.00  0.00           N
ATOM    497  CA  THR A  33      20.856  -7.299  -3.242  1.00  0.00           C
ATOM    498  C   THR A  33      20.336  -7.259  -4.682  1.00  0.00           C
ATOM    499  O   THR A  33      19.157  -7.538  -4.943  1.00  0.00           O
ATOM    510  N   LYS A  34      21.202  -6.890  -5.613  1.00  0.00           N
ATOM    511  CA  LYS A  34      20.783  -6.792  -7.003  1.00  0.00           C
ATOM    512  C   LYS A  34      20.787  -8.141  -7.700  1.00  0.00           C
ATOM    513  O   LYS A  34      21.833  -8.770  -7.853  1.00  0.00           O
ATOM    532  N   SER A  35      19.611  -8.544  -8.175  1.00  0.00           N
ATOM    533  CA  SER A  35      19.497  -9.784  -8.919  1.00  0.00           C
ATOM    534  C   SER A  35      19.856  -9.500 -10.372  1.00  0.00           C
ATOM    535  O   SER A  35      19.687  -8.379 -10.848  1.00  0.00           O
ATOM    543  N   GLU A  36      20.354 -10.499 -11.081  1.00  0.00           N
ATOM    544  CA  GLU A  36      20.718 -10.287 -12.468  1.00  0.00           C
ATOM    545  C   GLU A  36      19.486 -10.408 -13.361  1.00  0.00           C
```


Dieses Werk ist copyrightgeschützt und darf in keiner Form vervielfältigt werden noch an Dritte weitergegeben werden.
Es gilt nur für den persönlichen Gebrauch.

```
ATOM    546  O   GLU A  36      19.375  -9.715 -14.371  1.00  0.00           O
ATOM    558  N   ASN A  37      18.538 -11.259 -12.959  1.00  0.00           N
ATOM    559  CA  ASN A  37      17.303 -11.410 -13.721  1.00  0.00           C
ATOM    560  C   ASN A  37      16.525 -10.091 -13.693  1.00  0.00           C
ATOM    561  O   ASN A  37      15.965  -9.659 -14.703  1.00  0.00           O
ATOM    572  N   GLY A  38      16.501  -9.463 -12.519  1.00  0.00           N
ATOM    573  CA  GLY A  38      15.805  -8.204 -12.341  1.00  0.00           C
ATOM    574  C   GLY A  38      14.847  -8.283 -11.162  1.00  0.00           C
ATOM    575  O   GLY A  38      13.966  -7.442 -11.043  1.00  0.00           O
ATOM    579  N   LEU A  39      15.022  -9.307 -10.315  1.00  0.00           N
ATOM    580  CA  LEU A  39      14.155  -9.514  -9.152  1.00  0.00           C
ATOM    581  C   LEU A  39      14.271  -8.372  -8.147  1.00  0.00           C
ATOM    582  O   LEU A  39      13.277  -7.945  -7.565  1.00  0.00           O
ATOM    598  N   GLU A  40      15.491  -7.891  -7.944  1.00  0.00           N
ATOM    599  CA  GLU A  40      15.736  -6.791  -7.012  1.00  0.00           C
ATOM    600  C   GLU A  40      15.237  -7.132  -5.605  1.00  0.00           C
ATOM    601  O   GLU A  40      14.173  -6.663  -5.204  1.00  0.00           O
ATOM    613  N   PHE A  41      16.008  -7.911  -4.845  1.00  0.00           N
ATOM    614  CA  PHE A  41      15.609  -8.250  -3.478  1.00  0.00           C
ATOM    615  C   PHE A  41      16.264  -7.355  -2.450  1.00  0.00           C
ATOM    616  O   PHE A  41      17.471  -7.412  -2.225  1.00  0.00           O
ATOM    633  N   THR A  42      15.424  -6.563  -1.796  1.00  0.00           N
ATOM    634  CA  THR A  42      15.877  -5.676  -0.737  1.00  0.00           C
ATOM    635  C   THR A  42      15.088  -5.958   0.519  1.00  0.00           C
ATOM    636  O   THR A  42      13.912  -5.602   0.609  1.00  0.00           O
ATOM    647  N   SER A  43      15.720  -6.589   1.490  1.00  0.00           N
ATOM    648  CA  SER A  43      15.028  -6.884   2.729  1.00  0.00           C
ATOM    649  C   SER A  43      15.353  -5.808   3.748  1.00  0.00           C
ATOM    650  O   SER A  43      16.338  -5.084   3.601  1.00  0.00           O
ATOM    669  N   GLY A  45      14.987  -4.409   8.149  1.00  0.00           N
ATOM    670  CA  GLY A  45      14.796  -4.663   9.568  1.00  0.00           C
ATOM    671  C   GLY A  45      14.814  -3.327  10.288  1.00  0.00           C
ATOM    672  O   GLY A  45      15.755  -2.546  10.146  1.00  0.00           O
ATOM    676  N   SER A  46      13.786  -2.952  11.038  1.00  0.00           N
ATOM    677  CA  SER A  46      13.645  -1.601  11.631  1.00  0.00           C
ATOM    678  C   SER A  46      13.457  -1.647  13.118  1.00  0.00           C
ATOM    679  O   SER A  46      13.432  -2.690  13.677  1.00  0.00           O
ATOM    687  N   ALA A  47      13.324  -0.451  13.682  1.00  0.00           N
ATOM    688  CA  ALA A  47      12.782  -0.283  14.998  1.00  0.00           C
ATOM    689  C   ALA A  47      12.286   1.140  15.244  1.00  0.00           C
ATOM    690  O   ALA A  47      12.754   2.069  14.588  1.00  0.00           O
ATOM    697  N   ASN A  48      11.361   1.236  16.164  1.00  0.00           N
ATOM    698  CA  ASN A  48      10.609   2.450  16.469  1.00  0.00           C
ATOM    699  C   ASN A  48      11.291   3.068  17.698  1.00  0.00           C
ATOM    700  O   ASN A  48      11.594   2.322  18.637  1.00  0.00           O
ATOM    711  N   THR A  49      11.513   4.374  17.707  1.00  0.00           N
ATOM    712  CA  THR A  49      12.094   5.041  18.884  1.00  0.00           C
ATOM    713  C   THR A  49      11.155   5.040  20.099  1.00  0.00           C
ATOM    714  O   THR A  49      11.757   5.016  21.197  1.00  0.00           O
ATOM    725  N   GLU A  50       9.840   5.078  19.980  1.00  0.00           N
ATOM    726  CA  GLU A  50       8.980   5.021  21.170  1.00  0.00           C
ATOM    727  C   GLU A  50       9.033   3.622  21.797  1.00  0.00           C
ATOM    728  O   GLU A  50       9.510   3.554  22.947  1.00  0.00           O
ATOM    740  N   THR A  51       8.584   2.592  21.078  1.00  0.00           N
ATOM    741  CA  THR A  51       8.203   1.320  21.705  1.00  0.00           C
ATOM    742  C   THR A  51       9.335   0.290  21.744  1.00  0.00           C
ATOM    743  O   THR A  51       9.236  -0.698  22.469  1.00  0.00           O
ATOM    768  N   LYS A  53      10.025  -1.751  19.449  1.00  0.00           N
ATOM    769  CA  LYS A  53       9.562  -2.900  18.615  1.00  0.00           C
ATOM    770  C   LYS A  53      10.487  -3.066  17.417  1.00  0.00           C
ATOM    771  O   LYS A  53      11.299  -2.202  17.174  1.00  0.00           O
ATOM    790  N   VAL A  54      10.318  -4.205  16.720  1.00  0.00           N
ATOM    791  CA  VAL A  54      11.083  -4.624  15.566  1.00  0.00           C
ATOM    792  C   VAL A  54      10.076  -4.999  14.440  1.00  0.00           C
ATOM    793  O   VAL A  54       9.541  -6.114  14.523  1.00  0.00           O
ATOM    806  N   THR A  55       9.879  -4.126  13.468  1.00  0.00           N
ATOM    807  CA  THR A  55       9.179  -4.407  12.182  1.00  0.00           C
ATOM    808  C   THR A  55      10.222  -4.552  11.078  1.00  0.00           C
ATOM    809  O   THR A  55      11.385  -4.234  11.258  1.00  0.00           O
ATOM    820  N   GLY A  56       9.799  -5.060   9.929  1.00  0.00           N
ATOM    821  CA  GLY A  56      10.638  -5.110   8.725  1.00  0.00           C
ATOM    822  C   GLY A  56       9.790  -5.256   7.470  1.00  0.00           C
ATOM    823  O   GLY A  56       8.567  -5.053   7.540  1.00  0.00           O
ATOM    827  N   SER A  57      10.433  -5.606   6.377  1.00  0.00           N
ATOM    828  CA  SER A  57       9.766  -5.690   5.077  1.00  0.00           C
ATOM    829  C   SER A  57      10.641  -6.441   4.076  1.00  0.00           C
ATOM    830  O   SER A  57      11.850  -6.578   4.333  1.00  0.00           O
ATOM    838  N   LEU A  58       9.999  -6.897   3.013  1.00  0.00           N
ATOM    839  CA  LEU A  58      10.553  -7.605   1.877  1.00  0.00           C
ATOM    840  C   LEU A  58      10.174  -6.880   0.595  1.00  0.00           C
ATOM    841  O   LEU A  58       9.018  -6.948   0.167  1.00  0.00           O
ATOM    857  N   GLU A  59      11.079  -6.189  -0.084  1.00  0.00           N
ATOM    858  CA  GLU A  59      10.819  -5.321  -1.251  1.00  0.00           C
ATOM    859  C   GLU A  59      11.427  -6.015  -2.465  1.00  0.00           C
ATOM    860  O   GLU A  59      12.675  -5.938  -2.516  1.00  0.00           O
ATOM    872  N   THR A  60      10.655  -6.736  -3.321  1.00  0.00           N
ATOM    873  CA  THR A  60      11.098  -7.532  -4.463  1.00  0.00           C
ATOM    874  C   THR A  60      10.548  -6.957  -5.763  1.00  0.00           C
ATOM    875  O   THR A  60       9.336  -6.976  -5.995  1.00  0.00           O
ATOM    886  N   LYS A  61      11.358  -6.575  -6.761  1.00  0.00           N
ATOM    887  CA  LYS A  61      10.948  -5.697  -7.876  1.00  0.00           C
ATOM    888  C   LYS A  61      11.752  -6.040  -9.135  1.00  0.00           C
ATOM    889  O   LYS A  61      12.454  -7.041  -9.203  1.00  0.00           O
ATOM    908  N   TYR A  62      10.516  -7.160  -9.805  1.00  0.00           N
```


Dieses Werk ist copyrightgeschützt und darf in keiner Form vervielfältigt werden noch an Dritte weitergegeben werden.
Es gilt nur für den persönlichen Gebrauch.

```
ATOM    909  CA  TYR A  62      10.885  -7.913 -11.012  1.00  0.00           C
ATOM    910  C   TYR A  62      10.745  -7.022 -12.247  1.00  0.00           C
ATOM    911  O   TYR A  62       9.680  -6.425 -12.453  1.00  0.00           O
ATOM    929  N   ARG A  63      11.821  -6.947 -13.059  1.00  0.00           N
ATOM    930  CA  ARG A  63      11.816  -6.138 -14.300  1.00  0.00           C
ATOM    931  C   ARG A  63      12.026  -4.641 -14.027  1.00  0.00           C
ATOM    932  O   ARG A  63      13.099  -4.269 -13.579  1.00  0.00           O
ATOM    953  N   TRP A  64      10.981  -3.821 -14.286  1.00  0.00           N
ATOM    954  CA  TRP A  64      10.996  -2.358 -14.062  1.00  0.00           C
ATOM    955  C   TRP A  64      10.096  -1.711 -15.115  1.00  0.00           C
ATOM    956  O   TRP A  64       9.313  -2.399 -15.768  1.00  0.00           O
ATOM    977  N   THR A  65      10.194  -0.393 -15.270  1.00  0.00           N
ATOM    978  CA  THR A  65       9.369   0.308 -16.242  1.00  0.00           C
ATOM    979  C   THR A  65       9.944   0.183 -17.650  1.00  0.00           C
ATOM    980  O   THR A  65       9.561   0.939 -18.539  1.00  0.00           O
ATOM    991  N   GLU A  66      10.858  -0.775 -17.858  1.00  0.00           N
ATOM    992  CA  GLU A  66      11.448  -0.968 -19.185  1.00  0.00           C
ATOM    993  C   GLU A  66      10.358  -0.953 -20.244  1.00  0.00           C
ATOM    994  O   GLU A  66       9.932   0.116 -20.688  1.00  0.00           O
ATOM   1006  N   TYR A  67       9.900  -2.134 -20.664  1.00  0.00           N
ATOM   1007  CA  TYR A  67       8.863  -2.207 -21.667  1.00  0.00           C
ATOM   1008  C   TYR A  67       7.491  -2.169 -20.999  1.00  0.00           C
ATOM   1009  O   TYR A  67       6.502  -2.640 -21.561  1.00  0.00           O
ATOM   1027  N   GLY A  68       7.441  -1.541 -19.819  1.00  0.00           N
ATOM   1028  CA  GLY A  68       6.181  -1.370 -19.103  1.00  0.00           C
ATOM   1029  C   GLY A  68       5.722  -2.639 -18.396  1.00  0.00           C
ATOM   1030  O   GLY A  68       4.555  -2.740 -18.028  1.00  0.00           O
ATOM   1034  N   LEU A  69       6.632  -3.601 -18.218  1.00  0.00           N
ATOM   1035  CA  LEU A  69       6.289  -4.856 -17.554  1.00  0.00           C
ATOM   1036  C   LEU A  69       6.868  -4.911 -16.149  1.00  0.00           C
ATOM   1037  O   LEU A  69       7.736  -5.732 -15.857  1.00  0.00           O
ATOM   1053  N   THR A  70       6.351  -4.055 -15.282  1.00  0.00           N
ATOM   1054  CA  THR A  70       6.804  -4.032 -13.896  1.00  0.00           C
ATOM   1055  C   THR A  70       5.946  -4.942 -13.042  1.00  0.00           C
ATOM   1056  O   THR A  70       4.762  -4.655 -12.831  1.00  0.00           O
ATOM   1067  N   PHE A  71       6.541  -6.023 -12.525  1.00  0.00           N
ATOM   1068  CA  PHE A  71       5.800  -6.919 -11.655  1.00  0.00           C
ATOM   1069  C   PHE A  71       6.374  -6.745 -10.251  1.00  0.00           C
ATOM   1070  O   PHE A  71       7.412  -7.309  -9.904  1.00  0.00           O
ATOM   1087  N   THR A  72       5.711  -5.910  -9.473  1.00  0.00           N
ATOM   1088  CA  THR A  72       6.176  -5.596  -8.126  1.00  0.00           C
ATOM   1089  C   THR A  72       5.631  -6.586  -7.113  1.00  0.00           C
ATOM   1090  O   THR A  72       4.460  -6.947  -7.154  1.00  0.00           O
ATOM   1101  N   VAL A  73       6.496  -6.991  -6.181  1.00  0.00           N
ATOM   1102  CA  VAL A  73       6.092  -7.912  -5.130  1.00  0.00           C
ATOM   1103  C   VAL A  73       6.496  -7.371  -3.757  1.00  0.00           C
ATOM   1104  O   VAL A  73       7.673  -7.134  -3.485  1.00  0.00           O
ATOM   1117  N   LYS A  74       5.498  -7.170  -2.902  1.00  0.00           N
ATOM   1118  CA  LYS A  74       5.724  -6.649  -1.557  1.00  0.00           C
ATOM   1119  C   LYS A  74       5.228  -7.626  -0.494  1.00  0.00           C
ATOM   1120  O   LYS A  74       4.025  -7.842  -0.358  1.00  0.00           O
ATOM   1139  N   TRP A  75       6.154  -8.181   0.275  1.00  0.00           N
ATOM   1140  CA  TRP A  75       5.798  -9.101   1.353  1.00  0.00           C
ATOM   1141  C   TRP A  75       6.213  -8.478   2.690  1.00  0.00           C
ATOM   1142  O   TRP A  75       7.258  -7.831   2.778  1.00  0.00           O
ATOM   1163  N   ASN A  76       5.458  -8.662   3.785  1.00  0.00           N
ATOM   1164  CA  ASN A  76       5.759  -8.127   5.145  1.00  0.00           C
ATOM   1165  C   ASN A  76       5.519  -9.172   6.240  1.00  0.00           C
ATOM   1166  O   ASN A  76       4.864 -10.191   6.044  1.00  0.00           O
ATOM   1177  N   THR A  77       6.076  -8.879   7.422  1.00  0.00           N
ATOM   1178  CA  THR A  77       6.041  -9.728   8.618  1.00  0.00           C
ATOM   1179  C   THR A  77       4.711  -9.747   9.368  1.00  0.00           C
ATOM   1180  O   THR A  77       4.326 -10.792   9.907  1.00  0.00           O
ATOM   1191  N   ASP A  78       3.878  -8.697   9.226  1.00  0.00           N
ATOM   1192  CA  ASP A  78       2.422  -8.821   9.369  1.00  0.00           C
ATOM   1193  C   ASP A  78       1.698  -9.755   8.387  1.00  0.00           C
ATOM   1194  O   ASP A  78       0.461  -9.693   8.598  1.00  0.00           O
ATOM   1203  N   ASN A  79       2.252 -10.492   7.388  1.00  0.00           N
ATOM   1204  CA  ASN A  79       1.687 -11.485   6.467  1.00  0.00           C
ATOM   1205  C   ASN A  79       1.082 -10.859   5.206  1.00  0.00           C
ATOM   1206  O   ASN A  79       0.648 -11.589   4.318  1.00  0.00           O
ATOM   1217  N   THR A  80       1.064  -9.531   5.096  1.00  0.00           N
ATOM   1218  CA  THR A  80       0.509  -8.915   3.883  1.00  0.00           C
ATOM   1219  C   THR A  80       1.360  -9.293   2.679  1.00  0.00           C
ATOM   1220  O   THR A  80       2.579  -9.106   2.688  1.00  0.00           O
ATOM   1231  N   LEU A  81       0.696  -9.780   1.632  1.00  0.00           N
ATOM   1232  CA  LEU A  81       1.378 -10.147   0.395  1.00  0.00           C
ATOM   1233  C   LEU A  81       0.797  -9.312  -0.740  1.00  0.00           C
ATOM   1234  O   LEU A  81      -0.424  -9.226  -0.853  1.00  0.00           O
ATOM   1250  N   GLY A  82       1.632  -8.689  -1.572  1.00  0.00           N
ATOM   1251  CA  GLY A  82       1.100  -7.874  -2.662  1.00  0.00           C
ATOM   1252  C   GLY A  82       1.882  -8.065  -3.954  1.00  0.00           C
ATOM   1253  O   GLY A  82       3.078  -7.830  -3.989  1.00  0.00           O
ATOM   1257  N   THR A  83       1.182  -8.441  -5.024  1.00  0.00           N
ATOM   1258  CA  THR A  83       1.818  -8.606  -6.334  1.00  0.00           C
ATOM   1259  C   THR A  83       1.081  -7.764  -7.376  1.00  0.00           C
ATOM   1260  O   THR A  83      -0.126  -7.921  -7.572  1.00  0.00           O
ATOM   1271  N   GLU A  84       1.805  -6.855  -8.023  1.00  0.00           N
ATOM   1272  CA  GLU A  84       1.195  -5.977  -9.028  1.00  0.00           C
ATOM   1273  C   GLU A  84       1.831  -6.154 -10.404  1.00  0.00           C
ATOM   1274  O   GLU A  84       2.965  -5.734 -10.612  1.00  0.00           O
ATOM   1286  N   ILE A  85       1.089  -6.722 -11.363  1.00  0.00           N
ATOM   1287  CA  ILE A  85       1.623  -6.878 -12.721  1.00  0.00           C
ATOM   1288  C   ILE A  85       1.031  -5.801 -13.621  1.00  0.00           C
```


Dieses Werk ist copyrightgeschützt und darf in keiner Form vervielfältigt werden noch an Dritte weitergegeben werden.
Es gilt nur für den persönlichen Gebrauch.

```
ATOM   1289  O   ILE A  85      -0.178  -5.758 -13.817  1.00  0.00           O
ATOM   1305  N   THR A  86       1.893  -4.924 -14.138  1.00  0.00           N
ATOM   1306  CA  THR A  86       1.435  -3.823 -14.987  1.00  0.00           C
ATOM   1307  C   THR A  86       2.006  -3.871 -16.401  1.00  0.00           C
ATOM   1308  O   THR A  86       3.218  -3.999 -16.582  1.00  0.00           O
ATOM   1319  N   VAL A  87       1.124  -3.693 -17.397  1.00  0.00           N
ATOM   1320  CA  VAL A  87       1.555  -3.637 -18.796  1.00  0.00           C
ATOM   1321  C   VAL A  87       1.166  -2.281 -19.380  1.00  0.00           C
ATOM   1322  O   VAL A  87       0.004  -2.055 -19.718  1.00  0.00           O
ATOM   1335  N   GLU A  88       2.134  -1.383 -19.492  1.00  0.00           N
ATOM   1336  CA  GLU A  88       1.869  -0.046 -20.032  1.00  0.00           C
ATOM   1337  C   GLU A  88       2.183   0.025 -21.535  1.00  0.00           C
ATOM   1338  O   GLU A  88       3.017  -0.731 -22.026  1.00  0.00           O
ATOM   1350  N   ASP A  89       1.523   0.952 -22.247  1.00  0.00           N
ATOM   1351  CA  ASP A  89       1.761   1.143 -23.690  1.00  0.00           C
ATOM   1352  C   ASP A  89       1.411  -0.105 -24.504  1.00  0.00           C
ATOM   1353  O   ASP A  89       2.148  -0.467 -25.422  1.00  0.00           O
ATOM   1362  N   GLN A  90       0.422  -0.933 -24.148  1.00  0.00           N
ATOM   1363  CA  GLN A  90       0.066  -2.096 -24.985  1.00  0.00           C
ATOM   1364  C   GLN A  90      -0.423  -1.682 -26.380  1.00  0.00           C
ATOM   1365  O   GLN A  90       0.192  -2.366 -27.254  1.00  0.00           O
ATOM   1379  N   LEU A  91      -1.250  -0.668 -26.572  1.00  0.00           N
ATOM   1380  CA  LEU A  91      -1.692  -0.368 -27.935  1.00  0.00           C
ATOM   1381  C   LEU A  91      -0.657   0.532 -28.609  1.00  0.00           C
ATOM   1382  O   LEU A  91       0.030   0.121 -29.552  1.00  0.00           O
ATOM   1398  N   ALA A  92      -0.542   1.757 -28.106  1.00  0.00           N
ATOM   1399  CA  ALA A  92       0.420   2.711 -28.648  1.00  0.00           C
ATOM   1400  C   ALA A  92       0.314   4.082 -27.964  1.00  0.00           C
ATOM   1401  O   ALA A  92       1.334   4.699 -27.652  1.00  0.00           O
ATOM   1408  N   ARG A  93      -0.907   4.556 -27.704  1.00  0.00           N
ATOM   1409  CA  ARG A  93      -1.069   5.842 -27.045  1.00  0.00           C
ATOM   1410  C   ARG A  93      -0.781   5.684 -25.562  1.00  0.00           C
ATOM   1411  O   ARG A  93       0.309   5.995 -25.081  1.00  0.00           O
ATOM   1432  N   GLY A  94      -1.627   4.998 -24.825  1.00  0.00           N
ATOM   1433  CA  GLY A  94      -1.593   4.980 -23.376  1.00  0.00           C
ATOM   1434  C   GLY A  94      -2.581   3.906 -22.925  1.00  0.00           C
ATOM   1435  O   GLY A  94      -3.736   4.276 -22.718  1.00  0.00           O
ATOM   1439  N   LEU A  95      -2.119   2.673 -22.903  1.00  0.00           N
ATOM   1440  CA  LEU A  95      -2.896   1.511 -22.475  1.00  0.00           C
ATOM   1441  C   LEU A  95      -2.174   0.836 -21.302  1.00  0.00           C
ATOM   1442  O   LEU A  95      -1.011   0.440 -21.427  1.00  0.00           O
ATOM   1458  N   LYS A  96      -2.792   0.799 -20.112  1.00  0.00           N
ATOM   1459  CA  LYS A  96      -2.234   0.286 -18.830  1.00  0.00           C
ATOM   1460  C   LYS A  96      -3.108  -0.898 -18.402  1.00  0.00           C
ATOM   1461  O   LYS A  96      -4.262  -0.518 -18.357  1.00  0.00           O
ATOM   1480  N   LEU A  97      -2.597  -2.126 -18.149  1.00  0.00           N
ATOM   1481  CA  LEU A  97      -3.371  -3.257 -17.629  1.00  0.00           C
ATOM   1482  C   LEU A  97      -2.724  -3.752 -16.354  1.00  0.00           C
ATOM   1483  O   LEU A  97      -1.656  -4.362 -16.418  1.00  0.00           O
ATOM   1499  N   THR A  98      -3.348  -3.467 -15.199  1.00  0.00           N
ATOM   1500  CA  THR A  98      -2.760  -3.885 -13.927  1.00  0.00           C
ATOM   1501  C   THR A  98      -3.513  -4.986 -13.189  1.00  0.00           C
ATOM   1502  O   THR A  98      -4.470  -4.709 -12.456  1.00  0.00           O
ATOM   1513  N   PHE A  99      -3.036  -6.224 -13.307  1.00  0.00           N
ATOM   1514  CA  PHE A  99      -3.646  -7.290 -12.541  1.00  0.00           C
ATOM   1515  C   PHE A  99      -2.992  -7.208 -11.182  1.00  0.00           C
ATOM   1516  O   PHE A  99      -1.764  -7.140 -11.091  1.00  0.00           O
ATOM   1533  N   ASP A 100      -3.753  -7.049 -10.117  1.00  0.00           N
ATOM   1534  CA  ASP A 100      -3.269  -6.903  -8.743  1.00  0.00           C
ATOM   1535  C   ASP A 100      -3.550  -8.215  -8.014  1.00  0.00           C
ATOM   1536  O   ASP A 100      -4.451  -8.909  -8.415  1.00  0.00           O
ATOM   1545  N   SER A 101      -2.801  -8.486  -6.963  1.00  0.00           N
ATOM   1546  CA  SER A 101      -3.055  -9.578  -6.024  1.00  0.00           C
ATOM   1547  C   SER A 101      -2.602  -9.188  -4.631  1.00  0.00           C
ATOM   1548  O   SER A 101      -1.406  -9.081  -4.370  1.00  0.00           O
ATOM   1567  N   PHE A 103      -3.136 -10.341  -0.727  1.00  0.00           N
ATOM   1568  CA  PHE A 103      -3.606 -11.319   0.252  1.00  0.00           C
ATOM   1569  C   PHE A 103      -3.261 -10.843   1.671  1.00  0.00           C
ATOM   1570  O   PHE A 103      -2.094 -10.894   2.059  1.00  0.00           O
ATOM   1587  N   SER A 104      -4.261 -10.386   2.442  1.00  0.00           N
ATOM   1588  CA  SER A 104      -3.998  -9.909   3.810  1.00  0.00           C
ATOM   1589  C   SER A 104      -4.601 -10.835   4.889  1.00  0.00           C
ATOM   1590  O   SER A 104      -5.524 -11.618   4.622  1.00  0.00           O
ATOM   1598  N   PRO A 105      -4.087 -10.740   6.105  1.00  0.00           N
ATOM   1599  CA  PRO A 105      -4.544 -11.555   7.275  1.00  0.00           C
ATOM   1600  C   PRO A 105      -6.056 -11.771   7.353  1.00  0.00           C
ATOM   1601  O   PRO A 105      -6.508 -12.898   7.550  1.00  0.00           O
ATOM   1612  N   ASN A 106      -6.830 -10.693   7.233  1.00  0.00           N
ATOM   1613  CA  ASN A 106      -8.288 -10.794   7.328  1.00  0.00           C
ATOM   1614  C   ASN A 106      -8.798 -12.090   6.693  1.00  0.00           C
ATOM   1615  O   ASN A 106      -9.049 -12.139   5.494  1.00  0.00           O
ATOM   1626  N   THR A 107      -8.955 -13.126   7.520  1.00  0.00           N
ATOM   1627  CA  THR A 107      -9.437 -14.432   7.057  1.00  0.00           C
ATOM   1628  C   THR A 107      -8.949 -14.734   5.644  1.00  0.00           C
ATOM   1629  O   THR A 107      -9.727 -15.174   4.798  1.00  0.00           O
ATOM   1640  N   GLY A 108      -7.665 -14.497   5.391  1.00  0.00           N
ATOM   1641  CA  GLY A 108      -7.104 -14.754   4.067  1.00  0.00           C
ATOM   1642  C   GLY A 108      -7.839 -13.941   3.007  1.00  0.00           C
ATOM   1643  O   GLY A 108      -8.243 -14.474   1.975  1.00  0.00           O
ATOM   1647  N   LYS A 109      -8.015 -12.652   3.278  1.00  0.00           N
ATOM   1648  CA  LYS A 109      -8.717 -11.772   2.343  1.00  0.00           C
ATOM   1649  C   LYS A 109      -7.932 -11.634   1.043  1.00  0.00           C
ATOM   1650  O   LYS A 109      -6.829 -11.086   1.028  1.00  0.00           O
ATOM   1669  N   LYS A 110      -8.512 -12.148  -0.040  1.00  0.00           N
```


Dieses Werk ist copyrightgeschützt und darf in keiner Form vervielfältigt werden noch an Dritte weitergegeben werden.
Es gilt nur für den persönlichen Gebrauch.

```
ATOM   1670  CA  LYS A 110      -7.874 -12.104  -1.356  1.00  0.00           C
ATOM   1671  C   LYS A 110      -8.410 -10.945  -2.189  1.00  0.00           C
ATOM   1672  O   LYS A 110      -9.612 -10.855  -2.447  1.00  0.00           O
ATOM   1691  N   ASN A 111      -7.604 -10.019  -2.719  1.00  0.00           N
ATOM   1692  CA  ASN A 111      -8.048  -8.885  -3.578  1.00  0.00           C
ATOM   1693  C   ASN A 111      -7.439  -9.049  -4.973  1.00  0.00           C
ATOM   1694  O   ASN A 111      -6.286  -8.669  -5.139  1.00  0.00           O
ATOM   1705  N   ALA A 112      -8.215  -9.517  -5.939  1.00  0.00           N
ATOM   1706  CA  ALA A 112      -7.803  -9.787  -7.320  1.00  0.00           C
ATOM   1707  C   ALA A 112      -8.438  -8.753  -8.256  1.00  0.00           C
ATOM   1708  O   ALA A 112      -9.521  -9.047  -8.786  1.00  0.00           O
ATOM   1715  N   LYS A 113      -7.779  -7.608  -8.445  1.00  0.00           N
ATOM   1716  CA  LYS A 113      -8.255  -6.489  -9.309  1.00  0.00           C
ATOM   1717  C   LYS A 113      -7.586  -6.523 -10.685  1.00  0.00           C
ATOM   1718  O   LYS A 113      -6.438  -6.817 -10.598  1.00  0.00           O
ATOM   1737  N   ILE A 114      -8.281  -6.227 -11.754  1.00  0.00           N
ATOM   1738  CA  ILE A 114      -7.775  -6.106 -13.146  1.00  0.00           C
ATOM   1739  C   ILE A 114      -8.047  -4.648 -13.545  1.00  0.00           C
ATOM   1740  O   ILE A 114      -9.186  -4.551 -13.943  1.00  0.00           O
ATOM   1756  N   LYS A 115      -7.147  -3.692 -13.579  1.00  0.00           N
ATOM   1757  CA  LYS A 115      -7.446  -2.275 -13.912  1.00  0.00           C
ATOM   1758  C   LYS A 115      -7.098  -2.102 -15.385  1.00  0.00           C
ATOM   1759  O   LYS A 115      -5.984  -2.493 -15.542  1.00  0.00           O
ATOM   1778  N   THR A 116      -7.935  -1.631 -16.299  1.00  0.00           N
ATOM   1779  CA  THR A 116      -7.637  -1.391 -17.698  1.00  0.00           C
ATOM   1780  C   THR A 116      -7.941   0.060 -17.985  1.00  0.00           C
ATOM   1781  O   THR A 116      -9.099   0.446 -18.024  1.00  0.00           O
ATOM   1792  N   GLY A 117      -6.909   0.873 -18.218  1.00  0.00           N
ATOM   1793  CA  GLY A 117      -6.942   2.315 -18.399  1.00  0.00           C
ATOM   1794  C   GLY A 117      -6.491   2.691 -19.793  1.00  0.00           C
ATOM   1795  O   GLY A 117      -5.315   3.041 -19.959  1.00  0.00           O
ATOM   1796  H   GLY A 117      -5.985   0.603 -18.291  1.00  0.00           H
ATOM   1797  HA2 GLY A 117      -7.890   2.732 -18.254  1.00  0.00           H
ATOM   1798  HA3 GLY A 117      -6.281   2.759 -17.664  1.00  0.00           H
ATOM   1799  N   TYR A 118      -7.408   2.637 -20.743  1.00  0.00           N
ATOM   1800  CA  TYR A 118      -7.181   3.165 -22.086  1.00  0.00           C
ATOM   1801  C   TYR A 118      -7.174   4.682 -22.007  1.00  0.00           C
ATOM   1802  O   TYR A 118      -8.085   5.143 -21.301  1.00  0.00           O
ATOM   1820  N   LYS A 119      -6.270   5.326 -22.699  1.00  0.00           N
ATOM   1821  CA  LYS A 119      -6.076   6.771 -22.735  1.00  0.00           C
ATOM   1822  C   LYS A 119      -6.100   7.214 -24.205  1.00  0.00           C
ATOM   1823  O   LYS A 119      -5.654   6.458 -25.074  1.00  0.00           O
ATOM   1842  N   ARG A 120      -6.555   8.422 -24.454  1.00  0.00           N
ATOM   1843  CA  ARG A 120      -6.633   9.001 -25.795  1.00  0.00           C
ATOM   1844  C   ARG A 120      -6.914  10.482 -25.649  1.00  0.00           C
ATOM   1845  O   ARG A 120      -8.066  10.889 -25.650  1.00  0.00           O
ATOM   1866  N   GLU A 121      -5.850  11.275 -25.486  1.00  0.00           N
ATOM   1867  CA  GLU A 121      -5.970  12.718 -25.319  1.00  0.00           C
ATOM   1868  C   GLU A 121      -7.232  13.115 -24.536  1.00  0.00           C
ATOM   1869  O   GLU A 121      -8.362  12.908 -24.971  1.00  0.00           O
ATOM   1881  N   HIS A 122      -7.004  13.757 -23.405  1.00  0.00           N
ATOM   1882  CA  HIS A 122      -8.092  14.268 -22.560  1.00  0.00           C
ATOM   1883  C   HIS A 122      -9.091  13.192 -22.121  1.00  0.00           C
ATOM   1884  O   HIS A 122      -9.897  13.461 -21.222  1.00  0.00           O
ATOM   1898  N   ILE A 123      -9.078  12.003 -22.754  1.00  0.00           N
ATOM   1899  CA  ILE A 123     -10.031  10.950 -22.387  1.00  0.00           C
ATOM   1900  C   ILE A 123      -9.355   9.732 -21.772  1.00  0.00           C
ATOM   1901  O   ILE A 123      -8.661   8.993 -22.476  1.00  0.00           O
ATOM   1917  N   ASN A 124      -9.582   9.427 -20.481  1.00  0.00           N
ATOM   1918  CA  ASN A 124      -9.011   8.240 -19.787  1.00  0.00           C
ATOM   1919  C   ASN A 124     -10.197   7.406 -19.241  1.00  0.00           C
ATOM   1920  O   ASN A 124     -11.081   8.043 -18.665  1.00  0.00           O
ATOM   1931  N   LEU A 125     -10.182   6.086 -19.420  1.00  0.00           N
ATOM   1932  CA  LEU A 125     -11.295   5.165 -19.113  1.00  0.00           C
ATOM   1933  C   LEU A 125     -10.772   3.948 -18.346  1.00  0.00           C
ATOM   1934  O   LEU A 125     -10.441   2.901 -18.877  1.00  0.00           O
ATOM   1950  N   GLY A 126     -10.689   4.046 -17.000  1.00  0.00           N
ATOM   1951  CA  GLY A 126     -10.302   2.934 -16.136  1.00  0.00           C
ATOM   1952  C   GLY A 126     -11.398   1.883 -16.057  1.00  0.00           C
ATOM   1953  O   GLY A 126     -12.543   2.370 -16.032  1.00  0.00           O
ATOM   1957  N   CYS A 127     -11.072   0.576 -15.989  1.00  0.00           N
ATOM   1958  CA  CYS A 127     -11.994  -0.473 -15.555  1.00  0.00           C
ATOM   1959  C   CYS A 127     -11.319  -1.420 -14.547  1.00  0.00           C
ATOM   1960  O   CYS A 127     -10.488  -2.243 -14.916  1.00  0.00           O
ATOM   1968  N   ASP A 128     -11.561  -1.342 -13.263  1.00  0.00           N
ATOM   1969  CA  ASP A 128     -11.003  -2.148 -12.160  1.00  0.00           C
ATOM   1970  C   ASP A 128     -12.071  -3.167 -11.698  1.00  0.00           C
ATOM   1971  O   ASP A 128     -13.019  -2.710 -11.038  1.00  0.00           O
ATOM   1980  N   MET A 129     -11.888  -4.450 -11.985  1.00  0.00           N
ATOM   1981  CA  MET A 129     -12.812  -5.569 -11.686  1.00  0.00           C
ATOM   1982  C   MET A 129     -12.252  -6.366 -10.509  1.00  0.00           C
ATOM   1983  O   MET A 129     -11.429  -7.255 -10.738  1.00  0.00           O
ATOM   1997  N   ASP A 130     -12.716  -6.132  -9.290  1.00  0.00           N
ATOM   1998  CA  ASP A 130     -12.163  -6.764  -8.084  1.00  0.00           C
ATOM   1999  C   ASP A 130     -12.831  -8.110  -7.817  1.00  0.00           C
ATOM   2000  O   ASP A 130     -13.810  -8.174  -7.112  1.00  0.00           O
ATOM   2009  N   PHE A 131     -12.261  -9.211  -8.334  1.00  0.00           N
ATOM   2010  CA  PHE A 131     -12.789 -10.553  -8.062  1.00  0.00           C
ATOM   2011  C   PHE A 131     -12.511 -10.953  -6.612  1.00  0.00           C
ATOM   2012  O   PHE A 131     -11.570 -11.684  -6.299  1.00  0.00           O
ATOM   2029  N   ASP A 132     -13.375 -10.485  -5.740  1.00  0.00           N
ATOM   2030  CA  ASP A 132     -13.435 -10.796  -4.304  1.00  0.00           C
ATOM   2031  C   ASP A 132     -14.744 -11.555  -4.050  1.00  0.00           C
ATOM   2032  O   ASP A 132     -15.478 -11.725  -5.013  1.00  0.00           O
```


Dieses Werk ist copyrightgeschützt und darf in keiner Form vervielfältigt werden noch an Dritte weitergegeben werden.
Es gilt nur für den persönlichen Gebrauch.

```
ATOM   2041  N   ILE A 133     -15.043 -12.056  -2.863  1.00  0.00           N
ATOM   2042  CA  ILE A 133     -16.299 -12.692  -2.516  1.00  0.00           C
ATOM   2043  C   ILE A 133     -17.402 -11.644  -2.470  1.00  0.00           C
ATOM   2044  O   ILE A 133     -18.483 -11.868  -3.016  1.00  0.00           O
ATOM   2060  N   ALA A 134     -17.110 -10.468  -1.907  1.00  0.00           N
ATOM   2061  CA  ALA A 134     -18.094  -9.393  -1.920  1.00  0.00           C
ATOM   2062  C   ALA A 134     -18.226  -8.921  -3.367  1.00  0.00           C
ATOM   2063  O   ALA A 134     -19.309  -8.586  -3.839  1.00  0.00           O
ATOM   2070  N   GLY A 135     -17.098  -8.971  -4.081  1.00  0.00           N
ATOM   2071  CA  GLY A 135     -17.067  -8.636  -5.502  1.00  0.00           C
ATOM   2072  C   GLY A 135     -17.647  -9.834  -6.247  1.00  0.00           C
ATOM   2073  O   GLY A 135     -18.151 -10.759  -5.603  1.00  0.00           O
ATOM   2077  N   PRO A 136     -17.595  -9.903  -7.553  1.00  0.00           N
ATOM   2078  CA  PRO A 136     -17.014  -8.867  -8.485  1.00  0.00           C
ATOM   2079  C   PRO A 136     -17.568  -7.455  -8.318  1.00  0.00           C
ATOM   2080  O   PRO A 136     -18.766  -7.235  -8.520  1.00  0.00           O
ATOM   2091  N   SER A 137     -16.694  -6.473  -8.014  1.00  0.00           N
ATOM   2092  CA  SER A 137     -17.022  -5.037  -7.872  1.00  0.00           C
ATOM   2093  C   SER A 137     -16.499  -4.360  -9.145  1.00  0.00           C
ATOM   2094  O   SER A 137     -15.285  -4.699  -9.289  1.00  0.00           O
ATOM   2102  N   ILE A 138     -17.200  -3.514  -9.916  1.00  0.00           N
ATOM   2103  CA  ILE A 138     -16.637  -2.818 -11.074  1.00  0.00           C
ATOM   2104  C   ILE A 138     -16.393  -1.347 -10.754  1.00  0.00           C
ATOM   2105  O   ILE A 138     -17.325  -0.557 -10.736  1.00  0.00           O
ATOM   2121  N   ARG A 139     -15.186  -1.097 -10.306  1.00  0.00           N
ATOM   2122  CA  ARG A 139     -14.719   0.254 -10.160  1.00  0.00           C
ATOM   2123  C   ARG A 139     -14.212   0.641 -11.571  1.00  0.00           C
ATOM   2124  O   ARG A 139     -13.466  -0.007 -12.069  1.00  0.00           O
ATOM   2145  N   GLY A 140     -14.620   1.883 -12.091  1.00  0.00           N
ATOM   2146  CA  GLY A 140     -13.940   2.514 -13.242  1.00  0.00           C
ATOM   2147  C   GLY A 140     -13.930   4.028 -13.091  1.00  0.00           C
ATOM   2148  O   GLY A 140     -14.709   4.519 -12.309  1.00  0.00           O
ATOM   2152  N   ALA A 141     -13.049   4.768 -13.800  1.00  0.00           N
ATOM   2153  CA  ALA A 141     -12.895   6.221 -13.753  1.00  0.00           C
ATOM   2154  C   ALA A 141     -13.105   6.715 -15.175  1.00  0.00           C
ATOM   2155  O   ALA A 141     -12.284   6.127 -15.929  1.00  0.00           O
ATOM   2162  N   LEU A 142     -14.022   7.609 -15.511  1.00  0.00           N
ATOM   2163  CA  LEU A 142     -14.108   8.188 -16.852  1.00  0.00           C
ATOM   2164  C   LEU A 142     -13.750   9.650 -16.770  1.00  0.00           C
ATOM   2165  O   LEU A 142     -14.527  10.417 -16.215  1.00  0.00           O
ATOM   2181  N   VAL A 143     -12.576  10.009 -17.326  1.00  0.00           N
ATOM   2182  CA  VAL A 143     -11.990  11.357 -17.218  1.00  0.00           C
ATOM   2183  C   VAL A 143     -12.166  12.067 -18.555  1.00  0.00           C
ATOM   2184  O   VAL A 143     -11.721  11.324 -19.364  1.00  0.00           O
ATOM   2197  N   LEU A 144     -12.676  13.293 -18.654  1.00  0.00           N
ATOM   2198  CA  LEU A 144     -12.748  14.088 -19.869  1.00  0.00           C
ATOM   2199  C   LEU A 144     -11.959  15.356 -19.647  1.00  0.00           C
ATOM   2200  O   LEU A 144     -12.057  15.957 -18.577  1.00  0.00           O
ATOM   2216  N   GLY A 145     -11.182  15.774 -20.645  1.00  0.00           N
ATOM   2217  CA  GLY A 145     -10.380  16.985 -20.507  1.00  0.00           C
ATOM   2218  C   GLY A 145     -10.952  18.142 -21.324  1.00  0.00           C
ATOM   2219  O   GLY A 145     -11.528  17.930 -22.392  1.00  0.00           O
ATOM   2223  N   TYR A 146     -10.757  19.373 -20.847  1.00  0.00           N
ATOM   2224  CA  TYR A 146     -11.228  20.544 -21.588  1.00  0.00           C
ATOM   2225  C   TYR A 146     -10.260  21.693 -21.365  1.00  0.00           C
ATOM   2226  O   TYR A 146      -9.130  21.437 -20.972  1.00  0.00           O
ATOM   2244  N   GLU A 147     -10.726  22.939 -21.619  1.00  0.00           N
ATOM   2245  CA  GLU A 147      -9.927  24.177 -21.462  1.00  0.00           C
ATOM   2246  C   GLU A 147      -9.150  24.237 -20.137  1.00  0.00           C
ATOM   2247  O   GLU A 147      -9.262  25.213 -19.398  1.00  0.00           O
ATOM   2259  N   GLY A 148      -8.384  23.207 -19.836  1.00  0.00           N
ATOM   2260  CA  GLY A 148      -7.633  23.156 -18.593  1.00  0.00           C
ATOM   2261  C   GLY A 148      -8.480  22.539 -17.474  1.00  0.00           C
ATOM   2262  O   GLY A 148      -8.370  22.937 -16.319  1.00  0.00           O
ATOM   2266  N   TRP A 149      -9.328  21.571 -17.824  1.00  0.00           N
ATOM   2267  CA  TRP A 149     -10.173  20.925 -16.809  1.00  0.00           C
ATOM   2268  C   TRP A 149     -10.142  19.418 -16.943  1.00  0.00           C
ATOM   2269  O   TRP A 149     -10.162  18.887 -18.038  1.00  0.00           O
ATOM   2290  N   LEU A 150     -10.144  18.762 -15.792  1.00  0.00           N
ATOM   2291  CA  LEU A 150     -10.181  17.306 -15.686  1.00  0.00           C
ATOM   2292  C   LEU A 150     -11.414  16.903 -14.857  1.00  0.00           C
ATOM   2293  O   LEU A 150     -11.424  17.122 -13.647  1.00  0.00           O
ATOM   2309  N   ALA A 151     -12.414  16.280 -15.466  1.00  0.00           N
ATOM   2310  CA  ALA A 151     -13.589  15.824 -14.700  1.00  0.00           C
ATOM   2311  C   ALA A 151     -13.598  14.307 -14.712  1.00  0.00           C
ATOM   2312  O   ALA A 151     -13.263  13.742 -15.735  1.00  0.00           O
ATOM   2319  N   GLY A 152     -13.940  13.632 -13.597  1.00  0.00           N
ATOM   2320  CA  GLY A 152     -13.921  12.170 -13.582  1.00  0.00           C
ATOM   2321  C   GLY A 152     -15.195  11.583 -12.990  1.00  0.00           C
ATOM   2322  O   GLY A 152     -15.832  12.195 -12.125  1.00  0.00           O
ATOM   2326  N   TYR A 153     -15.550  10.379 -13.446  1.00  0.00           N
ATOM   2327  CA  TYR A 153     -16.744   9.702 -12.954  1.00  0.00           C
ATOM   2328  C   TYR A 153     -16.344   8.315 -12.535  1.00  0.00           C
ATOM   2329  O   TYR A 153     -15.985   7.507 -13.393  1.00  0.00           O
ATOM   2347  N   GLN A 154     -16.392   8.016 -11.234  1.00  0.00           N
ATOM   2348  CA  GLN A 154     -16.002   6.713 -10.769  1.00  0.00           C
ATOM   2349  C   GLN A 154     -17.232   5.893 -10.423  1.00  0.00           C
ATOM   2350  O   GLN A 154     -17.926   6.238  -9.485  1.00  0.00           O
ATOM   2364  N   MET A 155     -17.488   4.822 -11.178  1.00  0.00           N
ATOM   2365  CA  MET A 155     -18.659   3.976 -10.918  1.00  0.00           C
ATOM   2366  C   MET A 155     -18.271   2.637 -10.289  1.00  0.00           C
ATOM   2367  O   MET A 155     -17.598   1.814 -10.909  1.00  0.00           O
ATOM   2381  N   ASN A 156     -18.754   2.421  -9.070  1.00  0.00           N
ATOM   2382  CA  ASN A 156     -18.521   1.172  -8.362  1.00  0.00           C
```


Dieses Werk ist copyrightgeschützt und darf in keiner Form vervielfältigt werden noch an Dritte weitergegeben werden.
Es gilt nur für den persönlichen Gebrauch.

```
ATOM   2383  C   ASN A 156     -19.795   0.338  -8.427  1.00  0.00           C
ATOM   2384  O   ASN A 156     -20.830   0.712  -7.868  1.00  0.00           O
ATOM   2395  N   PHE A 157     -19.707  -0.784  -9.115  1.00  0.00           N
ATOM   2396  CA  PHE A 157     -20.857  -1.669  -9.266  1.00  0.00           C
ATOM   2397  C   PHE A 157     -20.680  -2.945  -8.461  1.00  0.00           C
ATOM   2398  O   PHE A 157     -20.048  -3.892  -8.914  1.00  0.00           O
ATOM   2415  N   GLU A 158     -21.234  -2.958  -7.262  1.00  0.00           N
ATOM   2416  CA  GLU A 158     -21.142  -4.142  -6.408  1.00  0.00           C
ATOM   2417  C   GLU A 158     -22.094  -5.200  -6.963  1.00  0.00           C
ATOM   2418  O   GLU A 158     -23.299  -5.136  -6.753  1.00  0.00           O
ATOM   2430  N   THR A 159     -21.554  -6.143  -7.732  1.00  0.00           N
ATOM   2431  CA  THR A 159     -22.391  -7.164  -8.378  1.00  0.00           C
ATOM   2432  C   THR A 159     -23.040  -8.143  -7.392  1.00  0.00           C
ATOM   2433  O   THR A 159     -24.148  -8.617  -7.644  1.00  0.00           O
ATOM   2444  N   ALA A 160     -22.372  -8.464  -6.285  1.00  0.00           N
ATOM   2445  CA  ALA A 160     -22.960  -9.409  -5.334  1.00  0.00           C
ATOM   2446  C   ALA A 160     -24.291  -8.869  -4.830  1.00  0.00           C
ATOM   2447  O   ALA A 160     -25.270  -9.603  -4.708  1.00  0.00           O
ATOM   2454  N   LYS A 161     -24.323  -7.567  -4.576  1.00  0.00           N
ATOM   2455  CA  LYS A 161     -25.545  -6.912  -4.126  1.00  0.00           C
ATOM   2456  C   LYS A 161     -26.203  -6.244  -5.329  1.00  0.00           C
ATOM   2457  O   LYS A 161     -27.352  -5.813  -5.273  1.00  0.00           O
ATOM   2476  N   SER A 162     -25.431  -6.144  -6.403  1.00  0.00           N
ATOM   2477  CA  SER A 162     -25.890  -5.497  -7.629  1.00  0.00           C
ATOM   2478  C   SER A 162     -26.352  -4.084  -7.302  1.00  0.00           C
ATOM   2479  O   SER A 162     -27.461  -3.681  -7.650  1.00  0.00           O
ATOM   2487  N   ARG A 163     -25.483  -3.343  -6.612  1.00  0.00           N
ATOM   2488  CA  ARG A 163     -25.789  -1.975  -6.216  1.00  0.00           C
ATOM   2489  C   ARG A 163     -24.685  -1.009  -6.628  1.00  0.00           C
ATOM   2490  O   ARG A 163     -23.497  -1.287  -6.447  1.00  0.00           O
ATOM   2511  N   VAL A 164     -25.096   0.161  -7.103  1.00  0.00           N
ATOM   2512  CA  VAL A 164     -24.166   1.203  -7.445  1.00  0.00           C
ATOM   2513  C   VAL A 164     -24.270   2.226  -6.335  1.00  0.00           C
ATOM   2514  O   VAL A 164     -25.227   3.001  -6.275  1.00  0.00           O
ATOM   2527  N   THR A 165     -23.311   2.193  -5.447  1.00  0.00           N
ATOM   2528  CA  THR A 165     -23.309   3.102  -4.297  1.00  0.00           C
ATOM   2529  C   THR A 165     -22.067   3.967  -4.298  1.00  0.00           C
ATOM   2530  O   THR A 165     -22.120   5.198  -4.286  1.00  0.00           O
ATOM   2541  N   GLN A 166     -20.955   3.281  -4.297  1.00  0.00           N
ATOM   2542  CA  GLN A 166     -19.664   3.944  -4.286  1.00  0.00           C
ATOM   2543  C   GLN A 166     -19.401   4.641  -5.620  1.00  0.00           C
ATOM   2544  O   GLN A 166     -19.147   3.996  -6.639  1.00  0.00           O
ATOM   2558  N   SER A 167     -19.446   5.969  -5.594  1.00  0.00           N
ATOM   2559  CA  SER A 167     -19.190   6.762  -6.791  1.00  0.00           C
ATOM   2560  C   SER A 167     -18.358   7.989  -6.426  1.00  0.00           C
ATOM   2561  O   SER A 167     -18.558   8.585  -5.364  1.00  0.00           O
ATOM   2569  N   ASN A 168     -17.400   8.340  -7.288  1.00  0.00           N
ATOM   2570  CA  ASN A 168     -16.529   9.475  -7.019  1.00  0.00           C
ATOM   2571  C   ASN A 168     -16.478  10.455  -8.198  1.00  0.00           C
ATOM   2572  O   ASN A 168     -16.063  10.094  -9.300  1.00  0.00           O
ATOM   2583  N   PHE A 169     -16.869  11.706  -7.944  1.00  0.00           N
ATOM   2584  CA  PHE A 169     -16.834  12.749  -8.978  1.00  0.00           C
ATOM   2585  C   PHE A 169     -15.509  13.497  -8.891  1.00  0.00           C
ATOM   2586  O   PHE A 169     -15.266  14.195  -7.911  1.00  0.00           O
ATOM   2603  N   ALA A 170     -14.671  13.390  -9.909  1.00  0.00           N
ATOM   2604  CA  ALA A 170     -13.405  14.110  -9.895  1.00  0.00           C
ATOM   2605  C   ALA A 170     -13.570  15.450 -10.582  1.00  0.00           C
ATOM   2606  O   ALA A 170     -14.085  15.501 -11.675  1.00  0.00           O
ATOM   2613  N   VAL A 171     -13.104  16.522  -9.958  1.00  0.00           N
ATOM   2614  CA  VAL A 171     -13.182  17.844 -10.575  1.00  0.00           C
ATOM   2615  C   VAL A 171     -11.817  18.518 -10.462  1.00  0.00           C
ATOM   2616  O   VAL A 171     -11.252  18.607  -9.370  1.00  0.00           O
ATOM   2629  N   GLY A 172     -11.286  18.962 -11.599  1.00  0.00           N
ATOM   2630  CA  GLY A 172      -9.995  19.595 -11.597  1.00  0.00           C
ATOM   2631  C   GLY A 172      -9.946  20.835 -12.465  1.00  0.00           C
ATOM   2632  O   GLY A 172     -10.577  20.915 -13.520  1.00  0.00           O
ATOM   2636  N   TYR A 173      -9.147  21.780 -12.002  1.00  0.00           N
ATOM   2637  CA  TYR A 173      -8.937  23.034 -12.703  1.00  0.00           C
ATOM   2638  C   TYR A 173      -7.445  23.256 -12.853  1.00  0.00           C
ATOM   2639  O   TYR A 173      -6.695  23.128 -11.886  1.00  0.00           O
ATOM   2657  N   LYS A 174      -7.001  23.528 -14.063  1.00  0.00           N
ATOM   2658  CA  LYS A 174      -5.575  23.696 -14.321  1.00  0.00           C
ATOM   2659  C   LYS A 174      -5.077  25.142 -14.207  1.00  0.00           C
ATOM   2660  O   LYS A 174      -5.749  26.103 -14.571  1.00  0.00           O
ATOM   2679  N   THR A 175      -3.846  25.234 -13.746  1.00  0.00           N
ATOM   2680  CA  THR A 175      -3.129  26.494 -13.600  1.00  0.00           C
ATOM   2681  C   THR A 175      -1.683  26.253 -14.049  1.00  0.00           C
ATOM   2682  O   THR A 175      -1.205  25.121 -13.979  1.00  0.00           O
ATOM   2693  N   ASP A 176      -1.003  27.283 -14.549  1.00  0.00           N
ATOM   2694  CA  ASP A 176       0.368  27.105 -15.045  1.00  0.00           C
ATOM   2695  C   ASP A 176       1.166  26.140 -14.172  1.00  0.00           C
ATOM   2696  O   ASP A 176       1.327  26.372 -12.974  1.00  0.00           O
ATOM   2705  N   GLU A 177       1.653  25.050 -14.788  1.00  0.00           N
ATOM   2706  CA  GLU A 177       2.442  24.032 -14.075  1.00  0.00           C
ATOM   2707  C   GLU A 177       1.672  23.394 -12.916  1.00  0.00           C
ATOM   2708  O   GLU A 177       2.084  22.353 -12.385  1.00  0.00           O
ATOM   2720  N   PHE A 178       0.624  24.070 -12.458  1.00  0.00           N
ATOM   2721  CA  PHE A 178      -0.128  23.606 -11.299  1.00  0.00           C
ATOM   2722  C   PHE A 178      -1.471  22.963 -11.691  1.00  0.00           C
ATOM   2723  O   PHE A 178      -2.206  23.515 -12.501  1.00  0.00           O
ATOM   2740  N   GLN A 179      -1.812  21.818 -11.062  1.00  0.00           N
ATOM   2741  CA  GLN A 179      -3.104  21.147 -11.306  1.00  0.00           C
ATOM   2742  C   GLN A 179      -3.947  21.119 -10.031  1.00  0.00           C
ATOM   2743  O   GLN A 179      -3.421  20.817  -8.954  1.00  0.00           O
```


Dieses Werk ist copyrightgeschützt und darf in keiner Form vervielfältigt werden noch an Dritte weitergegeben werden.
Es gilt nur für den persönlichen Gebrauch.

```
ATOM   2757  N   LEU A 180      -5.260  21.335 -10.175  1.00  0.00           N
ATOM   2758  CA  LEU A 180      -6.175  21.258  -9.032  1.00  0.00           C
ATOM   2759  C   LEU A 180      -7.005  19.991  -9.167  1.00  0.00           C
ATOM   2760  O   LEU A 180      -7.822  19.893 -10.060  1.00  0.00           O
ATOM   2776  N   HIS A 181      -6.754  19.022  -8.294  1.00  0.00           N
ATOM   2777  CA  HIS A 181      -7.475  17.748  -8.327  1.00  0.00           C
ATOM   2778  C   HIS A 181      -8.258  17.496  -7.027  1.00  0.00           C
ATOM   2779  O   HIS A 181      -7.664  17.357  -5.955  1.00  0.00           O
ATOM   2793  N   THR A 182      -9.583  17.396  -7.136  1.00  0.00           N
ATOM   2794  CA  THR A 182     -10.447  17.111  -5.974  1.00  0.00           C
ATOM   2795  C   THR A 182     -11.452  16.034  -6.349  1.00  0.00           C
ATOM   2796  O   THR A 182     -11.788  15.924  -7.534  1.00  0.00           O
ATOM   2807  N   ASN A 183     -11.976  15.239  -5.384  1.00  0.00           N
ATOM   2808  CA  ASN A 183     -12.956  14.238  -5.737  1.00  0.00           C
ATOM   2809  C   ASN A 183     -14.044  14.194  -4.675  1.00  0.00           C
ATOM   2810  O   ASN A 183     -13.754  14.206  -3.480  1.00  0.00           O
ATOM   2821  N   VAL A 184     -15.290  14.112  -5.111  1.00  0.00           N
ATOM   2822  CA  VAL A 184     -16.392  14.037  -4.169  1.00  0.00           C
ATOM   2823  C   VAL A 184     -16.645  12.582  -3.918  1.00  0.00           C
ATOM   2824  O   VAL A 184     -16.972  11.847  -4.845  1.00  0.00           O
ATOM   2837  N   ASN A 185     -16.479  12.152  -2.679  1.00  0.00           N
ATOM   2838  CA  ASN A 185     -16.674  10.770  -2.360  1.00  0.00           C
ATOM   2839  C   ASN A 185     -18.056  10.558  -1.800  1.00  0.00           C
ATOM   2840  O   ASN A 185     -18.358  11.042  -0.709  1.00  0.00           O
ATOM   2851  N   ASP A 186     -18.864   9.860  -2.589  1.00  0.00           N
ATOM   2852  CA  ASP A 186     -20.247   9.528  -2.228  1.00  0.00           C
ATOM   2853  C   ASP A 186     -21.070  10.751  -1.835  1.00  0.00           C
ATOM   2854  O   ASP A 186     -22.064  10.620  -1.117  1.00  0.00           O
ATOM   2863  N   GLY A 187     -20.679  11.931  -2.304  1.00  0.00           N
ATOM   2864  CA  GLY A 187     -21.432  13.134  -1.969  1.00  0.00           C
ATOM   2865  C   GLY A 187     -21.267  13.467  -0.493  1.00  0.00           C
ATOM   2866  O   GLY A 187     -22.082  14.191   0.078  1.00  0.00           O
ATOM   2870  N   THR A 188     -20.243  12.881   0.130  1.00  0.00           N
ATOM   2871  CA  THR A 188     -20.019  13.071   1.558  1.00  0.00           C
ATOM   2872  C   THR A 188     -18.633  13.652   1.888  1.00  0.00           C
ATOM   2873  O   THR A 188     -18.538  14.775   2.383  1.00  0.00           O
ATOM   2884  N   GLU A 189     -17.562  12.894   1.657  1.00  0.00           N
ATOM   2885  CA  GLU A 189     -16.213  13.404   1.994  1.00  0.00           C
ATOM   2886  C   GLU A 189     -15.380  13.741   0.757  1.00  0.00           C
ATOM   2887  O   GLU A 189     -15.173  12.888  -0.104  1.00  0.00           O
ATOM   2899  N   PHE A 190     -14.880  14.985   0.674  1.00  0.00           N
ATOM   2900  CA  PHE A 190     -14.059  15.407  -0.455  1.00  0.00           C
ATOM   2901  C   PHE A 190     -12.584  15.143  -0.167  1.00  0.00           C
ATOM   2902  O   PHE A 190     -12.148  15.187   0.986  1.00  0.00           O
ATOM   2919  N   GLY A 191     -11.815  14.896  -1.221  1.00  0.00           N
ATOM   2920  CA  GLY A 191     -10.384  14.651  -1.064  1.00  0.00           C
ATOM   2921  C   GLY A 191      -9.672  14.565  -2.403  1.00  0.00           C
ATOM   2922  O   GLY A 191     -10.234  14.067  -3.382  1.00  0.00           O
ATOM   2926  N   GLY A 192      -8.445  15.094  -2.469  1.00  0.00           N
ATOM   2927  CA  GLY A 192      -7.689  15.072  -3.717  1.00  0.00           C
ATOM   2928  C   GLY A 192      -6.308  15.682  -3.516  1.00  0.00           C
ATOM   2929  O   GLY A 192      -5.829  15.794  -2.384  1.00  0.00           O
ATOM   2933  N   SER A 193      -5.669  16.072  -4.618  1.00  0.00           N
ATOM   2934  CA  SER A 193      -4.329  16.647  -4.541  1.00  0.00           C
ATOM   2935  C   SER A 193      -4.161  17.859  -5.443  1.00  0.00           C
ATOM   2936  O   SER A 193      -5.013  18.168  -6.277  1.00  0.00           O
ATOM   2944  N   ILE A 194      -3.010  18.499  -5.314  1.00  0.00           N
ATOM   2945  CA  ILE A 194      -2.667  19.632  -6.145  1.00  0.00           C
ATOM   2946  C   ILE A 194      -1.263  19.384  -6.674  1.00  0.00           C
ATOM   2947  O   ILE A 194      -0.313  19.382  -5.899  1.00  0.00           O
ATOM   2963  N   TYR A 195      -1.129  19.165  -7.971  1.00  0.00           N
ATOM   2964  CA  TYR A 195       0.198  18.903  -8.544  1.00  0.00           C
ATOM   2965  C   TYR A 195       0.872  20.222  -8.844  1.00  0.00           C
ATOM   2966  O   TYR A 195       0.342  21.005  -9.621  1.00  0.00           O
ATOM   2984  N   GLN A 196       2.017  20.482  -8.211  1.00  0.00           N
ATOM   2985  CA  GLN A 196       2.702  21.745  -8.429  1.00  0.00           C
ATOM   2986  C   GLN A 196       4.137  21.564  -8.912  1.00  0.00           C
ATOM   2987  O   GLN A 196       5.038  21.347  -8.100  1.00  0.00           O
ATOM   3001  N   LYS A 197       4.376  21.757 -10.212  1.00  0.00           N
ATOM   3002  CA  LYS A 197       5.749  21.704 -10.699  1.00  0.00           C
ATOM   3003  C   LYS A 197       6.293  23.109 -10.493  1.00  0.00           C
ATOM   3004  O   LYS A 197       5.990  24.026 -11.258  1.00  0.00           O
ATOM   3023  N   VAL A 198       7.027  23.285  -9.401  1.00  0.00           N
ATOM   3024  CA  VAL A 198       7.543  24.590  -9.022  1.00  0.00           C
ATOM   3025  C   VAL A 198       8.727  25.010  -9.871  1.00  0.00           C
ATOM   3026  O   VAL A 198       8.834  26.166 -10.280  1.00  0.00           O
ATOM   3039  N   ASN A 199       9.605  24.069 -10.137  1.00  0.00           N
ATOM   3040  CA  ASN A 199      10.780  24.342 -10.954  1.00  0.00           C
ATOM   3041  C   ASN A 199      11.446  23.022 -11.316  1.00  0.00           C
ATOM   3042  O   ASN A 199      10.865  21.961 -11.108  1.00  0.00           O
ATOM   3053  N   LYS A 200      12.641  23.084 -11.876  1.00  0.00           N
ATOM   3054  CA  LYS A 200      13.337  21.864 -12.278  1.00  0.00           C
ATOM   3055  C   LYS A 200      13.635  20.957 -11.081  1.00  0.00           C
ATOM   3056  O   LYS A 200      13.506  19.739 -11.178  1.00  0.00           O
ATOM   3075  N   LYS A 201      14.069  21.543  -9.968  1.00  0.00           N
ATOM   3076  CA  LYS A 201      14.418  20.744  -8.791  1.00  0.00           C
ATOM   3077  C   LYS A 201      13.303  20.658  -7.738  1.00  0.00           C
ATOM   3078  O   LYS A 201      13.479  19.964  -6.737  1.00  0.00           O
ATOM   3097  N   LEU A 202      12.194  21.397  -7.805  1.00  0.00           N
ATOM   3098  CA  LEU A 202      11.032  21.429  -6.854  1.00  0.00           C
ATOM   3099  C   LEU A 202       9.756  20.801  -7.456  1.00  0.00           C
ATOM   3100  O   LEU A 202       9.147  21.460  -8.335  1.00  0.00           O
ATOM   3116  N   GLU A 203       9.380  19.609  -6.992  1.00  0.00           N
ATOM   3117  CA  GLU A 203       8.077  18.975  -7.322  1.00  0.00           C
```


Dieses Werk ist copyrightgeschützt und darf in keiner Form vervielfältigt werden noch an Dritte weitergegeben werden.
Es gilt nur für den persönlichen Gebrauch.

```
ATOM   3118  C   GLU A 203       7.319  18.795  -6.019  1.00  0.00           C
ATOM   3119  O   GLU A 203       7.774  17.877  -5.301  1.00  0.00           O
ATOM   3131  N   THR A 204       6.301  19.643  -5.686  1.00  0.00           N
ATOM   3132  CA  THR A 204       5.548  19.562  -4.443  1.00  0.00           C
ATOM   3133  C   THR A 204       4.092  19.199  -4.719  1.00  0.00           C
ATOM   3134  O   THR A 204       3.613  19.364  -5.842  1.00  0.00           O
ATOM   3145  N   ALA A 205       3.377  18.708  -3.701  1.00  0.00           N
ATOM   3146  CA  ALA A 205       1.983  18.346  -3.876  1.00  0.00           C
ATOM   3147  C   ALA A 205       1.184  18.695  -2.627  1.00  0.00           C
ATOM   3148  O   ALA A 205       1.529  18.277  -1.520  1.00  0.00           O
ATOM   3155  N   VAL A 206       0.100  19.446  -2.815  1.00  0.00           N
ATOM   3156  CA  VAL A 206      -0.759  19.831  -1.687  1.00  0.00           C
ATOM   3157  C   VAL A 206      -2.005  18.939  -1.667  1.00  0.00           C
ATOM   3158  O   VAL A 206      -2.719  18.832  -2.664  1.00  0.00           O
ATOM   3171  N   ASN A 207      -2.268  18.299  -0.532  1.00  0.00           N
ATOM   3172  CA  ASN A 207      -3.435  17.434  -0.428  1.00  0.00           C
ATOM   3173  C   ASN A 207      -4.575  18.175   0.240  1.00  0.00           C
ATOM   3174  O   ASN A 207      -4.382  18.730   1.309  1.00  0.00           O
ATOM   3185  N   LEU A 208      -5.754  18.179  -0.401  1.00  0.00           N
ATOM   3186  CA  LEU A 208      -6.923  18.875   0.166  1.00  0.00           C
ATOM   3187  C   LEU A 208      -8.004  17.881   0.574  1.00  0.00           C
ATOM   3188  O   LEU A 208      -8.645  17.285  -0.289  1.00  0.00           O
ATOM   3204  N   ALA A 209      -8.160  17.620   1.869  1.00  0.00           N
ATOM   3205  CA  ALA A 209      -9.215  16.783   2.467  1.00  0.00           C
ATOM   3206  C   ALA A 209     -10.227  17.690   3.147  1.00  0.00           C
ATOM   3207  O   ALA A 209      -9.711  18.531   3.912  1.00  0.00           O
ATOM   3214  N   TRP A 210     -11.539  17.546   2.906  1.00  0.00           N
ATOM   3215  CA  TRP A 210     -12.539  18.206   3.720  1.00  0.00           C
ATOM   3216  C   TRP A 210     -13.776  17.328   3.832  1.00  0.00           C
ATOM   3217  O   TRP A 210     -13.881  16.293   3.177  1.00  0.00           O
ATOM   3238  N   THR A 211     -14.693  17.716   4.686  1.00  0.00           N
ATOM   3239  CA  THR A 211     -15.890  16.906   4.904  1.00  0.00           C
ATOM   3240  C   THR A 211     -17.154  17.730   4.796  1.00  0.00           C
ATOM   3241  O   THR A 211     -17.374  18.632   5.602  1.00  0.00           O
ATOM   3252  N   ALA A 212     -17.990  17.428   3.793  1.00  0.00           N
ATOM   3253  CA  ALA A 212     -19.223  18.192   3.629  1.00  0.00           C
ATOM   3254  C   ALA A 212     -19.878  18.446   4.971  1.00  0.00           C
ATOM   3255  O   ALA A 212     -20.550  17.579   5.535  1.00  0.00           O
ATOM   3262  N   GLY A 213     -19.660  19.655   5.457  1.00  0.00           N
ATOM   3263  CA  GLY A 213     -20.190  20.102   6.724  1.00  0.00           C
ATOM   3264  C   GLY A 213     -19.617  21.482   7.035  1.00  0.00           C
ATOM   3265  O   GLY A 213     -19.153  22.185   6.137  1.00  0.00           O
ATOM   3269  N   ASN A 214     -19.625  21.867   8.295  1.00  0.00           N
ATOM   3270  CA  ASN A 214     -19.081  23.162   8.665  1.00  0.00           C
ATOM   3271  C   ASN A 214     -17.667  22.973   9.206  1.00  0.00           C
ATOM   3272  O   ASN A 214     -17.083  23.889   9.776  1.00  0.00           O
ATOM   3283  N   SER A 215     -16.966  21.852   8.992  1.00  0.00           N
ATOM   3284  CA  SER A 215     -15.632  21.562   9.564  1.00  0.00           C
ATOM   3285  C   SER A 215     -14.536  22.132   8.643  1.00  0.00           C
ATOM   3286  O   SER A 215     -14.805  22.476   7.490  1.00  0.00           O
ATOM   3294  N   ASN A 216     -13.302  22.216   9.147  1.00  0.00           N
ATOM   3295  CA  ASN A 216     -12.212  22.805   8.353  1.00  0.00           C
ATOM   3296  C   ASN A 216     -11.758  21.909   7.201  1.00  0.00           C
ATOM   3297  O   ASN A 216     -12.174  20.734   7.187  1.00  0.00           O
ATOM   3308  N   THR A 217     -10.947  22.493   6.313  1.00  0.00           N
ATOM   3309  CA  THR A 217     -10.249  21.852   5.190  1.00  0.00           C
ATOM   3310  C   THR A 217      -8.874  21.906   5.561  1.00  0.00           C
ATOM   3311  O   THR A 217      -8.330  22.939   5.837  1.00  0.00           O
ATOM   3322  N   ARG A 218      -8.703  21.292   5.320  1.00  0.00           N
ATOM   3323  CA  ARG A 218      -7.551  20.824   5.995  1.00  0.00           C
ATOM   3324  C   ARG A 218      -6.626  20.324   4.929  1.00  0.00           C
ATOM   3325  O   ARG A 218      -7.160  19.810   3.932  1.00  0.00           O
ATOM   3346  N   PHE A 219      -5.310  20.462   5.073  1.00  0.00           N
ATOM   3347  CA  PHE A 219      -4.434  20.241   3.944  1.00  0.00           C
ATOM   3348  C   PHE A 219      -2.962  20.124   4.190  1.00  0.00           C
ATOM   3349  O   PHE A 219      -2.624  21.000   4.984  1.00  0.00           O
ATOM   3366  N   GLY A 220      -2.245  19.210   3.484  1.00  0.00           N
ATOM   3367  CA  GLY A 220      -0.808  19.110   3.667  1.00  0.00           C
ATOM   3368  C   GLY A 220      -0.056  19.725   2.518  1.00  0.00           C
ATOM   3369  O   GLY A 220      -0.594  19.819   1.420  1.00  0.00           O
ATOM   3373  N   ILE A 221       1.201  20.118   2.769  1.00  0.00           N
ATOM   3374  CA  ILE A 221       2.026  20.686   1.709  1.00  0.00           C
ATOM   3375  C   ILE A 221       3.298  19.888   1.670  1.00  0.00           C
ATOM   3376  O   ILE A 221       4.139  20.059   2.546  1.00  0.00           O
ATOM   3392  N   ALA A 222       3.436  19.013   0.680  1.00  0.00           N
ATOM   3393  CA  ALA A 222       4.627  18.192   0.597  1.00  0.00           C
ATOM   3394  C   ALA A 222       5.554  18.681  -0.495  1.00  0.00           C
ATOM   3395  O   ALA A 222       5.179  18.721  -1.661  1.00  0.00           O
ATOM   3402  N   ALA A 223       6.763  19.047  -0.091  1.00  0.00           N
ATOM   3403  CA  ALA A 223       7.755  19.542  -1.030  1.00  0.00           C
ATOM   3404  C   ALA A 223       8.952  18.608  -1.116  1.00  0.00           C
ATOM   3405  O   ALA A 223       9.615  18.347  -0.113  1.00  0.00           O
ATOM   3412  N   LYS A 224       9.237  17.885  -2.241  1.00  0.00           N
ATOM   3413  CA  LYS A 224      10.476  17.126  -2.508  1.00  0.00           C
ATOM   3414  C   LYS A 224      11.381  18.162  -3.162  1.00  0.00           C
ATOM   3415  O   LYS A 224      10.995  18.451  -4.341  1.00  0.00           O
ATOM   3434  N   TYR A 225      12.433  18.609  -2.460  1.00  0.00           N
ATOM   3435  CA  TYR A 225      13.468  19.481  -2.997  1.00  0.00           C
ATOM   3436  C   TYR A 225      14.764  18.755  -3.274  1.00  0.00           C
ATOM   3437  O   TYR A 225      15.591  18.552  -2.385  1.00  0.00           O
ATOM   3455  N   GLN A 226      14.996  18.424  -4.534  1.00  0.00           N
ATOM   3456  CA  GLN A 226      16.175  17.704  -4.978  1.00  0.00           C
ATOM   3457  C   GLN A 226      17.290  18.718  -4.932  1.00  0.00           C
ATOM   3458  O   GLN A 226      17.333  19.594  -5.622  1.00  0.00           O
```


Dieses Werk ist copyrightgeschützt und darf in keiner Form vervielfältigt werden noch an Dritte weitergegeben werden.
Es gilt nur für den persönlichen Gebrauch.

```
ATOM   3472  N   ILE A 227      18.238  18.567  -4.034  1.00  0.00           N
ATOM   3473  CA  ILE A 227      19.236  19.514  -3.808  1.00  0.00           C
ATOM   3474  C   ILE A 227      20.307  19.534  -4.903  1.00  0.00           C
ATOM   3475  O   ILE A 227      20.528  20.532  -5.607  1.00  0.00           O
ATOM   3491  N   ASP A 228      20.912  18.354  -5.016  1.00  0.00           N
ATOM   3492  CA  ASP A 228      21.953  18.039  -5.993  1.00  0.00           C
ATOM   3493  C   ASP A 228      21.675  16.592  -6.336  1.00  0.00           C
ATOM   3494  O   ASP A 228      20.741  16.023  -5.777  1.00  0.00           O
ATOM   3503  N   PRO A 229      22.366  15.978  -7.229  1.00  0.00           N
ATOM   3504  CA  PRO A 229      22.032  14.583  -7.603  1.00  0.00           C
ATOM   3505  C   PRO A 229      22.214  13.598  -6.445  1.00  0.00           C
ATOM   3506  O   PRO A 229      21.736  12.467  -6.520  1.00  0.00           O
ATOM   3517  N   ASP A 230      22.943  14.012  -5.400  1.00  0.00           N
ATOM   3518  CA  ASP A 230      23.222  13.133  -4.272  1.00  0.00           C
ATOM   3519  C   ASP A 230      22.447  13.502  -2.996  1.00  0.00           C
ATOM   3520  O   ASP A 230      22.665  12.875  -1.963  1.00  0.00           O
ATOM   3529  N   ALA A 231      21.558  14.504  -3.035  1.00  0.00           N
ATOM   3530  CA  ALA A 231      20.817  14.867  -1.813  1.00  0.00           C
ATOM   3531  C   ALA A 231      19.461  15.517  -2.120  1.00  0.00           C
ATOM   3532  O   ALA A 231      19.319  16.238  -3.109  1.00  0.00           O
ATOM   3539  N   CYS A 232      18.447  15.236  -1.265  1.00  0.00           N
ATOM   3540  CA  CYS A 232      17.018  15.602  -1.466  1.00  0.00           C
ATOM   3541  C   CYS A 232      16.344  15.976  -0.121  1.00  0.00           C
ATOM   3542  O   CYS A 232      16.525  15.076   0.717  1.00  0.00           O
ATOM   3550  N   PHE A 233      15.618  17.110   0.038  1.00  0.00           N
ATOM   3551  CA  PHE A 233      14.903  17.441   1.286  1.00  0.00           C
ATOM   3552  C   PHE A 233      13.384  17.326   1.122  1.00  0.00           C
ATOM   3553  O   PHE A 233      12.782  18.039   0.320  1.00  0.00           O
ATOM   3570  N   SER A 234      12.772  16.379   1.841  1.00  0.00           N
ATOM   3571  CA  SER A 234      11.317  16.142   1.862  1.00  0.00           C
ATOM   3572  C   SER A 234      10.736  16.901   3.065  1.00  0.00           C
ATOM   3573  O   SER A 234      11.392  16.769   4.107  1.00  0.00           O
ATOM   3581  N   ALA A 235       9.643  17.651   2.934  1.00  0.00           N
ATOM   3582  CA  ALA A 235       8.936  18.249   4.071  1.00  0.00           C
ATOM   3583  C   ALA A 235       7.445  18.215   3.813  1.00  0.00           C
ATOM   3584  O   ALA A 235       7.035  18.328   2.668  1.00  0.00           O
ATOM   3591  N   LYS A 236       6.961  18.140   5.172  1.00  0.00           N
ATOM   3592  CA  LYS A 236       5.659  18.392   5.652  1.00  0.00           C
ATOM   3593  C   LYS A 236       5.048  19.617   5.870  1.00  0.00           C
ATOM   3594  O   LYS A 236       5.937  20.492   6.092  1.00  0.00           O
ATOM   3613  N   VAL A 237       3.711  19.742   5.640  1.00  0.00           N
ATOM   3614  CA  VAL A 237       2.990  20.415   6.745  1.00  0.00           C
ATOM   3615  C   VAL A 237       1.489  20.259   6.622  1.00  0.00           C
ATOM   3616  O   VAL A 237       0.905  20.730   5.657  1.00  0.00           O
ATOM   3629  N   ASN A 238       0.690  19.804   7.655  1.00  0.00           N
ATOM   3630  CA  ASN A 238      -0.786  19.868   7.627  1.00  0.00           C
ATOM   3631  C   ASN A 238      -1.270  21.223   8.200  1.00  0.00           C
ATOM   3632  O   ASN A 238      -0.675  21.888   9.006  1.00  0.00           O
ATOM   3643  N   ASN A 239      -2.468  21.641   7.785  1.00  0.00           N
ATOM   3644  CA  ASN A 239      -3.218  22.781   8.335  1.00  0.00           C
ATOM   3645  C   ASN A 239      -3.620  22.666   9.806  1.00  0.00           C
ATOM   3646  O   ASN A 239      -3.590  23.698  10.491  1.00  0.00           O
ATOM   3657  N   SER A 240      -3.916  21.445  10.293  1.00  0.00           N
ATOM   3658  CA  SER A 240      -4.038  21.139  11.737  1.00  0.00           C
ATOM   3659  C   SER A 240      -2.745  21.045  12.525  1.00  0.00           C
ATOM   3660  O   SER A 240      -2.901  20.586  13.701  1.00  0.00           O
ATOM   3668  N   SER A 241      -1.508  21.425  12.100  1.00  0.00           N
ATOM   3669  CA  SER A 241      -0.296  21.982  12.696  1.00  0.00           C
ATOM   3670  C   SER A 241       0.835  20.960  12.845  1.00  0.00           C
ATOM   3671  O   SER A 241       1.595  21.043  13.801  1.00  0.00           O
ATOM   3679  N   LEU A 242       1.001  19.950  11.966  1.00  0.00           N
ATOM   3680  CA  LEU A 242       2.066  18.892  12.036  1.00  0.00           C
ATOM   3681  C   LEU A 242       3.091  19.116  10.916  1.00  0.00           C
ATOM   3682  O   LEU A 242       2.845  18.633   9.826  1.00  0.00           O
ATOM   3698  N   ILE A 243       4.259  19.717  11.224  1.00  0.00           N
ATOM   3699  CA  ILE A 243       5.343  19.951  10.246  1.00  0.00           C
ATOM   3700  C   ILE A 243       6.270  18.754  10.210  1.00  0.00           C
ATOM   3701  O   ILE A 243       6.742  18.362  11.278  1.00  0.00           O
ATOM   3717  N   GLY A 244       7.192  18.282   9.452  1.00  0.00           N
ATOM   3718  CA  GLY A 244       7.763  17.049   9.504  1.00  0.00           C
ATOM   3719  C   GLY A 244       8.755  17.415   8.444  1.00  0.00           C
ATOM   3720  O   GLY A 244       8.521  17.833   7.358  1.00  0.00           O
ATOM   3724  N   LEU A 245       9.843  17.548   8.981  1.00  0.00           N
ATOM   3725  CA  LEU A 245      11.196  17.674   8.409  1.00  0.00           C
ATOM   3726  C   LEU A 245      11.731  16.273   8.154  1.00  0.00           C
ATOM   3727  O   LEU A 245      11.545  15.424   9.048  1.00  0.00           O
ATOM   3743  N   GLY A 246      12.376  16.006   7.041  1.00  0.00           N
ATOM   3744  CA  GLY A 246      13.129  14.760   6.940  1.00  0.00           C
ATOM   3745  C   GLY A 246      14.042  14.708   5.708  1.00  0.00           C
ATOM   3746  O   GLY A 246      13.490  14.826   4.600  1.00  0.00           O
ATOM   3750  N   TYR A 247      15.353  14.581   5.909  1.00  0.00           N
ATOM   3751  CA  TYR A 247      16.373  15.057   4.951  1.00  0.00           C
ATOM   3752  C   TYR A 247      17.103  13.829   4.408  1.00  0.00           C
ATOM   3753  O   TYR A 247      17.687  13.185   5.274  1.00  0.00           O
ATOM   3771  N   THR A 248      16.984  13.522   3.125  1.00  0.00           N
ATOM   3772  CA  THR A 248      17.515  12.290   2.508  1.00  0.00           C
ATOM   3773  C   THR A 248      18.890  12.609   1.923  1.00  0.00           C
ATOM   3774  O   THR A 248      18.933  13.714   1.347  1.00  0.00           O
ATOM   3785  N   GLN A 249      19.891  11.722   2.070  1.00  0.00           N
ATOM   3786  CA  GLN A 249      21.195  11.871   1.452  1.00  0.00           C
ATOM   3787  C   GLN A 249      21.595  10.606   0.690  1.00  0.00           C
ATOM   3788  O   GLN A 249      21.900   9.582   1.298  1.00  0.00           O
ATOM   3802  N   THR A 250      21.649  10.637  -0.641  1.00  0.00           N
ATOM   3803  CA  THR A 250      21.845   9.464  -1.524  1.00  0.00           C
```


Dieses Werk ist copyrightgeschützt und darf in keiner Form vervielfältigt werden noch an Dritte weitergegeben werden.
Es gilt nur für den persönlichen Gebrauch.

```
ATOM   3804  C   THR A 250      23.290   9.559  -2.041  1.00  0.00           C
ATOM   3805  O   THR A 250      23.530  10.120  -3.073  1.00  0.00           O
ATOM   3816  N   LEU A 251      24.260   8.948  -1.366  1.00  0.00           N
ATOM   3817  CA  LEU A 251      25.667   9.150  -1.745  1.00  0.00           C
ATOM   3818  C   LEU A 251      26.020   8.287  -2.981  1.00  0.00           C
ATOM   3819  O   LEU A 251      25.316   7.270  -3.090  1.00  0.00           O
ATOM   3835  N   LYS A 252      26.975   8.679  -3.876  1.00  0.00           N
ATOM   3836  CA  LYS A 252      27.457   7.928  -5.059  1.00  0.00           C
ATOM   3837  C   LYS A 252      27.893   6.543  -4.578  1.00  0.00           C
ATOM   3838  O   LYS A 252      27.417   5.523  -5.082  1.00  0.00           O
ATOM   3857  N   PRO A 253      28.775   6.484  -3.602  1.00  0.00           N
ATOM   3858  CA  PRO A 253      29.241   5.197  -3.022  1.00  0.00           C
ATOM   3859  C   PRO A 253      28.112   4.161  -2.895  1.00  0.00           C
ATOM   3860  O   PRO A 253      28.376   2.973  -2.731  1.00  0.00           O
ATOM   3871  N   GLY A 254      26.858   4.612  -2.989  1.00  0.00           N
ATOM   3872  CA  GLY A 254      25.719   3.697  -2.905  1.00  0.00           C
ATOM   3873  C   GLY A 254      25.147   3.603  -1.492  1.00  0.00           C
ATOM   3874  O   GLY A 254      24.672   2.542  -1.084  1.00  0.00           O
ATOM   3878  N   ILE A 255      25.191   4.708  -0.755  1.00  0.00           N
ATOM   3879  CA  ILE A 255      24.666   4.714   0.617  1.00  0.00           C
ATOM   3880  C   ILE A 255      23.586   5.784   0.816  1.00  0.00           C
ATOM   3881  O   ILE A 255      23.786   6.951   0.475  1.00  0.00           O
ATOM   3897  N   LYS A 256      22.363   5.388   1.258  1.00  0.00           N
ATOM   3898  CA  LYS A 256      21.252   6.331   1.556  1.00  0.00           C
ATOM   3899  C   LYS A 256      21.290   6.566   3.073  1.00  0.00           C
ATOM   3900  O   LYS A 256      21.392   5.534   3.737  1.00  0.00           O
ATOM   3919  N   LEU A 257      21.258   7.813   3.536  1.00  0.00           N
ATOM   3920  CA  LEU A 257      21.127   8.208   4.937  1.00  0.00           C
ATOM   3921  C   LEU A 257      19.991   9.219   5.092  1.00  0.00           C
ATOM   3922  O   LEU A 257      20.150  10.375   4.708  1.00  0.00           O
ATOM   3938  N   THR A 258      18.820   8.777   5.549  1.00  0.00           N
ATOM   3939  CA  THR A 258      17.678   9.665   5.839  1.00  0.00           C
ATOM   3940  C   THR A 258      17.703  10.046   7.319  1.00  0.00           C
ATOM   3941  O   THR A 258      18.196   9.234   8.082  1.00  0.00           O
ATOM   3952  N   LEU A 259      17.223  11.223   7.658  1.00  0.00           N
ATOM   3953  CA  LEU A 259      16.703  11.600   8.984  1.00  0.00           C
ATOM   3954  C   LEU A 259      15.213  11.844   8.783  1.00  0.00           C
ATOM   3955  O   LEU A 259      14.869  12.292   7.691  1.00  0.00           O
ATOM   3971  N   SER A 260      14.408  11.596   9.811  1.00  0.00           N
ATOM   3972  CA  SER A 260      13.017  12.076   9.892  1.00  0.00           C
ATOM   3973  C   SER A 260      12.684  12.530  11.324  1.00  0.00           C
ATOM   3974  O   SER A 260      13.405  12.211  12.266  1.00  0.00           O
ATOM   3982  N   ALA A 261      11.590  13.263  11.401  1.00  0.00           N
ATOM   3983  CA  ALA A 261      10.973  13.774  12.624  1.00  0.00           C
ATOM   3984  C   ALA A 261       9.584  14.330  12.293  1.00  0.00           C
ATOM   3985  O   ALA A 261       9.441  14.558  11.067  1.00  0.00           O
ATOM   3992  N   LEU A 262       8.591  14.425  13.143  1.00  0.00           N
ATOM   3993  CA  LEU A 262       7.152  14.653  12.845  1.00  0.00           C
ATOM   3994  C   LEU A 262       6.591  15.622  13.895  1.00  0.00           C
ATOM   3995  O   LEU A 262       5.908  15.079  14.792  1.00  0.00           O
ATOM   4011  N   LEU A 263       6.859  16.945  13.882  1.00  0.00           N
ATOM   4012  CA  LEU A 263       6.686  17.746  15.126  1.00  0.00           C
ATOM   4013  C   LEU A 263       5.276  18.390  15.131  1.00  0.00           C
ATOM   4014  O   LEU A 263       5.075  19.197  14.210  1.00  0.00           O
ATOM   4030  N   ASP A 264       4.397  18.085  16.123  1.00  0.00           N
ATOM   4031  CA  ASP A 264       3.024  18.590  16.153  1.00  0.00           C
ATOM   4032  C   ASP A 264       2.911  19.887  16.934  1.00  0.00           C
ATOM   4033  O   ASP A 264       2.945  19.900  18.147  1.00  0.00           O
ATOM   4042  N   GLY A 265       2.781  20.963  16.196  1.00  0.00           N
ATOM   4043  CA  GLY A 265       2.671  22.307  16.742  1.00  0.00           C
ATOM   4044  C   GLY A 265       1.571  22.464  17.781  1.00  0.00           C
ATOM   4045  O   GLY A 265       1.643  23.366  18.619  1.00  0.00           O
ATOM   4049  N   LYS A 266       0.608  21.546  17.767  1.00  0.00           N
ATOM   4050  CA  LYS A 266      -0.468  21.516  18.753  1.00  0.00           C
ATOM   4051  C   LYS A 266      -0.062  20.555  19.853  1.00  0.00           C
ATOM   4052  O   LYS A 266      -0.646  20.563  20.935  1.00  0.00           O
ATOM   4071  N   ASN A 267       1.001  19.771  19.593  1.00  0.00           N
ATOM   4072  CA  ASN A 267       1.490  18.877  20.569  1.00  0.00           C
ATOM   4073  C   ASN A 267       3.027  18.905  20.594  1.00  0.00           C
ATOM   4074  O   ASN A 267       3.619  17.924  20.985  1.00  0.00           O
ATOM   4085  N   VAL A 268       3.692  20.018  20.218  1.00  0.00           N
ATOM   4086  CA  VAL A 268       5.165  20.039  20.320  1.00  0.00           C
ATOM   4087  C   VAL A 268       5.513  19.947  21.742  1.00  0.00           C
ATOM   4088  O   VAL A 268       6.570  19.441  22.123  1.00  0.00           O
ATOM   4101  N   ASN A 269       4.566  20.412  22.510  1.00  0.00           N
ATOM   4102  CA  ASN A 269       4.657  20.356  23.957  1.00  0.00           C
ATOM   4103  C   ASN A 269       3.978  19.101  24.484  1.00  0.00           C
ATOM   4104  O   ASN A 269       4.092  18.804  25.659  1.00  0.00           O
ATOM   4115  N   ALA A 270       3.348  18.309  23.603  1.00  0.00           N
ATOM   4116  CA  ALA A 270       2.801  17.040  24.039  1.00  0.00           C
ATOM   4117  C   ALA A 270       3.723  15.944  23.484  1.00  0.00           C
ATOM   4118  O   ALA A 270       3.963  14.948  24.169  1.00  0.00           O
ATOM   4125  N   GLY A 271       4.293  16.134  22.258  1.00  0.00           N
ATOM   4126  CA  GLY A 271       5.204  15.176  21.726  1.00  0.00           C
ATOM   4127  C   GLY A 271       4.633  14.438  20.546  1.00  0.00           C
ATOM   4128  O   GLY A 271       4.268  15.010  19.520  1.00  0.00           O
ATOM   4132  N   GLY A 272       4.601  13.146  20.707  1.00  0.00           N
ATOM   4133  CA  GLY A 272       4.132  12.265  19.663  1.00  0.00           C
ATOM   4134  C   GLY A 272       4.790  12.671  18.351  1.00  0.00           C
ATOM   4135  O   GLY A 272       4.100  12.926  17.367  1.00  0.00           O
ATOM   4139  N   HIS A 273       6.122  12.623  18.406  1.00  0.00           N
ATOM   4140  CA  HIS A 273       7.147  12.713  17.364  1.00  0.00           C
ATOM   4141  C   HIS A 273       7.661  11.353  16.991  1.00  0.00           C
ATOM   4142  O   HIS A 273       7.522  10.426  17.812  1.00  0.00           O
```


Dieses Werk ist copyrightgeschützt und darf in keiner Form vervielfältigt werden noch an Dritte weitergegeben werden.
Es gilt nur für den persönlichen Gebrauch.

```
ATOM   4156  N   LYS A 274       8.198  11.212  15.819  1.00  0.00           N
ATOM   4157  CA  LYS A 274       8.685   9.958  15.253  1.00  0.00           C
ATOM   4158  C   LYS A 274      10.042  10.256  14.617  1.00  0.00           C
ATOM   4159  O   LYS A 274      10.208  10.439  13.419  1.00  0.00           O
ATOM   4178  N   LEU A 275      11.009  10.307  15.524  1.00  0.00           N
ATOM   4179  CA  LEU A 275      12.448  10.366  15.195  1.00  0.00           C
ATOM   4180  C   LEU A 275      12.822   9.083  14.447  1.00  0.00           C
ATOM   4181  O   LEU A 275      12.320   8.017  14.847  1.00  0.00           O
ATOM   4197  N   GLY A 276      13.628   9.178  13.407  1.00  0.00           N
ATOM   4198  CA  GLY A 276      13.847   8.054  12.486  1.00  0.00           C
ATOM   4199  C   GLY A 276      15.052   8.280  11.582  1.00  0.00           C
ATOM   4200  O   GLY A 276      15.489   9.421  11.434  1.00  0.00           O
ATOM   4204  N   LEU A 277      15.563   7.165  11.054  1.00  0.00           N
ATOM   4205  CA  LEU A 277      16.916   7.019  10.498  1.00  0.00           C
ATOM   4206  C   LEU A 277      16.889   5.895   9.435  1.00  0.00           C
ATOM   4207  O   LEU A 277      16.984   4.708   9.730  1.00  0.00           O
ATOM   4223  N   GLY A 278      16.736   6.245   8.163  1.00  0.00           N
ATOM   4224  CA  GLY A 278      16.513   5.313   7.047  1.00  0.00           C
ATOM   4225  C   GLY A 278      17.850   4.961   6.401  1.00  0.00           C
ATOM   4226  O   GLY A 278      18.311   5.942   5.761  1.00  0.00           O
ATOM   4230  N   LEU A 279      18.404   3.754   6.561  1.00  0.00           N
ATOM   4231  CA  LEU A 279      19.786   3.403   6.250  1.00  0.00           C
ATOM   4232  C   LEU A 279      19.802   2.302   5.216  1.00  0.00           C
ATOM   4233  O   LEU A 279      19.646   1.125   5.610  1.00  0.00           O
ATOM   4249  N   GLU A 280      19.961   2.675   3.903  1.00  0.00           N
ATOM   4250  CA  GLU A 280      19.841   1.723   2.791  1.00  0.00           C
ATOM   4251  C   GLU A 280      21.224   1.552   2.178  1.00  0.00           C
ATOM   4252  O   GLU A 280      21.644   2.649   1.713  1.00  0.00           O
ATOM   4264  N   PHE A 281      21.834   0.353   2.209  1.00  0.00           N
ATOM   4265  CA  PHE A 281      23.152   0.120   1.641  1.00  0.00           C
ATOM   4266  C   PHE A 281      23.054  -0.705   0.361  1.00  0.00           C
ATOM   4267  O   PHE A 281      22.318  -1.701   0.305  1.00  0.00           O
ATOM   4284  N   GLN A 282      23.792  -0.273  -0.664  1.00  0.00           N
ATOM   4285  CA  GLN A 282      23.792  -0.958  -1.950  1.00  0.00           C
ATOM   4286  C   GLN A 282      24.829  -2.079  -1.958  1.00  0.00           C
ATOM   4287  O   GLN A 282      26.031  -1.828  -1.872  1.00  0.00           O
ATOM   4301  N   ALA A 283      24.351  -3.317  -2.054  1.00  0.00           N
ATOM   4302  CA  ALA A 283      25.236  -4.479  -2.068  1.00  0.00           C
ATOM   4303  C   ALA A 283      26.272  -4.394  -0.951  1.00  0.00           C
ATOM   4304  O   ALA A 283      26.243  -3.479  -0.128  1.00  0.00           O
ATOM   4311  N   ARG A 284      27.187  -5.362  -0.928  1.00  0.00           N
ATOM   4312  CA  ARG A 284      28.230  -5.397   0.092  1.00  0.00           C
ATOM   4313  C   ARG A 284      29.386  -4.481  -0.296  1.00  0.00           C
ATOM   4314  O   ARG A 284      29.687  -4.313  -1.478  1.00  0.00           O
ATOM   4335  N   SER A 285      30.030  -3.891   0.710  1.00  0.00           N
ATOM   4336  CA  SER A 285      31.155  -2.989   0.468  1.00  0.00           C
ATOM   4337  C   SER A 285      32.466  -3.628   0.921  1.00  0.00           C
ATOM   4338  O   SER A 285      33.335  -2.895   1.361  1.00  0.00           O
END
```


Dieses Werk ist copyrightgeschützt und darf in keiner Form vervielfältigt werden noch an Dritte weitergegeben werden.
Es gilt nur für den persönlichen Gebrauch.

D.2 Model 2

```
HEADER 5jdp
ATOM      1  N   SER A   1      17.791  -1.898  -4.458  1.00  0.00           N
ATOM      2  CA  SER A   1      16.470  -2.608  -4.563  1.00  0.00           C
ATOM      3  C   SER A   1      16.126  -3.317  -3.256  1.00  0.00           C
ATOM      4  O   SER A   1      14.899  -3.689  -3.218  1.00  0.00           O
ATOM     14  N   ALA A   2      16.953  -3.488  -2.270  1.00  0.00           N
ATOM     15  CA  ALA A   2      16.543  -3.683  -0.880  1.00  0.00           C
ATOM     16  C   ALA A   2      15.605  -2.561  -0.458  1.00  0.00           C
ATOM     17  O   ALA A   2      14.473  -2.972  -0.103  1.00  0.00           O
ATOM     24  N   VAL A   3      16.030  -1.363  -0.592  1.00  0.00           N
ATOM     25  CA  VAL A   3      15.407  -0.057  -0.468  1.00  0.00           C
ATOM     26  C   VAL A   3      14.550  -0.074   0.838  1.00  0.00           C
ATOM     27  O   VAL A   3      13.383  -0.346   0.760  1.00  0.00           O
ATOM     40  N   PRO A   4      15.099   0.241   2.018  1.00  0.00           N
ATOM     41  CA  PRO A   4      14.364   0.444   3.339  1.00  0.00           C
ATOM     42  C   PRO A   4      13.618   1.786   3.677  1.00  0.00           C
ATOM     43  O   PRO A   4      14.423   2.795   3.699  1.00  0.00           O
ATOM     68  N   THR A   6      11.057   4.212   6.513  1.00  0.00           N
ATOM     69  CA  THR A   6      11.127   2.935   7.255  1.00  0.00           C
ATOM     70  C   THR A   6       9.849   2.930   8.114  1.00  0.00           C
ATOM     71  O   THR A   6       9.240   4.004   8.294  1.00  0.00           O
ATOM     82  N   TYR A   7       9.513   1.781   8.606  1.00  0.00           N
ATOM     83  CA  TYR A   7       8.274   1.668   9.380  1.00  0.00           C
ATOM     84  C   TYR A   7       8.355   2.358  10.761  1.00  0.00           C
ATOM     85  O   TYR A   7       7.313   2.883  11.190  1.00  0.00           O
ATOM    103  N   ALA A   8       9.461   2.332  11.463  1.00  0.00           N
ATOM    104  CA  ALA A   8       9.402   2.347  12.935  1.00  0.00           C
ATOM    105  C   ALA A   8       9.106   3.734  13.567  1.00  0.00           C
ATOM    106  O   ALA A   8       8.146   3.715  14.378  1.00  0.00           O
ATOM    113  N   ASP A   9       9.821   4.736  13.198  1.00  0.00           N
ATOM    114  CA  ASP A   9       9.618   6.112  13.718  1.00  0.00           C
ATOM    115  C   ASP A   9       8.675   6.925  12.802  1.00  0.00           C
ATOM    116  O   ASP A   9       9.035   7.992  12.264  1.00  0.00           O
ATOM    125  N   LEU A  10       7.428   6.409  12.653  1.00  0.00           N
ATOM    126  CA  LEU A  10       6.482   7.002  11.713  1.00  0.00           C
ATOM    127  C   LEU A  10       5.948   8.271  12.356  1.00  0.00           C
ATOM    128  O   LEU A  10       5.037   8.172  13.195  1.00  0.00           O
ATOM    144  N   GLY A  11       6.517   9.404  11.997  1.00  0.00           N
ATOM    145  CA  GLY A  11       6.073  10.713  12.464  1.00  0.00           C
ATOM    146  C   GLY A  11       6.774  11.072  13.782  1.00  0.00           C
ATOM    147  O   GLY A  11       6.043  11.476  14.699  1.00  0.00           O
ATOM    151  N   LYS A  12       8.103  10.968  13.842  1.00  0.00           N
ATOM    152  CA  LYS A  12       8.883  11.402  15.023  1.00  0.00           C
ATOM    153  C   LYS A  12       9.327  12.885  14.911  1.00  0.00           C
ATOM    154  O   LYS A  12      10.288  13.385  15.492  1.00  0.00           O
ATOM    173  N   SER A  13       8.546  13.791  14.250  1.00  0.00           N
ATOM    174  CA  SER A  13       8.292  15.139  14.830  1.00  0.00           C
ATOM    175  C   SER A  13       6.824  15.596  14.720  1.00  0.00           C
ATOM    176  O   SER A  13       6.566  16.808  14.933  1.00  0.00           O
ATOM    184  N   ALA A  14       5.821  14.741  14.635  1.00  0.00           N
ATOM    185  CA  ALA A  14       4.652  14.768  15.513  1.00  0.00           C
ATOM    186  C   ALA A  14       5.021  14.222  16.888  1.00  0.00           C
ATOM    187  O   ALA A  14       4.343  14.749  17.811  1.00  0.00           O
ATOM    194  N   ARG A  15       5.945  13.314  17.053  1.00  0.00           N
ATOM    195  CA  ARG A  15       6.135  12.496  18.250  1.00  0.00           C
ATOM    196  C   ARG A  15       7.641  12.366  18.497  1.00  0.00           C
ATOM    197  O   ARG A  15       8.121  11.193  18.568  1.00  0.00           O
ATOM    218  N   ASP A  16       8.554  13.315  18.444  1.00  0.00           N
ATOM    219  CA  ASP A  16       8.566  14.630  19.133  1.00  0.00           C
ATOM    220  C   ASP A  16       7.406  15.514  18.782  1.00  0.00           C
ATOM    221  O   ASP A  16       7.195  16.186  17.799  1.00  0.00           O
ATOM    230  N   VAL A  17       6.409  15.927  19.551  1.00  0.00           N
ATOM    231  CA  VAL A  17       6.634  16.331  20.927  1.00  0.00           C
ATOM    232  C   VAL A  17       6.495  15.117  21.861  1.00  0.00           C
ATOM    233  O   VAL A  17       7.548  14.935  22.464  1.00  0.00           O
ATOM    246  N   PHE A  18       5.415  14.421  21.946  1.00  0.00           N
ATOM    247  CA  PHE A  18       4.799  13.560  22.985  1.00  0.00           C
ATOM    248  C   PHE A  18       5.666  13.239  24.233  1.00  0.00           C
ATOM    249  O   PHE A  18       5.178  13.367  25.351  1.00  0.00           O
ATOM    266  N   THR A  19       6.944  12.941  23.997  1.00  0.00           N
ATOM    267  CA  THR A  19       8.003  13.043  25.015  1.00  0.00           C
ATOM    268  C   THR A  19       8.558  14.481  25.152  1.00  0.00           C
ATOM    269  O   THR A  19       7.642  15.331  25.299  1.00  0.00           O
ATOM    280  N   LYS A  20       9.788  14.860  25.180  1.00  0.00           N
ATOM    281  CA  LYS A  20      10.372  15.983  26.023  1.00  0.00           C
ATOM    282  C   LYS A  20       9.715  16.230  27.416  1.00  0.00           C
ATOM    283  O   LYS A  20       9.284  17.221  27.996  1.00  0.00           O
ATOM    302  N   GLY A  21      10.408  15.220  27.805  1.00  0.00           N
ATOM    303  CA  GLY A  21      11.228  15.266  29.039  1.00  0.00           C
ATOM    304  C   GLY A  21      10.820  14.100  30.039  1.00  0.00           C
ATOM    305  O   GLY A  21       9.786  13.915  29.567  1.00  0.00           O
ATOM    309  N   TYR A  22      11.954  14.182  30.622  1.00  0.00           N
ATOM    310  CA  TYR A  22      12.815  13.027  30.944  1.00  0.00           C
ATOM    311  C   TYR A  22      13.534  12.575  29.673  1.00  0.00           C
ATOM    312  O   TYR A  22      12.872  12.057  28.765  1.00  0.00           O
ATOM    330  N   GLY A  23      14.846  12.772  29.595  1.00  0.00           N
ATOM    331  CA  GLY A  23      15.630  12.296  28.454  1.00  0.00           C
ATOM    332  C   GLY A  23      15.433  13.203  27.243  1.00  0.00           C
ATOM    333  O   GLY A  23      14.557  12.825  26.429  1.00  0.00           O
ATOM    337  N   PHE A  24      16.234  14.279  27.226  1.00  0.00           N
```


Dieses Werk ist copyrightgeschützt und darf in keiner Form vervielfältigt werden noch an Dritte weitergegeben werden.
Es gilt nur für den persönlichen Gebrauch.

```
ATOM    338  CA  PHE A  24      16.407  14.790  25.841  1.00  0.00           C
ATOM    339  C   PHE A  24      17.202  13.765  24.981  1.00  0.00           C
ATOM    340  O   PHE A  24      17.943  12.891  25.403  1.00  0.00           O
ATOM    357  N   GLY A  25      16.746  14.138  23.806  1.00  0.00           N
ATOM    358  CA  GLY A  25      17.212  12.519  23.025  1.00  0.00           C
ATOM    359  C   GLY A  25      17.044  11.000  23.083  1.00  0.00           C
ATOM    360  O   GLY A  25      17.924  11.018  22.224  1.00  0.00           O
ATOM    364  N   LEU A  26      16.763   9.273  23.204  1.00  0.00           N
ATOM    365  CA  LEU A  26      17.860   8.427  22.757  1.00  0.00           C
ATOM    366  C   LEU A  26      17.591   8.024  21.319  1.00  0.00           C
ATOM    367  O   LEU A  26      16.449   7.781  20.933  1.00  0.00           O
ATOM    383  N   ILE A  27      18.561   7.547  21.007  1.00  0.00           N
ATOM    384  CA  ILE A  27      18.970   7.585  19.726  1.00  0.00           C
ATOM    385  C   ILE A  27      18.893   6.062  19.439  1.00  0.00           C
ATOM    386  O   ILE A  27      18.980   5.299  20.455  1.00  0.00           O
ATOM    402  N   LYS A  28      18.590   5.516  18.084  1.00  0.00           N
ATOM    403  CA  LYS A  28      18.557   4.074  17.867  1.00  0.00           C
ATOM    404  C   LYS A  28      20.005   4.089  18.345  1.00  0.00           C
ATOM    405  O   LYS A  28      20.990   4.283  17.619  1.00  0.00           O
ATOM    424  N   LEU A  29      20.865   3.186  18.841  1.00  0.00           N
ATOM    425  CA  LEU A  29      22.279   2.759  18.950  1.00  0.00           C
ATOM    426  C   LEU A  29      22.419   1.295  18.544  1.00  0.00           C
ATOM    427  O   LEU A  29      21.423   0.604  18.519  1.00  0.00           O
ATOM    443  N   ASP A  30      23.661   0.848  18.297  1.00  0.00           N
ATOM    444  CA  ASP A  30      23.944  -0.578  18.097  1.00  0.00           C
ATOM    445  C   ASP A  30      25.432  -0.914  18.286  1.00  0.00           C
ATOM    446  O   ASP A  30      26.226  -0.017  17.988  1.00  0.00           O
ATOM    455  N   LEU A  31      25.748  -2.124  18.725  1.00  0.00           N
ATOM    456  CA  LEU A  31      27.106  -2.612  19.046  1.00  0.00           C
ATOM    457  C   LEU A  31      27.312  -3.990  18.380  1.00  0.00           C
ATOM    458  O   LEU A  31      26.491  -4.848  18.731  1.00  0.00           O
ATOM    474  N   LYS A  32      28.315  -4.182  17.517  1.00  0.00           N
ATOM    475  CA  LYS A  32      28.615  -5.471  16.840  1.00  0.00           C
ATOM    476  C   LYS A  32      29.758  -6.200  17.563  1.00  0.00           C
ATOM    477  O   LYS A  32      30.699  -5.466  17.907  1.00  0.00           O
ATOM    496  N   THR A  33      29.660  -7.536  17.731  1.00  0.00           N
ATOM    497  CA  THR A  33      30.732  -8.419  18.194  1.00  0.00           C
ATOM    498  C   THR A  33      30.867  -9.594  17.221  1.00  0.00           C
ATOM    499  O   THR A  33      29.939 -10.398  17.059  1.00  0.00           O
ATOM    510  N   LYS A  34      32.009  -9.683  16.557  1.00  0.00           N
ATOM    511  CA  LYS A  34      32.209 -10.750  15.587  1.00  0.00           C
ATOM    512  C   LYS A  34      32.626 -12.053  16.246  1.00  0.00           C
ATOM    513  O   LYS A  34      33.691 -12.139  16.856  1.00  0.00           O
ATOM    532  N   SER A  35      31.802 -13.080  16.057  1.00  0.00           N
ATOM    533  CA  SER A  35      32.123 -14.395  16.579  1.00  0.00           C
ATOM    534  C   SER A  35      33.035 -15.093  15.577  1.00  0.00           C
ATOM    535  O   SER A  35      32.984 -14.806  14.382  1.00  0.00           O
ATOM    543  N   GLU A  36      33.872 -16.001  16.049  1.00  0.00           N
ATOM    544  CA  GLU A  36      34.767 -16.695  15.144  1.00  0.00           C
ATOM    545  C   GLU A  36      34.043 -17.862  14.479  1.00  0.00           C
ATOM    546  O   GLU A  36      34.308 -18.184  13.321  1.00  0.00           O
ATOM    558  N   ASN A  37      33.094 -18.466  15.199  1.00  0.00           N
ATOM    559  CA  ASN A  37      32.314 -19.561  14.632  1.00  0.00           C
ATOM    560  C   ASN A  37      31.483 -19.039  13.457  1.00  0.00           C
ATOM    561  O   ASN A  37      31.366 -19.692  12.417  1.00  0.00           O
ATOM    572  N   GLY A  38      30.910 -17.850  13.642  1.00  0.00           N
ATOM    573  CA  GLY A  38      30.096 -17.228  12.617  1.00  0.00           C
ATOM    574  C   GLY A  38      28.741 -16.827  13.179  1.00  0.00           C
ATOM    575  O   GLY A  38      27.821 -16.571  12.414  1.00  0.00           O
ATOM    579  N   LEU A  39      28.632 -16.794  14.514  1.00  0.00           N
ATOM    580  CA  LEU A  39      27.377 -16.447  15.187  1.00  0.00           C
ATOM    581  C   LEU A  39      26.957 -15.009  14.895  1.00  0.00           C
ATOM    582  O   LEU A  39      25.776 -14.728  14.703  1.00  0.00           O
ATOM    598  N   GLU A  40      28.044 -14.015  15.029  1.00  0.00           N
ATOM    599  CA  GLU A  40      27.785 -12.625  14.649  1.00  0.00           C
ATOM    600  C   GLU A  40      26.710 -12.006  15.558  1.00  0.00           C
ATOM    601  O   GLU A  40      25.688 -11.481  15.104  1.00  0.00           O
ATOM    613  N   PHE A  41      26.937 -12.054  16.879  1.00  0.00           N
ATOM    614  CA  PHE A  41      26.085 -11.343  17.840  1.00  0.00           C
ATOM    615  C   PHE A  41      26.219  -9.836  17.696  1.00  0.00           C
ATOM    616  O   PHE A  41      27.334  -9.340  17.864  1.00  0.00           O
ATOM    633  N   THR A  42      25.119  -9.168  17.440  1.00  0.00           N
ATOM    634  CA  THR A  42      24.988  -7.714  17.392  1.00  0.00           C
ATOM    635  C   THR A  42      23.785  -7.341  18.258  1.00  0.00           C
ATOM    636  O   THR A  42      22.693  -7.710  17.757  1.00  0.00           O
ATOM    647  N   SER A  43      23.959  -6.690  19.376  1.00  0.00           N
ATOM    648  CA  SER A  43      22.905  -6.274  20.314  1.00  0.00           C
ATOM    649  C   SER A  43      22.777  -4.758  20.236  1.00  0.00           C
ATOM    650  O   SER A  43      23.826  -4.125  20.013  1.00  0.00           O
ATOM    658  N   SER A  44      21.595  -4.255  20.476  1.00  0.00           N
ATOM    659  CA  SER A  44      21.214  -2.830  20.411  1.00  0.00           C
ATOM    660  C   SER A  44      20.483  -2.370  21.672  1.00  0.00           C
ATOM    661  O   SER A  44      19.964  -3.181  22.441  1.00  0.00           O
ATOM    669  N   GLY A  45      20.506  -1.051  21.836  1.00  0.00           N
ATOM    670  CA  GLY A  45      20.188  -0.332  23.066  1.00  0.00           C
ATOM    671  C   GLY A  45      19.537   0.987  22.671  1.00  0.00           C
ATOM    672  O   GLY A  45      20.142   2.054  22.803  1.00  0.00           O
ATOM    676  N   SER A  46      18.343   0.863  22.144  1.00  0.00           N
ATOM    677  CA  SER A  46      17.763   1.826  21.219  1.00  0.00           C
ATOM    678  C   SER A  46      16.679   2.644  21.892  1.00  0.00           C
ATOM    679  O   SER A  46      16.568   2.575  23.108  1.00  0.00           O
ATOM    687  N   ALA A  47      15.875   3.328  21.120  1.00  0.00           N
ATOM    688  CA  ALA A  47      14.531   3.693  21.494  1.00  0.00           C
ATOM    689  C   ALA A  47      13.614   3.651  20.261  1.00  0.00           C
```


Dieses Werk ist copyrightgeschützt und darf in keiner Form vervielfältigt werden noch an Dritte weitergegeben werden.
Es gilt nur für den persönlichen Gebrauch.

```
ATOM    690  O   ALA A  47      13.954   4.381  19.314  1.00  0.00           O
ATOM    697  N   ASN A  48      12.562   2.887  20.275  1.00  0.00           N
ATOM    698  CA  ASN A  48      11.478   2.851  19.283  1.00  0.00           C
ATOM    699  C   ASN A  48      10.320   3.620  19.907  1.00  0.00           C
ATOM    700  O   ASN A  48       9.362   3.017  20.415  1.00  0.00           O
ATOM    711  N   THR A  49      10.430   4.958  19.928  1.00  0.00           N
ATOM    712  CA  THR A  49       9.577   5.752  20.809  1.00  0.00           C
ATOM    713  C   THR A  49       8.137   5.852  20.294  1.00  0.00           C
ATOM    714  O   THR A  49       7.778   6.758  19.541  1.00  0.00           O
ATOM    725  N   GLU A  50       7.295   4.921  20.761  1.00  0.00           N
ATOM    726  CA  GLU A  50       5.867   5.224  20.920  1.00  0.00           C
ATOM    727  C   GLU A  50       5.333   4.499  22.164  1.00  0.00           C
ATOM    728  O   GLU A  50       4.368   3.747  22.184  1.00  0.00           O
ATOM    740  N   THR A  51       6.082   4.656  23.267  1.00  0.00           N
ATOM    741  CA  THR A  51       5.981   3.901  24.535  1.00  0.00           C
ATOM    742  C   THR A  51       6.597   4.695  25.706  1.00  0.00           C
ATOM    743  O   THR A  51       5.786   5.171  26.508  1.00  0.00           O
ATOM    754  N   THR A  52       7.892   4.857  25.798  1.00  0.00           N
ATOM    755  CA  THR A  52       8.741   5.535  26.819  1.00  0.00           C
ATOM    756  C   THR A  52      10.194   5.358  26.366  1.00  0.00           C
ATOM    757  O   THR A  52      10.624   6.393  25.729  1.00  0.00           O
ATOM    768  N   LYS A  53      11.013   4.357  26.356  1.00  0.00           N
ATOM    769  CA  LYS A  53      11.603   3.174  26.995  1.00  0.00           C
ATOM    770  C   LYS A  53      13.128   3.141  26.744  1.00  0.00           C
ATOM    771  O   LYS A  53      13.624   4.064  26.082  1.00  0.00           O
ATOM    790  N   VAL A  54      13.823   2.073  27.158  1.00  0.00           N
ATOM    791  CA  VAL A  54      14.957   1.481  26.480  1.00  0.00           C
ATOM    792  C   VAL A  54      14.471   0.123  25.895  1.00  0.00           C
ATOM    793  O   VAL A  54      14.666  -0.924  26.531  1.00  0.00           O
ATOM    806  N   THR A  55      13.877   0.121  24.696  1.00  0.00           N
ATOM    807  CA  THR A  55      13.765  -1.107  23.861  1.00  0.00           C
ATOM    808  C   THR A  55      15.127  -1.398  23.225  1.00  0.00           C
ATOM    809  O   THR A  55      16.016  -0.562  23.285  1.00  0.00           O
ATOM    820  N   GLY A  56      15.266  -2.567  22.609  1.00  0.00           N
ATOM    821  CA  GLY A  56      16.510  -2.995  21.953  1.00  0.00           C
ATOM    822  C   GLY A  56      16.244  -4.015  20.854  1.00  0.00           C
ATOM    823  O   GLY A  56      15.139  -4.107  20.317  1.00  0.00           O
ATOM    827  N   SER A  57      17.270  -4.779  20.551  1.00  0.00           N
ATOM    828  CA  SER A  57      17.164  -5.986  19.726  1.00  0.00           C
ATOM    829  C   SER A  57      18.392  -6.865  19.935  1.00  0.00           C
ATOM    830  O   SER A  57      19.370  -6.383  20.536  1.00  0.00           O
ATOM    838  N   LEU A  58      18.292  -8.072  19.447  1.00  0.00           N
ATOM    839  CA  LEU A  58      19.362  -9.062  19.416  1.00  0.00           C
ATOM    840  C   LEU A  58      19.400  -9.672  18.008  1.00  0.00           C
ATOM    841  O   LEU A  58      18.470 -10.458  17.717  1.00  0.00           O
ATOM    857  N   GLU A  59      20.364  -9.326  17.192  1.00  0.00           N
ATOM    858  CA  GLU A  59      20.591  -9.839  15.837  1.00  0.00           C
ATOM    859  C   GLU A  59      21.734 -10.851  15.933  1.00  0.00           C
ATOM    860  O   GLU A  59      22.783 -10.429  16.469  1.00  0.00           O
ATOM    872  N   THR A  60      21.544 -12.074  15.504  1.00  0.00           N
ATOM    873  CA  THR A  60      22.458 -13.224  15.691  1.00  0.00           C
ATOM    874  C   THR A  60      22.415 -14.075  14.414  1.00  0.00           C
ATOM    875  O   THR A  60      21.344 -14.636  14.208  1.00  0.00           O
ATOM    886  N   LYS A  61      23.474 -14.142  13.616  1.00  0.00           N
ATOM    887  CA  LYS A  61      23.368 -14.509  12.197  1.00  0.00           C
ATOM    888  C   LYS A  61      24.329 -15.650  11.852  1.00  0.00           C
ATOM    889  O   LYS A  61      25.402 -15.743  12.437  1.00  0.00           O
ATOM    908  N   TYR A  62      24.161 -16.867  12.240  1.00  0.00           N
ATOM    909  CA  TYR A  62      25.070 -18.020  12.201  1.00  0.00           C
ATOM    910  C   TYR A  62      25.386 -18.390  10.751  1.00  0.00           C
ATOM    911  O   TYR A  62      24.459 -18.579   9.953  1.00  0.00           O
ATOM    929  N   ARG A  63      26.693 -18.494  10.429  1.00  0.00           N
ATOM    930  CA  ARG A  63      27.141 -18.866   9.066  1.00  0.00           C
ATOM    931  C   ARG A  63      27.082 -17.684   8.086  1.00  0.00           C
ATOM    932  O   ARG A  63      27.828 -16.734   8.262  1.00  0.00           O
ATOM    953  N   TRP A  64      26.175 -17.767   7.084  1.00  0.00           N
ATOM    954  CA  TRP A  64      25.965 -16.715   6.064  1.00  0.00           C
ATOM    955  C   TRP A  64      25.540 -17.399   4.764  1.00  0.00           C
ATOM    956  O   TRP A  64      25.170 -18.572   4.773  1.00  0.00           O
ATOM    977  N   THR A  65      25.577 -16.667   3.653  1.00  0.00           N
ATOM    978  CA  THR A  65      25.181 -17.232   2.373  1.00  0.00           C
ATOM    979  C   THR A  65      26.305 -18.065   1.762  1.00  0.00           C
ATOM    980  O   THR A  65      26.267 -18.369   0.573  1.00  0.00           O
ATOM    991  N   GLU A  66      27.302 -18.440   2.575  1.00  0.00           N
ATOM    992  CA  GLU A  66      28.412 -19.252   2.069  1.00  0.00           C
ATOM    993  C   GLU A  66      27.874 -20.397   1.227  1.00  0.00           C
ATOM    994  O   GLU A  66      27.582 -20.219   0.042  1.00  0.00           O
ATOM   1006  N   TYR A  67      27.742 -21.584   1.824  1.00  0.00           N
ATOM   1007  CA  TYR A  67      27.237 -22.724   1.094  1.00  0.00           C
ATOM   1008  C   TYR A  67      25.714 -22.764   1.186  1.00  0.00           C
ATOM   1009  O   TYR A  67      25.100 -23.821   1.037  1.00  0.00           O
ATOM   1027  N   GLY A  68      25.115 -21.582   1.369  1.00  0.00           N
ATOM   1028  CA  GLY A  68      23.660 -21.465   1.405  1.00  0.00           C
ATOM   1029  C   GLY A  68      23.060 -21.923   2.729  1.00  0.00           C
ATOM   1030  O   GLY A  68      21.861 -22.178   2.795  1.00  0.00           O
ATOM   1034  N   LEU A  69      23.891 -22.035   3.769  1.00  0.00           N
ATOM   1035  CA  LEU A  69      23.413 -22.469   5.079  1.00  0.00           C
ATOM   1036  C   LEU A  69      23.347 -21.305   6.054  1.00  0.00           C
ATOM   1037  O   LEU A  69      24.080 -21.267   7.042  1.00  0.00           O
ATOM   1053  N   THR A  70      22.439 -20.382   5.784  1.00  0.00           N
ATOM   1054  CA  THR A  70      22.261 -19.231   6.663  1.00  0.00           C
ATOM   1055  C   THR A  70      21.207 -19.521   7.710  1.00  0.00           C
ATOM   1056  O   THR A  70      20.025 -19.656   7.376  1.00  0.00           O
ATOM   1067  N   PHE A  71      21.622 -19.591   8.981  1.00  0.00           N
```


Dieses Werk ist copyrightgeschützt und darf in keiner Form vervielfältigt werden noch an Dritte weitergegeben werden.
Es gilt nur für den persönlichen Gebrauch.

```
ATOM   1068  CA  PHE A  71      20.665 -19.818  10.050  1.00  0.00           C
ATOM   1069  C   PHE A  71      20.575 -18.516  10.843  1.00  0.00           C
ATOM   1070  O   PHE A  71      21.415 -18.220  11.693  1.00  0.00           O
ATOM   1087  N   THR A  72      19.575 -17.723  10.509  1.00  0.00           N
ATOM   1088  CA  THR A  72      19.399 -16.419  11.138  1.00  0.00           C
ATOM   1089  C   THR A  72      18.567 -16.527  12.403  1.00  0.00           C
ATOM   1090  O   THR A  72      17.559 -17.225  12.435  1.00  0.00           O
ATOM   1101  N   VAL A  73      18.990 -15.794  13.434  1.00  0.00           N
ATOM   1102  CA  VAL A  73      18.263 -15.780  14.695  1.00  0.00           C
ATOM   1103  C   VAL A  73      18.001 -14.343  15.147  1.00  0.00           C
ATOM   1104  O   VAL A  73      18.926 -13.557  15.348  1.00  0.00           O
ATOM   1117  N   LYS A  74      16.734 -13.951  15.304  1.00  0.00           N
ATOM   1118  CA  LYS A  74      16.244 -12.610  15.694  1.00  0.00           C
ATOM   1119  C   LYS A  74      15.360 -12.709  16.945  1.00  0.00           C
ATOM   1120  O   LYS A  74      14.184 -13.100  16.826  1.00  0.00           O
ATOM   1139  N   TRP A  75      15.912 -12.406  18.113  1.00  0.00           N
ATOM   1140  CA  TRP A  75      15.183 -12.186  19.380  1.00  0.00           C
ATOM   1141  C   TRP A  75      15.048 -10.664  19.599  1.00  0.00           C
ATOM   1142  O   TRP A  75      15.890  -9.912  19.106  1.00  0.00           O
ATOM   1163  N   ASN A  76      14.008 -10.258  20.316  1.00  0.00           N
ATOM   1164  CA  ASN A  76      13.713  -8.871  20.745  1.00  0.00           C
ATOM   1165  C   ASN A  76      13.146  -8.848  22.164  1.00  0.00           C
ATOM   1166  O   ASN A  76      12.726  -9.862  22.713  1.00  0.00           O
ATOM   1177  N   THR A  77      13.145  -7.647  22.757  1.00  0.00           N
ATOM   1178  CA  THR A  77      12.639  -7.444  24.105  1.00  0.00           C
ATOM   1179  C   THR A  77      11.120  -7.639  24.219  1.00  0.00           C
ATOM   1180  O   THR A  77      10.718  -8.115  25.299  1.00  0.00           O
ATOM   1191  N   ASP A  78      10.308  -7.325  23.211  1.00  0.00           N
ATOM   1192  CA  ASP A  78       8.891  -7.730  23.166  1.00  0.00           C
ATOM   1193  C   ASP A  78       8.641  -9.253  23.291  1.00  0.00           C
ATOM   1194  O   ASP A  78       7.425  -9.489  23.540  1.00  0.00           O
ATOM   1203  N   ASN A  79       9.547 -10.155  23.166  1.00  0.00           N
ATOM   1204  CA  ASN A  79       9.635 -11.624  23.357  1.00  0.00           C
ATOM   1205  C   ASN A  79       9.497 -12.392  22.020  1.00  0.00           C
ATOM   1206  O   ASN A  79       9.229 -13.605  22.042  1.00  0.00           O
ATOM   1217  N   THR A  80       9.707 -11.805  20.853  1.00  0.00           N
ATOM   1218  CA  THR A  80       9.439 -12.480  19.555  1.00  0.00           C
ATOM   1219  C   THR A  80      10.621 -13.406  19.294  1.00  0.00           C
ATOM   1220  O   THR A  80      11.704 -13.273  19.832  1.00  0.00           O
ATOM   1231  N   LEU A  81      10.707 -14.298  19.057  1.00  0.00           N
ATOM   1232  CA  LEU A  81      11.877 -15.117  18.758  1.00  0.00           C
ATOM   1233  C   LEU A  81      11.757 -15.621  17.324  1.00  0.00           C
ATOM   1234  O   LEU A  81      10.696 -16.116  16.952  1.00  0.00           O
ATOM   1250  N   GLY A  82      12.807 -15.498  16.511  1.00  0.00           N
ATOM   1251  CA  GLY A  82      12.714 -15.963  15.129  1.00  0.00           C
ATOM   1252  C   GLY A  82      13.982 -16.676  14.679  1.00  0.00           C
ATOM   1253  O   GLY A  82      15.055 -16.097  14.707  1.00  0.00           O
ATOM   1257  N   THR A  83      13.836 -17.917  14.215  1.00  0.00           N
ATOM   1258  CA  THR A  83      14.977 -18.682  13.705  1.00  0.00           C
ATOM   1259  C   THR A  83      14.677 -19.176  12.290  1.00  0.00           C
ATOM   1260  O   THR A  83      13.685 -19.872  12.063  1.00  0.00           O
ATOM   1271  N   GLU A  84      15.523 -18.794  11.337  1.00  0.00           N
ATOM   1272  CA  GLU A  84      15.319 -19.192   9.940  1.00  0.00           C
ATOM   1273  C   GLU A  84      16.489 -20.010   9.401  1.00  0.00           C
ATOM   1274  O   GLU A  84      17.563 -19.463   9.170  1.00  0.00           O
ATOM   1286  N   ILE A  85      16.275 -21.307   9.145  1.00  0.00           N
ATOM   1287  CA  ILE A  85      17.343 -22.140   8.580  1.00  0.00           C
ATOM   1288  C   ILE A  85      17.093 -22.337   7.091  1.00  0.00           C
ATOM   1289  O   ILE A  85      16.081 -22.912   6.707  1.00  0.00           O
ATOM   1305  N   THR A  86      18.011 -21.830   6.266  1.00  0.00           N
ATOM   1306  CA  THR A  86      17.859 -21.926   4.814  1.00  0.00           C
ATOM   1307  C   THR A  86      18.975 -22.717   4.138  1.00  0.00           C
ATOM   1308  O   THR A  86      20.156 -22.454   4.371  1.00  0.00           O
ATOM   1319  N   VAL A  87      18.584 -23.639   3.245  1.00  0.00           N
ATOM   1320  CA  VAL A  87      19.559 -24.410   2.469  1.00  0.00           C
ATOM   1321  C   VAL A  87      19.334 -24.141   0.984  1.00  0.00           C
ATOM   1322  O   VAL A  87      18.408 -24.684   0.381  1.00  0.00           O
ATOM   1335  N   GLU A  88      20.174 -23.299   0.399  1.00  0.00           N
ATOM   1336  CA  GLU A  88      20.045 -22.963  -1.022  1.00  0.00           C
ATOM   1337  C   GLU A  88      20.956 -23.842  -1.893  1.00  0.00           C
ATOM   1338  O   GLU A  88      21.983 -24.323  -1.420  1.00  0.00           O
ATOM   1350  N   ASP A  89      20.579 -24.026  -3.168  1.00  0.00           N
ATOM   1351  CA  ASP A  89      21.386 -24.821  -4.114  1.00  0.00           C
ATOM   1352  C   ASP A  89      21.525 -26.280  -3.673  1.00  0.00           C
ATOM   1353  O   ASP A  89      22.609 -26.854  -3.778  1.00  0.00           O
ATOM   1362  N   GLN A  90      20.462 -26.878  -3.155  1.00  0.00           N
ATOM   1363  CA  GLN A  90      20.569 -28.261  -2.693  1.00  0.00           C
ATOM   1364  C   GLN A  90      20.738 -29.271  -3.835  1.00  0.00           C
ATOM   1365  O   GLN A  90      21.512 -30.218  -3.701  1.00  0.00           O
ATOM   1379  N   LEU A  91      20.046 -29.081  -4.953  1.00  0.00           N
ATOM   1380  CA  LEU A  91      20.196 -30.014  -6.071  1.00  0.00           C
ATOM   1381  C   LEU A  91      21.335 -29.537  -6.972  1.00  0.00           C
ATOM   1382  O   LEU A  91      22.388 -30.177  -7.064  1.00  0.00           O
ATOM   1398  N   ALA A  92      21.117 -28.398  -7.622  1.00  0.00           N
ATOM   1399  CA  ALA A  92      22.129 -27.824  -8.503  1.00  0.00           C
ATOM   1400  C   ALA A  92      21.624 -26.555  -9.206  1.00  0.00           C
ATOM   1401  O   ALA A  92      22.357 -25.571  -9.311  1.00  0.00           O
ATOM   1408  N   ARG A  93      20.370 -26.556  -9.667  1.00  0.00           N
ATOM   1409  CA  ARG A  93      19.831 -25.378 -10.328  1.00  0.00           C
ATOM   1410  C   ARG A  93      19.479 -24.334  -9.283  1.00  0.00           C
ATOM   1411  O   ARG A  93      20.232 -23.392  -9.035  1.00  0.00           O
ATOM   1432  N   GLY A  94      18.323 -24.531  -8.668  1.00  0.00           N
ATOM   1433  CA  GLY A  94      17.840 -23.635  -7.639  1.00  0.00           C
ATOM   1434  C   GLY A  94      16.872 -24.372  -6.720  1.00  0.00           C
```


Dieses Werk ist copyrightgeschützt und darf in keiner Form vervielfältigt werden noch an Dritte weitergegeben werden.
Es gilt nur für den persönlichen Gebrauch.

```
ATOM   1435  O   GLY A  94      15.679 -24.492  -6.996  1.00  0.00           O
ATOM   1439  N   LEU A  95      17.417 -24.835  -5.619  1.00  0.00           N
ATOM   1440  CA  LEU A  95      16.638 -25.544  -4.605  1.00  0.00           C
ATOM   1441  C   LEU A  95      16.855 -24.863  -3.247  1.00  0.00           C
ATOM   1442  O   LEU A  95      17.992 -24.743  -2.781  1.00  0.00           O
ATOM   1458  N   LYS A  96      15.754 -24.378  -2.655  1.00  0.00           N
ATOM   1459  CA  LYS A  96      15.801 -23.658  -1.374  1.00  0.00           C
ATOM   1460  C   LYS A  96      14.879 -24.323  -0.349  1.00  0.00           C
ATOM   1461  O   LYS A  96      13.700 -24.533  -0.631  1.00  0.00           O
ATOM   1480  N   LEU A  97      15.405 -24.639   0.845  1.00  0.00           N
ATOM   1481  CA  LEU A  97      14.588 -25.264   1.888  1.00  0.00           C
ATOM   1482  C   LEU A  97      14.677 -24.431   3.149  1.00  0.00           C
ATOM   1483  O   LEU A  97      15.722 -24.435   3.801  1.00  0.00           O
ATOM   1499  N   THR A  98      13.601 -23.695   3.476  1.00  0.00           N
ATOM   1500  CA  THR A  98      13.632 -22.841   4.662  1.00  0.00           C
ATOM   1501  C   THR A  98      12.739 -23.288   5.813  1.00  0.00           C
ATOM   1502  O   THR A  98      11.542 -22.979   5.834  1.00  0.00           O
ATOM   1513  N   PHE A  99      13.329 -23.940   6.814  1.00  0.00           N
ATOM   1514  CA  PHE A  99      12.550 -24.291   7.982  1.00  0.00           C
ATOM   1515  C   PHE A  99      12.559 -23.046   8.838  1.00  0.00           C
ATOM   1516  O   PHE A  99      13.623 -22.469   9.076  1.00  0.00           O
ATOM   1533  N   ASP A 100      11.390 -22.595   9.243  1.00  0.00           N
ATOM   1534  CA  ASP A 100      11.288 -21.370  10.005  1.00  0.00           C
ATOM   1535  C   ASP A 100      10.671 -21.636  11.370  1.00  0.00           C
ATOM   1536  O   ASP A 100       9.842 -22.529  11.514  1.00  0.00           O
ATOM   1545  N   SER A 101      11.065 -20.822  12.342  1.00  0.00           N
ATOM   1546  CA  SER A 101      10.536 -20.932  13.701  1.00  0.00           C
ATOM   1547  C   SER A 101      10.322 -19.554  14.295  1.00  0.00           C
ATOM   1548  O   SER A 101      11.281 -18.848  14.596  1.00  0.00           O
ATOM   1556  N   SER A 102       9.059 -19.188  14.467  1.00  0.00           N
ATOM   1557  CA  SER A 102       8.714 -17.901  15.033  1.00  0.00           C
ATOM   1558  C   SER A 102       7.775 -18.082  16.215  1.00  0.00           C
ATOM   1559  O   SER A 102       6.628 -18.500  16.073  1.00  0.00           O
ATOM   1567  N   PHE A 103       8.295 -17.750  17.376  1.00  0.00           N
ATOM   1568  CA  PHE A 103       7.544 -17.846  18.626  1.00  0.00           C
ATOM   1569  C   PHE A 103       7.214 -16.439  19.146  1.00  0.00           C
ATOM   1570  O   PHE A 103       8.108 -15.752  19.640  1.00  0.00           O
ATOM   1587  N   SER A 104       5.947 -16.010  19.039  1.00  0.00           N
ATOM   1588  CA  SER A 104       5.564 -14.670  19.512  1.00  0.00           C
ATOM   1589  C   SER A 104       4.647 -14.716  20.754  1.00  0.00           C
ATOM   1590  O   SER A 104       3.996 -15.732  21.036  1.00  0.00           O
ATOM   1598  N   PRO A 105       4.506 -13.569  21.465  1.00  0.00           N
ATOM   1599  CA  PRO A 105       3.622 -13.370  22.691  1.00  0.00           C
ATOM   1600  C   PRO A 105       2.191 -13.886  22.732  1.00  0.00           C
ATOM   1601  O   PRO A 105       1.775 -14.208  23.861  1.00  0.00           O
ATOM   1612  N   ASN A 106       1.512 -13.860  21.585  1.00  0.00           N
ATOM   1613  CA  ASN A 106       0.115 -14.296  21.436  1.00  0.00           C
ATOM   1614  C   ASN A 106      -0.056 -15.746  21.904  1.00  0.00           C
ATOM   1615  O   ASN A 106      -0.104 -16.621  21.025  1.00  0.00           O
ATOM   1626  N   THR A 107      -0.188 -15.958  23.245  1.00  0.00           N
ATOM   1627  CA  THR A 107      -0.312 -17.259  23.911  1.00  0.00           C
ATOM   1628  C   THR A 107       0.751 -18.236  23.420  1.00  0.00           C
ATOM   1629  O   THR A 107       0.445 -19.390  23.122  1.00  0.00           O
ATOM   1640  N   GLY A 108       1.996 -17.773  23.336  1.00  0.00           N
ATOM   1641  CA  GLY A 108       3.082 -18.633  22.877  1.00  0.00           C
ATOM   1642  C   GLY A 108       2.795 -19.157  21.474  1.00  0.00           C
ATOM   1643  O   GLY A 108       2.913 -20.353  21.213  1.00  0.00           O
ATOM   1647  N   LYS A 109       2.408 -18.252  20.581  1.00  0.00           N
ATOM   1648  CA  LYS A 109       2.091 -18.636  19.205  1.00  0.00           C
ATOM   1649  C   LYS A 109       3.336 -19.152  18.491  1.00  0.00           C
ATOM   1650  O   LYS A 109       4.289 -18.405  18.265  1.00  0.00           O
ATOM   1669  N   LYS A 110       3.315 -20.440  18.152  1.00  0.00           N
ATOM   1670  CA  LYS A 110       4.442 -21.082  17.475  1.00  0.00           C
ATOM   1671  C   LYS A 110       4.207 -21.161  15.970  1.00  0.00           C
ATOM   1672  O   LYS A 110       3.224 -21.747  15.514  1.00  0.00           O
ATOM   1691  N   ASN A 111       5.121 -20.569  15.206  1.00  0.00           N
ATOM   1692  CA  ASN A 111       5.026 -20.573  13.752  1.00  0.00           C
ATOM   1693  C   ASN A 111       6.157 -21.407  13.155  1.00  0.00           C
ATOM   1694  O   ASN A 111       7.305 -20.961  13.112  1.00  0.00           O
ATOM   1705  N   ALA A 112       5.824 -22.613  12.691  1.00  0.00           N
ATOM   1706  CA  ALA A 112       6.809 -23.501  12.092  1.00  0.00           C
ATOM   1707  C   ALA A 112       6.496 -23.709  10.619  1.00  0.00           C
ATOM   1708  O   ALA A 112       5.501 -24.343  10.276  1.00  0.00           O
ATOM   1715  N   LYS A 113       7.347 -23.159   9.751  1.00  0.00           N
ATOM   1716  CA  LYS A 113       7.121 -23.280   8.301  1.00  0.00           C
ATOM   1717  C   LYS A 113       8.238 -24.033   7.595  1.00  0.00           C
ATOM   1718  O   LYS A 113       9.403 -23.846   7.902  1.00  0.00           O
ATOM   1737  N   ILE A 114       7.864 -24.789   6.570  1.00  0.00           N
ATOM   1738  CA  ILE A 114       8.842 -25.481   5.734  1.00  0.00           C
ATOM   1739  C   ILE A 114       8.599 -25.078   4.285  1.00  0.00           C
ATOM   1740  O   ILE A 114       7.656 -25.546   3.655  1.00  0.00           O
ATOM   1756  N   LYS A 115       9.458 -24.199   3.772  1.00  0.00           N
ATOM   1757  CA  LYS A 115       9.341 -23.721   2.408  1.00  0.00           C
ATOM   1758  C   LYS A 115      10.291 -24.497   1.527  1.00  0.00           C
ATOM   1759  O   LYS A 115      11.488 -24.488   1.765  1.00  0.00           O
ATOM   1778  N   THR A 116       9.764 -25.106   0.490  1.00  0.00           N
ATOM   1779  CA  THR A 116      10.603 -25.816  -0.456  1.00  0.00           C
ATOM   1780  C   THR A 116      10.321 -25.250  -1.828  1.00  0.00           C
ATOM   1781  O   THR A 116       9.258 -25.487  -2.381  1.00  0.00           O
ATOM   1792  N   GLY A 117      11.271 -24.474  -2.347  1.00  0.00           N
ATOM   1793  CA  GLY A 117      11.128 -23.840  -3.631  1.00  0.00           C
ATOM   1794  C   GLY A 117      12.074 -24.439  -4.640  1.00  0.00           C
ATOM   1795  O   GLY A 117      13.264 -24.122  -4.658  1.00  0.00           O
ATOM   1799  N   TYR A 118      11.536 -25.286  -5.505  1.00  0.00           N
```


Dieses Werk ist copyrightgeschützt und darf in keiner Form vervielfältigt werden noch an Dritte weitergegeben werden.
Es gilt nur für den persönlichen Gebrauch.

```
ATOM   1800  CA  TYR A 118      12.344 -25.886  -6.547  1.00  0.00           C
ATOM   1801  C   TYR A 118      12.232 -25.017  -7.778  1.00  0.00           C
ATOM   1802  O   TYR A 118      11.147 -24.549  -8.128  1.00  0.00           O
ATOM   1820  N   LYS A 119      13.373 -24.744  -8.376  1.00  0.00           N
ATOM   1821  CA  LYS A 119      13.440 -23.858  -9.511  1.00  0.00           C
ATOM   1822  C   LYS A 119      13.952 -24.594 -10.751  1.00  0.00           C
ATOM   1823  O   LYS A 119      14.703 -25.562 -10.645  1.00  0.00           O
ATOM   1842  N   ARG A 120      13.559 -24.119 -11.923  1.00  0.00           N
ATOM   1843  CA  ARG A 120      14.004 -24.728 -13.176  1.00  0.00           C
ATOM   1844  C   ARG A 120      13.558 -23.834 -14.315  1.00  0.00           C
ATOM   1845  O   ARG A 120      12.483 -24.030 -14.861  1.00  0.00           O
ATOM   1866  N   GLU A 121      14.378 -22.829 -14.637  1.00  0.00           N
ATOM   1867  CA  GLU A 121      14.072 -21.881 -15.701  1.00  0.00           C
ATOM   1868  C   GLU A 121      12.567 -21.582 -15.804  1.00  0.00           C
ATOM   1869  O   GLU A 121      11.749 -22.444 -16.115  1.00  0.00           O
ATOM   1881  N   HIS A 122      12.239 -20.318 -15.606  1.00  0.00           N
ATOM   1882  CA  HIS A 122      10.855 -19.839 -15.729  1.00  0.00           C
ATOM   1883  C   HIS A 122       9.864 -20.573 -14.819  1.00  0.00           C
ATOM   1884  O   HIS A 122       8.734 -20.095 -14.665  1.00  0.00           O
ATOM   1898  N   ILE A 123      10.248 -21.730 -14.248  1.00  0.00           N
ATOM   1899  CA  ILE A 123       9.327 -22.483 -13.390  1.00  0.00           C
ATOM   1900  C   ILE A 123       9.785 -22.537 -11.939  1.00  0.00           C
ATOM   1901  O   ILE A 123      10.774 -23.209 -11.631  1.00  0.00           O
ATOM   1917  N   ASN A 124       9.025 -21.895 -11.045  1.00  0.00           N
ATOM   1918  CA  ASN A 124       9.339 -21.964  -9.614  1.00  0.00           C
ATOM   1919  C   ASN A 124       8.143 -22.530  -8.835  1.00  0.00           C
ATOM   1920  O   ASN A 124       7.019 -22.037  -8.957  1.00  0.00           O
ATOM   1931  N   LEU A 125       8.399 -23.571  -8.038  1.00  0.00           N
ATOM   1932  CA  LEU A 125       7.346 -24.203  -7.240  1.00  0.00           C
ATOM   1933  C   LEU A 125       7.708 -24.169  -5.763  1.00  0.00           C
ATOM   1934  O   LEU A 125       8.608 -24.893  -5.368  1.00  0.00           O
ATOM   1950  N   GLY A 126       7.007 -23.383  -4.934  1.00  0.00           N
ATOM   1951  CA  GLY A 126       7.289 -23.329  -3.511  1.00  0.00           C
ATOM   1952  C   GLY A 126       6.191 -23.996  -2.707  1.00  0.00           C
ATOM   1953  O   GLY A 126       5.016 -23.802  -2.995  1.00  0.00           O
ATOM   1957  N   CYS A 127       6.608 -24.754  -1.681  1.00  0.00           N
ATOM   1958  CA  CYS A 127       5.685 -25.446  -0.781  1.00  0.00           C
ATOM   1959  C   CYS A 127       5.953 -25.063   0.685  1.00  0.00           C
ATOM   1960  O   CYS A 127       6.932 -25.500   1.281  1.00  0.00           O
ATOM   1968  N   ASP A 128       5.107 -24.197   1.223  1.00  0.00           N
ATOM   1969  CA  ASP A 128       5.247 -23.723   2.589  1.00  0.00           C
ATOM   1970  C   ASP A 128       4.271 -24.474   3.497  1.00  0.00           C
ATOM   1971  O   ASP A 128       3.062 -24.242   3.444  1.00  0.00           O
ATOM   1980  N   MET A 129       4.800 -25.364   4.338  1.00  0.00           N
ATOM   1981  CA  MET A 129       3.950 -26.122   5.254  1.00  0.00           C
ATOM   1982  C   MET A 129       4.038 -25.494   6.632  1.00  0.00           C
ATOM   1983  O   MET A 129       5.083 -25.537   7.266  1.00  0.00           O
ATOM   1997  N   ASP A 130       2.938 -24.906   7.082  1.00  0.00           N
ATOM   1998  CA  ASP A 130       2.906 -24.249   8.380  1.00  0.00           C
ATOM   1999  C   ASP A 130       2.332 -25.166   9.449  1.00  0.00           C
ATOM   2000  O   ASP A 130       1.119 -25.327   9.531  1.00  0.00           O
ATOM   2009  N   PHE A 131       3.201 -25.748  10.280  1.00  0.00           N
ATOM   2010  CA  PHE A 131       2.739 -26.634  11.345  1.00  0.00           C
ATOM   2011  C   PHE A 131       2.280 -25.830  12.554  1.00  0.00           C
ATOM   2012  O   PHE A 131       3.032 -25.641  13.514  1.00  0.00           O
ATOM   2029  N   ASP A 132       1.036 -25.372  12.501  1.00  0.00           N
ATOM   2030  CA  ASP A 132       0.456 -24.598  13.592  1.00  0.00           C
ATOM   2031  C   ASP A 132      -0.843 -25.262  14.027  1.00  0.00           C
ATOM   2032  O   ASP A 132      -1.337 -26.160  13.344  1.00  0.00           O
ATOM   2041  N   ILE A 133      -1.394 -24.855  15.159  1.00  0.00           N
ATOM   2042  CA  ILE A 133      -2.618 -25.484  15.617  1.00  0.00           C
ATOM   2043  C   ILE A 133      -3.725 -25.239  14.602  1.00  0.00           C
ATOM   2044  O   ILE A 133      -4.450 -26.170  14.250  1.00  0.00           O
ATOM   2060  N   ALA A 134      -3.804 -24.021  14.060  1.00  0.00           N
ATOM   2061  CA  ALA A 134      -4.782 -23.754  13.013  1.00  0.00           C
ATOM   2062  C   ALA A 134      -4.331 -24.522  11.771  1.00  0.00           C
ATOM   2063  O   ALA A 134      -5.139 -25.062  11.020  1.00  0.00           O
ATOM   2070  N   GLY A 135      -3.008 -24.614  11.614  1.00  0.00           N
ATOM   2071  CA  GLY A 135      -2.410 -25.384  10.528  1.00  0.00           C
ATOM   2072  C   GLY A 135      -2.513 -26.854  10.925  1.00  0.00           C
ATOM   2073  O   GLY A 135      -3.157 -27.163  11.931  1.00  0.00           O
ATOM   2077  N   PRO A 136      -1.908 -27.782  10.228  1.00  0.00           N
ATOM   2078  CA  PRO A 136      -1.083 -27.576   8.981  1.00  0.00           C
ATOM   2079  C   PRO A 136      -1.778 -26.814   7.856  1.00  0.00           C
ATOM   2080  O   PRO A 136      -2.793 -27.281   7.332  1.00  0.00           O
ATOM   2091  N   SER A 137      -1.177 -25.708   7.388  1.00  0.00           N
ATOM   2092  CA  SER A 137      -1.704 -25.006   6.231  1.00  0.00           C
ATOM   2093  C   SER A 137      -0.676 -25.161   5.112  1.00  0.00           C
ATOM   2094  O   SER A 137       0.531 -25.092   5.372  1.00  0.00           O
ATOM   2102  N   ILE A 138      -1.122 -25.384   3.888  1.00  0.00           N
ATOM   2103  CA  ILE A 138      -0.187 -25.547   2.775  1.00  0.00           C
ATOM   2104  C   ILE A 138      -0.232 -24.337   1.848  1.00  0.00           C
ATOM   2105  O   ILE A 138      -1.151 -24.202   1.054  1.00  0.00           O
ATOM   2121  N   ARG A 139       0.774 -23.467   1.973  1.00  0.00           N
ATOM   2122  CA  ARG A 139       0.853 -22.259   1.145  1.00  0.00           C
ATOM   2123  C   ARG A 139       1.988 -22.378   0.129  1.00  0.00           C
ATOM   2124  O   ARG A 139       3.160 -22.298   0.479  1.00  0.00           O
ATOM   2145  N   GLY A 140       1.646 -22.618  -1.132  1.00  0.00           N
ATOM   2146  CA  GLY A 140       2.689 -22.771  -2.168  1.00  0.00           C
ATOM   2147  C   GLY A 140       2.500 -21.741  -3.272  1.00  0.00           C
ATOM   2148  O   GLY A 140       1.424 -21.199  -3.356  1.00  0.00           O
ATOM   2152  N   ALA A 141       3.507 -21.503  -4.147  1.00  0.00           N
ATOM   2153  CA  ALA A 141       3.352 -20.572  -5.236  1.00  0.00           C
ATOM   2154  C   ALA A 141       3.916 -21.219  -6.487  1.00  0.00           C
```


Dieses Werk ist copyrightgeschützt und darf in keiner Form vervielfältigt werden noch an Dritte weitergegeben werden.
Es gilt nur für den persönlichen Gebrauch.

```
ATOM   2155  O   ALA A 141       5.066 -21.661  -6.495  1.00  0.00           O
ATOM   2162  N   LEU A 142       3.120 -21.278  -7.525  1.00  0.00           N
ATOM   2163  CA  LEU A 142       3.557 -21.889  -8.781  1.00  0.00           C
ATOM   2164  C   LEU A 142       3.716 -20.806  -9.816  1.00  0.00           C
ATOM   2165  O   LEU A 142       2.713 -20.252 -10.248  1.00  0.00           O
ATOM   2181  N   VAL A 143       4.950 -20.501 -10.218  1.00  0.00           N
ATOM   2182  CA  VAL A 143       5.144 -19.454 -11.212  1.00  0.00           C
ATOM   2183  C   VAL A 143       5.703 -20.019 -12.500  1.00  0.00           C
ATOM   2184  O   VAL A 143       6.575 -20.896 -12.512  1.00  0.00           O
ATOM   2197  N   LEU A 144       5.157 -19.483 -13.578  1.00  0.00           N
ATOM   2198  CA  LEU A 144       5.535 -19.870 -14.927  1.00  0.00           C
ATOM   2199  C   LEU A 144       6.040 -18.642 -15.644  1.00  0.00           C
ATOM   2200  O   LEU A 144       5.447 -17.571 -15.513  1.00  0.00           O
ATOM   2216  N   GLY A 145       7.125 -18.781 -16.403  1.00  0.00           N
ATOM   2217  CA  GLY A 145       7.683 -17.640 -17.121  1.00  0.00           C
ATOM   2218  C   GLY A 145       7.409 -17.724 -18.621  1.00  0.00           C
ATOM   2219  O   GLY A 145       7.359 -18.816 -19.189  1.00  0.00           O
ATOM   2223  N   TYR A 146       7.275 -16.568 -19.276  1.00  0.00           N
ATOM   2224  CA  TYR A 146       7.058 -16.552 -20.723  1.00  0.00           C
ATOM   2225  C   TYR A 146       7.736 -15.325 -21.311  1.00  0.00           C
ATOM   2226  O   TYR A 146       8.612 -14.773 -20.660  1.00  0.00           O
ATOM   2244  N   GLU A 147       7.312 -14.923 -22.532  1.00  0.00           N
ATOM   2245  CA  GLU A 147       7.857 -13.753 -23.261  1.00  0.00           C
ATOM   2246  C   GLU A 147       7.993 -12.497 -22.384  1.00  0.00           C
ATOM   2247  O   GLU A 147       7.494 -11.434 -22.745  1.00  0.00           O
ATOM   2259  N   GLY A 148       8.649 -12.620 -21.247  1.00  0.00           N
ATOM   2260  CA  GLY A 148       8.806 -11.500 -20.336  1.00  0.00           C
ATOM   2261  C   GLY A 148       7.625 -11.425 -19.362  1.00  0.00           C
ATOM   2262  O   GLY A 148       7.202 -10.339 -18.981  1.00  0.00           O
ATOM   2266  N   TRP A 149       7.093 -12.583 -18.968  1.00  0.00           N
ATOM   2267  CA  TRP A 149       5.959 -12.596 -18.032  1.00  0.00           C
ATOM   2268  C   TRP A 149       6.178 -13.594 -16.915  1.00  0.00           C
ATOM   2269  O   TRP A 149       6.669 -14.685 -17.139  1.00  0.00           O
ATOM   2290  N   LEU A 150       5.749 -13.195 -15.728  1.00  0.00           N
ATOM   2291  CA  LEU A 150       5.799 -14.022 -14.525  1.00  0.00           C
ATOM   2292  C   LEU A 150       4.373 -14.166 -13.964  1.00  0.00           C
ATOM   2293  O   LEU A 150       3.834 -13.197 -13.433  1.00  0.00           O
ATOM   2309  N   ALA A 151       3.782 -15.352 -14.022  1.00  0.00           N
ATOM   2310  CA  ALA A 151       2.439 -15.549 -13.446  1.00  0.00           C
ATOM   2311  C   ALA A 151       2.571 -16.485 -12.258  1.00  0.00           C
ATOM   2312  O   ALA A 151       3.356 -17.410 -12.344  1.00  0.00           O
ATOM   2319  N   GLY A 152       1.852 -16.252 -11.143  1.00  0.00           N
ATOM   2320  CA  GLY A 152       1.993 -17.125  -9.978  1.00  0.00           C
ATOM   2321  C   GLY A 152       0.646 -17.561  -9.418  1.00  0.00           C
ATOM   2322  O   GLY A 152      -0.349 -16.833  -9.520  1.00  0.00           O
ATOM   2326  N   TYR A 153       0.625 -18.746  -8.804  1.00  0.00           N
ATOM   2327  CA  TYR A 153      -0.600 -19.276  -8.216  1.00  0.00           C
ATOM   2328  C   TYR A 153      -0.293 -19.675  -6.800  1.00  0.00           C
ATOM   2329  O   TYR A 153       0.464 -20.624  -6.593  1.00  0.00           O
ATOM   2347  N   GLN A 154      -0.859 -18.972  -5.815  1.00  0.00           N
ATOM   2348  CA  GLN A 154      -0.588 -19.292  -4.440  1.00  0.00           C
ATOM   2349  C   GLN A 154      -1.771 -20.024  -3.832  1.00  0.00           C
ATOM   2350  O   GLN A 154      -2.824 -19.430  -3.693  1.00  0.00           O
ATOM   2364  N   MET A 155      -1.588 -21.298  -3.478  1.00  0.00           N
ATOM   2365  CA  MET A 155      -2.679 -22.083  -2.887  1.00  0.00           C
ATOM   2366  C   MET A 155      -2.476 -22.312  -1.389  1.00  0.00           C
ATOM   2367  O   MET A 155      -1.535 -22.984  -0.970  1.00  0.00           O
ATOM   2381  N   ASN A 156      -3.407 -21.783  -0.603  1.00  0.00           N
ATOM   2382  CA  ASN A 156      -3.384 -21.962   0.841  1.00  0.00           C
ATOM   2383  C   ASN A 156      -4.433 -23.004   1.212  1.00  0.00           C
ATOM   2384  O   ASN A 156      -5.636 -22.786   1.041  1.00  0.00           O
ATOM   2395  N   PHE A 157      -3.964 -24.130   1.713  1.00  0.00           N
ATOM   2396  CA  PHE A 157      -4.859 -25.216   2.099  1.00  0.00           C
ATOM   2397  C   PHE A 157      -4.926 -25.366   3.609  1.00  0.00           C
ATOM   2398  O   PHE A 157      -4.081 -26.013   4.215  1.00  0.00           O
ATOM   2415  N   GLU A 158      -5.931 -24.754   4.210  1.00  0.00           N
ATOM   2416  CA  GLU A 158      -6.103 -24.846   5.660  1.00  0.00           C
ATOM   2417  C   GLU A 158      -6.634 -26.241   5.985  1.00  0.00           C
ATOM   2418  O   GLU A 158      -7.815 -26.521   5.821  1.00  0.00           O
ATOM   2430  N   THR A 159      -5.738 -27.141   6.386  1.00  0.00           N
ATOM   2431  CA  THR A 159      -6.130 -28.533   6.651  1.00  0.00           C
ATOM   2432  C   THR A 159      -7.046 -28.694   7.871  1.00  0.00           C
ATOM   2433  O   THR A 159      -7.897 -29.583   7.881  1.00  0.00           O
ATOM   2444  N   ALA A 160      -6.882 -27.864   8.899  1.00  0.00           N
ATOM   2445  CA  ALA A 160      -7.730 -28.005  10.085  1.00  0.00           C
ATOM   2446  C   ALA A 160      -9.191 -27.837   9.693  1.00  0.00           C
ATOM   2447  O   ALA A 160     -10.060 -28.577  10.152  1.00  0.00           O
ATOM   2454  N   LYS A 161      -9.442 -26.882   8.808  1.00  0.00           N
ATOM   2455  CA  LYS A 161     -10.793 -26.641   8.315  1.00  0.00           C
ATOM   2456  C   LYS A 161     -10.938 -27.323   6.959  1.00  0.00           C
ATOM   2457  O   LYS A 161     -12.037 -27.464   6.427  1.00  0.00           O
ATOM   2476  N   SER A 162      -9.798 -27.710   6.404  1.00  0.00           N
ATOM   2477  CA  SER A 162      -9.751 -28.344   5.089  1.00  0.00           C
ATOM   2478  C   SER A 162     -10.431 -27.436   4.076  1.00  0.00           C
ATOM   2479  O   SER A 162     -11.321 -27.858   3.339  1.00  0.00           O
ATOM   2487  N   ARG A 163     -10.004 -26.171   4.063  1.00  0.00           N
ATOM   2488  CA  ARG A 163     -10.569 -25.181   3.156  1.00  0.00           C
ATOM   2489  C   ARG A 163      -9.485 -24.455   2.369  1.00  0.00           C
ATOM   2490  O   ARG A 163      -8.465 -24.043   2.926  1.00  0.00           O
ATOM   2511  N   VAL A 164      -9.759 -24.231   1.090  1.00  0.00           N
ATOM   2512  CA  VAL A 164      -8.868 -23.477   0.250  1.00  0.00           C
ATOM   2513  C   VAL A 164      -9.521 -22.123   0.070  1.00  0.00           C
ATOM   2514  O   VAL A 164     -10.478 -21.978  -0.693  1.00  0.00           O
ATOM   2527  N   THR A 165      -9.027 -21.158   0.801  1.00  0.00           N
```


Dieses Werk ist copyrightgeschützt und darf in keiner Form vervielfältigt werden noch an Dritte weitergegeben werden.
Es gilt nur für den persönlichen Gebrauch.

```
ATOM   2528  CA  THR A 165      -9.591 -19.807   0.754  1.00  0.00           C
ATOM   2529  C   THR A 165      -8.547 -18.804   0.315  1.00  0.00           C
ATOM   2530  O   THR A 165      -8.709 -18.067  -0.659  1.00  0.00           O
ATOM   2541  N   GLN A 166      -7.484 -18.792   1.073  1.00  0.00           N
ATOM   2542  CA  GLN A 166      -6.383 -17.885   0.809  1.00  0.00           C
ATOM   2543  C   GLN A 166      -5.644 -18.285  -0.467  1.00  0.00           C
ATOM   2544  O   GLN A 166      -4.927 -19.288  -0.503  1.00  0.00           O
ATOM   2558  N   SER A 167      -5.813 -17.477  -1.508  1.00  0.00           N
ATOM   2559  CA  SER A 167      -5.148 -17.727  -2.782  1.00  0.00           C
ATOM   2560  C   SER A 167      -4.660 -16.407  -3.374  1.00  0.00           C
ATOM   2561  O   SER A 167      -5.341 -15.385  -3.264  1.00  0.00           O
ATOM   2569  N   ASN A 168      -3.463 -16.424  -3.967  1.00  0.00           N
ATOM   2570  CA  ASN A 168      -2.891 -15.211  -4.535  1.00  0.00           C
ATOM   2571  C   ASN A 168      -2.434 -15.414  -5.985  1.00  0.00           C
ATOM   2572  O   ASN A 168      -1.562 -16.239  -6.262  1.00  0.00           O
ATOM   2583  N   PHE A 169      -3.006 -14.627  -6.900  1.00  0.00           N
ATOM   2584  CA  PHE A 169      -2.630 -14.697  -8.318  1.00  0.00           C
ATOM   2585  C   PHE A 169      -1.537 -13.671  -8.598  1.00  0.00           C
ATOM   2586  O   PHE A 169      -1.794 -12.473  -8.530  1.00  0.00           O
ATOM   2603  N   ALA A 170      -0.342 -14.121  -8.944  1.00  0.00           N
ATOM   2604  CA  ALA A 170       0.730 -13.186  -9.257  1.00  0.00           C
ATOM   2605  C   ALA A 170       0.752 -12.912 -10.747  1.00  0.00           C
ATOM   2606  O   ALA A 170       0.745 -13.837 -11.524  1.00  0.00           O
ATOM   2613  N   VAL A 171       0.814 -11.647 -11.137  1.00  0.00           N
ATOM   2614  CA  VAL A 171       0.887 -11.300 -12.555  1.00  0.00           C
ATOM   2615  C   VAL A 171       2.011 -10.287 -12.754  1.00  0.00           C
ATOM   2616  O   VAL A 171       2.053  -9.258 -12.077  1.00  0.00           O
ATOM   2629  N   GLY A 172       2.931 -10.602 -13.664  1.00  0.00           N
ATOM   2630  CA  GLY A 172       4.038  -9.719 -13.909  1.00  0.00           C
ATOM   2631  C   GLY A 172       4.339  -9.548 -15.383  1.00  0.00           C
ATOM   2632  O   GLY A 172       4.208 -10.475 -16.185  1.00  0.00           O
ATOM   2636  N   TYR A 173       4.781  -8.345 -15.703  1.00  0.00           N
ATOM   2637  CA  TYR A 173       5.154  -7.987 -17.060  1.00  0.00           C
ATOM   2638  C   TYR A 173       6.545  -7.382 -17.031  1.00  0.00           C
ATOM   2639  O   TYR A 173       6.824  -6.501 -16.219  1.00  0.00           O
ATOM   2657  N   LYS A 174       7.431  -7.887 -17.864  1.00  0.00           N
ATOM   2658  CA  LYS A 174       8.812  -7.414 -17.869  1.00  0.00           C
ATOM   2659  C   LYS A 174       9.085  -6.264 -18.845  1.00  0.00           C
ATOM   2660  O   LYS A 174       8.547  -6.191 -19.947  1.00  0.00           O
ATOM   2679  N   THR A 175       9.993  -5.415 -18.409  1.00  0.00           N
ATOM   2680  CA  THR A 175      10.467  -4.272 -19.177  1.00  0.00           C
ATOM   2681  C   THR A 175      11.982  -4.173 -18.967  1.00  0.00           C
ATOM   2682  O   THR A 175      12.484  -4.630 -17.940  1.00  0.00           O
ATOM   2693  N   ASP A 176      12.715  -3.632 -19.938  1.00  0.00           N
ATOM   2694  CA  ASP A 176      14.178  -3.558 -19.819  1.00  0.00           C
ATOM   2695  C   ASP A 176      14.615  -3.233 -18.393  1.00  0.00           C
ATOM   2696  O   ASP A 176      14.234  -2.197 -17.846  1.00  0.00           O
ATOM   2705  N   GLU A 177      15.411  -4.136 -17.798  1.00  0.00           N
ATOM   2706  CA  GLU A 177      15.912  -3.957 -16.425  1.00  0.00           C
ATOM   2707  C   GLU A 177      14.785  -3.837 -15.396  1.00  0.00           C
ATOM   2708  O   GLU A 177      15.024  -3.943 -14.186  1.00  0.00           O
ATOM   2720  N   PHE A 178      13.586  -3.510 -15.867  1.00  0.00           N
ATOM   2721  CA  PHE A 178      12.459  -3.277 -14.972  1.00  0.00           C
ATOM   2722  C   PHE A 178      11.470  -4.457 -14.956  1.00  0.00           C
ATOM   2723  O   PHE A 178      11.100  -4.966 -16.007  1.00  0.00           O
ATOM   2740  N   GLN A 179      10.999  -4.848 -13.753  1.00  0.00           N
ATOM   2741  CA  GLN A 179       9.995  -5.923 -13.618  1.00  0.00           C
ATOM   2742  C   GLN A 179       8.699  -5.378 -13.017  1.00  0.00           C
ATOM   2743  O   GLN A 179       8.746  -4.613 -12.048  1.00  0.00           O
ATOM   2757  N   LEU A 180       7.556  -5.852 -13.528  1.00  0.00           N
ATOM   2758  CA  LEU A 180       6.255  -5.457 -12.979  1.00  0.00           C
ATOM   2759  C   LEU A 180       5.676  -6.641 -12.221  1.00  0.00           C
ATOM   2760  O   LEU A 180       5.324  -7.635 -12.824  1.00  0.00           O
ATOM   2776  N   HIS A 181       5.619  -6.528 -10.899  1.00  0.00           N
ATOM   2777  CA  HIS A 181       5.096  -7.604 -10.054  1.00  0.00           C
ATOM   2778  C   HIS A 181       3.863  -7.155  -9.250  1.00  0.00           C
ATOM   2779  O   HIS A 181       3.959  -6.268  -8.399  1.00  0.00           O
ATOM   2793  N   THR A 182       2.723  -7.802  -9.494  1.00  0.00           N
ATOM   2794  CA  THR A 182       1.478  -7.501  -8.760  1.00  0.00           C
ATOM   2795  C   THR A 182       0.825  -8.803  -8.325  1.00  0.00           C
ATOM   2796  O   THR A 182       1.031  -9.822  -8.995  1.00  0.00           O
ATOM   2807  N   ASN A 183       0.016  -8.818  -7.239  1.00  0.00           N
ATOM   2808  CA  ASN A 183      -0.631 -10.049  -6.846  1.00  0.00           C
ATOM   2809  C   ASN A 183      -2.057  -9.757  -6.404  1.00  0.00           C
ATOM   2810  O   ASN A 183      -2.301  -8.808  -5.660  1.00  0.00           O
ATOM   2821  N   VAL A 184      -2.990 -10.589  -6.837  1.00  0.00           N
ATOM   2822  CA  VAL A 184      -4.375 -10.404  -6.444  1.00  0.00           C
ATOM   2823  C   VAL A 184      -4.580 -11.212  -5.199  1.00  0.00           C
ATOM   2824  O   VAL A 184      -4.419 -12.429  -5.224  1.00  0.00           O
ATOM   2837  N   ASN A 185      -4.915 -10.550  -4.105  1.00  0.00           N
ATOM   2838  CA  ASN A 185      -5.104 -11.245  -2.868  1.00  0.00           C
ATOM   2839  C   ASN A 185      -6.568 -11.517  -2.644  1.00  0.00           C
ATOM   2840  O   ASN A 185      -7.344 -10.581  -2.448  1.00  0.00           O
ATOM   2851  N   ASP A 186      -6.901 -12.800  -2.711  1.00  0.00           N
ATOM   2852  CA  ASP A 186      -8.272 -13.283  -2.508  1.00  0.00           C
ATOM   2853  C   ASP A 186      -9.289 -12.582  -3.405  1.00  0.00           C
ATOM   2854  O   ASP A 186     -10.477 -12.546  -3.077  1.00  0.00           O
ATOM   2863  N   GLY A 187      -8.844 -12.040  -4.533  1.00  0.00           N
ATOM   2864  CA  GLY A 187      -9.771 -11.364  -5.433  1.00  0.00           C
ATOM   2865  C   GLY A 187     -10.274 -10.074  -4.802  1.00  0.00           C
ATOM   2866  O   GLY A 187     -11.314  -9.550  -5.200  1.00  0.00           O
ATOM   2870  N   THR A 188      -9.561  -9.604  -3.777  1.00  0.00           N
ATOM   2871  CA  THR A 188      -9.979  -8.412  -3.051  1.00  0.00           C
ATOM   2872  C   THR A 188      -8.919  -7.296  -3.046  1.00  0.00           C
```


Dieses Werk ist copyrightgeschützt und darf in keiner Form vervielfältigt werden noch an Dritte weitergegeben werden.
Es gilt nur für den persönlichen Gebrauch.

```
ATOM   2873  O   THR A 188      -9.142  -6.232  -3.624  1.00  0.00           O
ATOM   2884  N   GLU A 189      -7.788  -7.506  -2.373  1.00  0.00           N
ATOM   2885  CA  GLU A 189      -6.759  -6.442  -2.316  1.00  0.00           C
ATOM   2886  C   GLU A 189      -5.514  -6.776  -3.140  1.00  0.00           C
ATOM   2887  O   GLU A 189      -4.889  -7.813  -2.929  1.00  0.00           O
ATOM   2899  N   PHE A 190      -5.139  -5.884  -4.073  1.00  0.00           N
ATOM   2900  CA  PHE A 190      -3.959  -6.095  -4.903  1.00  0.00           C
ATOM   2901  C   PHE A 190      -2.726  -5.488  -4.239  1.00  0.00           C
ATOM   2902  O   PHE A 190      -2.823  -4.494  -3.516  1.00  0.00           O
ATOM   2919  N   GLY A 191      -1.566  -6.075  -4.509  1.00  0.00           N
ATOM   2920  CA  GLY A 191      -0.319  -5.565  -3.944  1.00  0.00           C
ATOM   2921  C   GLY A 191       0.896  -6.273  -4.518  1.00  0.00           C
ATOM   2922  O   GLY A 191       0.846  -7.472  -4.806  1.00  0.00           O
ATOM   2926  N   GLY A 192       2.008  -5.540  -4.683  1.00  0.00           N
ATOM   2927  CA  GLY A 192       3.216  -6.124  -5.266  1.00  0.00           C
ATOM   2928  C   GLY A 192       4.395  -5.149  -5.219  1.00  0.00           C
ATOM   2929  O   GLY A 192       4.372  -4.244  -4.364  1.00  0.00           O
ATOM   2933  N   SER A 193       5.361  -5.361  -6.097  1.00  0.00           N
ATOM   2934  CA  SER A 193       6.540  -4.491  -6.274  1.00  0.00           C
ATOM   2935  C   SER A 193       6.917  -4.322  -7.736  1.00  0.00           C
ATOM   2936  O   SER A 193       6.329  -5.092  -8.529  1.00  0.00           O
ATOM   2944  N   ILE A 194       7.787  -3.338  -8.017  1.00  0.00           N
ATOM   2945  CA  ILE A 194       8.346  -3.094  -9.329  1.00  0.00           C
ATOM   2946  C   ILE A 194       9.858  -3.072  -9.167  1.00  0.00           C
ATOM   2947  O   ILE A 194      10.388  -2.170  -8.529  1.00  0.00           O
ATOM   2963  N   TYR A 195      10.562  -4.092  -9.644  1.00  0.00           N
ATOM   2964  CA  TYR A 195      12.038  -4.159  -9.565  1.00  0.00           C
ATOM   2965  C   TYR A 195      12.611  -3.216 -10.598  1.00  0.00           C
ATOM   2966  O   TYR A 195      12.321  -3.387 -11.773  1.00  0.00           O
ATOM   2984  N   GLN A 196      13.368  -2.209 -10.289  1.00  0.00           N
ATOM   2985  CA  GLN A 196      13.966  -1.329 -11.279  1.00  0.00           C
ATOM   2986  C   GLN A 196      15.481  -1.223 -11.138  1.00  0.00           C
ATOM   2987  O   GLN A 196      15.970  -0.445 -10.317  1.00  0.00           O
ATOM   3001  N   LYS A 197      16.248  -1.997 -11.926  1.00  0.00           N
ATOM   3002  CA  LYS A 197      17.711  -1.858 -11.931  1.00  0.00           C
ATOM   3003  C   LYS A 197      17.931  -0.572 -12.727  1.00  0.00           C
ATOM   3004  O   LYS A 197      17.925  -0.585 -13.955  1.00  0.00           O
ATOM   3023  N   VAL A 198      18.142   0.596 -12.216  1.00  0.00           N
ATOM   3024  CA  VAL A 198      18.332   1.852 -12.923  1.00  0.00           C
ATOM   3025  C   VAL A 198      19.721   1.974 -13.518  1.00  0.00           C
ATOM   3026  O   VAL A 198      19.888   2.434 -14.648  1.00  0.00           O
ATOM   3039  N   ASN A 199      20.709   1.554 -12.760  1.00  0.00           N
ATOM   3040  CA  ASN A 199      22.090   1.604 -13.222  1.00  0.00           C
ATOM   3041  C   ASN A 199      22.961   0.806 -12.263  1.00  0.00           C
ATOM   3042  O   ASN A 199      22.443   0.082 -11.417  1.00  0.00           O
ATOM   3053  N   LYS A 200      24.270   0.915 -12.404  1.00  0.00           N
ATOM   3054  CA  LYS A 200      25.175   0.161 -11.541  1.00  0.00           C
ATOM   3055  C   LYS A 200      25.020   0.555 -10.069  1.00  0.00           C
ATOM   3056  O   LYS A 200      25.052  -0.303  -9.190  1.00  0.00           O
ATOM   3075  N   LYS A 201      24.889   1.851  -9.798  1.00  0.00           N
ATOM   3076  CA  LYS A 201      24.779   2.316  -8.413  1.00  0.00           C
ATOM   3077  C   LYS A 201      23.336   2.566  -7.949  1.00  0.00           C
ATOM   3078  O   LYS A 201      23.133   2.906  -6.784  1.00  0.00           O
ATOM   3097  N   LEU A 202      22.361   2.638  -8.841  1.00  0.00           N
ATOM   3098  CA  LEU A 202      20.919   2.970  -8.697  1.00  0.00           C
ATOM   3099  C   LEU A 202      20.032   1.783  -9.083  1.00  0.00           C
ATOM   3100  O   LEU A 202      19.504   1.643 -10.211  1.00  0.00           O
ATOM   3116  N   GLU A 203      19.895   0.942  -8.075  1.00  0.00           N
ATOM   3117  CA  GLU A 203      18.837  -0.052  -7.986  1.00  0.00           C
ATOM   3118  C   GLU A 203      17.679   0.615  -7.240  1.00  0.00           C
ATOM   3119  O   GLU A 203      18.052   1.199  -6.182  1.00  0.00           O
ATOM   3131  N   THR A 204      16.446   0.550  -7.649  1.00  0.00           N
ATOM   3132  CA  THR A 204      15.269   1.221  -7.036  1.00  0.00           C
ATOM   3133  C   THR A 204      14.128   0.207  -6.929  1.00  0.00           C
ATOM   3134  O   THR A 204      14.407  -0.892  -7.497  1.00  0.00           O
ATOM   3145  N   ALA A 205      12.999   0.457  -6.241  1.00  0.00           N
ATOM   3146  CA  ALA A 205      11.943  -0.551  -6.150  1.00  0.00           C
ATOM   3147  C   ALA A 205      10.552   0.021  -5.835  1.00  0.00           C
ATOM   3148  O   ALA A 205      10.247   0.248  -4.661  1.00  0.00           O
ATOM   3155  N   VAL A 206       9.650   0.162  -6.828  1.00  0.00           N
ATOM   3156  CA  VAL A 206       8.400   0.929  -6.631  1.00  0.00           C
ATOM   3157  C   VAL A 206       7.383  -0.077  -6.034  1.00  0.00           C
ATOM   3158  O   VAL A 206       7.233  -1.106  -6.746  1.00  0.00           O
ATOM   3171  N   ASN A 207       6.744   0.113  -4.908  1.00  0.00           N
ATOM   3172  CA  ASN A 207       5.632  -0.739  -4.418  1.00  0.00           C
ATOM   3173  C   ASN A 207       4.321  -0.198  -4.963  1.00  0.00           C
ATOM   3174  O   ASN A 207       4.253   0.980  -4.876  1.00  0.00           O
ATOM   3185  N   LEU A 208       3.413  -1.026  -5.468  1.00  0.00           N
ATOM   3186  CA  LEU A 208       2.007  -0.675  -5.829  1.00  0.00           C
ATOM   3187  C   LEU A 208       1.042  -1.405  -4.890  1.00  0.00           C
ATOM   3188  O   LEU A 208       1.396  -2.543  -4.596  1.00  0.00           O
ATOM   3204  N   ALA A 209      -0.044  -0.802  -4.422  1.00  0.00           N
ATOM   3205  CA  ALA A 209      -1.072  -1.509  -3.641  1.00  0.00           C
ATOM   3206  C   ALA A 209      -2.434  -0.833  -3.756  1.00  0.00           C
ATOM   3207  O   ALA A 209      -2.432   0.350  -3.389  1.00  0.00           O
ATOM   3214  N   TRP A 210      -3.483  -1.529  -4.202  1.00  0.00           N
ATOM   3215  CA  TRP A 210      -4.814  -0.936  -4.341  1.00  0.00           C
ATOM   3216  C   TRP A 210      -5.828  -1.858  -3.675  1.00  0.00           C
ATOM   3217  O   TRP A 210      -5.715  -3.082  -3.744  1.00  0.00           O
ATOM   3238  N   THR A 211      -6.906  -1.366  -3.850  1.00  0.00           N
ATOM   3239  CA  THR A 211      -8.006  -2.167  -3.318  1.00  0.00           C
ATOM   3240  C   THR A 211      -9.174  -2.227  -4.277  1.00  0.00           C
ATOM   3241  O   THR A 211      -9.792  -1.203  -4.562  1.00  0.00           O
ATOM   3252  N   ALA A 212      -9.477  -3.429  -4.787  1.00  0.00           N
```


Dieses Werk ist copyrightgeschützt und darf in keiner Form vervielfältigt werden noch an Dritte weitergegeben werden.
Es gilt nur für den persönlichen Gebrauch.

```
ATOM   3253  CA  ALA A 212     -10.588  -3.552  -5.726  1.00  0.00           C
ATOM   3254  C   ALA A 212     -11.768  -2.717  -5.271  1.00  0.00           C
ATOM   3255  O   ALA A 212     -12.536  -3.111  -4.390  1.00  0.00           O
ATOM   3262  N   GLY A 213     -11.884  -1.560  -5.900  1.00  0.00           N
ATOM   3263  CA  GLY A 213     -12.937  -0.612  -5.617  1.00  0.00           C
ATOM   3264  C   GLY A 213     -12.674   0.663  -6.412  1.00  0.00           C
ATOM   3265  O   GLY A 213     -11.939   0.645  -7.399  1.00  0.00           O
ATOM   3269  N   ASN A 214     -13.247   1.769  -5.982  1.00  0.00           N
ATOM   3270  CA  ASN A 214     -13.027   3.023  -6.681  1.00  0.00           C
ATOM   3271  C   ASN A 214     -11.962   3.828  -5.941  1.00  0.00           C
ATOM   3272  O   ASN A 214     -11.758   5.005  -6.217  1.00  0.00           O
ATOM   3283  N   SER A 215     -11.309   3.181  -4.970  1.00  0.00           N
ATOM   3284  CA  SER A 215     -10.293   3.847  -4.155  1.00  0.00           C
ATOM   3285  C   SER A 215      -8.939   3.989  -4.875  1.00  0.00           C
ATOM   3286  O   SER A 215      -8.708   3.375  -5.915  1.00  0.00           O
ATOM   3294  N   ASN A 216      -8.095   4.959  -4.372  1.00  0.00           N
ATOM   3295  CA  ASN A 216      -6.775   5.140  -4.995  1.00  0.00           C
ATOM   3296  C   ASN A 216      -5.776   4.040  -4.647  1.00  0.00           C
ATOM   3297  O   ASN A 216      -5.982   3.261  -3.715  1.00  0.00           O
ATOM   3308  N   THR A 217      -4.685   4.022  -5.429  1.00  0.00           N
ATOM   3309  CA  THR A 217      -3.516   3.186  -5.175  1.00  0.00           C
ATOM   3310  C   THR A 217      -2.557   3.937  -4.237  1.00  0.00           C
ATOM   3311  O   THR A 217      -2.000   4.960  -4.639  1.00  0.00           O
ATOM   3322  N   ARG A 218      -2.343   3.443  -3.023  1.00  0.00           N
ATOM   3323  CA  ARG A 218      -1.154   3.820  -2.258  1.00  0.00           C
ATOM   3324  C   ARG A 218       0.032   3.193  -2.975  1.00  0.00           C
ATOM   3325  O   ARG A 218      -0.115   1.981  -3.201  1.00  0.00           O
ATOM   3346  N   PHE A 219       1.083   3.929  -3.308  1.00  0.00           N
ATOM   3347  CA  PHE A 219       2.267   3.394  -4.001  1.00  0.00           C
ATOM   3348  C   PHE A 219       3.529   4.070  -3.505  1.00  0.00           C
ATOM   3349  O   PHE A 219       3.490   5.290  -3.403  1.00  0.00           O
ATOM   3366  N   GLY A 220       4.552   3.300  -3.215  1.00  0.00           N
ATOM   3367  CA  GLY A 220       5.882   3.764  -2.826  1.00  0.00           C
ATOM   3368  C   GLY A 220       6.778   3.821  -4.027  1.00  0.00           C
ATOM   3369  O   GLY A 220       6.937   2.728  -4.442  1.00  0.00           O
ATOM   3373  N   ILE A 221       7.273   4.983  -4.438  1.00  0.00           N
ATOM   3374  CA  ILE A 221       8.528   5.071  -5.201  1.00  0.00           C
ATOM   3375  C   ILE A 221       9.551   5.065  -4.128  1.00  0.00           C
ATOM   3376  O   ILE A 221       9.319   5.771  -3.121  1.00  0.00           O
ATOM   3392  N   ALA A 222      10.599   4.323  -4.343  1.00  0.00           N
ATOM   3393  CA  ALA A 222      11.601   4.170  -3.336  1.00  0.00           C
ATOM   3394  C   ALA A 222      12.947   4.084  -4.029  1.00  0.00           C
ATOM   3395  O   ALA A 222      12.823   3.592  -5.184  1.00  0.00           O
ATOM   3402  N   ALA A 223      14.079   4.504  -3.545  1.00  0.00           N
ATOM   3403  CA  ALA A 223      15.376   4.424  -4.252  1.00  0.00           C
ATOM   3404  C   ALA A 223      16.577   4.324  -3.306  1.00  0.00           C
ATOM   3405  O   ALA A 223      16.590   5.142  -2.404  1.00  0.00           O
ATOM   3412  N   LYS A 224      17.522   3.436  -3.564  1.00  0.00           N
ATOM   3413  CA  LYS A 224      18.758   3.186  -2.804  1.00  0.00           C
ATOM   3414  C   LYS A 224      19.881   3.585  -3.771  1.00  0.00           C
ATOM   3415  O   LYS A 224      20.186   2.760  -4.660  1.00  0.00           O
ATOM   3434  N   TYR A 225      20.451   4.760  -3.583  1.00  0.00           N
ATOM   3435  CA  TYR A 225      21.607   5.268  -4.336  1.00  0.00           C
ATOM   3436  C   TYR A 225      22.910   5.030  -3.593  1.00  0.00           C
ATOM   3437  O   TYR A 225      23.168   5.809  -2.678  1.00  0.00           O
ATOM   3455  N   GLN A 226      23.682   4.054  -4.000  1.00  0.00           N
ATOM   3456  CA  GLN A 226      25.000   3.807  -3.450  1.00  0.00           C
ATOM   3457  C   GLN A 226      25.852   4.916  -4.001  1.00  0.00           C
ATOM   3458  O   GLN A 226      26.089   5.009  -5.087  1.00  0.00           O
ATOM   3472  N   ILE A 227      26.411   5.763  -3.177  1.00  0.00           N
ATOM   3473  CA  ILE A 227      27.132   6.880  -3.597  1.00  0.00           C
ATOM   3474  C   ILE A 227      28.558   6.544  -4.043  1.00  0.00           C
ATOM   3475  O   ILE A 227      28.966   6.747  -5.197  1.00  0.00           O
ATOM   3491  N   ASP A 228      29.257   5.980  -3.060  1.00  0.00           N
ATOM   3492  CA  ASP A 228      30.636   5.510  -3.178  1.00  0.00           C
ATOM   3493  C   ASP A 228      30.658   4.284  -2.291  1.00  0.00           C
ATOM   3494  O   ASP A 228      29.630   3.967  -1.698  1.00  0.00           O
ATOM   3503  N   PRO A 229      31.713   3.556  -2.192  1.00  0.00           N
ATOM   3504  CA  PRO A 229      31.693   2.320  -1.376  1.00  0.00           C
ATOM   3505  C   PRO A 229      31.456   2.595   0.112  1.00  0.00           C
ATOM   3506  O   PRO A 229      31.157   1.671   0.867  1.00  0.00           O
ATOM   3517  N   ASP A 230      31.636   3.852   0.537  1.00  0.00           N
ATOM   3518  CA  ASP A 230      31.489   4.208   1.943  1.00  0.00           C
ATOM   3519  C   ASP A 230      30.219   5.020   2.244  1.00  0.00           C
ATOM   3520  O   ASP A 230      30.035   5.439   3.384  1.00  0.00           O
ATOM   3529  N   ALA A 231      29.294   5.277   1.322  1.00  0.00           N
ATOM   3530  CA  ALA A 231      28.023   5.983   1.637  1.00  0.00           C
ATOM   3531  C   ALA A 231      26.885   5.482   0.733  1.00  0.00           C
ATOM   3532  O   ALA A 231      27.223   4.980  -0.357  1.00  0.00           O
ATOM   3539  N   CYS A 232      25.637   5.538   1.213  1.00  0.00           N
ATOM   3540  CA  CYS A 232      24.417   5.227   0.436  1.00  0.00           C
ATOM   3541  C   CYS A 232      23.279   6.209   0.820  1.00  0.00           C
ATOM   3542  O   CYS A 232      23.135   6.409   2.031  1.00  0.00           O
ATOM   3550  N   PHE A 233      22.553   6.768  -0.146  1.00  0.00           N
ATOM   3551  CA  PHE A 233      21.319   7.575   0.066  1.00  0.00           C
ATOM   3552  C   PHE A 233      20.076   6.748  -0.305  1.00  0.00           C
ATOM   3553  O   PHE A 233      20.126   5.941  -1.234  1.00  0.00           O
ATOM   3570  N   SER A 234      19.024   6.965   0.428  1.00  0.00           N
ATOM   3571  CA  SER A 234      17.831   6.180   0.721  1.00  0.00           C
ATOM   3572  C   SER A 234      16.665   7.211   0.777  1.00  0.00           C
ATOM   3573  O   SER A 234      16.717   7.932   1.771  1.00  0.00           O
ATOM   3581  N   ALA A 235      15.696   7.294  -0.149  1.00  0.00           N
ATOM   3582  CA  ALA A 235      14.668   8.372  -0.139  1.00  0.00           C
ATOM   3583  C   ALA A 235      13.471   8.194  -1.049  1.00  0.00           C
```


Dieses Werk ist copyrightgeschützt und darf in keiner Form vervielfältigt werden noch an Dritte weitergegeben werden.
Es gilt nur für den persönlichen Gebrauch.

```
ATOM   3584  O   ALA A 235      13.714   7.845  -2.214  1.00  0.00           O
ATOM   3591  N   LYS A 236      11.751   8.349  -0.061  1.00  0.00           N
ATOM   3592  CA  LYS A 236      11.059   7.182  -0.597  1.00  0.00           C
ATOM   3593  C   LYS A 236       9.547   7.342  -0.416  1.00  0.00           C
ATOM   3594  O   LYS A 236       9.111   8.051   0.497  1.00  0.00           O
ATOM   3613  N   VAL A 237       8.929   7.748  -1.310  1.00  0.00           N
ATOM   3614  CA  VAL A 237       7.739   8.647  -1.340  1.00  0.00           C
ATOM   3615  C   VAL A 237       6.488   7.804  -1.543  1.00  0.00           C
ATOM   3616  O   VAL A 237       6.289   7.294  -2.625  1.00  0.00           O
ATOM   3629  N   ASN A 238       5.637   7.651  -0.503  1.00  0.00           N
ATOM   3630  CA  ASN A 238       4.424   6.820  -0.618  1.00  0.00           C
ATOM   3631  C   ASN A 238       3.458   7.657  -1.385  1.00  0.00           C
ATOM   3632  O   ASN A 238       3.585   8.768  -1.605  1.00  0.00           O
ATOM   3643  N   ASN A 239       2.370   7.656  -1.940  1.00  0.00           N
ATOM   3644  CA  ASN A 239       1.404   8.476  -2.690  1.00  0.00           C
ATOM   3645  C   ASN A 239       0.425   9.203  -1.749  1.00  0.00           C
ATOM   3646  O   ASN A 239       0.015  10.306  -2.143  1.00  0.00           O
ATOM   3657  N   SER A 240       0.130   8.704  -0.550  1.00  0.00           N
ATOM   3658  CA  SER A 240      -0.500   9.510   0.516  1.00  0.00           C
ATOM   3659  C   SER A 240       0.435  10.615   1.049  1.00  0.00           C
ATOM   3660  O   SER A 240      -0.155  11.321   1.934  1.00  0.00           O
ATOM   3668  N   SER A 241       1.633  10.867   0.637  1.00  0.00           N
ATOM   3669  CA  SER A 241       2.517  12.058   0.566  1.00  0.00           C
ATOM   3670  C   SER A 241       3.598  12.040   1.669  1.00  0.00           C
ATOM   3671  O   SER A 241       3.939  13.096   2.167  1.00  0.00           O
ATOM   3679  N   LEU A 242       4.204  11.016   2.136  1.00  0.00           N
ATOM   3680  CA  LEU A 242       5.268  10.762   3.125  1.00  0.00           C
ATOM   3681  C   LEU A 242       6.582  10.579   2.359  1.00  0.00           C
ATOM   3682  O   LEU A 242       6.969   9.468   1.984  1.00  0.00           O
ATOM   3698  N   ILE A 243       7.279  11.704   2.117  1.00  0.00           N
ATOM   3699  CA  ILE A 243       8.571  11.714   1.389  1.00  0.00           C
ATOM   3700  C   ILE A 243       9.620  11.446   2.465  1.00  0.00           C
ATOM   3701  O   ILE A 243       9.950  12.317   3.262  1.00  0.00           O
ATOM   3717  N   GLY A 244      10.132  10.188   2.525  1.00  0.00           N
ATOM   3718  CA  GLY A 244      11.289   9.850   3.327  1.00  0.00           C
ATOM   3719  C   GLY A 244      12.554  10.456   2.716  1.00  0.00           C
ATOM   3720  O   GLY A 244      12.574  10.798   1.531  1.00  0.00           O
ATOM   3724  N   LEU A 245      13.598  10.527   3.531  1.00  0.00           N
ATOM   3725  CA  LEU A 245      14.996  10.724   3.108  1.00  0.00           C
ATOM   3726  C   LEU A 245      15.912   9.852   3.955  1.00  0.00           C
ATOM   3727  O   LEU A 245      15.668   9.720   5.159  1.00  0.00           O
ATOM   3743  N   GLY A 246      17.032   9.321   4.134  1.00  0.00           N
ATOM   3744  CA  GLY A 246      17.603   8.241   4.999  1.00  0.00           C
ATOM   3745  C   GLY A 246      19.137   8.080   4.954  1.00  0.00           C
ATOM   3746  O   GLY A 246      19.580   6.929   4.914  1.00  0.00           O
ATOM   3750  N   TYR A 247      19.933   9.148   5.047  1.00  0.00           N
ATOM   3751  CA  TYR A 247      21.306   9.176   4.487  1.00  0.00           C
ATOM   3752  C   TYR A 247      22.298   8.307   5.282  1.00  0.00           C
ATOM   3753  O   TYR A 247      22.475   8.635   6.453  1.00  0.00           O
ATOM   3771  N   THR A 248      22.879   7.258   4.694  1.00  0.00           N
ATOM   3772  CA  THR A 248      23.733   6.249   5.375  1.00  0.00           C
ATOM   3773  C   THR A 248      25.201   6.500   4.997  1.00  0.00           C
ATOM   3774  O   THR A 248      25.413   6.717   3.793  1.00  0.00           O
ATOM   3785  N   GLN A 249      26.119   6.464   5.956  1.00  0.00           N
ATOM   3786  CA  GLN A 249      27.560   6.692   5.798  1.00  0.00           C
ATOM   3787  C   GLN A 249      28.373   5.562   6.455  1.00  0.00           C
ATOM   3788  O   GLN A 249      28.690   5.662   7.639  1.00  0.00           O
ATOM   3802  N   THR A 250      28.771   4.553   5.695  1.00  0.00           N
ATOM   3803  CA  THR A 250      29.538   3.398   6.190  1.00  0.00           C
ATOM   3804  C   THR A 250      31.023   3.791   6.129  1.00  0.00           C
ATOM   3805  O   THR A 250      31.618   3.642   5.079  1.00  0.00           O
ATOM   3816  N   LEU A 251      31.662   4.155   7.236  1.00  0.00           N
ATOM   3817  CA  LEU A 251      33.087   4.516   7.175  1.00  0.00           C
ATOM   3818  C   LEU A 251      33.936   3.239   7.092  1.00  0.00           C
ATOM   3819  O   LEU A 251      33.404   2.251   7.653  1.00  0.00           O
ATOM   3835  N   LYS A 252      35.104   3.216   6.418  1.00  0.00           N
ATOM   3836  CA  LYS A 252      36.104   2.123   6.415  1.00  0.00           C
ATOM   3837  C   LYS A 252      36.418   1.782   7.873  1.00  0.00           C
ATOM   3838  O   LYS A 252      36.292   0.628   8.291  1.00  0.00           O
ATOM   3857  N   PRO A 253      36.806   2.763   8.660  1.00  0.00           N
ATOM   3858  CA  PRO A 253      37.097   2.561  10.105  1.00  0.00           C
ATOM   3859  C   PRO A 253      36.116   1.585  10.776  1.00  0.00           C
ATOM   3860  O   PRO A 253      36.391   1.078  11.859  1.00  0.00           O
ATOM   3871  N   GLY A 254      34.984   1.311  10.121  1.00  0.00           N
ATOM   3872  CA  GLY A 254      34.002   0.375  10.669  1.00  0.00           C
ATOM   3873  C   GLY A 254      32.898   1.079  11.454  1.00  0.00           C
ATOM   3874  O   GLY A 254      32.392   0.534  12.436  1.00  0.00           O
ATOM   3878  N   ILE A 255      32.423   2.240  11.038  1.00  0.00           N
ATOM   3879  CA  ILE A 255      31.413   3.064  11.764  1.00  0.00           C
ATOM   3880  C   ILE A 255      30.298   3.332  10.735  1.00  0.00           C
ATOM   3881  O   ILE A 255      30.693   3.814   9.658  1.00  0.00           O
ATOM   3897  N   LYS A 256      29.041   3.064  11.067  1.00  0.00           N
ATOM   3898  CA  LYS A 256      27.858   3.446  10.258  1.00  0.00           C
ATOM   3899  C   LYS A 256      27.187   4.624  10.971  1.00  0.00           C
ATOM   3900  O   LYS A 256      26.937   4.429  12.164  1.00  0.00           O
ATOM   3919  N   LEU A 257      26.966   5.726  10.305  1.00  0.00           N
ATOM   3920  CA  LEU A 257      26.176   6.885  10.762  1.00  0.00           C
ATOM   3921  C   LEU A 257      24.999   7.064   9.803  1.00  0.00           C
ATOM   3922  O   LEU A 257      25.165   7.720   8.768  1.00  0.00           O
ATOM   3938  N   THR A 258      23.856   6.459  10.144  1.00  0.00           N
ATOM   3939  CA  THR A 258      22.586   6.680   9.431  1.00  0.00           C
ATOM   3940  C   THR A 258      21.868   7.887  10.033  1.00  0.00           C
ATOM   3941  O   THR A 258      21.828   7.838  11.242  1.00  0.00           O
ATOM   3952  N   LEU A 259      21.422   8.852   9.267  1.00  0.00           N
```


Dieses Werk ist copyrightgeschützt und darf in keiner Form vervielfältigt werden noch an Dritte weitergegeben werden.
Es gilt nur für den persönlichen Gebrauch.

```
ATOM   3953  CA  LEU A 259      20.477   9.922   9.652  1.00  0.00           C
ATOM   3954  C   LEU A 259      19.152   9.559   9.018  1.00  0.00           C
ATOM   3955  O   LEU A 259      19.167   8.636   8.172  1.00  0.00           O
ATOM   3971  N   SER A 260      18.061  10.401   9.564  1.00  0.00           N
ATOM   3972  CA  SER A 260      16.930  10.312   8.633  1.00  0.00           C
ATOM   3973  C   SER A 260      16.077  11.593   8.672  1.00  0.00           C
ATOM   3974  O   SER A 260      16.285  12.453   9.541  1.00  0.00           O
ATOM   3982  N   ALA A 261      15.133  11.684   7.739  1.00  0.00           N
ATOM   3983  CA  ALA A 261      14.038  12.639   7.814  1.00  0.00           C
ATOM   3984  C   ALA A 261      12.791  12.087   7.120  1.00  0.00           C
ATOM   3985  O   ALA A 261      12.888  10.999   6.519  1.00  0.00           O
ATOM   3992  N   LEU A 262      11.658  12.783   7.224  1.00  0.00           N
ATOM   3993  CA  LEU A 262      10.390  12.256   6.706  1.00  0.00           C
ATOM   3994  C   LEU A 262       9.407  13.416   6.541  1.00  0.00           C
ATOM   3995  O   LEU A 262       8.555  13.694   7.375  1.00  0.00           O
ATOM   4011  N   LEU A 263       9.557  14.137   5.431  1.00  0.00           N
ATOM   4012  CA  LEU A 263       8.794  15.381   5.155  1.00  0.00           C
ATOM   4013  C   LEU A 263       7.412  15.000   4.558  1.00  0.00           C
ATOM   4014  O   LEU A 263       7.367  14.621   3.390  1.00  0.00           O
ATOM   4030  N   ASP A 264       6.350  15.126   5.372  1.00  0.00           N
ATOM   4031  CA  ASP A 264       5.032  14.569   5.069  1.00  0.00           C
ATOM   4032  C   ASP A 264       4.146  15.683   4.518  1.00  0.00           C
ATOM   4033  O   ASP A 264       3.163  16.057   5.046  1.00  0.00           O
ATOM   4042  N   GLY A 265       3.832  15.460   3.333  1.00  0.00           N
ATOM   4043  CA  GLY A 265       3.210  16.583   2.608  1.00  0.00           C
ATOM   4044  C   GLY A 265       1.726  16.928   2.860  1.00  0.00           C
ATOM   4045  O   GLY A 265       1.431  18.094   2.567  1.00  0.00           O
ATOM   4049  N   LYS A 266       0.935  16.039   3.421  1.00  0.00           N
ATOM   4050  CA  LYS A 266      -0.377  16.286   4.059  1.00  0.00           C
ATOM   4051  C   LYS A 266      -0.222  16.526   5.557  1.00  0.00           C
ATOM   4052  O   LYS A 266      -1.279  17.051   6.024  1.00  0.00           O
ATOM   4071  N   ASN A 267       0.842  16.221   6.269  1.00  0.00           N
ATOM   4072  CA  ASN A 267       1.108  16.562   7.639  1.00  0.00           C
ATOM   4073  C   ASN A 267       2.485  17.225   7.859  1.00  0.00           C
ATOM   4074  O   ASN A 267       2.925  17.112   8.985  1.00  0.00           O
ATOM   4085  N   VAL A 268       3.147  17.943   6.907  1.00  0.00           N
ATOM   4086  CA  VAL A 268       4.257  18.908   7.248  1.00  0.00           C
ATOM   4087  C   VAL A 268       3.760  19.897   8.175  1.00  0.00           C
ATOM   4088  O   VAL A 268       4.428  20.111   9.128  1.00  0.00           O
ATOM   4101  N   ASN A 269       2.773  20.422   8.310  1.00  0.00           N
ATOM   4102  CA  ASN A 269       2.203  21.354   9.253  1.00  0.00           C
ATOM   4103  C   ASN A 269       1.574  20.600  10.448  1.00  0.00           C
ATOM   4104  O   ASN A 269       1.499  21.354  11.440  1.00  0.00           O
ATOM   4115  N   ALA A 270       1.211  19.331  10.429  1.00  0.00           N
ATOM   4116  CA  ALA A 270       0.925  18.528  11.630  1.00  0.00           C
ATOM   4117  C   ALA A 270       2.234  17.820  12.032  1.00  0.00           C
ATOM   4118  O   ALA A 270       2.468  17.923  13.278  1.00  0.00           O
ATOM   4125  N   GLY A 271       3.081  17.129  11.250  1.00  0.00           N
ATOM   4126  CA  GLY A 271       4.344  16.676  11.781  1.00  0.00           C
ATOM   4127  C   GLY A 271       5.303  16.117  10.746  1.00  0.00           C
ATOM   4128  O   GLY A 271       5.363  16.642   9.669  1.00  0.00           O
ATOM   4132  N   GLY A 272       6.020  15.100  11.105  1.00  0.00           N
ATOM   4133  CA  GLY A 272       6.604  14.127  10.187  1.00  0.00           C
ATOM   4134  C   GLY A 272       8.052  13.832  10.578  1.00  0.00           C
ATOM   4135  O   GLY A 272       8.366  12.640  10.636  1.00  0.00           O
ATOM   4139  N   HIS A 273       8.925  14.838  10.715  1.00  0.00           N
ATOM   4140  CA  HIS A 273      10.349  14.658  10.416  1.00  0.00           C
ATOM   4141  C   HIS A 273      11.090  13.842  11.466  1.00  0.00           C
ATOM   4142  O   HIS A 273      11.005  14.122  12.607  1.00  0.00           O
ATOM   4156  N   LYS A 274      11.861  12.859  11.055  1.00  0.00           N
ATOM   4157  CA  LYS A 274      12.737  12.135  11.964  1.00  0.00           C
ATOM   4158  C   LYS A 274      13.904  13.046  12.371  1.00  0.00           C
ATOM   4159  O   LYS A 274      14.506  13.705  11.539  1.00  0.00           O
ATOM   4178  N   LEU A 275      13.671  13.348  13.524  1.00  0.00           N
ATOM   4179  CA  LEU A 275      14.819  13.476  14.407  1.00  0.00           C
ATOM   4180  C   LEU A 275      15.224  12.068  14.866  1.00  0.00           C
ATOM   4181  O   LEU A 275      14.565  11.464  15.703  1.00  0.00           O
ATOM   4197  N   GLY A 276      16.249  11.457  14.457  1.00  0.00           N
ATOM   4198  CA  GLY A 276      16.791  10.164  14.878  1.00  0.00           C
ATOM   4199  C   GLY A 276      17.931   9.705  13.980  1.00  0.00           C
ATOM   4200  O   GLY A 276      18.006  10.210  12.841  1.00  0.00           O
ATOM   4204  N   LEU A 277      18.734   8.798  14.512  1.00  0.00           N
ATOM   4205  CA  LEU A 277      19.997   8.306  13.926  1.00  0.00           C
ATOM   4206  C   LEU A 277      20.042   6.780  14.029  1.00  0.00           C
ATOM   4207  O   LEU A 277      19.278   6.277  14.866  1.00  0.00           O
ATOM   4223  N   GLY A 278      20.889   6.129  13.259  1.00  0.00           N
ATOM   4224  CA  GLY A 278      21.253   4.717  13.401  1.00  0.00           C
ATOM   4225  C   GLY A 278      22.768   4.595  13.519  1.00  0.00           C
ATOM   4226  O   GLY A 278      23.374   4.829  12.449  1.00  0.00           O
ATOM   4230  N   LEU A 279      23.300   4.266  14.676  1.00  0.00           N
ATOM   4231  CA  LEU A 279      24.733   4.331  14.999  1.00  0.00           C
ATOM   4232  C   LEU A 279      25.206   2.909  15.258  1.00  0.00           C
ATOM   4233  O   LEU A 279      24.658   2.381  16.255  1.00  0.00           O
ATOM   4249  N   GLU A 280      26.076   2.337  14.435  1.00  0.00           N
ATOM   4250  CA  GLU A 280      26.513   0.932  14.510  1.00  0.00           C
ATOM   4251  C   GLU A 280      28.038   0.922  14.512  1.00  0.00           C
ATOM   4252  O   GLU A 280      28.548   1.489  13.510  1.00  0.00           O
ATOM   4264  N   PHE A 281      28.684   0.372  15.508  1.00  0.00           N
ATOM   4265  CA  PHE A 281      30.142   0.394  15.701  1.00  0.00           C
ATOM   4266  C   PHE A 281      30.687  -1.031  15.545  1.00  0.00           C
ATOM   4267  O   PHE A 281      30.165  -1.913  16.262  1.00  0.00           O
ATOM   4284  N   GLN A 282      31.669  -1.245  14.686  1.00  0.00           N
ATOM   4285  CA  GLN A 282      32.364  -2.530  14.528  1.00  0.00           C
ATOM   4286  C   GLN A 282      33.468  -2.630  15.577  1.00  0.00           C
```


Dieses Werk ist copyrightgeschützt und darf in keiner Form vervielfältigt werden noch an Dritte weitergegeben werden.
Es gilt nur für den persönlichen Gebrauch.

```
ATOM   4287  O   GLN A 282      34.465  -1.913  15.520  1.00  0.00           O
ATOM   4301  N   ALA A 283      33.032  -3.828  16.429  1.00  0.00           N
ATOM   4302  CA  ALA A 283      33.939  -4.204  17.510  1.00  0.00           C
ATOM   4303  C   ALA A 283      34.394  -2.978  18.296  1.00  0.00           C
ATOM   4304  O   ALA A 283      33.940  -1.862  18.048  1.00  0.00           O
ATOM   4311  N   ARG A 284      35.296  -3.200  19.251  1.00  0.00           N
ATOM   4312  CA  ARG A 284      35.810  -2.112  20.078  1.00  0.00           C
ATOM   4313  C   ARG A 284      36.936  -1.379  19.354  1.00  0.00           C
ATOM   4314  O   ARG A 284      37.691  -1.982  18.592  1.00  0.00           O
ATOM   4335  N   SER A 285      37.040  -0.074  19.602  1.00  0.00           N
ATOM   4336  CA  SER A 285      38.077   0.739  18.969  1.00  0.00           C
ATOM   4337  C   SER A 285      39.125   1.169  19.992  1.00  0.00           C
ATOM   4338  O   SER A 285      39.658   2.255  19.842  1.00  0.00           O
END
```


Dieses Werk ist copyrightgeschützt und darf in keiner Form vervielfältigt werden noch an Dritte weitergegeben werden.
Es gilt nur für den persönlichen Gebrauch.

Bibliography

[1] E. Wallin, G. von Heijne, *Protein Sci.* **1998**, *7*, 1029–1038.

[2] J. Liu, B. Rost, *Protein Sci.* **2001**, *10*, 1970–1979.

[3] M. Ahram, Z. I. Litou, R. Fang, G. Al-Tawallbeh, *In Silico Biol.* **2006**, *6*, 379–86.

[4] B. Alberts, A. Johnson, J. Lewis, M. Raff, K. Roberts, P. Walter, *Molecular Biology of the Cell 4th ed.*, Garland Science, New York, **2002**.

[5] R. B. Russell, D. S. Eggleston, *Nat. Struct. Mol. Biol.* **2000**, *7*, 928–930.

[6] R. Santos, O. Ursu, A. Gaulton, A. P. Bento, R. S. Donadi, C. G. Bologa, A. Karlsson, B. Al-Lazikani, A. Hersey, T. I. Oprea, J. P. Overington, *Nat. Rev. Drug Discovery* **2017**, *16*, 19–34.

[7] E. Callaway, *Nature* **2015**, *525*, 172–174.

[8] S. Hiller, F. Fiorito, K. Wüthrich, G. Wider, *Proc. Natl. Acad. Sci. U. S. A.* **2005**, *102*, 10876–10881.

[9] K. Kazimierczuk, V. Orekhov, *Magn. Reson. Chem.* **2015**, *53*, 921–926.

[10] A. C. Chadwick, D. R. Jensen, P. J. Hanson, P. T. Lange, S. C. Proudfoot, F. C. Peterson, B. F. Volkman, D. Sahoo, *Structure* **2017**, *25*, 446 – 457.

[11] E. V. Bocharov, P. E. Bragin, K. V. Pavlov, O. V. Bocharova, K. S. Mineev, A. A. Polyansky, P. E. Volynsky, R. G. Efremov, A. S. Arseniev, *Biochemistry* **2017**, *56*, 1697–1705.

Dieses Werk ist copyrightgeschützt und darf in keiner Form vervielfältigt werden noch an Dritte weitergegeben werden.
Es gilt nur für den persönlichen Gebrauch.

[12] A. Karnkowska, V. Vacek, Z. Zubáčová, S. C. Treitli, R. Petrželková, L. Eme, L. Novák, V. Žárský, L. D. Barlow, E. K. Herman, P. Soukal, M. Hroudová, P. Doležal, C. W. Stairs, A. J. Roger, M. Eliáš, J. B. Dacks, ČestmÃr Vlček, V. Hampl, *Curr. Biol.* **2016**, *26*, 1274–1284.

[13] M. Saraste, *Science* **1999**, *283*, 1488–1493.

[14] W. F. Martin, M. Müller, *Origin of mitochondria and hydrogenosomes*, Springer, Heidelberg, **2007**.

[15] H. M. McBride, M. Neuspiel, S. Wasiak, *Curr. Biol.* **2006**, *16*, R551 – R560.

[16] E. Pfaff, M. Klingenberg, *Eur. J. Biochem.* **1968**, *6*, 66–79.

[17] M. Klingenberg, *Biochim. Biophys. Acta, Biomembr.* **2008**, *1778*, 1978 – 2021.

[18] P. L. Yeagle (Ed.), *The Structure of Biological Membranes third edition ed.*, CRC Press, **2011**.

[19] K. Hill, K. Model, M. T. Ryan, K. Dietmeier, F. Martin, R. Wagner, N. Pfanner, *Nature* **1998**, *395*, 516–521.

[20] C. Meisinger, M. Rissler, A. Chacinska, L. K. Sanjuán Szklarz, D. Milenkovic, V. Kozjak, B. Schönfisch, C. Lohaus, H. E. Meyer, M. P. Yaffe, B. Guiard, N. Wiedemann, N. Pfanner, *Dev. Cell* **2004**, *7*, 61–71.

[21] C. Meisinger, S. Pfannschmidt, M. Rissler, D. Milenkovic, T. Becker, D. Stojanovski, M. J. Youngman, R. E. Jensen, A. Chacinska, B. Guiard, N. Pfanner, N. Wiedemann, *EMBO J.* **2007**, *26*, 2229–2239.

[22] N. Wiedemann, V. Kozjak, A. Chacinska, B. Schönfisch, S. Rospert, M. T. Ryan, N. Pfanner, C. Meisinger, *Nature* **2003**, *424*, 565–571.

[23] N. Bolender, A. Sickmann, R. Wagner, C. Meisinger, N. Pfanner, *EMBO Rep.* **2008**, *9*, 42–49.

[24] R. Benz, *Biochim. Biophys. Acta, Rev. Biomembr.* **1994**, *1197*, 167–196.

Dieses Werk ist copyrightgeschützt und darf in keiner Form vervielfältigt werden noch an Dritte weitergegeben werden.
Es gilt nur für den persönlichen Gebrauch.

[25] S. J. Schein, M. Colombini, A. Finkelstein, *J. Membr. Biol.* **1976**, *30*, 99–120.

[26] E. Blachly-Dyson, M. Forte, *IUBMB Life* **2001**, *52*, 113–118.

[27] R. P. Gonçalves, N. Buzhynskyy, V. Prima, J. N. Sturgis, S. Scheuring, *J. Mol. Biol.* **2007**, *369*, 413–418.

[28] B. W. Hoogenboom, K. Suda, A. Engel, D. Fotiadis, *J. Mol. Biol.* **2007**, *370*, 246 – 255.

[29] M. Colombini, C. A. Mannella, *Biochim. Biophys. Acta, Biomembr.* **2012**, *1818*, 1438–1443.

[30] P. Mueller, D. Rudin, H. Ti Tien, W. C. Wescott, *Nature* **1962**, *194*, 979–980.

[31] M. Montal, P. Mueller, *Proc. Natl. Acad. Sci. U. S. A.* **1972**, *69*, 3561–3566.

[32] E. Neher, B. Sakmann, *Nature* **1976**, *260*, 799–802.

[33] W. C. Werkheiser, W. Bartley, *Biochem. J.* **1957**, *66*, 79–91.

[34] M. Colombini, *Nature* **1979**, *279*, 643–645.

[35] L. S. Zalman, H. Nikaido, Y. Kagawa, *J. Biol. Chem.* **1980**, *255*, 1771–1774.

[36] D. F. Parsons, W. D. B. Jr., J. G. Verboon, *Can. J. Bot.* **1965**, *43*, 647–655.

[37] C. A. Mannella, W. D. Bonner, *Biochim. Biophys. Acta, Biomembr.* **1975**, *413*, 213 – 225.

[38] C. A. Mannella, *J. Cell Biol.* **1982**, *94*, 680–687.

[39] V. Adams, L. Griffin, J. Towbin, B. Gelb, K. Worley, E. R. McCabe, *Biochem. Med. Metab. Biol.* **1991**, *45*, 271 – 291.

[40] M. J. Sampson, R. S. Lovell, D. B. Davison, W. J. Craigen, *Genomics* **1996**, *36*, 192–196.

[41] Z. Rahmani, C. Maunoury, A. Siddiqui, *Eur. J. Hum. Genet.* **1998**, *6*, 337–340.

[42] R. Buettner, G. Papoutsoglou, E. Scemes, D. C. Spray, R. Dermietzel, *Proc. Natl. Acad. Sci. U. S. A.* **2000**, *97*, 3201–3206.

Dieses Werk ist copyrightgeschützt und darf in keiner Form vervielfältigt werden noch an Dritte weitergegeben werden.
Es gilt nur für den persönlichen Gebrauch.

[43] V. D. Pinto, F. Guarino, A. Guarnera, A. Messina, S. Reina, F. M. Tomasello, V. Palermo, C. Mazzoni, *Biochim. Biophys. Acta, Bioenerg.* **2010**, *1797*, 1268 – 1275.

[44] X. Xu, W. Decker, M. Sampson, W. Craigen, M. Colombini, *J. Membr. Biol.* **1999**, *170*, 89–102.

[45] M. Colombini, *J. Membr. Biol.* **1989**, *111*, 103–111.

[46] R. Ujwal, D. Cascio, J.-P. Colletier, S. Faham, J. Zhang, L. Toro, P. Ping, J. Abramson, *Proc. Natl. Acad. Sci. U. S. A.* **2008**, *105*, 17742–17747.

[47] S. Abu-Hamad, N. Arbel, D. Calo, L. Arzoine, A. Israelson, N. Keinan, R. Ben-Romano, O. Friedman, V. Shoshan-Barmatz, *J. Cell Sci.* **2009**, *122*, 1906–1916.

[48] S. Hiller, R. G. Garces, T. J. Malia, V. Y. Orekhov, M. Colombini, G. Wagner, *Science* **2008**, *321*, 1206–1210.

[49] H. Engelhardt, T. Meins, M. Poynor, V. Adams, S. Nussberger, W. Welte, K. Zeth, *J. Membr. Biol.* **2007**, *216*, 93–105.

[50] B. Popp, D. A. Court, R. Benz, W. Neupert, R. Lill, *J. Biol. Chem.* **1996**, *271*, 13593–13599.

[51] B. Shanmugavadivu, H.-J. Apell, T. Meins, K. Zeth, J. H. Kleinschmidt, *J. Mol. Biol.* **2007**, *368*, 66 – 78.

[52] B. Mertins, G. Psakis, W. Grosse, K. C. Back, A. Salisowski, P. Reiss, U. Koert, L.-O. Essen, *PLoS One* **2012**, *7*, e47938.

[53] M. Colombini, *Ion channel reconstitution*, C. Miller (Ed.), Plenum, New York, **1986**, chapter Voltage gating in VDAC: Toward a molecular mechanism, pp. 533–552.

[54] T. Rostovtseva, M. Colombini, *Biophys. J.* **1997**, *72*, 1954–1962.

[55] E. Pavlov, S. M. Grigoriev, L. M. Dejean, C. L. Zweihorn, C. A. Mannella, K. W. Kinnally, *Biochim. Biophys. Acta, Bioenerg.* **2005**, *1710*, 96–102.

Dieses Werk ist copyrightgeschützt und darf in keiner Form vervielfältigt werden noch an Dritte weitergegeben werden.
Es gilt nur für den persönlichen Gebrauch.

[56] R. Benz, M. Kottke, D. Brdiczka, *Biochim. Biophys. Acta, Biomembr.* **1990**, *1022*, 311–318.

[57] E. Blachly-Dyson, S. Z. Peng, M. Colombini, M. Forte, *J. Bioenerg. Biomembr.* **1989**, *21*, 471–483.

[58] E. Blachly-Dyson, S. Peng, M. Colombini, M. Forte, *Science* **1990**, *247*, 1233–1236.

[59] L. Thomas, E. Blachly-Dyson, M. Colombini, M. Forte, *Proc. Natl. Acad. Sci. U. S. A.* **1993**, *90*, 5446–5449.

[60] J. Song, C. Midson, E. Blachly-Dyson, M. Forte, M. Colombini, *J. Biol. Chem.* **1998**, *273*, 24406–24413.

[61] V. De Pinto, G. Prezioso, F. Thinnes, T. A. Link, F. Palmieri, *Biochemistry* **1991**, *30*, 10191–10200.

[62] G. Rauch, O. Moran, *Biochem. Biophys. Res. Commun.* **1994**, *200*, 908–915.

[63] R. Casadio, I. Jacoboni, A. Messina, V. De Pinto, *FEBS Lett.* **2002**, *520*, 1–7.

[64] M. Bayrhuber, Ph.D. thesis, Max Planck Institute for Biophysical Chemistry, Göttingen, **2007**.

[65] F. Al Bitar, N. Roosens, M. Smeyers, M. Vauterin, J. V. Boxtel, M. Jacobs, F. Homblé, *Biochim. Biophys. Acta, Gene Struct. Expression* **2003**, *1625*, 43 – 51.

[66] M. Forte, H. R. Guy, C. A. Mannella, *J. Bioenerg. Biomembr.* **1987**, *19*, 341–350.

[67] S. Stanley, J. A. Dias, D. D'Arcangelis, C. A. Mannella, *J. Biol. Chem.* **1995**, *270*, 16694–16700.

[68] J. Kyte, R. F. Doolittle, *J. Mol. Biol.* **1982**, *157*, 105–132.

[69] M. Colombini, *Biochim. Biophys. Acta, Mol. Cell Res.* **2016**, *1863*, 2498–2502.

Dieses Werk ist copyrightgeschützt und darf in keiner Form vervielfältigt werden noch an Dritte weitergegeben werden.
Es gilt nur für den persönlichen Gebrauch.

[70] M. Bayrhuber, T. Meins, M. Habeck, S. Becker, K. Giller, S. Villinger, C. Vonrhein, C. Griesinger, M. Zweckstetter, K. Zeth, *Proc. Natl. Acad. Sci. U. S. A.* **2008**, *105*, 15370–15375.

[71] Schrödinger, LLC, *The PyMOL Molecular Graphics System, Version 1.8*, **2015**, http://www.pymol.org.

[72] M. F. Tomasello, F. Guarino, S. Reina, A. Messina, V. De Pinto, *PLoS One* **2013**, *8*.

[73] S.-Y. Lee, M.-G. Kang, S. Shin, C. Kwak, T. Kwon, J. K. Seo, J.-S. Kim, H.-W. Rhee, *J. Am. Chem. Soc.* **2017**, *139*, 3651–3662.

[74] S. Villinger, Ph.D. thesis, Max Planck Institute for Biophysical Chemistry, Göttingen, **2012**.

[75] J. Schredelseker, A. Paz, C. J. López, C. Altenbach, C. S. Leung, M. K. Drexler, J.-N. Chen, W. L. Hubbell, J. Abramson, *J. Biol. Chem.* **2014**, *289*, 12566–12577.

[76] M. Colombini, *Trends Biochem. Sci.* **2009**, *34*, 382–389.

[77] X. W. Guo, P. Smith, B. Cognon, D. D'Arcangelis, E. Dolginova, C. A. Mannella, *J. Struct. Biol.* **1995**, *114*, 41–59.

[78] C. A. Mannella, *J. Bioenerg. Biomembr.* **1989**, *21*, 427–437.

[79] S. Hiller, J. Abramson, C. Mannella, G. Wagner, K. Zeth, *Trends Biochem. Sci.* **2010**, *35*, 514–521.

[80] O. P. Choudhary, A. Paz, J. L. Adelman, J.-P. Colletier, J. Abramson, M. Grabe, *Nat. Struct. Mol. Biol.* **2014**, *21*, 626–632.

[81] J. Zimmerberg, V. A. Parsegian, *Nature* **1986**, *323*, 36–39.

[82] M. Zizi, L. Thomas, E. Blachly-Dyson, M. Forte, M. Colombini, *J. Membr. Biol.* **1995**, *144*, 121–129.

Dieses Werk ist copyrightgeschützt und darf in keiner Form vervielfältigt werden noch an Dritte weitergegeben werden.
Es gilt nur für den persönlichen Gebrauch.

[83] K. A. Bowen, K. Tam, M. Colombini, *J. Membr. Biol.* **1985**, *86*, 51–59.

[84] A. K. Bera, S. Ghosh, *J. Struct. Biol.* **2001**, *135*, 67–72.

[85] T. K. Rostovtseva, S. M. Bezrukov, *J. Bioenerg. Biomembr.* **2008**, *40*, 163.

[86] S. Peng, E. Blachly-Dyson, M. Forte, M. Colombini, *Biophys. J.* **1992**, *62*, 123–135.

[87] J. Song, C. Midson, E. Blachly-Dyson, M. Forte, M. Colombini, *Biophys. J.* **1998**, *74*, 2926–2944.

[88] C. A. Mannella, *J. Struct. Biol.* **1998**, *121*, 207–218.

[89] D. A. Koppel, K. W. Kinnally, P. Masters, M. Forte, E. Blachly-Dyson, C. A. Mannella, *J. Biol. Chem.* **1998**, *273*, 13794–13800.

[90] V. De Pinto, S. Reina, F. Guarino, A. Messina, *J. Bioenerg. Biomembr.* **2008**, *40*, 139–147.

[91] U. Zachariae, R. Schneider, R. Briones, Z. Gattin, J.-P. Demers, K. Giller, E. Maier, M. Zweckstetter, C. Griesinger, S. Becker, R. Benz, B. de Groot, A. Lange, *Structure* **2012**, *20*, 1540–1549.

[92] S. Törnroth-Horsefield, R. Neutze, *Proc. Natl. Acad. Sci. U. S. A.* **2008**, *105*, 19565–19566.

[93] S. Hiller, G. Wagner, *Curr. Opin. Struct. Biol.* **2009**, *19*, 396–401.

[94] O. P. Choudhary, R. Ujwal, W. Kowallis, R. Coalson, J. Abramson, M. Grabe, *J. Mol. Biol.* **2010**, *396*, 580–592.

[95] C. Kutzner, H. Grubmüller, B. de Groot, U. Zachariae, *Biophys. J.* **2011**, *101*, 809–817.

[96] M. Colombini, *Chem. Rev.* **2012**, *112*, 6373–6387.

[97] A. M. Porcelli, A. Ghelli, C. Zanna, P. Pinton, R. Rizzuto, M. Rugolo, *Biochem. Biophys. Res. Commun.* **2005**, *326*, 799–804.

Dieses Werk ist copyrightgeschützt und darf in keiner Form vervielfältigt werden noch an Dritte weitergegeben werden.
Es gilt nur für den persönlichen Gebrauch.

[98] J. D. Cortese, A. L. Voglino, C. R. Hackenbrock, *Biochim. Biophys. Acta, Bioenerg.* **1992**, *1100*, 189 – 197.

[99] S. Y. Noskov, T. K. Rostovtseva, A. C. Chamberlin, O. Teijido, W. Jiang, S. M. Bezrukov, *Biochim. Biophys. Acta, Biomembr.* **2016**, *1858*, 1778–1790.

[100] V. Shoshan-Barmatz, V. D. Pinto, M. Zweckstetter, Z. Raviv, N. Keinan, N. Arbel, *Mol. Aspects Med.* **2010**, *31*, 227–285.

[101] T. K. Rostovtseva, K. L. Sheldon, E. Hassanzadeh, C. Monge, V. Saks, S. M. Bezrukov, D. L. Sackett, *Proc. Natl. Acad. Sci. U. S. A.* **2008**, *105*, 18746–18751.

[102] T. K. Rostovtseva, S. M. Bezrukov, *Biochim. Biophys. Acta, Biomembr.* **2012**, *1818*, 1526 – 1535, {VDAC} Structure, Function and Regulation of Mitochondrial and Cellular Metabolism.

[103] H. Azoulay-Zohar, A. Israelson, S. Abu-Hamad, V. Shoshan-Barmatz, *Biochem. J.* **2004**, *377*, 347–355.

[104] T. Meins, Ph.D. thesis, Max Planck Institute for Biochemistry, Munich, **2008**.

[105] F. Delaglio, S. Grzesiek, G. W. Vuister, G. Zhu, J. Pfeifer, A. Bax, *J. Biomol. NMR* **1995**, *6*, 277–293.

[106] Bruker BioSpin GmbH, *TopSpin^{TM}, different versions*, **2015**, http://www.bruker.com/products/mr/nmr/nmr-software/nmr-software/topspin/overview.html.

[107] T. D. Goddard, D. G. Kneller, *SPARKY 3*, University of California, San Francisco.

[108] W. F. Vranken, W. Boucher, T. J. Stevens, R. H. Fogh, A. Pajon, M. Llinas, E. L. Ulrich, J. L. Markley, J. Ionides, E. D. Laue, *Proteins: Struct., Funct., Bioinf.* **2005**, *59*, 687–696.

[109] M. Salzmann, G. Wider, K. Pervushin, H. Senn, K. Wüthrich, *J. Am. Chem. Soc.* **1999**, *121*, 844–848.

Dieses Werk ist copyrightgeschützt und darf in keiner Form vervielfältigt werden noch an Dritte weitergegeben werden.
Es gilt nur für den persönlichen Gebrauch.

[110] A. Eletsky, A. Kienhöfer, K. Pervushin, *J. Biomol. NMR* **2001**, *20*, 177–180.

[111] J. Ying, J. H. Chill, J. M. Louis, A. Bax, *J. Biomol. NMR* **2007**, *37*, 195–204.

[112] G. Zhu, X. M. Kong, K. H. Sze, *J. Biomol. NMR* **1999**, *13*, 77–81.

[113] R. Schneider, M. Etzkorn, K. Giller, V. Daebel, J. Eisfeld, M. Zweckstetter, C. Griesinger, S. Becker, A. Lange, *Angew. Chem. Int. Ed.* **2010**, *49*, 1882–1885; *Angew. Chem.* **2010**, *122*, 1926–1929.

[114] V. Sklenář, A. Bax, *J. Magn. Reson. (1969)* **1987**, *74*, 469 – 479.

[115] M. Jaremko, Ł. Jaremko, S. Villinger, C. D. Schmidt, C. Griesinger, S. Becker, M. Zweckstetter, *Angew. Chem. Int. Ed.* **2016**, *55*, 10518–10521; *Angew. Chem.* **2016**, *128*, 10674–10678.

[116] N.-A. Lakomek, J. Ying, A. Bax, *J. Biomol. NMR* **2012**, *53*, 209–221.

[117] P. Damberg, J. Jarvet, A. Gräslund, *J. Am. Chem. Soc.* **2005**, *127*, 1995–2005.

[118] Ł. Jaremko, M. Jaremko, M. Nowakowski, A. Ejchart, *J. Phys. Chem. B* **2015**, *119*, 11978–11987.

[119] K. V. Pervushin, G. Wider, K. Wüthrich, *J. Biomol. NMR* **1998**, *12*, 345–348.

[120] L. Kay, P. Keifer, T. Saarinen, *J. Am. Chem. Soc.* **1992**, *114*, 10663–10665.

[121] J. MacDonald, *J. Magn. Reson. (1969)* **1980**, *38*, 381 – 384.

[122] D. E. Woessner, *J. Chem. Phys.* **1962**, *37*, 647–654.

[123] G. Lipari, A. Szabo, *J. Am. Chem. Soc.* **1982**, *104*, 4559–4570.

[124] G. Lipari, A. Szabo, R. M. Levy, *Nature* **1982**, *300*, 197–198.

[125] W. Press, S. Teukolsky, W. Vetterling, B. Flannery, E. Ziegel, *Numerical Recipes: The Art of Scientific Computing*, Cambridge University Press, **1987**.

Dieses Werk ist copyrightgeschützt und darf in keiner Form vervielfältigt werden noch an Dritte weitergegeben werden.
Es gilt nur für den persönlichen Gebrauch.

[126] C. D. Schwieters, J. J. Kuszewski, N. Tjandra, G. M. Clore, *J. Magn. Reson.* **2003**, *160*, 65 – 73.

[127] Y. Shen, A. Bax, *J. Biomol. NMR* **2013**, *56*, 227–241.

[128] C. D. Schwieters, J. J. Kuszewski, G. M. Clore, *Prog. Nucl. Magn. Reson. Spectrosc.* **2006**, *48*, 47 – 62.

[129] N. Tjandra, D. S. Garrett, A. M. Gronenborn, A. Bax, G. M. Clore, *Nat. Struct. Mol. Biol.* **1997**, *4*, 443–449.

[130] G. A. Bermejo, G. M. Clore, C. D. Schwieters, *Protein Sci.* **2012**, *21*, 1824–1836.

[131] A. Grishaev, A. Bax, *J. Am. Chem. Soc.* **2004**, *126*, 7281–7292.

[132] S. Villinger, R. Briones, K. Giller, U. Zachariae, A. Lange, B. L. de Groot, C. Griesinger, S. Becker, M. Zweckstetter, *Proc. Natl. Acad. Sci. U. S. A.* **2010**, *107*, 22546–22551.

[133] R. Kaptein, G. Wagner, *J. Biomol. NMR* **2015**, *61*, 181–184.

[134] D. M. LeMaster, F. M. Richards, *Biochemistry* **1988**, *27*, 142–150.

[135] S. Grzesiek, J. Anglister, H. Ren, A. Bax, *J. Am. Chem. Soc.* **1993**, *115*, 4369–4370.

[136] H. Kalbitzer, R. Leberman, A. Wittinghofer, *FEBS Lett.* **1985**, *180*, 40–42.

[137] N. Tjandra, A. Bax, *Science* **1997**, *278*, 1111–1114.

[138] R. S. Lipsitz, N. Tjandra, *Annu. Rev. Biophys. Biomol. Struct.* **2004**, *33*, 387–413.

[139] R. Bruschweiler, X. Liao, P. Wright, *Science* **1995**, *268*, 886–889.

[140] J. W. Peng, G. Wagner, *Biochemistry* **1995**, *34*, 16733–16752.

[141] A. K. Mittermaier, L. E. Kay, *Trends Biochem. Sci.* **2009**, *34*, 601–611.

[142] G. Lipari, A. Szabo, *J. Am. Chem. Soc.* **1982**, *104*, 4546–4559.

Dieses Werk ist copyrightgeschützt und darf in keiner Form vervielfältigt werden noch an Dritte weitergegeben werden.
Es gilt nur für den persönlichen Gebrauch.

[143] D. Fushman, R. Xu, D. Cowburn, *Biochemistry* **1999**, *38*, 10225–10230.

[144] E. Gallucci, S. Micelli, V. Picciarelli in *Planar Lipid Bilayers (BLMs) and their Applications*, H. T. Tien, A. Ottova-Leitmannova (Eds.), Elsevier Science, **2003**.

[145] S. Geula, D. Ben-Hail, V. Shoshan-Barmatz, *Biochem. J.* **2012**, *444*, 475–485.

[146] L. Aram, S. Geula, N. Arbel, V. Shoshan-Barmatz, *Biochem. J.* **2010**, *427*, 445–454.

[147] W. A.T.Summers, D. A.Court, *Biochem. Cell Biol.* **2010**, *88*, 425–438.

[148] S. Hovmöller, T. Zhou, T. Ohlson, *Acta Crystallogr., Sect. D: Struct. Biol.* **2002**, *58*, 768–776.

[149] K. Pervushin, R. Riek, G. Wider, , K. Wüthrich, *J. Am. Chem. Soc.* **1998**, *120*, 6394–6400.

[150] K. Takeuchi, H. Arthanari, G. Wagner, *J. Biomol. NMR* **2016**, *66*, 221–225.

[151] Z. Gattin, R. Schneider, Y. Laukat, K. Giller, E. Maier, M. Zweckstetter, C. Griesinger, R. Benz, S. Becker, A. Lange, *J. Biomol. NMR* **2015**, *61*, 311–320.

[152] H. McWilliam, W. Li, M. Uludag, S. Squizzato, Y. M. Park, N. Buso, A. P. Cowley, R. Lopez, *Nucleic Acids Res.* **2013**, *41*, W597–W600.

[153] M. Colombini, *Biochim. Biophys. Acta, Biomembr.* **2012**, *1818*, 1457–1465.

[154] E. T. Dill, Ph.D. thesis, University of Maryland (College Park, Md.), **1987**.

[155] P. Vallurupalli, G. Bouvignies, L. E. Kay, *J. Am. Chem. Soc.* **2012**, *134*, 8148–8161.

[156] N. L. Fawzi, J. Ying, D. A. Torchia, G. M. Clore, *Nat. Protocols* **2012**, *7*, 1523–1533.

[157] O. Teijido, R. Ujwal, C.-O. Hillerdal, L. Kullman, T. K. Rostovtseva, J. Abramson, *J. Biol. Chem.* **2012**, *287*, 11437–11445.

[158] S.-Y. Sheu, D.-Y. Yang, H. L. Selzle, E. W. Schlag, *Proc. Natl. Acad. Sci. U. S. A.* **2003**, *100*, 12683–12687.

Dieses Werk ist copyrightgeschützt und darf in keiner Form vervielfältigt werden noch an Dritte weitergegeben werden.
Es gilt nur für den persönlichen Gebrauch.

[159] I. Moraes, *The Next Generation in Membrane Protein Structure Determination*, I. Moraes (Ed.), Springer International Publishing, **2016**.

[160] M. L. Nasr, D. Baptista, M. Strauss, Z.-Y. J. Sun, S. Grigoriu, S. Huser, A. Pluckthun, F. Hagn, T. Walz, J. M. Hogle, G. Wagner, *Nat. Meth.* **2017**, *14*, 49–52.

[161] A. M. Waterhouse, J. B. Procter, D. M. A. Martin, M. Clamp, G. J. Barton, *Bioinformatics* **2009**, *25*, 1189.

Dieses Werk ist copyrightgeschützt und darf in keiner Form vervielfältigt werden noch an Dritte weitergegeben werden.
Es gilt nur für den persönlichen Gebrauch.

Curriculum vitae

Personal information

Name	Christian Daniel Schmidt
Date of birth	13.10.1988
Place of birth	Leipzig, Germany
Citizenship	German

Education

1995–1999	82. & 80. Grundschule, primary school in Leipzig
1999–2007	Wilhelm-Ostwald-Gymnasium, grammar school in Leipzig
2008–2011	Academic studies of Chemistry (Bachelor of Science) at the Georg-August-Universität Göttingen, Bachelor thesis in the Institute of Organic and Biomolecular Chemistry, title “Reaktionen donor-akzeptor-substituierter Cyclopropane zum Aufbau von Thiophenen”, principal investigator Dr. Daniel B. Werz
2011–2013	Academic studies of Chemistry (Master of Science) at the Georg-August-Universität Göttingen, Master thesis in the Institute of Organic and Biomolecular Chemistry, title “Untersuchungen zur Umlagerung von Nitrocyclopropanen in Nitrone”, principal investigator PD Dr. Daniel B. Werz
2013–2017	Doctoral thesis at the Max Planck Institute for Biophysical Chemistry, department of NMR-based Structural Biology, Göttingen with the title “NMR spectroscopic investigations on VDAC”

Scholarships

10/2011	Stipend of the “Otto Vahlbruch-Stiftung”
12/2012	Stipend of the “Otto Vahlbruch-Stiftung”
2009–today	Stipend of the “Dr. Jost Henkel Stiftung”

Göttingen, May 2017

Dieses Werk ist copyrightgeschützt und darf in keiner Form vervielfältigt werden noch an Dritte weitergegeben werden.
Es gilt nur für den persönlichen Gebrauch.

Dieses Werk ist copyrightgeschützt und darf in keiner Form vervielfältigt werden noch an Dritte weitergegeben werden.
Es gilt nur für den persönlichen Gebrauch.

Dieses Werk ist copyrightgeschützt und darf in keiner Form vervielfältigt werden noch an Dritte weitergegeben werden.
Es gilt nur für den persönlichen Gebrauch.

Dieses Werk ist copyrightgeschützt und darf in keiner Form vervielfältigt werden noch an Dritte weitergegeben werden.
Es gilt nur für den persönlichen Gebrauch.